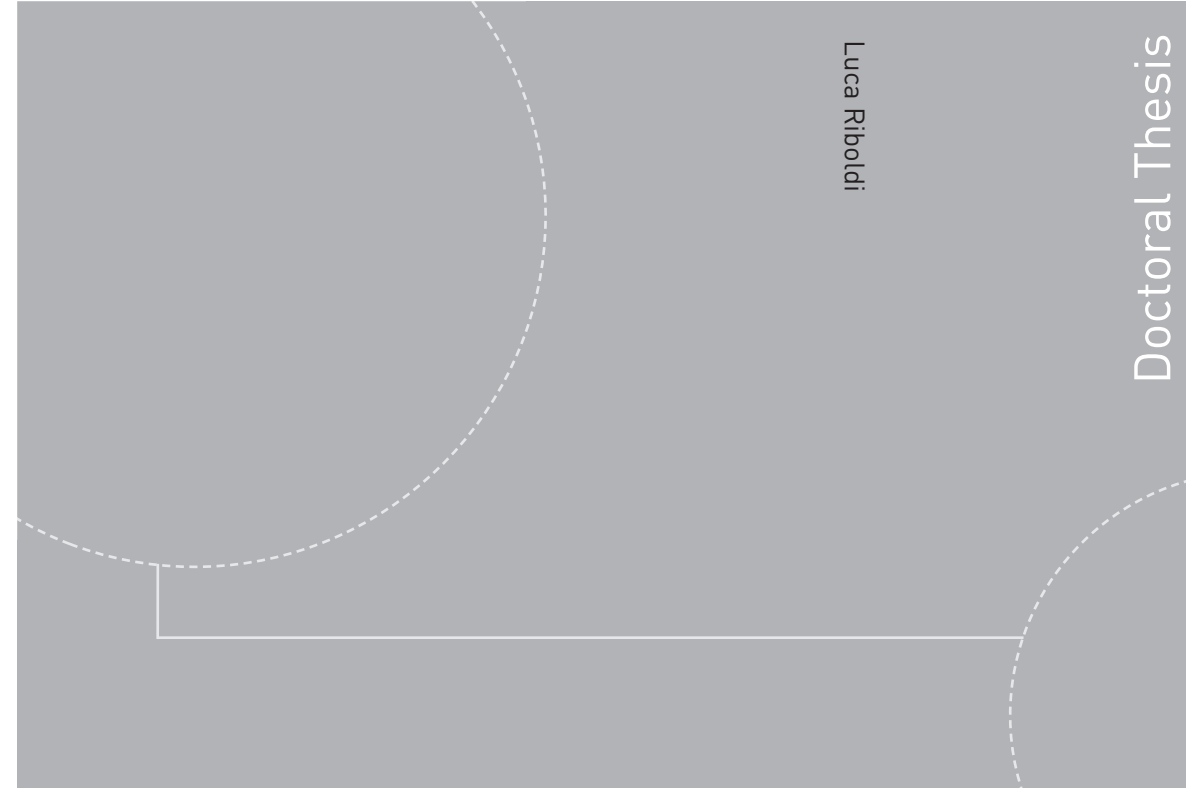


ISBN 978-82-326-1638-1 (printed version)
ISBN 978-82-326-1639-8 (electronic version)
ISSN 1503-8181



Doctoral theses at NTNU, 2016:150

Luca Riboldi

**Assessment of pressure swing
adsorption as CO₂
capture technology in coal-fired
power plants**

Luca Riboldi

Assessment of pressure swing adsorption as CO₂ capture technology in coal-fired power plants

Thesis for the degree of Philosophiae Doctor

Trondheim, June 2016

Norwegian University of Science and Technology
Faculty of Engineering
Science and Technology
Department of Energy and Process Engineering



Norwegian University of
Science and Technology

NTNU

Norwegian University of Science and Technology

Thesis for the degree of Philosophiae Doctor

Faculty of Engineering

Science and Technology

Department of Energy and Process Engineering

© Luca Riboldi

ISBN 978-82-326-1638-1 (printed version)

ISBN 978-82-326-1639-8 (electronic version)

ISSN 1503-8181

Doctoral theses at NTNU, 2016:150



Printed by Skipnes Kommunikasjon as

Preface

The thesis is submitted as partial fulfilment of the requirements for the degree of philosophiæ doctor (PhD) at the Norwegian University of Science and Technology (NTNU). The work was carried out at the Department of Energy and Process Engineering at the Faculty of Engineering Science and Technology, with Prof. Olav Bolland as supervisor. Prof. Nicola Wagner from University of the Witwatersrand (WITS) was appointed co-supervisor.

The research was supported by the Norwegian University of Science and Technology (NTNU).

Abstract

Coal-based power generation is responsible for a significant share of CO₂ emissions on a global scale. Technologies to drastically reduce coal carbon footprint are critical for meeting mitigation targets. Absorption, whether chemical or physical depending on the process framework, is commonly regarded as the most mature technology in this context. Nevertheless, absorption suffers from some drawbacks, such as high energy requirements and corrosion of process equipment. Adsorption is considered as a promising alternative, with potential for reducing energy penalty, environmental impact and cost of CO₂ capture.

The main objective of this thesis is to assess the viability of a process relying on adsorption, i.e. pressure swing adsorption (PSA), as CO₂ capture technology in coal-fired power plants.

In order to get a comprehensive overview on the prospects of PSA, different cases were considered. Post-combustion CO₂ capture was studied by integrating a PSA unit into an advanced supercritical pulverized coal (ASC) plant. Pre-combustion CO₂ capture was studied by integrating a PSA unit into an integrated gasification combined cycle (IGCC) plant. Proper designs for these process frameworks were defined, taking into account characteristics, requirements and constraints of the systems. PSA is a discontinuous process, made of different steps undergone by each column of a PSA train. A dynamic model was built, based on material, energy and momentum balances. The developed dynamic model was then linked to the steady-state model of the power plant, by exploiting appropriate process scheduling and the cyclic steady state (CSS) condition of the PSA process (a condition in which the process transient behavior becomes steady throughout different cycles). The resulting composite model allowed performing simulations and analyses on a system level.

The post-combustion case (ASC + PSA) showed competitive energy performance. The net electric efficiency obtained was 34.8%, whereas the reference plant without CO₂ capture had 45.1%. The CO₂ capture requirement was also fulfilled with more than 90% CO₂ sequestered. A comparison with chemical absorption - performing with 34.2% net electric efficiency - confirmed the competitiveness of PSA. A serious issue ascertained concerned the required footprint of the PSA unit. A first estimation suggested the necessity of more than 260 adsorption columns for processing the entire flue gas coming from the boiler. The feasibility of PSA in the post-combustion case appeared less attractive because of the number of vessels needed.

The pre-combustion case (IGCC + PSA) returned good results for all the performance indicators investigated. A comparison with physical absorption showed that PSA is slightly outperformed in terms of energy efficiency (36.2% versus 37.1%, with the reference plant without CO₂ capture having 47.3%), CO₂ recovery (86.1% versus 90.6%) and footprint. However, the performance gap was evaluated to be rather small, thus additional investigations were carried out in this process framework.

Improvements in the performance of the pre-combustion case were sought by considering two domains, the process and the adsorbent material. Several possible process configurations were analysed and a range of results obtained. Improved energy performance could be obtained but to the detriment of the CO₂ separation performance and vice versa. Modifications in the adsorbent material properties (attempting to simulate different adsorbents and/or advancements in the materials) showed a significant influence not only on the gas separation process but on the whole plant performance. The utilization of improved adsorbents demonstrated the capability to give a substantial contribution to close the gap with absorption, though it may not be sufficient. None of the cases studied succeeded to fully match absorption-based performance both in terms of energy and CO₂ capture efficiency. Further, an approach to exploit possible synergies between the two studied domains and realize the full potential of PSA in this framework was outlined. It consisted of tuning the material properties according to a specific process configuration. The results achieved were encouraging as net electric efficiencies up to 37.1% were obtained without drastic decrease in the CO₂ capture efficiency.

The knowledge developed in the pre-combustion process framework suggested a further case which was believed interesting for PSA. An IGCC plant was defined coproducing power and ultrapure H₂ with CO₂ capture. The system is of interest both because it allows capturing CO₂ and because differentiating the plant products can be advantageous in terms of flexible operation. Two novel process configurations were developed, entirely relying on PSA. The first consists of two consecutive PSA stages (*Two-train PSA*), while the second configuration carries out both CO₂ separation and H₂ purification within a single PSA stage (*One-train PSA*). Both these configurations succeeded to provide a varying power-to-hydrogen output ratio - the net power output could be reduced from 346 MW to 300 MW by increasing the ultrapure H₂ throughput - with a constant coal feed to the gasifier and retaining plant efficiency on a good level. The common process design for an IGCC coproduction layout encompasses absorption for CO₂ capture and PSA for H₂ production. With regard to that, a comparative analysis seems to confirm the expected advantages brought by the utilization of PSA as the only gas separation technology. A higher integration level could be achieved, allowing significant energy savings. The assessment of PSA in this framework was concluded to be promising and worth further analyses.

Summing up, it was demonstrated that PSA can be successfully integrated in coal-fired power plants as CO₂ capture technology. However, the analyses carried out showed also that PSA is generally outperformed by absorption in an overall evaluation taking into account different performance indicators. Potentials and limits of the technology have been highlighted and recommendations for optimizing the performance have been outlined. The knowledge developed can be useful to address further work on PSA technology, especially in those specific frameworks (e.g. coproduction of power and H₂) where PSA can reach competitiveness.

Acknowledgements

First I would like to acknowledge Prof. Olav Bolland which made all of this possible and for the trust he put on me. His guidance throughout the PhD period has been precious.

I would like to express my gratitude to all the people which gave a contribution to the development of this thesis. In particular I would like to mention Prof. Lars Nord. He has always been very available for a good advice or a nice word. I am very glad to have the opportunity to work with him in the future. Prof. Nicola Wagner, Prof. Salam Titinchi and Dr. Jacob M. Ngoy for the time we spent together working on the project and for the kind hospitality. Prof. Hugo A. Jakobsen and Dr. Rafael A. Sánchez for the work we did together. Prof. Hallvard F. Svendsen for letting me joining meetings with his students and for his valuable advices.

Other people at university were likewise important in order to help me out during these years and to create a perfect work environment. I would like to acknowledge the administration staff of EPT. No matter how annoying I was, they have always been nice, professional and helpful. Sincere thanks to my colleagues and friends. Many people came and go during these years. I have been so lucky to find some who became close friends during our common struggle for the completion of a PhD. I will try to mention most of them: Vu, Bjørn, Tian, Renga, Jonas, Donghoi, Ruben, Shareq, Karl, Christoph, Fredrik, Karl Oskar. Thank you for your friendship (and sometimes for your patience). The relaxing moments we spent together, whether to have a coffee, a lunch or a grøte (no that is not considered a lunch), inside or outside university, will remain as good memories to me.

Bring a PhD to completion is an effort which influence your everyday life. Therefore I cannot avoid expressing my gratitude to the extraordinary people which surrounded me during this period.

The first of my list is my mother Patrizia. Your unconditioned love and support has been fundamental during hard days of these years. You are an important cornerstone of my life. The rest of my family had also a primary role. My sister Valentina, my father Luciano, my sister Anna, my grandmother Luciana, my uncle and aunt Gianmario and Roberta, my cousin Tommaso and all the other additional members. It's because of your affection if after a number of years away I still call you home. I cannot forget my lifetime-friends in Italy. The fact that we are still close as we were before is the sign of the strength of our friendship.

My years in Trondheim brought me to know more people which enriched my life. They would all deserve some words to highlight their importance but I'm scared the space would not be enough. At least I would like to mention them by name. Thanks to my friends Claudio, Giancarlo, Roberta, Eirini, Nicola, Sepideh, Walter, Luca, Maria and Eleni. You are great people and I hope I get to count on you for many years to come. A special thanks to Annette. You made me a better person.

Finally, thanks to all friends, to my former flatmates, to the football and cageball group and to the many people that have been part of my life during these years in Trondheim. No matter how small, the role of each of you has been essential.

Table of Contents

Preface	iii
Abstract	iv
Acknowledgements	vii
Table of Contents	ix
Nomenclature	xii
Chapter 1 Introduction.....	1
1.1 Background and motivation.....	1
1.2 Objectives	2
1.3 Contribution	3
1.4 Thesis structure	3
1.5 List of publications	4
Chapter 2 Technical background.....	6
2.1 Climate change and the role of CCS.....	6
2.2 CO ₂ capture systems	10
2.2.1 Post-combustion CO ₂ capture.....	10
2.2.2 Pre-combustion CO ₂ capture	11
2.2.3 Oxy-combustion CO ₂ capture.....	13
2.3 Adsorption for gas separation	14
2.3.1 Adsorbent materials.....	15
2.3.2 Pressure Swing Adsorption (PSA)	17
2.3.3 PSA for CO ₂ capture	19
2.3.4 PSA for H ₂ purification	21
2.4 The role of coal in the energy sector.....	23
2.4.1 Coal-fired power plants	24

2.4.2	Advanced supercritical pulverized coal (ASC) plant	24
2.4.3	Integrated gasification combined cycle (IGCC) plant.....	27
Chapter 3 Methodology		33
3.1	Composite model for system analysis	33
3.2	Process design and modeling of ASC plant.....	35
3.2.1	Pulverized coal boiler	35
3.2.2	Steam cycle.....	37
3.2.3	Gas cleaning	38
3.2.4	CO ₂ separation.....	39
3.2.5	CO ₂ compression	40
3.3	Process design and modeling of IGCC plant	40
3.3.1	Air separation	41
3.3.2	Gasification and syngas treatment.....	42
3.3.3	CO ₂ separation and H ₂ production	44
3.3.4	CO ₂ compression and purification.....	45
3.3.5	Power island	46
3.4	Process design and modeling of PSA process	47
3.4.1	Governing equations.....	48
3.4.2	Boundary and initial conditions.....	58
3.4.3	PSA configuration	61
3.4.4	Solution of the PSA model.....	66
3.5	Definition of efficiencies and performance indicators.....	67
3.5.1	Energy performance	67
3.5.2	Gas separation performance	69
3.5.3	Footprint of the gas separation technology.....	70
3.6	Specifications and constraints of the systems.....	70
Chapter 4 Results and discussions		71
4.1	Paper I - Evaluating Pressure Swing Adsorption as a CO ₂ separation technique in coal-fired power plants	71
4.2	Paper II - Comprehensive analysis on the performance of an IGCC plant with a PSA process integrated for CO ₂ capture.....	73

4.3	Paper III - Pressure swing adsorption for coproduction of power and ultrapure H ₂ in an IGCC plant with CO ₂ capture.....	75
Chapter 5 Conclusions and further work		77
5.1	Conclusions.....	77
5.2	Further work	78
References		81
Papers		87

Nomenclature

a_i	neighboring sites occupied by adsorbate molecule for component i
a_p	particle surface area per unit volume, m^2/m^3
a_w	ratio of internal surface area to volume of the column wall, m^2/m^3
a_u	ratio of external surface area to volume of column wall, m^2/m^3
C_i	gas phase concentration of component i, mol/m^3
$C_{ads,i}$	specific heat of component i in the adsorbed phase, $J/(mol\ K)$
$C_{p,g}$	gas specific heat at constant pressure, $J/(mol\ K)$
$C_{por,i}$	macropore concentration of component i, mol/m^3
$C_{por,i}^s$	macropore concentration of component i at the particle surface, mol/m^3
C_S	particle specific heat, $J/(kg\ K)$
C_{tot}	total gas phase concentration, mol/m^3
$C_{v,G}$	gas specific heat at constant volume, $J/(mol\ K)$
C_w	wall specific heat, $J/(kg\ K)$
$D_{ax,i}$	axial dispersion coefficient of component i, m^2/s
$D_{c,i}$	micropore diffusivity of component i, m^2/s
$D_{0c,i}$	limiting micropore diffusivity at infinite temp. of component i, m^2/s
$D_{g,i}^m$	multicomponent molecular diffusivity of component i, m^2/s
$D_{g,ij}$	binary diffusion coefficient of the ij system, m^2/s
$D_{k,i}$	Knudsen diffusivity for component i, m^2/s
d_p	adsorbent particle diameter, m
$D_{p,i}$	macropore diffusivity of component i, m^2/s
$E_{a,i}$	activation energy of component i, J/mol
f_D	correction term
h_f	film heat transfer coefficient between the gas and particle, $J/(m^2\ s\ K)$
h_u	external convective heat transfer coefficient ($J/m^2\ s\ K$)
h_w	wall heat transfer coefficient, $J/(m^2\ s\ K)$
k	Boltzmann constant
K_D	parameters corresponding to the viscous pressure loss term
$k_{f,i}$	external mass transfer coefficient of component i, m/s
k_g	thermal conductivity of the gas phase, $J/(m\ s\ K)$
$k_{g,e}$	thermal conductivity of the external air, $J/(m\ s\ K)$
k_i	equilibrium constant of component i, Pa^{-1}
$k_{LDF,i}$	linear driving force coefficient of component i, s^{-1}
K_V	parameters corresponding to the kinetic pressure loss term
k_w	wall conductivity, $J/m\ s\ K$
L	length of the adsorption column, m
LHV_f	coal lower heating value, kJ/kg
LHV_{H_2}	ultrapure H_2 lower heating value, kJ/kg

LHV_s	syngas lower heating value, kJ/kg
\dot{m}	mass flow rate, kg/s
\dot{m}_f	coal mass flow rate, kg/s
\dot{m}_{H_2}	ultrapure H_2 mass flow rate, kg/s
\dot{m}_s	syngas mass flow rate, kg/s
MW_i	molecular weight of component i, g/mol
\dot{n}	mole flow rate, mol/s
Nu	Nusselt number
P	pressure, Pa
$PSA-R_{CO_2}$	PSA CO_2 recovery
$PSA-Y_{CO_2}$	PSA CO_2 purity
Pr	Prandtl number
q_i	distributed concentration of component i in the micropore, mol/kg
q_i^*	equilibrium adsorbed concentration of component i, mol/kg
\hat{q}_i	average concentration of component i in the particle, mol/kg
\bar{q}_i	averaged adsorbed concentration of component i, mol/kg
$q_{m,i}$	specific saturation adsorption capacity of component i, mol/kg
r	distance along the micropore radius, m
R	distance along the macroparticle radius, m
r_c	micropore radius, m
R_{CO_2}	CO_2 recovery
Ra	Rayleigh number
Re	Reynolds number
R_g	universal gas constant, Pa m ³ /(mol K)
R_{H_2}	H_2 recovery
R_p	macroparticle radius, m
$R_{w,i}$	internal radius of the column, m
$R_{w,e}$	external radius of the column, m
Sc	Schmidt number
Sh	Sherwood number
t	step time, s
T	temperature, K
T_s	temperature in solid phase, K
T_s^s	temperature at the particle surface, K
T_w	wall temperature, K
U	overall heat transfer coefficient, J/m ² s K
u_s	superficial velocity, m/s
\dot{W}	electric power, MW
Y_{CO_2}	CO_2 purity
Y_{H_2}	H_2 purity
y_i	mole fraction of component i

z distance along the axial direction, m

Greek letters

$\Delta H_{r,i}$ heat of adsorption of component i , J/mol
 ε bed porosity
 ε_p particle porosity
 η_{CO_2} CO₂ capture efficiency
 η_{drive} efficiency of the drives for the different compressors and pumps
 η_{el} net electric efficiency
 η_g generator efficiency
 η_m mechanical efficiency
 $\eta_{el\ prod}$ power production efficiency
 η_{H_2} hydrogen efficiency
 η_{tot60} cumulative energy efficiency (with a factor 0.6)
 η_{tot}^* cumulative energy efficiency (with a factor $\eta_{el\ prod}$)
 λ_{ax} axial thermal dispersion coefficient, J/(m s K)
 μ dynamic viscosity, Pa s
 ξ_i diffusion parameter for component i
 ρ_g gas volumetric mass density, kg/m³
 ρ_p volumetric mass density of the particle, kg/m³
 σ_{ij} characteristic length of the intermolecular force law, Å
 χ_{LDF}^c linear driving force geometrical factor
 τ tortuosity factor
 Ω_D collision integral for diffusion

Abbreviations

AC activated carbon
AGR acid gas removal
ASC advance supercritical pulverized coal
ASU air separation unit
CCS carbon dioxide capture and storage
CFBC circulating fluidized bed combustion
CSS cyclic steady state
DHU dehydration unit
EBTF European benchmarking task force
ECO economizer
ESP electrostatic precipitators
EV evaporator
FC flash column
FGD flue gas desulfurization
GHG greenhouse gas

GT	gas turbine
HHV	higher heating value
HP	high pressure
HRSG	heat recovery steam generator
IEA	international energy agency
IGCC	integrated gasification combined cycle
IP	intermediate pressure
IPCC	intergovernmental panel on climate change
LHV	lower heating value
LP	low pressure
MOF	metal organic framework
MSHE	multi-stream heat exchanger
PCC	pulverized coal combustion
PDAE	partial differential and algebraic equations
PEM	proton exchange membrane
PFBC	pressurize fluidized bed combustion
PSA	pressure swing adsorption
RH	reheater
SCR	selective catalytic reduction
SEWGS	sorption enhanced water-gas shift
SH	superheater
SNCR	selective non-catalytic reduction
ST	steam turbine
TIT	turbine inlet temperature
VPSA	vacuum pressure swing adsorption
WGS	water-gas shift

Chapter 1 Introduction

1.1 Background and motivation

Global warming mitigation has been widely accepted as one of the major challenges of our time. Emissions reduction with reasonable economics and impact needs to be targeted. In this sense, carbon capture and storage (CCS) is an important measure in the portfolio of available mitigation options. CCS allows a significant reduction of the carbon footprint of fossil fuels. Therefore, CCS can be a bridge technology, contributing to a smooth transition towards an energy system no longer depending on fossil fuels. Many models could not limit warming to below 2°C if CCS is not in the mix of mitigation technologies or in limited use. In this context, the energy need is at the core of the discussion. Energy production and use accounts for two-thirds of the world's greenhouse-gas (GHG) emissions. The majority of the energy-related emissions are from coal. Given the significant role that coal is predicted to retain in the near future world energy supply, this thesis was decided to focus on coal-based power generation with CO₂ capture.

To date, the most applicable technology for CO₂ capture is absorption, both in post- and pre-combustion applications [1–3]. The vast majority of commercial CO₂ capture plants use absorption-based processes and, likewise, the ongoing industrial-scale projects in the energy sector. Absorption demonstrated to be a reliable technology, offering high CO₂ capture efficiency and selectivity. However, it is plagued by a series of issues which slowed down its deployment [4–6]. The solvent regeneration process is energy intensive, mainly due to the large amount of water to be evaporated. Corrosion, toxicity and amine degradation are also to be carefully taken into account. Furthermore, some studies suggested that absorption may not be the most cost-effective technology in the future [7,8]. The investigation of alternative mitigation technologies is, thus, highly recommended.

Pressure swing adsorption (PSA) is regarded as a promising process for CO₂ capture, with potential for reduced energy penalty and environmental impact. A considerable research effort is currently addressed to develop materials and processes for effective CO₂ capture based on adsorption. However, a gap in knowledge has been observed with

respect to information and approaches for the integration of a PSA unit within power plants. There are very few system analyses reported in the literature, dealing with this topic. The thesis work aimed to close this gap and, consequently, give an actual contribution to the development of CCS.

The PhD project constituted a part of the project of collaboration called “EnPe – NORAD’s Programme within the energy and petroleum sector”. The project scope is a specialization within environmental challenges related to climate change, here in particular related to CCS. A specific objective of the project was to transfer CCS competence from NTNU to the South African institutions selected as partners and to contribute to further development of competence focused on CCS. South Africa is regarded as a very interesting partner being the largest emitter of CO₂ in Africa, a major exporter of hard coal and with limited expertise on CCS.

1.2 Objectives

This thesis work wanted to assess PSA as a CO₂ emission mitigation technology. The primary objective of the thesis was to provide an evaluation based on system level analyses of coal-fired power plants integrating a PSA unit for CO₂ capture.

Different process frameworks were considered, in order to return a complete overview on the status of PSA technology.

In the accomplishment of the main objective, a series of sub-tasks can be listed:

- Process design and integration of the PSA unit for CO₂ capture into the power plant, both for a post- and a pre-combustion application.
- Development of a composite model of the systems investigated, including a steady-state model of the coal-fired power plant and a dynamic model of the PSA process.
- Performing system analyses through process simulations to assess the performance and to provide plant-level comparisons with other techniques of decarbonization, absorption in the first instance.
- Evaluating prospects and potentials of the concepts studied. The following questions aimed to be answered: *is PSA currently a competitive technology for CO₂ capture in coal-fired power plants? If not, does it have the potential to become competitive under some assumptions? How should further research efforts be addressed?*

1.3 Contribution

The main contributions of the thesis can be so summarized:

- Development of tools and methodologies for assessing the viability of PSA as CO₂ capture technology into coal-fired power plants. A novel composite model was developed constituted by a dynamic model of the PSA unit and a steady-state model of the power plant. A performance framework was also defined to assess the process simulation outputs.
- Exhaustive understanding of the coupling principles and relationships between the various sub-units of the complex systems investigated, which involve the integration of a PSA unit and a CO₂ compression unit into a power plant.
- System level analysis of an advanced supercritical pulverized coal (ASC) plant and of an integrated gasification combined cycle (IGCC) plant integrating PSA for CO₂ capture (*Paper I*). Definition of advantages, issues and uncertainties of the defined systems. Comparative analysis with common approaches to CO₂ emission control in the energy generation sector (i.e. absorption) and general evaluation of the viability of adsorption as a valid mitigation technology.
- Comprehensive analysis on the performance realistically achievable by the pre-combustion case investigated, IGCC + PSA (*Paper II*). The analysis takes into account the state-of-the-art and the possible future advancements of the technology. Evaluations on the current status and on the potentials of PSA in this process framework are provided, together with guidelines to address future developments.
- Definition and evaluation of two novel configurations of an IGCC plant coproducing power and ultrapure H₂ with CO₂ capture (*Paper III*). Those configurations are completely based on PSA as gas separation technology. The advantages in terms of flexible operation, energy efficiency and process integration opportunities are outlined.

1.4 Thesis structure

The thesis includes five chapters and three papers. *Chapter 1* gives an introduction to the thesis work. The thesis framework is first set by discussing the background, the motivations and the objectives of the work. The achievements are then analysed reporting the contribution to the body of knowledge and the list of scientific publications. *Chapter 2* gives a technical background to the subject. An insight is provided on CSS and its role in climate change mitigation, on adsorption as gas separation technology and on coal-based power generation. A review of relevant works from the literature is included as well. *Chapter 3* outlines the methodologies adopted to

meet the objectives of the thesis. Composite models were developed to enable process simulations and system analyses. The basic characteristics and assumptions of these composite models are described, along with the established process design of the systems investigated. A framework for the analysis of the results is also set. *Chapter 4* provides a summary of the selected papers. The main results of the thesis work are reported and discussed. *Chapter 5* gives the conclusion of the work and some recommendations for further work. The papers selected to be the core of thesis work are enclosed at the end of the thesis.

1.5 List of publications

The papers included in the thesis and, thus, subject of the evaluation, are *Paper I*, *Paper II* and *Paper III*. With regard to these, Riboldi is the main author, responsible for the modelling, process simulations, critical analysis of the results and paper writing. Bolland (main supervisor) is the coauthor, contributing with discussions, suggestions and comments throughout the whole development of the paper and with the revision of the manuscript.

Additional papers realized during thesis work but not included in the thesis, are *Paper IV*, *Paper V*, *Paper VI* and *Paper VII*. For *Paper VI* the same authorship framework as in *Paper I,II* and *III* applies, with the authors giving the same type of contributions. In *Paper IV* also Wagner and Ngoy are coauthors, contributing with discussions to the definition of the paper. Wagner took also part in the revision of the manuscript. For *Paper V*, the situation is overturned with Ngoy as main author, Wagner as principal coauthor and Riboldi and Bolland contributing as coauthors to the definition of the paper with discussions and comments. For *Paper VII* Sánchez is the main author, responsible for the modelling and numerical implementation of the reforming simulations. Sánchez additionally carried out the critical analysis of the results and the paper writing. Riboldi did as coauthor the modelling and process simulation of the gas separation stage. Jakobsen provided guidelines for the paper.

Paper included in the thesis

International journal papers, first author

Paper I

Riboldi L., Bolland O. (2015) *Evaluating Pressure Swing Adsorption as a CO₂ separation technique in coal-fired power plants. International Journal of Greenhouse Gas Control* 39, 1-16.

Paper II

Riboldi L., Bolland O. (2015) *Comprehensive analysis on the performance of an IGCC plant with a PSA process integrated for CO₂ capture. International Journal of Greenhouse Gas Control* 43, 57-69.

Paper III

Riboldi L., Bolland O. (2016) *Pressure swing adsorption for coproduction of power and ultrapure H₂ in an IGCC plant with CO₂ capture. International Journal of Hydrogen Energy. In Press.*

Additional contributions (not included in the thesis)

Conference paper, first author

Paper IV

Riboldi L., Bolland O., Ngoy J. M., Wagner N. (2104) *Full-plant Analysis of a PSA CO₂ Capture Unit Integrated in Coal-fired Power Plants: Post-and Pre-combustion Scenarios. Energy Procedia* 63, 2289-2304.

Conference paper, coauthor

Paper V

Ngoy J. M., Wagner N., Riboldi L., Bolland O. (2104) *A CO₂ Capture Technology Using Multi-walled Carbon Nanotubes with Polyaspartamide Surfactant. Energy Procedia* 63, 2230-2248.

Conference paper with peer-reviewing, first author

Paper VI

Riboldi L., Bolland O. (2016) *Determining the potentials of PSA processes for CO₂ capture in Integrated Gasification Combined Cycle (IGCC). Energy Procedia* 86, 294-303.

International journal paper, coauthor

Paper VII

Sánchez R. A., Riboldi L., Jakobsen H. A. (2016) *Numerical modelling and simulation of hydrogen production via four different chemical reforming processes: Process performance and energy requirements. Submitted to The Canadian Journal of Chemical Engineering.*

Chapter 2 Technical background

2.1 Climate change and the role of CCS

«The *Conference of the Parties*, [...] *Recognizing* that climate change represents an urgent and potentially irreversible threat to human societies and the planet and thus requires the widest possible cooperation by all countries, and their participation in an effective and appropriate international response, with a view to accelerating the reduction of global greenhouse gas emissions, *Also recognizing* that deep reductions in global emissions will be required in order to achieve the ultimate objective of the Convention and emphasizing the need for urgency in addressing climate change, [...]»

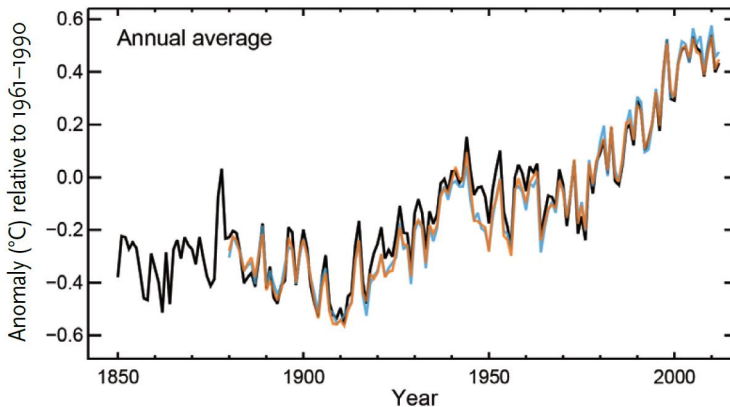


Figure 1. Earth's average surface air temperature from 1850 to 2012. The indicated anomaly (°C) is relative to the average surface temperature of the period 1961-1990. Sources: IPCC AR5, data from the HadCRUT4 dataset (black), UK Met Office Hadley Centre, the NCDC MLOST dataset (orange), US National Oceanic and Atmospheric Administration, and the NASA GISS dataset (blue). Figure reproduced from [9].

The reported excerpt from the Paris Agreement - dated December 12th 2015 - under the United Nations Framework Convention on Climate Change, clearly stresses that climate change has been widely recognized as a global issue to be tackled with the greatest urgency. Warming of the climate system is unequivocal, and since the 1950s, many of

the observed changes are unprecedented over decades to millennia. The clearest evidence for surface warming comes from widespread temperature records. Earth's average surface air temperature has increased by about 0.8°C since 1900, with much of this increase taking place since the mid-1970s (see *Figure 1*) [9]. There are robust evidences that the main cause of global warming is the accumulation of greenhouse gases (GHG) in the atmosphere, CO₂ in particular. The CO₂ level in 2012 was about 40% higher than it was in the nineteenth century. Most of this CO₂ increase has taken place since 1970. Continued emission of GHGs will cause further warming and long-lasting changes in all components of the climate system. Any major climate modification is known to be disruptive, especially when is as rapid as the one we are witnessing, increasing the likelihood of severe, pervasive and irreversible impacts for people and ecosystems.

There is a widespread agreement on setting to 2°C the threshold for the surface temperature increase compared to pre-industrial levels. Holding the global average temperature below that level would not prevent for the long-term changes caused by human activities which are irreversible. However, it would make them less disruptive and would increase the resilience of human societies. In order to reach the objective, it is fundamental to limit the total amount of GHGs emitted to the atmosphere. It has been estimated that keeping the cumulative CO₂ emissions from all anthropogenic sources since 1870 to remain below about 2900 Gt_{CO₂} would comply with the 2°C goal with a probability of > 66% [10]. About 1900 Gt_{CO₂} had already been emitted by 2011. Thus, an urgent and resolute action is needed. The peak of CO₂ emissions must be reached soon and must be followed by a fast decrease in the following decades leading to near zero emissions of CO₂ by the end of the century. Implementing such reductions poses substantial technological, economic, social and institutional challenges. On the other hand, additional delays would severely undermine the possibility to reach the 2°C goal. Energy production and use accounts for roughly two-thirds of all anthropogenic GHG emissions, meaning that effective action in this sector is essential [11]. In order to sustain the growth of the world economy and bringing modern energy to the billions who lack it today, the requested decrease in CO₂ emissions in the energy sector needs to be built on a drastic decarbonisation of the world's energy system. This trend already moved its first steps as there are signs that growth in the global economy and energy-related emissions are starting to decouple. A fundamental contribution to the reshaping of the energy system is given by the deployment of renewable energy sources and by the increased energy efficiency. However, many models show that the Earth's warming cannot be kept below the 2°C threshold without the contribution of carbon dioxide capture and storage (CCS). This does not mean that CCS should be supported to the detriment of other low-carbon technologies. A realistic pathway towards a carbon constrained energy system cannot disregard any of the available options. In the absence or under limited availability of any mitigation technology, mitigation costs can increase substantially and the emissions reduction goals become virtually unattainable.

CCS is a process consisting of the separation of CO₂ from industrial and energy-related sources, transport to a storage location and long-term isolation from the atmosphere [1]. CCS is a key component in the portfolio of mitigation technologies for two main reasons. In the first instance, CCS allows a decarbonisation of the energy system while continuing to exploit fossil fuels. Albeit in the long-term clean energy technologies are predicted to take over for a larger and larger share of the global energy production, coal and other fossil fuels will inevitably play a role for many decades to come. Further, CCS is currently the only technology available to deal with CO₂ emissions reductions in the industrial sector, including industries like cement, iron and steel, chemicals and refining. The CO₂ emissions from the industrial sector currently make up for one-fifth of total global CO₂ emissions and there are no signs of a future decrease [12]. Several models and relative emissions scenarios confirm the critical role of CCS (see for example *Figure 2* developed by IEA) [13]. If CCS is removed from the list of emissions reduction options in the electricity sector, the capital investment needed to meet the same emissions constraints increases by about 40%.

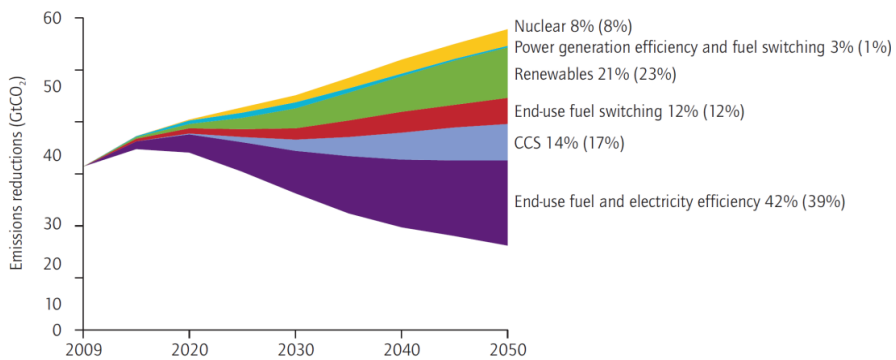


Figure 2. Emissions reduction contributions through 2050 of different mitigation technologies in 2°C Scenario compared to 6°C Scenario. The number besides each technology is the relative share in cumulative emission reductions through 2050, whereas the number in brackets is the relative share in 2050. Figure reproduced from [12].

Once established the necessity of CCS as mitigation technology, a question arising may be: is CCS ready to do its part to meet CO₂ emissions limits? An analysis on the status of CCS technology needs to take into consideration the three components constituting the CCS chain, namely CO₂ capture, transport and storage.

While assessing CO₂ capture readiness, a basic distinction needs to be done with regard to the framework considered. In some industrial applications, CO₂ capture processes are already commercially available and in common use (e.g. natural gas processing, hydrogen production, etc.). For other applications, like in the power generation sector, CO₂ capture is less advanced and more costly. However, many processes are approaching commercial maturity driven by an intense research activity.

Transport of CO₂ is a well-established and mature technology, mainly thanks to the extensive experience gained with the operation of more than 6000 km of CO₂ pipes in the United States. A possible issue may arise for the up-scaling of the transport network. In order to keep up with the IEA's least-cost pathway to halve energy-related CO₂ emissions by 2050, the estimated network of CO₂ transport infrastructure to be built in the coming 30-40 years is roughly 100 times larger than the current one [14]. Other options for CO₂ transport need to be developed likewise, for instance shipping.

The last step in the CCS process is the permanent storage into appropriate geologic formations. Suitable storage sites include saline aquifers, depleted oil and gas fields, oil fields with the potential for enhanced oil recovery (EOR) and unmineable coal seams. The fundamental physical processes and engineering aspects of geological storage are well understood, based on the accumulated experience in the petroleum sector and through CO₂ storage pilot and large-scale projects. There is a high degree of confidence that CO₂ storage can be undertaken safely. The timing seems to be the possible concern. Available large and storage-ready structures are required in order to store the huge CO₂ volumes predicted by emission constrained scenarios. Given the considerable period of time necessary to fully appraise a greenfield site, a thorough mapping of the possible storage sites must be undertaken well in advance not to slow down the CCS deployment in the next decades.

An important milestone in the development of CCS has been recently reached when the world's first large-scale¹ CCS project in the power sector commenced operation in October 2014 at the Boundary Dam power station in Saskatchewan, Canada. Two additional large-scale CCS projects in the power sector – at the Kemper County Energy Facility in Mississippi and the Petra Nova Carbon Capture Project in Texas – are planned to come into operation in 2016. The world's first large-scale CCS project in the iron and steel sector, the Abu Dhabi CCS Project in the United Arab Emirates (UAE), is currently under construction. The total number of large-scale CCS projects in operation or under construction is 22, while other 14 are in advanced planning, including 9 in the power sector [14]. These numbers represent a significant increase compared to 2010 (i.e. 11 large-scale projects) and attest the global commitment in CCS. *Figure 3* reports the large-scale projects in operation, under construction or in an advanced stage of development planning by industry and storage type. Even though tangible progress has been achieved, this progress is still below the trajectory required. The portfolio of CCS needs to be expanded to areas where capturing is more challenging (e.g. power generation sector) or where there is not alternative to CCS (e.g. cement industry). Further, immediate and longer-term policy support is vital in order to pursue CCS potential as mitigation technology.

¹ A CCS project is considered large-scale when involves capture, transport and storage of CO₂ at a scale of: at least 800000 tons of CO₂ per year for a coal-based power plant; at least 400000 tons of CO₂ per year for other emission-intensive industrial facilities.

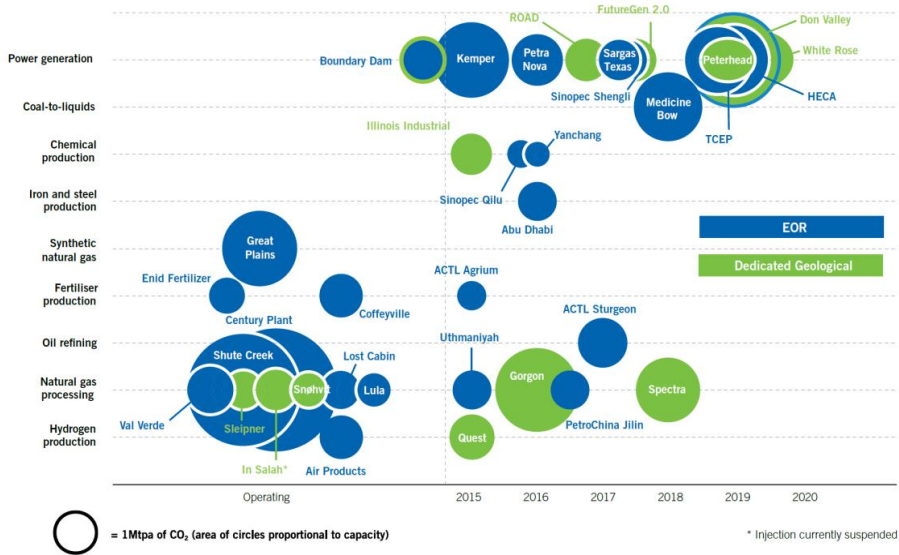


Figure 3. Actual and expected operation dates for large-scale CCS projects in operation, under construction or in an advanced stage of development planning by industry and storage type. Figure reproduced from [14].

2.2 CO₂ capture systems

There is a number of separation processes that can be used to capture CO₂ from a gas mixture. All the possible approaches can be classified in three basic principles:

- Post-combustion CO₂ capture
- Pre-combustion CO₂ capture
- Oxy-combustion CO₂ capture

2.2.1 Post-combustion CO₂ capture

Capture of CO₂ from flue gases produced by combustion of fossil fuels and biomass in air is referred to as post-combustion CO₂ capture (PostCCC) [1]. The process framework consists of passing the flue gas through a gas separation unit, which is responsible for the CO₂ removal. The CO₂-rich gas stream obtained is further conditioned (i.e. compressed and dehydrated) for being transported and finally stored, whereas the remaining flue gas is discharged to the atmosphere. A scheme of a general CO₂ post-combustion capture process is shown in Figure 4.

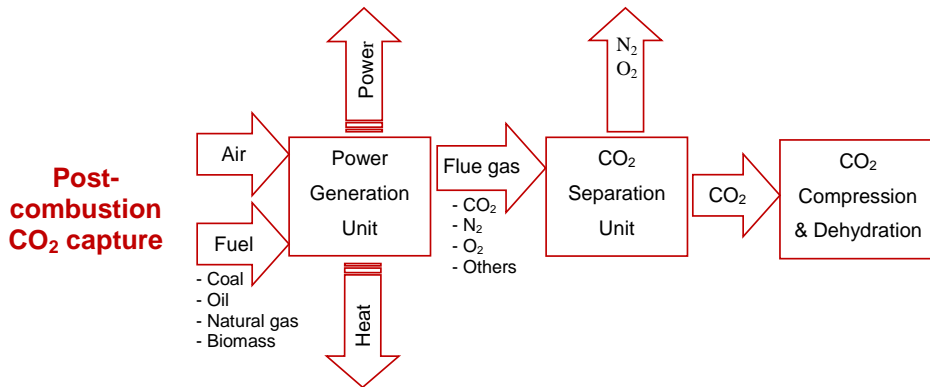


Figure 4. General post-combustion CO₂ capture process scheme.

A significant disadvantage of post-combustion method, in its common process framework, is the low partial pressure of CO₂ in flue gas (0.03 to 0.15 bar). This is due principally to two factors: flue gas resulting from combustion systems is usually at atmospheric pressure; the CO₂ content of flue gases is normally rather low, varying between 3% by volume for a natural gas combined cycle to less than 15% for a coal-fired combustion plant. Additional challenges connected to PostCCC are the huge volumes of flue gas to process and the presence of impurities that can be detrimental to the CO₂ capture unit. Despite the mentioned drawbacks, at the moment PostCCC is the only industrial CO₂ capture technology being demonstrated at full commercial-scale. The major examples are the Technology Center Mongstad in Norway (100000 tons per year CO₂ captured) and Boundary Dam power station in Canada (1 million tons per year CO₂ captured). Some advantages drove to a faster development of PostCCC [2]: it can be retrofitted to coal-fired power plants without substantial changes in their configuration; it is the most suitable candidate for gas-fired power plants; it offers operation flexibility to the plants which can keep on working when the capture unit is shut down. There are several commercially available process technologies which can in principle be used for CO₂ capture from flue gases. Currently the benchmark for PostCCC is the absorption process based on chemical solvents [2,15,16]. Other techniques are also being considered but these are not at such an advanced stage of development. Among these it is worth to mention: adsorption, membrane separation and phase separation through distillation or anti-sublimation.

2.2.2 Pre-combustion CO₂ capture

Pre-combustion CO₂ capture (PreCCC) involves reacting a primary fuel with oxygen or air and/or steam to give mainly a ‘synthesis gas (syngas)’ or ‘fuel gas’ composed of CO

and H₂. CO is reacted with steam in a catalytic reactor, called a shift converter, to give CO₂ and more H₂. CO₂ is then separated resulting in a H₂-rich fuel which can be used in many applications, such as boilers, furnaces, gas turbines, engines and fuel cells [1]. The input concentration of CO₂ in the separation stage can be in the range 15-60% vol. (dry basis) and the total pressure is typically 2-7 MPa, meaning that the CO₂ separation and compression process is less energy demanding than the post-combustion counterpart, where the total pressure and CO₂ concentration are lower. The separated CO₂ is then compressed and made available for transport and storage. A simple process scheme is shown in *Figure 5*.

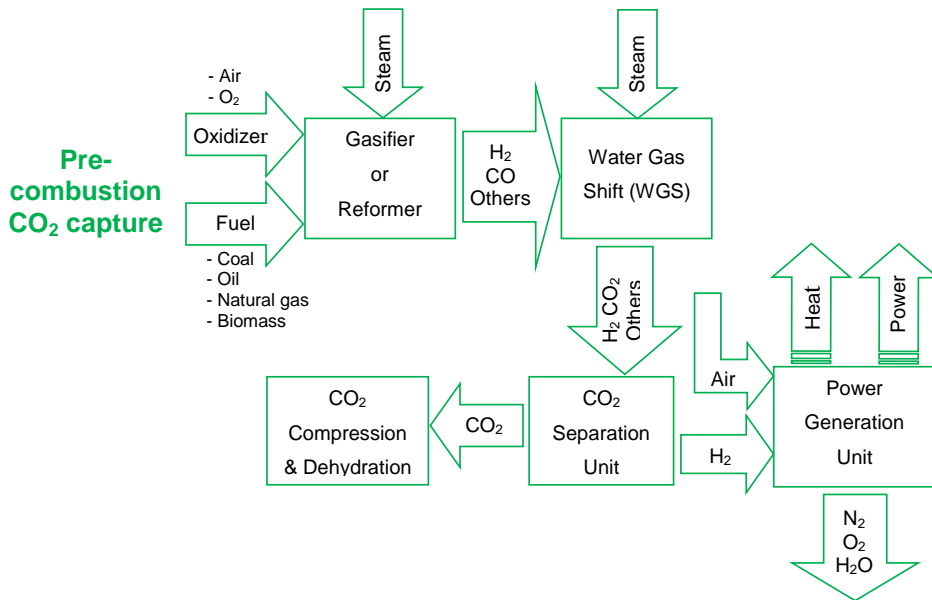


Figure 5. General pre-combustion CO₂ capture process scheme.

Pre-combustion CO₂ capture in power generation is based on processes that are used on industrial scale to produce hydrogen and chemical commodities, where CO₂ is a by-product that is being removed. In this respect, pre-combustion CO₂ capture in chemical industry is mature and in use for over 90 years [3]. The most common CO₂ capture technology is absorption with a chemical or a physical solvent. The liquid solvents used in absorption selectively remove both H₂S and CO₂, thus the unit is called acid gas removal (AGR) unit. The acid components are separately released upon regeneration. Chemical solvents are used to remove CO₂ from syngas at partial pressures below, typically, about 1.5 MPa. The tertiary amine methyldiethanolamine (MDEA) is widely used in modern industrial processes. Physical solvent processes are mostly applicable to gas streams which have a higher CO₂ partial pressure. Depending on the possibility of transport and storage of mixed CO₂ and H₂S or not, the main solvents used are

Sulphinol, Rectisol or Selexol. Alternative technologies are under development. Adsorption may be an option both for low and high-temperature gas separation. Especially interesting is the concept of sorption enhanced water-gas shift (SEWGS), where the CO conversion is combined with CO₂ removal by using a solid adsorbent. Membrane technology and low temperature separation processes (e.g. cryogenic distillation) are other possible options.

2.2.3 Oxy-combustion CO₂ capture

The oxy-combustion CO₂ capture process (OxyCCC) eliminates nitrogen from the flue gas by combusting a hydrocarbon or carbonaceous fuel in either pure oxygen or a mixture of pure oxygen and a CO₂-rich recycled flue gas [1]. Combustion of a fuel with pure oxygen has a combustion temperature of about 3500°C, which is far too high for typical power plant materials. The combustion temperature should be limited to about 1300-1400°C in a typical gas turbine cycle and to about 1900°C in an oxy-fuel coal-fired boiler, using current technology. The methodology commonly implemented to moderate the temperature is to recirculate a fraction of the flue gas to the combustor. The flue gas resulting from an oxy-combustion has high concentration of CO₂ and water vapour. CO₂ can be separated from water by dehydration and low temperature purification processes. Nevertheless, other impurities may be present depending on the fuel used (e.g. SO_x, NO_x, HCl, Hg), on the diluents in the oxygen stream supplied (e.g. N₂, Ar, excess O₂) and on possible air leakage into the system. The content of impurities may be so high that a separation process downstream the power plant has to be implemented anyway. The concentrated CO₂ stream is compressed and transported by pipeline. A simple scheme of an oxy-combustion configuration is shown in *Figure 6*.

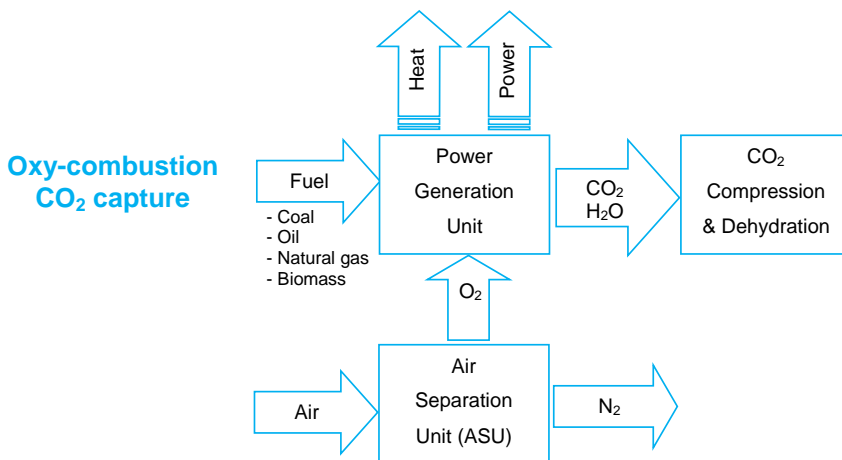


Figure 6. General oxy-combustion CO₂ capture process scheme.

Although elements of oxy-combustion technology are already in use in the aluminium, iron and steel and glass melting industries, oxy-combustion technology for CO₂ capture has yet to be deployed on a commercial scale. The last decade has seen significant R&D on oxy-combustion. Large-scale testing combined with targeted laboratory studies have provided fundamental scientific knowledge and has generated experience with the large individual and integrated unit operations [17]. However, it is important to emphasize that the key separation step in most oxy-combustion capture systems (i.e. O₂ from air) is a mature technology. Current methods of oxygen production by air separation comprise cryogenic distillation, adsorption using multi-bed pressure swing units and polymeric membranes. Adsorption and polymeric membrane methods of air separation are only economic for small oxygen production rates (less than 200 tons of O₂ per day). For all the larger applications, which include power station boilers, cryogenic air separation is the only economic and practical solution. A higher degree of integration between air separation and power cycle may also apply. Technologies being investigated in this case include: metal oxides as an oxygen carrier (such as chemical looping combustion); oxygen selective metal (the CAR-cycle); oxygen separated in a continuous operation using an oxygen transport membrane (OTM) or an ion transport membrane (ITM).

2.3 Adsorption for gas separation

In adsorption processes one or more components of a gas or liquid stream are adsorbed on the surface of a solid adsorbent and a separation is obtained [18]. This process differs from absorption, in which a fluid (the adsorbate) permeates or is dissolved by a liquid or solid (the adsorbent). Note that adsorption is a surface-based process while absorption involves the whole volume of the material. In commercial processes, the adsorbent is usually in the form of small particles in a fixed bed (even if there are applications with fluidized and moving beds). A fluid is passed through the bed and the solid particles selectively adsorb some components. When the bed is almost saturated, the flow is stopped and the bed is regenerated through a pressure decrease, a temperature increase or a combination of the two. The adsorbed components (adsorbate) are thus desorbed and recovered, and the solid adsorbent is ready for another cycle of adsorption. Similar to surface tension, adsorption is a consequence of surface energy. In a bulk material, all the bonding requirements (ionic, covalent, or metallic) of the constituent atoms are filled by other atoms in the material. However, atoms on the surface of the adsorbent are not wholly surrounded by other adsorbent atoms and therefore can attract adsorbates. The exact nature of the bonding depends on the nature of the species involved, but the adsorption process is generally classified as physisorption (characterised by weak van der Waals forces) or chemisorption (characterised by the formation of chemical bonds). Many adsorbents have been developed for a wide range of separation processes.

Typically the adsorbents are in the form of small pellets, beads or granules. A particle of adsorbents has a very porous structure with many fine pores and a pore volume up to 50% of total particle volume. The size and number of pores determine the internal surface area. It is normally advantageous to have a high surface area (large population of small pores). According to the International Union of Pure and Applied Chemistry (IUPAC), adsorbents can be classified on the basis of their pore sizes: microporous materials have pores smaller than 2 nm, mesoporous materials have pores between 2 and 50 nm, and macroporous materials have pores larger than 50 nm. Adsorption often occurs as a monolayer on the surface of the fine pores. However, several layers sometimes occur.

The selection of the proper adsorbent is a complex task, yet of paramount importance in the design of a separation process. Many different properties of an adsorbent are desirable in order to achieve an efficient gas separation. It is worthwhile to point out that no single ideal adsorbent exists for a given application. Trade-offs between the requested properties are likely to occur. Accordingly, an understanding of the system in which the adsorbent needs to perform is fundamental. Main criteria for the selection of an adsorbent include: adsorption capacity; selectivity; adsorption/desorption kinetics; regenerability and multicycle stability; chemical stability/tolerance to impurities; thermal stability; mechanical strength.

2.3.1 *Adsorbent materials*

Adsorbents can be categorized in many ways. The distinguishing factor can be the composition, the pore dimensions, the separation mechanism (physisorption or chemisorption but also equilibrium, kinetic, or molecular sieving mechanisms). The simple classification proposed here divides the adsorbents into two groups, the physisorbents and the chemisorbents. The first group includes zeolites, activated carbons (ACs), carbon molecular sieves, carbon nanotubes-based adsorbents and metal organic frameworks (MOFs). The second group includes hydrotalcites and all the amine functionalized adsorbents. The literature is rich in comprehensive reviews on adsorbent materials for CO₂ capture applications [19–22]. For a detailed overview of the characteristics and properties of different classes of adsorbents, reference should be made to the suggested literature. In this section, some general considerations are provided, with regard to the current status of significant families of adsorbents and their advantages/disadvantages in actual processes.

Physisorbents, especially zeolites and ACs, are the most extensively adsorbents studied for many applications, CO₂ separation included. They display a series of interesting characteristics which make them the natural choice in many instances. Both zeolites and ACs exhibit competitive CO₂ adsorption capacity near ambient temperature and good

CO₂ selectivity over other common gas components. At low CO₂ partial pressures (\approx 0.15 bar), typical of post-combustion applications, zeolites outperform ACs in terms of adsorption capacity and selectivity, due to the more favorable adsorption isotherm. The situation overturns at higher CO₂ partial pressures ($>$ 1.7 bar) [23], which makes ACs good candidates for pre-combustion applications, where such high pressure levels are common. Since the uptake mechanism for physisorbents does not involve chemical reactions, the kinetics of adsorption is typically mass transfer limited and the heat of adsorption is relatively low. Accordingly, zeolites and ACs generally display fast kinetics and excellent regenerability. However, the performance is strongly affected by the operating conditions. The CO₂ adsorption capacity decreases significantly at high temperatures ($>$ 373K). Additionally, the presence of water vapor, which is an inevitable component in flue gas, negatively affects the capacity of these adsorbents and reduces the availability of active surface area. Other contaminants in flue gas, such as SO_x and NO_x, may also have a detrimental impact on the CO₂ adsorption capacity. Pretreatment steps are most likely to be applied for the gas stream to treat, including cooling, dehydration and gas cleaning processes.

An emerging class of crystalline solids called metal organic frameworks (MOFs) has recently gained widespread attention. The related studies exponentially increased in the last years thanks to the extremely wide variety of MOF materials that can be synthesized [24–27]. One important characteristic of MOFs is the possibility to tune to a large extent their structural and chemical features (e.g. pore size, pore shape, chemical potential of the adsorbing surfaces) in order to obtain desired properties. Promising CO₂ adsorption capacities have been demonstrated in the materials with the highest surface area, and high adsorptive selectivities have also begun to emerge in materials furnished with functionalized surfaces. However, additional research effort needs to be undertaken to ensure the applicability of this family of adsorbents. Many issues are yet to be addressed, including: the effect of water and other impurities components (O₂, CO, CH₄, SO_x, NO_x) in the feed, the practical aspects of employing a PSA process [27], the stability over multiple adsorption/desorption cycles [19] and the material formulation and mechanical stability [28].

In contrast to physisorbents, the adsorptive properties of chemisorbents vary widely according to the nature of their chemical interactions with CO₂. In general, hydrotalcites display lower adsorption capacity than physisorbents and other chemisorbents. However, they have some peculiar characteristics which make them suitable for certain applications. Hydrotalcites adsorption capacity is positively affected by the presence of water and is retained at high temperatures (up to around 673K [19]). The ability to perform at higher operative temperature than physisorbents opens the way for process integration opportunities. For instance, hydrotalcites have been considered for sorption enhanced processes (e.g. sorption-enhanced water-gas shift). The adsorption kinetics is characterized by a fast followed by a slow stage and is slower than physisorbents.

Likewise, regenerability is not as good as with physisorbents, especially at high temperatures, which often give rise to structural changes in the adsorbents, resulting in substantial decreases in adsorption capacity with repeated cycles.

Another class of chemisorbents includes the amine-functionalized adsorbents. It is a rather wide family of adsorbents as differences can be found in the composition, in the functional group for chemisorption and in the solid support. Generally speaking, amine-functionalized adsorbents display high CO₂ adsorption capacity at low pressure levels, high CO₂ selectivity (especially over N₂) and robustness in presence of water in the gas. These characteristics make them promising candidates for post-combustion applications. Their regenerability appears to be good, even though a thermal swing may be needed. The issues yet to be addressed regard [19,21,22]: the possible amine degradation at high temperature; the adverse effects of impurities, especially acid gases such as COS, SO_x and NO_x; the slower adsorption kinetics that can be an intrinsic limit to the cycle times achievable.

2.3.2 *Pressure Swing Adsorption (PSA)*

Pressure swing adsorption (PSA) is a cyclic process where some components from a multicomponent gas mixture are selectively retained in a porous material. Before breakthrough of these components, the adsorbent is regenerated by rapidly reducing the partial pressure of the adsorbed components, either by lowering the total pressure or by using a purge gas, under a pre-defined schedule. When the pressure is reduced to a sub-atmospheric value, the process is called vacuum pressure swing adsorption (VPSA). For simplicity in the rest of the text, the process will be always termed PSA even though it involves sub-atmospheric pressures. The origin of PSA can be traced back to 1958, when a patent was registered by Skarstrom and independently, in a different version, by Guerin de Montegareuil and Domine [29]. In the more well-known Skarstrom cycle, two steps (adsorption and depressurization/purge) are carried out in two adsorbent beds operated in tandem, enabling the processing of a continuous feed. Since introduction of the Skarstrom cycle, many more sophisticated PSA processes have been developed and commercialized. Such processes have attracted increasing interest because of their low energy requirements and low capital investment costs. Nowadays, PSA is a mature technology for air drying, hydrogen purification, n-paraffin removal and small- to medium-scale air fractionation. Its utilization is under investigation for other applications, among them CO₂ separation. In modern PSA processes, a number of beds is used to synchronize and accommodate steps additional to those in the Skarstrom cycle while ensuring continuous operation (i.e. one bed of the train is always admitting the feed gas stream). Typical PSA steps are (see *Figure 7* for a schematic representation):

- *Adsorption or feed*: the high-pressure feed gas is co-currently injected at the bottom of the column. The heavy components (e.g. CO₂) of the gas stream start to be selectively adsorbed onto the surface of the adsorbent. The less adsorbed components (e.g. light gases like H₂ or N₂) flow out by the column end.
- *Blowdown*: the pressure is reduced in order to regenerate the bed. A fraction of the adsorbates are desorbed and flows out from one side of the column. In CO₂-separation applications a stream of CO₂-rich gas can be recovered during this step.
- *Purge*: the regeneration is completed by injecting a purge gas into the column, normally counter-currently, while the pressure is retained low. In order to further reduce CO₂ partial pressure and to ensure an effective CO₂ displacement, the purge gas has to be an inert or light gas. It can be the effluent from another step, e.g. the feed/adsorption step. In CO₂-separation applications, a stream of CO₂-rich gas can be recovered during this step.
- *Feed pressurization*: the bed pressure is increased to the feed pressure. The pressurization is carried out by sending the feed stream concurrently while the opposite side of the column is kept closed.
- *Light product pressurization*: the bed pressure is increased to the feed pressure. The pressurization is carried out by sending a light gas stream (e.g. H₂-rich gas stream) co-currently or counter-currently to the column while the opposite side is kept closed. The light gas can be the effluent from another step, e.g. the feed/adsorption step.
- *Pressure equalization - depressurization*: the column is connected to another at lower pressure. The pressure decreases as a fraction of the gas is displaced to the other column.
- *Pressure equalization - pressurization*: the column is connected to another at higher pressure. The pressure increases as some gas flows in, released from the other column.
- *Heavy reflux or rinse*: a heavy gas (normally a fraction of the CO₂-rich product gas) is fed to the column in order to displace the light components from the gas phase. This step is implemented before the regeneration process as it contributes to increase the purity of the recovered gas.
- *Null or idle*: the column is left idle.

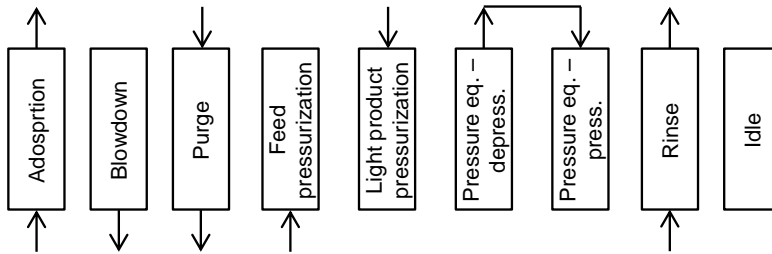


Figure 7. Schematic representation of the PSA steps.

Attempts have been made to develop a systematic methodology to define the optimal cycle configuration for a given application, in terms on number of beds, and number and duration of steps [30,31]. However, PSA process design often remains a trial and error procedure that demands some experience and specific knowledge of the system. What makes the optimization process such a complex task is the large number of parameters which influence PSA process, the cyclic nature of its operation and the multiple objectives to consider.

2.3.3 PSA for CO₂ capture

Utilization of PSA for CO₂ capture is the focus of the thesis, therefore a literature review on this subject is presented. A variety of PSA cycle configurations have been developed for concentrating the heavy component, CO₂ in the first instance, from a feed stream. Reynolds et al. provided an overview of different PSA cycles explored for concentrating CO₂ from stack and flue gases [32]. Additional studies have been lately published which contribute to understand the potentials of this process. Zhang et al. analysed experimentally 6- and 9-step VPSA cycles to remove CO₂ from a gas stream representative of the flue gas from a coal-fired boiler (12% vol. CO₂) [33]. The adsorbent used, a zeolite 13X, was able to achieve > 90% CO₂ purity with a CO₂ recovery exceeding 60%. Xiao et al. studied two VPSA cycles for removing CO₂ from the same type of gas mixture (i.e. 12% vol. CO₂) [34]. A 3-bed 9-step cycle and a 3-bed 12-step cycle were defined and simulated, a zeolite 13X again used as adsorbent. CO₂ purities over 95%, with CO₂ recoveries greater than 70%, were achieved provided a vacuum pressure of 0.03 bar. The performance dropped quickly when the vacuum level was raised to 0.1 bar. A novel VPSA cycle utilizing activated carbon as adsorbent was proposed by Delgado et al. [35]. The process consisted of a 3-bed 12-step cycle. It introduced a peculiar equalization step, termed over-equalization step, where the gas stream transferred from one column to the other undergoes a compression process. According to the simulated results, a large fraction of CO₂ (> 90%) could be recovered at high purity (> 93%) from a mixture with 13% CO₂, setting the regeneration pressure

between 0.01 and 0.02 bar. The specific energy consumption (defined as the energy supplied to the PSA process per kilo of CO₂ sequestrated) was also competitive (< 430 kJ/kg_{CO2}, considering 0.80 the compression efficiency) in comparison to values reported by other works. Liu et al. simulated different VPSA cycles, designed with up to four columns working in parallel, using zeolite 5A for CO₂ capture [36]. The gas mixture adopted was meant to resemble the dry flue gas of a coal-fired power station. They ascertained the necessity of a second VPSA stage in order to match the specifications for the CO₂ product stream (i.e. 90% CO₂ recovery and 95% CO₂ purity). The vacuum level was set to 0.1 bar and 0.15 bar respectively in the first and second stage. The overall performance of the process was 96.1% CO₂ purity and 92.0% CO₂ recovery with a specific energy consumption of 645.7 kJ/kg_{CO2} (ideal process, not considering a compression efficiency). A two-stage VPSA process was also studied by Shen et al. [37]. In this work activated carbon beads were adopted as adsorbent. A CO₂ purity of 95.3% was achieved with a related CO₂ recovery of 74.4%. The specific energy consumption was measured to be 723.6 kJ/kg_{CO2} (ideal process). Haghpanah et al. developed a robust and efficient adsorption process model [38], utilized to perform a systematic analysis of several VPSA cycles with a zeolite 13X as adsorbent to capture CO₂ from dry flue gas (15% vol. CO₂ in N₂) [39]. The pressure swing varied in the range between 1 bar and 0.03 bar. The optimization of the cycles showed that a 4-step VPSA cycle with light product pressurization was able to match 90% CO₂ purity and recovery constraints with a minimum energy penalty of 471.6 kJ/kg_{CO2} (considering 0.72 the compression efficiency). When the CO₂ purity required was set to 95% and 97%, the specific energy consumption increased, respectively to 554.4 kJ/kg_{CO2} and 669.6 kJ/kg_{CO2}. At a later stage the same operating framework was tested in a pilot plant [40]. The two sets of results showed good agreement for what concerns CO₂ purity and recovery, while the power consumption estimated from the process simulations was significantly lower than the experimental output. All the studies mentioned deal with post-combustion applications, where CO₂ is normally diluted in N₂ with low partial pressure. Pre-combustion applications set a different framework. CO₂ has to be removed from a shifted syngas, where the main components are H₂ and CO₂ but significant traces of CO and N₂ may be present. The high pressure, at which the upstream processes are commonly operated, is beneficial for the separation unit and permits the avoidance of vacuum pressure levels. Casas et al. analysed a PSA process for CO₂ separation from the syngas of an IGCC power plant using an activated carbon as adsorbent [41]. A simplified 60%/40% vol. H₂/CO₂ feed mixture was considered. The PSA design involved different pressure equalization steps leading to a significant number of columns working in parallel and to a complex scheduling of the cycle. Several process configurations and operating conditions were assessed and multi-objective optimizations carried out. The targets 90% CO₂ recovery and 95% CO₂ purity appeared within reach by utilizing a single PSA stage. The same multi-objective optimization procedure was utilized to evaluate the performance of PSA with two MOFs under the

same process framework [28]. The simulations showed promising outputs. The separation efficiency was on a similar level compared to the reference activated carbon, with the performance of the different materials ranking differently depending on the operating conditions selected. The two MOFs displayed a significant advantage in terms of adsorbent productivity, potentially leading to reduced process footprint. García et al. experimentally evaluated the performance of a commercial activated carbon adsorbent in a pressure-temperature swing adsorption (PTSA) process operated at simulated shifted-syngas conditions (i.e. 20/70/10% vol. CO₂/H₂/N₂ gas mixture) and under different regeneration conditions [42]. The experimental apparatus consisted of a bench-scale fixed-bed reactor. A maximum CO₂ purity of 91.6% could be achieved, at conditions which did not correspond to the optimum values of other performance indicators such as CO₂ recovery and adsorbent productivity.

Summing up, in post-combustion applications a 2-stage PSA system is likely necessary to meet the requested separation performance. Some studies seem to show that a single stage process may become able to achieve similar performance but would require high vacuum conditions, which are not simple to implement on large systems [43]. Conversely, a single stage PSA process can be able to reach the separation objectives in pre-combustion applications. This is due to the favourable operating conditions, especially in terms of high pressures. A drawback is the increased complexity of the PSA designs adopted, involving many columns working in parallel and a complex scheduling.

2.3.4 *PSA for H₂ purification*

Since PSA for producing ultrapure H₂ is considered in the thesis, the specific literature review is presented. PSA for H₂ purification is an established technology which has been used since the early 1980s. A comprehensive overview on the use of adsorption in such field was published by Ritter and Ebner [44]. Given that typical gas streams to be processed, either from coal gasification or from natural gas reforming, are composed by traces of several gases, such as H₂, CO₂, CH₄, CO and N₂, the common knowledge suggests to utilize a layered bed. The typical arrangement consists of a first activated carbon layer near the feed-end adsorbing mainly CO₂ and CH₄, with a following zeolite layer removing the remaining components, hence CO and N₂. The definition of the length of each layer is not straightforward. Both Park et al. [45] and Yang and Lee [46] studied the adsorber dynamics for multicomponent adsorption in layered beds, both experimentally and through numerical simulations. Their studies are helpful in the definition of layered beds optimal designs. The effects of feed composition on the adsorption dynamics were studied by Ahn et al. [47]. Optimal designs were determined from the experimental and simulated results in a layered bed PSA with activated carbon

and zeolite 5A. While the mentioned papers focused on the adsorption materials and on the adsorption dynamics, also the design of proper PSA cycles plays an important role in the H₂ purification process. Accordingly, many PSA designs have been evaluated in the literature. Sircar and Golden reviewed several key commercial H₂-PSA processes used for production of high purity H₂ from steam methane reforming off-gas and refinery off-gas [48]. Patented processes demonstrated to be able to produce a 99.999% pure H₂ with a H₂ recovery up to 86.0%. Ribeiro et al. analysed the performance of a 4-bed 8-step PSA process with layered activated carbon/zeolite bed for the purification of hydrogen from a five components mixture (H₂/CO₂/CH₄/CO/N₂; 73/17/4/3/4% vol.) [49]. The feed gas composition is representative of a natural gas reforming plant. The process simulation predicted a H₂ recovery and purity, respectively, of 52.1% and 99.996%. The influence of feed flow rate, purge-to-feed ratio and lengths of both adsorbent layers on the system performance was assessed. In another paper, Ribeiro et al. studied the purification of H₂ from the same gas mixture but saturated in water vapour [50]. A tailor-made activated carbon was considered as only adsorbent [51]. Water vapour did not affect significantly the breakthrough behavior of the other species. The multicolumn simulation predicted a H₂ recovery, purity, and productivity, respectively, of 62.7%, 99.999%, and 55.2 mol_{H2}/kg_{ads}/day. Lopes et al. adopted the same activated carbon and performed multicomponent breakthrough experiments [52]. A 10-step one-column VPSA experiment was performed obtaining a 99.981% H₂ purity stream with a H₂ recovery of 81.6% and an adsorbent productivity of 101 mol_{H2}/kg_{ads}/day. It was also verified that high-purity H₂ (> 99.99%) can be obtained with recoveries higher than 75% and unit productivities of 160 mol_{H2}/kg_{ads}/day. Ahn et al. investigated a PSA process with layered bed for hydrogen purification from a coal gas with relatively low H₂ concentrations (H₂/CO₂/CH₄/CO/N₂; 38/50/1/1/10% vol.) [53]. The evaluated 4-bed PSA process could produce H₂ with a purity of 96–99.5% and a recovery of 71–85%. Luberti et al. analysed different PSA configurations with the objective of maximizing the H₂ recovery and, accordingly, decreasing the power consumption for the H₂-PSA tail gas recompression in an IGCC plant coproducing H₂ and power [54]. A maximum H₂ recovery of around 93% was obtained with a Polybed H₂-PSA system (12-bed 13-step) using a zeolite 5A. Other options suggested in the literature in order to increase H₂ recovery, rely on an additional PSA unit or the integration with a selective surface membrane [48].

The main objective of the reported PSA designs is to obtain a highly concentrated H₂ gas stream. Few studies dealt with a set-up able to return multiple product streams. An example is a process called *Gemini* for contemporary production of high-purity H₂ and CO₂ [55]. The outputs are a primary H₂ product at a purity of 99.999+% with a H₂ recovery of 86-87% and a secondary CO₂ product at a purity of 99.4% with a CO₂ recovery of 90+%. It involves the utilization of two PSA trains consisting, respectively, of 6 and 3 columns, and the utilization of rotating machinery (i.e., vacuum pumps and CO₂ recycle compressors), which makes the process energy intensive. Krishnamurthy et

al. patented a two-train PSA system for producing ultrapure H₂ (99.999%+ vol.) and food grade liquid CO₂ [56]. The shifted syngas resulting from a hydrocarbon steam reforming process is routed to a first PSA unit for H₂ purification. The resulting effluent gas is processed by a second PSA unit, which main product is a CO₂-rich gas stream to be liquefied. The configuration encompasses a number of recycle streams and recompression processes. Chouce suggested and patented a PSA process able to produce a pure H₂ gas stream, a H₂-rich first tail-gas stream and a CO₂-rich second tail-gas stream [57]. Three different set-ups are described, which are capable of fulfilling the task. In particular, one configuration relies on a single PSA train. In all the options proposed the tail-gas streams are withdrawn during the regeneration steps and, accordingly, are made available at a low pressure level.

Summing up, PSA for H₂ purification is a well-established technology able to return high-purity H₂ product stream. Several bed designs and process configurations have been studied in order to optimise the process. High H₂ recovery can be obtained along with high purity, albeit it involves very complex PSA arrangements.

2.4 The role of coal in the energy sector

Coal is the most abundant and widely distributed energy source. Proven global coal reserves at the end of 2013 were estimated to be 968 Gt, of which around 688 Gt were hard coal and 280 Gt lignite² [58]. Coal is currently a key component of the global fuel mix for power generation. Coal-fired power plants provided in 2013 over 41% of global electricity supply [11]. Its low cost and wide availability makes coal very attractive in major developing economies for meeting their pressing energy needs. Therefore, coal is predicted to play a primary role in the world energy system under any foreseeable scenario [59]. A wide exploitation of coal inherently implies environmental concerns. Coal has the highest CO₂ emission index (defined as the mass of CO₂ generated per lower heating value of the fuel) among the fossil fuels energy sources. As a result, coal is responsible for the largest share of energy-related CO₂ emissions. This share has increased since 2000 from 38% to 44% in 2014 [11]. A global effort towards a carbon constrained world can lead to future scenarios where coal utilization is limited for environmental reasons. However, an energy mix without coal is not realistic in the short term and thus the role of coal cannot be disregarded in the world future outlook. Given its strong carbon footprint, coal exploitation has to be coupled with a strategy for limiting its negative environmental impact. An increase of the efficiency of the coal-fired power plant fleet is certainly required, but alone it would not be sufficient. The

² Coals have been distinguished between hard coal and lignite on the basis of their energy content (i.e. lower heating value LHV). Hard coal (LHV > 16500 kJ/kg) includes sub-bituminous coal, bituminous coal and anthracite. Lignite (LHV < 16500 kJ/kg) includes lower rank coals.

deployment of CCS is believed to be critical in order to reduce CO₂ emissions while allowing coal to meet the world's energy needs.

2.4.1 *Coal-fired power plants*

A number of methods can be used in large-scale plants in order to convert coal to power. The first distinction involves the fact that coal can be either combusted or gasified. Gasification of coal produces a syngas that can be subsequently fed to a gas turbine. A coal-fired power plant of such kind is called integrated gasification combined cycle (IGCC). Direct coal combustion can be carried out at atmospheric pressure or pressurized. The first instance includes pulverized coal combustion (PCC) plants and circulating fluidized bed combustion (CFBC) plants. The second instance includes pressurized fluidized bed combustion (PFBC) plants. The following sections provide a description of the two types of coal-fired power plant considered in this thesis, namely an advanced supercritical pulverized (ASC) coal plant, which is a subgroup of the PCC plants, and an IGCC plant.

2.4.2 *Advanced supercritical pulverized coal (ASC) plant*

Pulverized coal combustion is the most common process for coal-based power generation. The technology is well-developed and there are thousands of units around the world, accounting for well over 90% of the coal-fired capacity. When the system is designed for operation with supercritical to ultra-supercritical steam parameters, it may be termed advanced supercritical pulverized coal (ASC) plant. Last generation ASC can operate with steam pressures up to 32 MPa and temperatures up to 600/610°C. The shift from subcritical to supercritical operation entails a significant enhancement of the power generation efficiency.

The main sections of an ASC plant are:

- Pulverized coal boiler
- Steam cycle
- Gas cleaning

A typical block flow diagram of an ASC plant is shown in *Figure 8*.

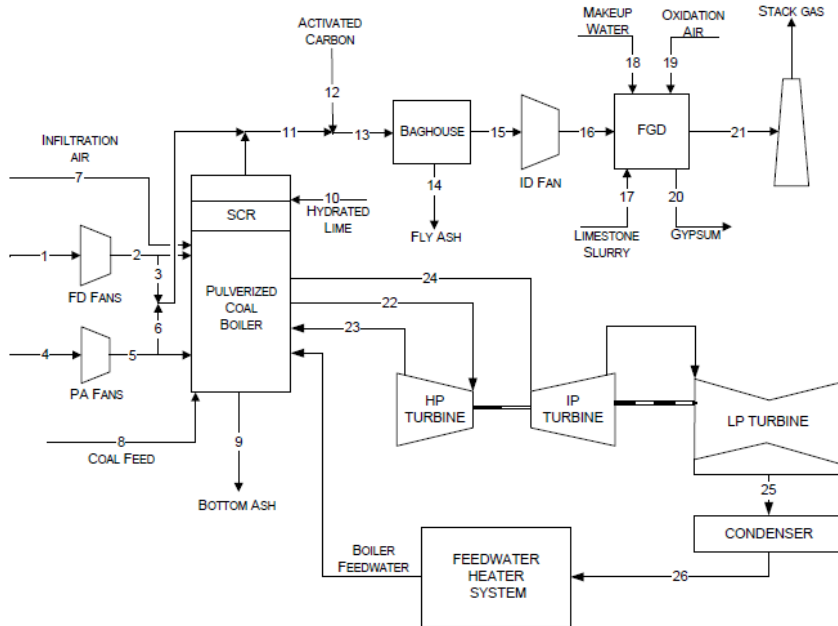


Figure 8. Block flow diagram of an ASC pulverised coal plant. Figure reproduced from [60].

Pulverized coal boiler - The pulverized coal is injected through burners into the furnace with combustion air. The bulk of the combustion air is then mixed into the flame to completely burn the coal char. The walls of the combustion chamber are made up by steel tubes, so-called water wall, to which much of the heat released by combustion is transferred by radiation. Inside these tubes, pressurized water flows at a saturated state and steam is generated. The flue gases then pass through additional heat transfer sections (e.g. superheater, reheater and economizer). At the exit of the boiler, the flue gas is cooled in a heat exchanger with incoming combustion air. The most common arrangement is to utilize as air preheater a Ljungström regenerative rotating wheel.

Steam cycle - The supercritical steam generated into the boiler is utilized in a steam cycle (also known as Rankine cycle) where power is produced by a steam turbine. Steam cycles based on pulverized coal boilers are the preferred technology worldwide for power generation from coal, ensuring high availability and the lowest cost of electricity. The main components of a steam cycle are:

- Heat supply: energy from the combustion of coal or sensible heat from the flue gas has to be transferred to generate pressurized steam. This process takes place in the boiler.
- Steam expansion in the turbine: the pressurized steam is routed to a turbine, where its energy is partly converted to work.

- Steam condensation: the steam condensation process takes place in a condenser where the heat of condensation is rejected from the cycle, using a cooling system.
- Cooling system: provides the cooling duty for steam condensation. Whenever abundant cooling water is available, the optimal system is a once-through open loop water system. Another option is to use a water cooled condenser integrated with a cooling tower for heat rejection to the air.
- Feedwater preheating: the liquid water from the condenser is heated, deaerated and pressurised before entering the boiler. The heating duty is provided by steam extracted from the turbine.

Gas cleaning – The flue gas coming from the boiler must be cleaned to meet the required emission standards. The pollutants of primary interest and currently regulated include particulate matter (PM), sulfur oxides (SO_x) and nitrogen oxides (NO_x).

Several particulate control technologies are available for coal-fired power plants, including electrostatic precipitators (ESPs), fabric filters (baghouses), wet particulate scrubbers, mechanical collectors (cyclones) and hot-gas particulate filtration. ESPs and fabric filters are currently the technologies of choice as they can meet current legislation PM levels. When operating properly, ESPs and fabric filters can achieve overall collection efficiencies of 99.9% of primary particulates (over 99% control of PM₁₀ and 95 % control of PM_{2.5}).

Methods to control SO_x emissions include switching to a lower sulfur fuel, cleaning the coal to remove the sulfur-bearing components, such as pyrite, or installing flue gas desulfurization (FGD) systems. FGD (especially wet FGD) is a proven technology and is commercially well-established. Wet scrubbing can achieve 95% SO_x removal without additives and 99+% SO_x removal with additives [59].

The measures to minimize NO_x emissions can be divided into two groups, namely primary measures and flue gas treatment methods. The primary measures aim to reduce NO_x formation at the source, thus during the combustion process. The mechanisms involved reduce peak flame temperature and residence time at peak flame temperature. The primary techniques available include low-NO_x burners, fuel or furnace air staging, flue gas recirculation and water/steam injection. The flue gas treatment methods involve a post-combustion NO_x emission reduction. The two most commonly used technologies are selective catalytic reduction (SCR) and selective non-catalytic reduction (SNCR). SCR can achieve 90% NO_x removal efficiency over inlet concentration, while SNCR reaches a removal efficiency of 30-50%.

The cleaned flue gas has a typical CO₂ volumetric fraction of ≈ 14%, whereas the other main components are N₂ (≈ 74%), O₂ (≈ 3%) and H₂O (≈ 8%). Ar and residual impurities make up for the remaining percentage. In plants without CO₂ capture unit, the flue gas is vented to the atmosphere. Otherwise, it is further processed to separate CO₂ by the other gas components.

Pulverised coal combustion plants show a wide range of efficiencies due to the several design parameters that have an impact on the performance, among those: steam pressure and temperature, number of steam reheats, number of feedwater preheaters, condenser pressure, turbine blading design, etc. The most advanced plants in operation reach an efficiency of about 45-47% (LHV). However, the average efficiency for the coal-fired power plant fleet is estimated to be about 35% (LHV) in 2011 [61].

2.4.3 *Integrated gasification combined cycle (IGCC) plant*

Gasification is a process to upgrade a solid feedstock, which is difficult to handle, by removing undesirable impurities and converting it into a gaseous form [62]. The output of the gasification process is a synthesis gas or syngas, whose main components are H₂, CO, CO₂ and steam. Depending on the feedstock, the process and the oxidiser, other gases that may be present are N₂ and sulfuric compounds like H₂S and COS. An integrated gasification combined cycle (IGCC) plant converts this syngas into electricity by means of a combined cycle. The main advantage of gasification lies in the fact that syngas is a cleaner fuel than coal. Fewer sulfur and nitrogen oxides are formed during combustion. If CO₂ capture is taken into account, IGCC plants may be favoured, as the high pressure typical of the gasification process is beneficial for CO₂ separation from the syngas. Further, IGCC plants can take advantage of the utilization of gas turbine technology and combined cycle arrangement, achieving high efficiency. On the other hand, the main challenges facing the IGCC technology in order to compete with conventional pulverized coal plants are capital cost, system complexity, availability and the development of effective gas turbine technology for a syngas feed [63].

There are many coal gasification plants in the world producing fuels, chemicals and/or steam. With regard to power generation, IGCC did not reach the deployment which was initially expected about 15-20 years ago. The following seven are the only commercial IGCC power stations using coal and/or coke as primary feedstock:

- Buggenum IGCC power station – the Netherlands (Startup in 1994, shutdown in 2013)
- Puertollano IGCC power station – Spain (Startup in 1997)
- Wabash River IGCC Power station – USA (Startup in 1995)
- Tampa electric Polk power IGCC – USA (Startup in 1995)
- Nakoso IGCC power station – Japan (Experimental demo startup in 2007, commercial operations in 2013)
- Tampa electric Polk power IGCC – USA (Startup in 1995)
- Edwardsport IGCC station – USA (Startup in 2013)
- Kemper County IGCC – USA (Startup in 2016)

The Kemper County IGCC will be the first-of-a-kind commercial-size IGCC plant implementing CO₂ capture, as it will be capturing 65% of the produced CO₂. If demonstrated, the benefits on a CO₂ capture point of view can contribute to revive the interest on IGCC technology.

The main sections of an IGCC plant are:

- Coal gasification
- Air separation
- Syngas treatment and clean up
- Power island

A typical block flow diagram of an IGCC plant is shown in *Figure 9*.

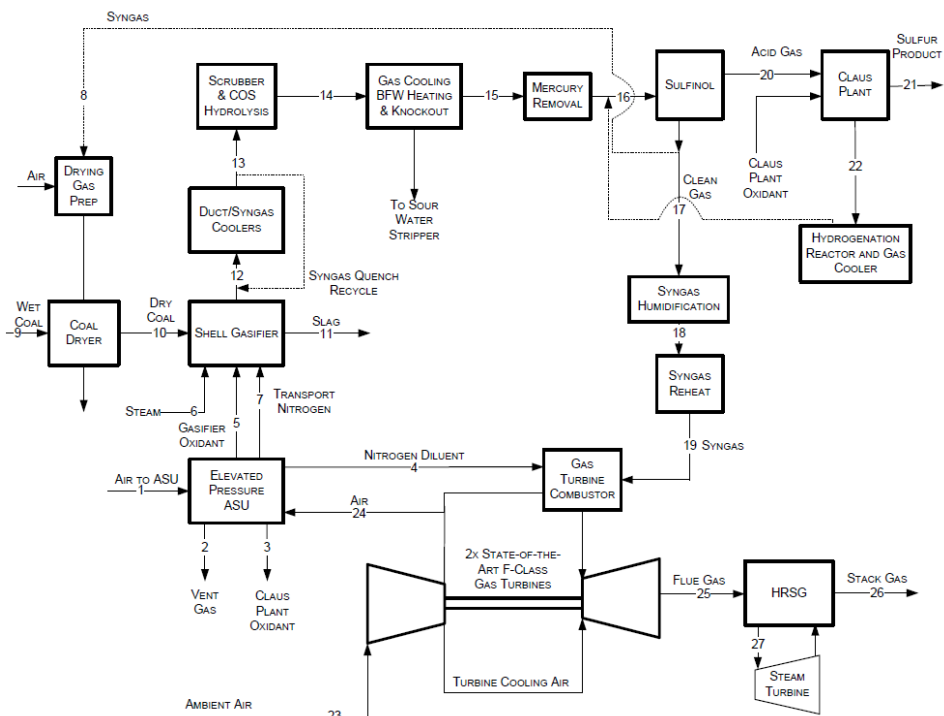
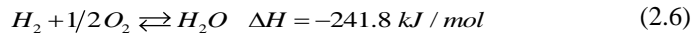
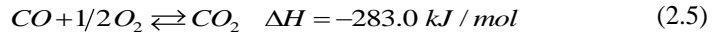
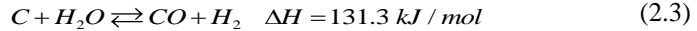
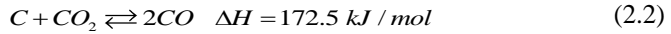
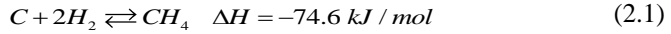


Figure 9. Block flow diagram of an IGCC plant with Shell gasification technology. Figure reproduced from [64].

Coal gasification - Gasification is a non-catalytic reaction converting carbonaceous materials into H₂, CO, CO₂ and steam. The main reactions involved in coal gasification are:



Entrained-flow gasifiers demonstrated to be the most suitable gasification technology for power generation in an IGCC plant. The benefits that made entrained-flow gasifiers to dominate the market can be listed to be:

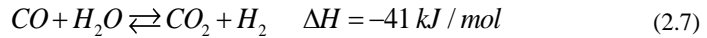
- Ability to handle practically any coal as feed
- Syngas is free of oils and tars
- High carbon conversion
- Low methane production, suitable for synthesis gas products
- High throughput because of high reaction rates at elevated temperature

Entrained-flow gasifiers are operated at high temperatures (1250-1600°C), in the so-called slagging range (the ash is fully liquid with low viscosity), and high pressures (40-70 bar). In most of the commercial entrained flow gasifiers the high slagging temperature is ensured by using oxygen or oxygen-enriched air as oxidation agent, entailing the presence of an air separation unit (ASU) in the plant design. The three commercial gasifier technologies with largest total installed capacity are the GE gasifier (entrained-flow, developed by Texaco), the Shell gasifier (entrained-flow) and the Sasol-Lurgi dry ash gasifier (moving bed, developed by Lurgi). Other gasifiers commercially available are the ConocoPhillips E-Gas gasifier (entrained-flow) and the Siemens gasifier (entrained-flow). For large-scale entrained-flow gasifiers operating at high pressure, two commercial coal feeding systems are available: coal-water slurry feed and dry feed based on lock hoppers. Dry-fed gasifiers tend to be somewhat more fuel flexible and more energy efficient than slurry-fed gasifiers. Despite its relatively low performance, the water slurry feeding system is attractive due to the high pressures it can achieve and, more importantly, because it is more compact and employs simpler equipment, which may lead to more favorable process economics [65]. Among the gasifier designs previously mentioned, both dry-fed systems (e.g. Shell, Siemens) and water-slurry systems (e.g. GE, ConocoPhillips) are adopted.

Air separation - There is a single technology commercially-ready to meet the O₂ throughput necessary for the coal-gasification process. That is distillation in a cryogenic air separation unit (ASU). Air is normally supplied to the ASU compressed to around 5 bar, while oxygen (with a typical composition of 95 % O₂, 3.5 % Ar and 1.5 % N₂ by volume) and nitrogen product streams are available at around 1 bar. However, the process may also operate at elevated pressure such that the air fed to the ASU is at a pressure closer to that of the gas turbine compressor outlet. In this case, the ASU product streams are at around 5 bar which reduces the recompression work [63]. Nitrogen, byproduct of the oxygen production, can be used in various parts of the plant: as fuel preparation gas (if a dry-fed gasifier applies); as fuel dilution gas in the gas turbine; and for periodic cleaning of candle filters. A fraction of the compressed air supplied to the ASU can be taken from the compressor of the gas turbine. The degree of integration of the ASU with the IGCC plant is an important design choice, influencing gas turbine performance and flexibility. With regard to the compressor duty, no significant advantages exist when power and gasification island are integrated: the GT compressor features higher isentropic efficiency whilst the ASU main compressor is intercooled; this results in an overall similar compression work at different integration levels [66]. The present experience with power plants based on coal gasification recommends a maximum of 50% integration, i.e. 50% of the mass flow of air entering the ASU comes from the GT compressor, on grounds of reliability and availability [67].

Syngas treatment and clean up - The temperature of the syngas leaving an entrained flow gasifier can be as high as 1500°C. Such temperature entails the fly ash to be in a liquid form (i.e. slagging condition). In order to protect downstream process equipment from possible fouling, the slag needs to be solidified and made non-sticky. This is achieved by reducing the syngas temperature. The most widespread technologies are water quench and gas recycle quench, while radiant syngas cooling and chemical quench are less common. Water quench uses sensible heat from syngas to evaporate water. It is the technology adopted by the basic GE gasifier. Shell-type gasifier adopts the gas recycle quench, which consists of recirculating the syngas (at about 300°C) back to the gasifier outlet. A final syngas temperature of about 900°C is obtained. Further temperature reduction is obtained through a syngas cooler. Syngas cooler allows cooling down the syngas to the temperature necessary for downstream gas clean up processes, while producing steam. Downstream the syngas cooling, entrained solid particles are removed. The main technologies adopted are candle filters (e.g. Shell process) or water scrubbers (e.g. GE process). Sulfur contained in solid coal is mainly converted to H₂S, and barely to COS, since the gasification is carried out in an oxygen-depleted environment. Accordingly, the derived syngas must be cleaned before use in the gas turbine. An acid gas removal (AGR) process is normally used, where H₂S is removed by means of an absorption cycle. The most common absorption processes adopted rely either on physical solvents (i.e. Selexol or Rectisol) or on chemical solvents (i.e.

MDEA). The total sulfur ($H_2S + COS$) content can be reduced to levels below 20 ppmv in the cleaned syngas. These solvents can be also effective for other acid components, for instance CO_2 . When CO_2 capture has to be implemented, it is common practice to adopt a two-stage process, selectively retaining H_2S and CO_2 , while releasing them separately upon regeneration. The CO_2 capture process demands for an upstream syngas treatment, namely a shift process. The water-gas shift (WGS) process, carried out in a catalytic reactor, increases the H_2/CO ratio of the syngas, according to the following reaction:



As a result, the shifted syngas has a higher content of CO_2 which is beneficial for its downstream removal. Two main system configurations may be considered when introducing WGS, depending whether the shift process is taking place before (sour WGS) or after (sweet WGS) the syngas desulfurization. Sweet WGS allows a multi-reactor process at higher temperatures, given the larger operating window of the catalyst, resulting in higher CO conversion. However, for sulfur containing fuel, such as coal, sour shift is the preferred option since avoids an additional thermal swing (sulfur removal is normally a cold process). A typical shifted syngas composition involves large volumetric fractions of H_2 ($\approx 54\%$) and CO_2 ($\approx 38\%$), significant contents of N_2 ($\approx 7\%$) and CO ($\approx 1\%$), and traces of other components like (CH_4 , Ar, H_2O , etc.).

Power island - The power island includes a gas turbine (GT), a heat recovery steam generator (HRSG) and a steam turbine (ST). Gas turbines run normally on natural gas. The utilization of syngas introduces some issues on their operability, which need to be addressed. This situation is amplified if H_2 -rich syngas is used, resulting from a CO_2 capture process. Syngas has a lower volumetric LHV compared to natural gas, due to its H_2 content. In order to maintain the same turbine inlet temperature (TIT), which is desirable to retain high efficiency, a higher fuel volumetric flow rate is needed. Further, the fuel needs a robust dilution for keeping the NO_x formation under control. Given that the gas turbine has a maximum swallowing capacity, the high H_2 content of the syngas feeding leads to higher pressure ratio and decreased air demand. As a result, compressor stall issues may arise. In order to deal with it, the integration with ASU (some compressed air sent to the ASU) can be a convenient procedure. Other possible countermeasures consist in modifications either of the turbine (i.e. increasing the nozzle area to allow a higher flow rate) or of the compressor (i.e. adding a compressor stage). The increased mass flow rate through the turbine results in an increased power output. The mechanical ability of the gas turbine rotor to handle increased power output may limit the maximum GT power output. The high content of H_2 in the syngas heavily influences the combustion. High flame speed is a concern, which does not allow using air pre-mixing technologies. Accordingly, dry low- NO_x (DLN) combustors cannot be

adopted and traditional diffusion combustors apply. The NO_x emissions need to be controlled with fuel dilution or other measures. Common practice is to use nitrogen from the ASU, water (syngas saturation) or a combination of both. Another consequence of using a H_2 -rich mixture as fuel, is the significant water fraction in the exhaust gas. The presence of water enhances heat transfer and therefore increases the metal temperatures, shortening the lifetime of the turbine materials. In practice, this will probably mean that the TIT must be reduced to avoid shorter lifetime of the blade materials and coatings. Any reduction in TIT reduces the efficiency of the combined cycle. It is worth mentioning that, while there is a good experience with gas turbines running on syngas (mixture of CO and H_2), there are no existing turbines running on a H_2 -rich fuel. E-class gas turbines have been proven on H_2 -rich fuel streams and would probably be offered on commercial basis from various vendors if asked. The problem with E-class gas turbines is that they will result in a plant concept with ca. 3 %-points lower electrical efficiency compared to a state-of-the-art F-class machine.

The exhaust gas from the gas turbine has a temperature of ca. 600°C . Such energy potential is normally exploited to produce steam in a HRSG. Similarly to a conventional combined cycle, a three pressure level heat recovery steam cycle (with or without reheating) is commonly used to recover heat from gas turbine flue gas and syngas cooling. Depending on the gasification process, the intermediate pressure level can be coupled with the gasifier reactor pressure such that the steam demand and the reactor wall cooling are optimized. The steam at different pressure levels is routed to proper sections of a steam turbine to generate additional electric power.

New IGCC plants are expected to perform with net plant efficiency in the range of 39-48% (LHV) [68]. A large variability in the possible efficiency values has to be noted. The reason for this lies in the complexity of those systems. A number of different designs and operating conditions can be considered which influences the performance of the plant. Among those, one can mention:

- Coal type
- Gasification technology
- Degree of ASU integration
- Technology level

Chapter 3 Methodology

The methodologies used in the thesis work will be covered in this chapter. In the first instance, the composite model developed for the analyses is defined, together with the simulation tools adopted. The following sections provide an overview of the process design and modeling concepts for both the power plants (i.e. ASC and IGCC plant) and for the PSA processes. The main modeling approaches, operating parameters and fundamental assumptions are outlined. An in-depth analysis of the theory at the basis of the PSA model is also provided. Furthermore, a performance evaluation system is defined, and specifications and constraints of the systems are discussed.

The same composite model may have been used in different analysis frameworks. In such cases, some modifications have been introduced, resulting in changed operating conditions or even process configuration. On the other hand, the overview in this chapter is general, aiming to provide the common modeling basis. For this reasons some information has not been reported (e.g. the characteristics of all the system streams), especially when those data are subject to change from case to case. However, all the necessary inputs to define the common modeling framework are present, whereas a more thorough overview of the specific system can be found in the relative *Paper*.

3.1 Composite model for system analysis

The main goal of the thesis is to assess PSA as CO₂ capture technology in coal-fired power plants. Process simulations are the tools selected for carrying out this sort of analysis. Therefore, the starting point of the work was to develop a composite model, able to simulate the overall plant.

Two plant configurations were considered, respectively to account for a post- and a pre-combustion CO₂ capture scenario. The selected thermal power plants aimed to represent the most common systems for coal-based power generation. The post-combustion case is an advanced supercritical pulverized coal (ASC) plant. The pre-combustion case is an integrated gasification combined cycle (IGCC) plant. A modeling framework was established for both cases. It includes the definition of a comprehensive set of design parameters and guidelines that serve as a basis for cycle definition, cycle analysis and comparison of different technologies. The objective is to make such comparisons

consistent and reliable, by using the same set of fundamental assumptions. For this reason, all the cases were based on the European Benchmarking Task Force (EBTF) recommendations [67]. For what concerns PSA processes, an extensive literature study allowed defining the most proper modeling approaches and process configurations to be applied to the different systems investigated.

Once the systems and their characteristics were specified, appropriate modeling tools were selected. For the steady-state model of the power plants the Thermoflow package was used (i.e. *STEAM PRO*, *GT PRO* and *THERMOFLEX*) [69]. The power plants were initially modeled through *STEAM PRO* and *GT PRO*, the basic programs for designing a conventional steam plant (e.g. ASC plant) and a combined cycle plant (e.g. IGCC plant), respectively. Whenever EBTF information was not sufficient or could not be superimposed to the model, the design was completed using reasonable assumptions or retaining program default values. Process simulations of reference power plants without CO₂ capture or implementing standard absorption processes for CO₂ capture, were obtained, based on the models built in *STEAM PRO* and *GT PRO*. The performances achieved by these cases were compared to those reported by EBTF. The differences were evaluated to be within an acceptable margin of error and the basis models were considered reliable. The integration of a PSA unit was not possible within those simulation platforms. It was necessary to use a program enabling a higher degree of customisation of the model. Thus, the models developed were exported into *THERMOFLEX*. *THERMOFLEX* allowed a plant design reconfiguration in order to accommodate the PSA unit. The inherently dynamic PSA processes needed to be modeled through another program, namely *gPROMS* [70]. *gPROMS* is a modeling platform to build and execute dynamic process models. A proper set of equations describing the dynamics of the adsorption bed was implemented and allowed simulating the PSA process. The resulting outputs of the model were checked against available literature data and were considered reliable. In some systems, a flash separation process was modeled in *Aspen HYSYS* [71], as a network of multistream heat-exchangers and separators. The models developed - one for the power plant, one for the PSA unit and, possibly, one for the flash separation unit - were connected through a common *Microsoft Excel* interface in order to exchange information. The process units upstream the CO₂ capture section provide the input data for the PSA model. That information is conveyed to the *gPROMS* model and a PSA process simulation is run. The obtained output data are sent back to the *THERMOFLEX* model of the power plant. When a flash separation is implemented, the same procedure applies. The overall plant simulation can then be completed and allows for full-plant analyses.

3.2 Process design and modeling of ASC plant

The post-combustion case studied involved an ASC plant integrating PSA for CO₂ capture. The plant produces about 827 MW gross electric output. When the auxiliary power is taken into account, the net power output is about 579 MW, giving a net electric efficiency of 34.8%. *Figure 10* shows a general flowsheet of the plant. The characteristics of the main plant streams can be found in *Paper 1*. The overall plant can be divided in 5 sections:

- Pulverised coal boiler
- Steam cycle
- Gas cleaning
- CO₂ separation
- CO₂ compression

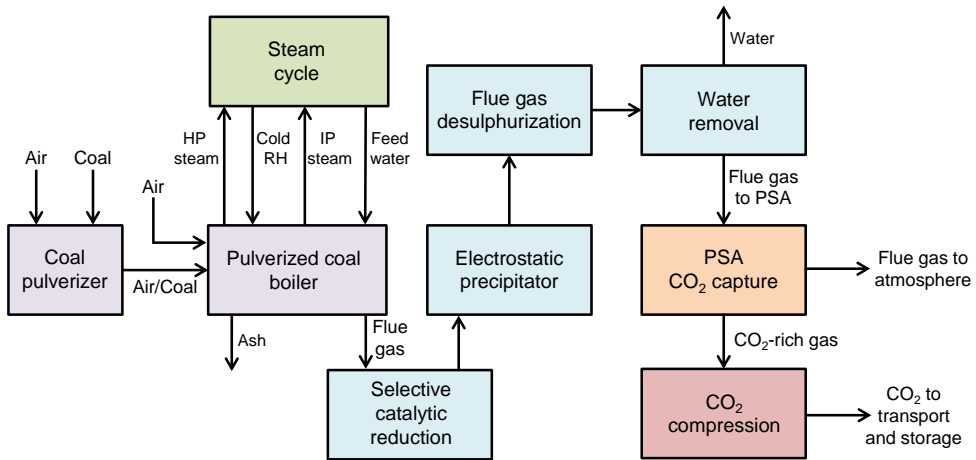


Figure 10. Flowsheet of an ASC plant integrating a PSA unit for CO₂ capture.

3.2.1 Pulverized coal boiler

A bituminous Douglas premium coal (66.2 kg/s) is fed to a pulverized coal boiler. The characteristics of the coal are given in *Table 1*.

Table 1. Douglas premium coal characteristics [67].

Douglas premium coal			
Proximate analysis (weight %)		Ultimate analysis (weight %)	
Moisture	8,0 %	Moisture	8,0 %
Ash	14,2 %	Ash	14,2 %
Volatile matter	22,9 %	Carbon	66,5 %
Fixed carbon	55,0 %	Hydrogen	3,8 %
Total	100,0 %	Nitrogen	1,6 %
		Chlorine	0,009 %
		Sulfur	0,5 %
		Oxygen	5,5 %
		Total	100,0 %
LHV (kJ/kg)	25170		
HHV (kJ/kg)	26190		
CO ₂ emission (g/kWh _{LHV})	349		

Supercritical steam (600°C) at one pressure level (300 bar) is generated in the boiler. A single reheat is present (620°C and 89 bar) and water coming from water preheaters is introduced to the boiler at 316°C. *Figure 11* shows the pulverized coal boiler section in detail. The THERMOFLEX boiler model consists of a water-wall evaporator, an economizer, a superheater and a single reheater. Additionally, a pulverizer model is connected, which calculates fuel processing details and defines the air/coal mixture sent to the furnace. The pulverizer is equipped with 6 vertical air-swept mills and mill fans. Drying air provides the right amount of energy to dry out certain percentage of the total moisture in the fuel and heat up the rest of the fuel to the desired exit temperature. Three inlet air streams are considered for the boiler: primary air (59 kg/s), secondary air (563 kg/s) and tempering air (57 kg/s). The primary air and tempering air flow rates are determined by the pulverizer model and the secondary air will supply the remaining air flow needed for combustion. The combustion calculations assume complete oxidation of coal with the exception of any unburned carbon explicitly cited to be part of the bottom ash and fly ash leaving the boiler. Boiler efficiency results to be $\approx 94\%$. The emission rate of NO_x is computed from user-defined production levels (188 mg/Nm³ at 6% reference O₂). The flue gas (736 kg/s) exits the boiler at 339°C. A Ljungström regenerative heat exchanger is used to preheat the combustion air to the boiler (285°C) and the air used for coal drying and pulverized fuel transport (299°C), while the flue gas is cooled to 117°C.

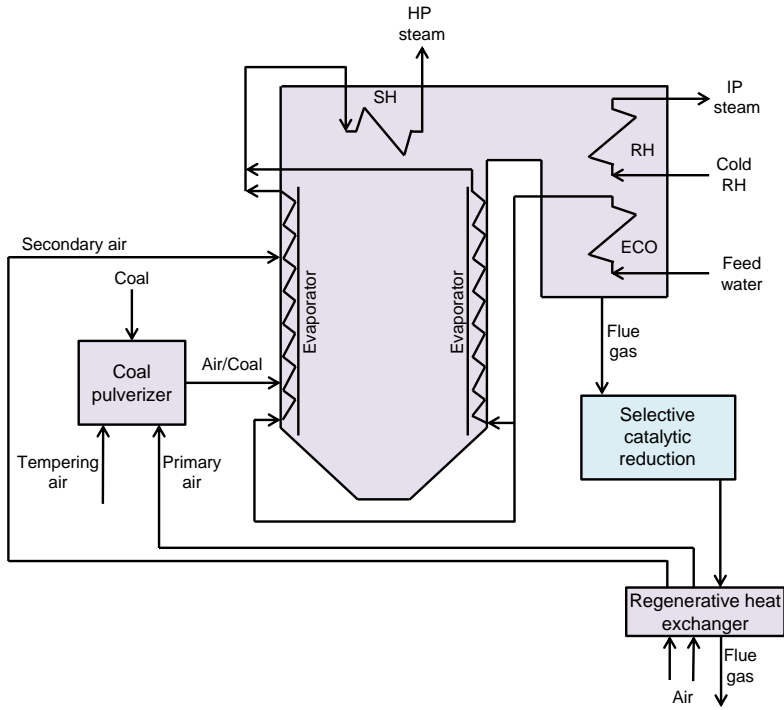


Figure 11. Detailed flowsheet of the pulverized coal boiler section of the ASC plant.

3.2.2 Steam cycle

The supercritical steam (600°C and 300 bar) produced in the pulverized coal boiler is processed in a steam cycle for power generation. Figure 12 shows the steam cycle section in detail. The steam turbine plant consists of high pressure (HP) turbine, intermediate pressure (IP) turbine and low pressure (LP) turbine with extraction points for regenerative heating of feed water and condensate. A single reheat is implemented. *THERMOFLEX* allows imposing a value for the dry step efficiency of each turbine group. This is the efficiency in the expansion path with dry steam and will be corrected in the case of wet steam (i.e. an efficiency decrement is applied to all steps with steam quality below the Wilson line). The efficiency of each step within a particular group is assumed to be the same in the absence of steam moisture. The overall isentropic efficiency is finally calculated taking into account exhaust loss and throttling effect. This efficiency results to be about 92%, 94% and 83%, respectively for the HP, IP and LP group. The expanded steam (0.048 bar) leaving the LP turbines is routed to the condenser. A water-cooled condenser is employed and the heat is rejected to the

environment through a natural draught wet cooling tower. Saturated condensate is assumed at the condenser outlet. A system of nine preheaters increases the feed water temperature to 316°C. Steam is extracted from the turbine at proper locations to provide the necessary heating duty for the preheaters. The boiler feed pumps selected are motor driven. The gross power output is about 827 MW.

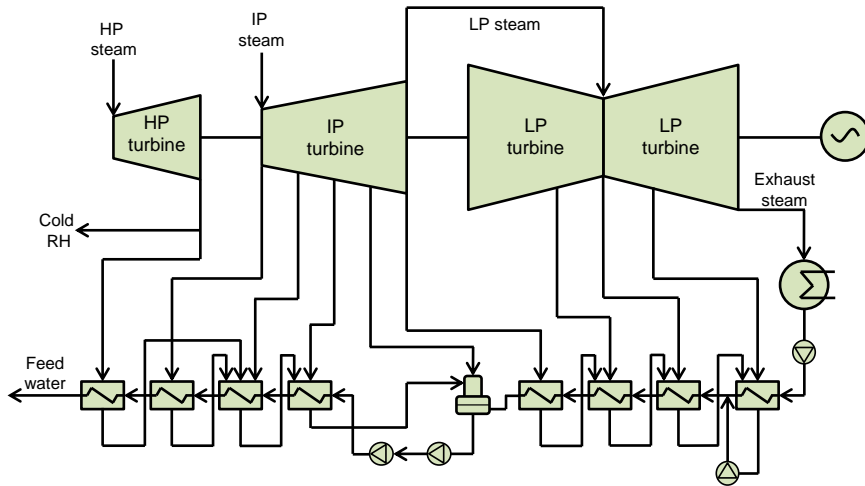


Figure 12. Detailed flowsheet of the steam cycle section of the ASC plant.

3.2.3 Gas cleaning

This section includes the gas cleaning processes and other gas treatment processes implemented before sending the flue gas to the CO₂ separation unit. Figure 13 shows the gas cleaning section in detail. The first cleaning process undergone by the flue gas is a selective catalytic reduction (SCR) to meet the NO_x emission limits (i.e. 120 mg/Nm³). SCR is located between the boiler's exit and the air heater inlet. Flue gas (736 kg/s) enters the SCR unit with a temperature of 339°C, compatible with the catalytic reaction. The NO_x reduction is obtained through ammonia injection with an effectiveness of 80%. Flue gas leaving the SCR is particle-laden. An electrostatic precipitator (ESP) device is included in the plant design to reduce the particle content down to the desired limit (i.e. 8 mg/Nm³). ESP is assumed to operate with a 99.5% particulate removal efficiency. The last cleaning process involves the removal of SO_x in a wet flue gas desulfurization (FGD) system. The flue gas (801 kg/s) at 127°C is introduced into an absorption reactor. Limestone is crushed into a fine powder and mixed with water in a slurry preparation tank. The sorbent slurry is then pumped to spray headers inside the absorber reactor in order to carry out the SO_x removal. The treated flue gas leaving the absorber is fulfilling

SO_x limits (i.e. 85 mg/Nm³) and is saturated with moisture. In order to convert absorbed SO_x to sulfate and cause gypsum to precipitate, forced oxidation is obtained by blowing air into the slurry in the reaction tank. A slurry bleed stream is pumped from the reactor to the dewatering system equipment, where byproduct or waste solids are separated from the bleed slurry and made ready for final delivery or disposal. The unit is assumed to reach a 98% SO_x removal efficiency. Before being routed to the PSA unit, the flue gas is going through a water removal unit. Such unit is included because of the detrimental effect of water on the considered adsorption process. An equilibrium separation is modeled. The flue gas stream is cooled down to approximately 20°C and fed to a flash separator where water is extracted as a liquid. This simple process can only lower the water content down to about 2%, given the atmospheric pressure of the flue gas. A much lower water content is advisable, but it would require a different dehydration strategy. This has not been included in the simulation. The partially dehydrated flue gas stream then enters the PSA unit.

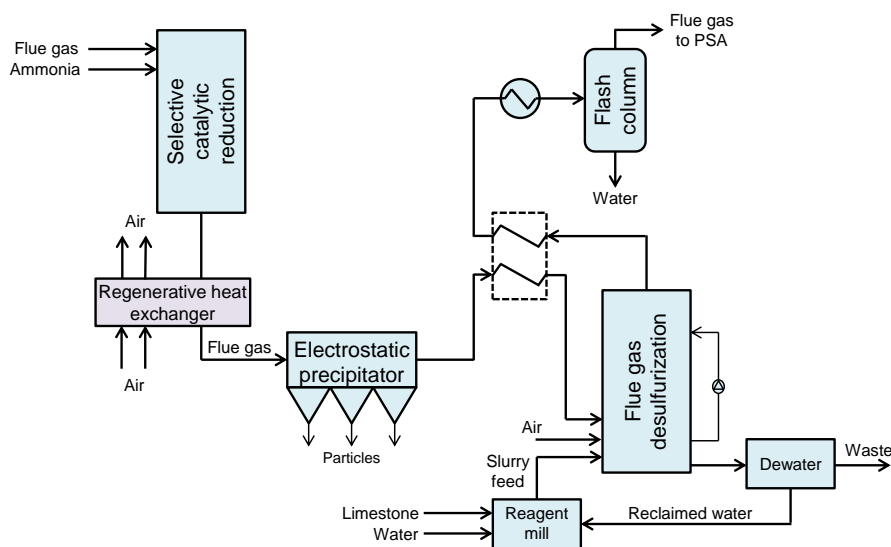


Figure 13. Detailed flowsheet of the gas cleaning section of the ASC plant.

3.2.4 CO₂ separation

The CO₂ is removed from the flue gas by means of a PSA process. Flue gas is introduced into the unit at atmospheric pressure and with a temperature of 20°C. The volumetric composition is the following: 14.3% CO₂, 77.8% N₂, 4.6% O₂, 0.9% Ar, 2.3% H₂O and 0.06% other components. A two-stage PSA process is considered. Each stage

consists of a number of columns working in parallel and synchronized. The multi-column configuration allows the PSA to accommodate a constant feed flow, ensuring continuous operation. The characteristics of the PSA unit are outlined in section 3.4.3. Two gas streams leave the unit: a CO₂-rich gas stream at 1 bar, which is sent to the CO₂ compression unit; a waste gas stream, mainly composed of N₂, which is vented to the atmosphere. The adsorption column regeneration process involves a vacuum pressure (0.1 bar). The relative vacuum pumps energy consumption has been computed considering an adiabatic compression process, corrected with an isentropic efficiency of 70%. The PSA unit is responsible for additional compression energy consumptions, due to the fans used to overcome the pressure drop in the column. In this case, the isentropic efficiency was set to 85%.

3.2.5 CO₂ compression

CO₂-rich gas stream leaving PSA unit needs to be compressed from 1 bar to 110 bar for transport. An intercooled compression arrangement is modeled. *Figure 14* shows the CO₂ compression section in detail. Five compression stages are implemented. *THERMOFLEX* sets an equal pressure ratio for each compression stage. The cooling fluid is water. The isentropic efficiency of each compressor stage was set to 85%. The efficiency of the compressor driver was assumed to be 95%. The compressors performance is simulated according to maps internal to the model. The CO₂-rich gas stream is cooled to 28°C in each intercooler. The specific energy consumption is calculated to be 0.36 MJ/kg_{CO2}.

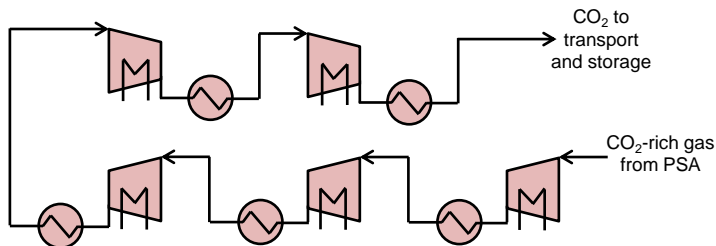


Figure 14. Detailed flowsheet of the CO₂ compression section of the ASC plant.

3.3 Process design and modeling of IGCC plant

The pre-combustion case studied involved an IGCC plant integrating PSA for CO₂ capture. If ultrapure H₂ is an additional power product, PSA technology was used both for CO₂ capture and H₂ purification. The plant produces a gross power output of about

460 MW (decreasing if H₂ is additionally produced). The net power output is about 350 MW, resulting in a net electric efficiency of 36.2%. *Figure 15* shows a general flowsheet of the plant (when electricity is the only plant product, the ultrapure H₂ stream does not apply). The characteristics of the main plant streams can be found in *Paper I*. The overall plant can be divided in 5 sections:

- Air separation
- Gasification and syngas treatment
- CO₂ separation and H₂ production
- CO₂ compression and purification
- Power island

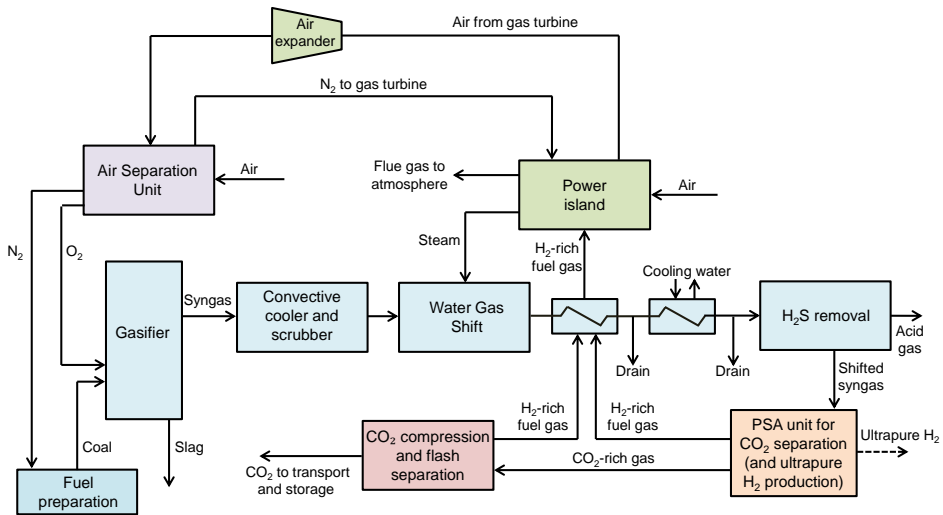


Figure 15. Flowsheet of an IGCC plant integrating a PSA unit for CO₂ capture.

3.3.1 Air separation

Figure 16 shows the air separation section in detail. The main duty of this section is to supply O₂ to the gasifier. A cryogenic air separation unit (ASU) is used for the purpose, which is modeled by *THERMOFLEX*. The distillation column is operated at 10 bar, producing a 95% pure O₂ gas stream, which is made available at 2.6 bar. The O₂ needs to be compressed to the pressure at which the gasification process takes place (i.e. 44.9 bar). Air is compressed (to 10 bar) and cooled (to 20°C) before being delivered to the cryogenic separation unit. Based on the total product demand flow and stream compositions, the ASU model computes the required flow of air. 50% of the compressed air entering the ASU is taken from the compressor of the gas turbine. As a

byproduct pure N_2 is made available at 2.6 bar (100% N_2 streams are considered in the model). A fraction of N_2 ($0.2207 \text{ kg}_{N_2}/\text{kg}_{\text{coal}}$) is sent to the fuel preparation unit where it is used as fuel transport stream. This N_2 gas stream is compressed to 88 bar. N_2 is also supplied to the combustor of the gas turbine for NO_x control. Accordingly, it is compressed to ≈ 24 bar. The dilution N_2 is preheated to 200°C by the air coming from the GT compressor. Preheating the N_2 improves system efficiency by reducing the fuel burnt in the GT to heat the N_2 and by reducing the cooling load handled by ASU coolers. The mentioned compression processes are modeled as multi-stage intercooled processes, with a polytropic efficiency of 90% and a mechanical efficiency of 95%. The overall power consumption consists of the computed power to drive the compressor motors and an additional miscellaneous power consumption term. The air separation section demands about 51.6 MW. The O_2 produced is 31.2 kg/s , which makes the specific consumption 1.74 MJ/kg_{O_2} . This value is higher than a normal ASU, mainly due to the additional N_2 compression power requirement.

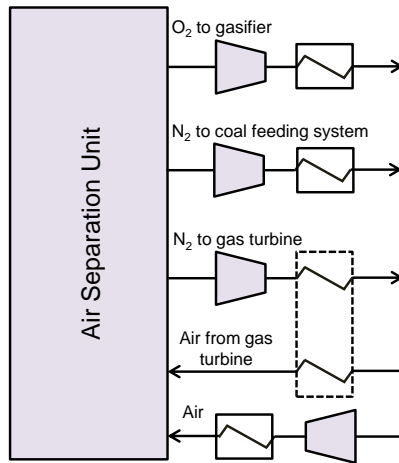


Figure 16. Detailed flowsheet of the air separation section of the IGCC plant.

3.3.2 Gasification and syngas treatment

This section includes the fuel preparation unit, the gasifier and the units for syngas treatment and clean-up. Figure 17 shows the gasification and syngas treatment section in detail. A bituminous Douglas premium coal (38.5 kg/s , see Table 1 for its characteristics) is fed to the gasifier using N_2 as fuel preparation gas. N_2 coming off the ASU conveys fuel to the pulverizing mills and into the gasifier. O_2 is supplied from the ASU as well, at the gasifier pressure. The gasifier is assumed to be a Shell-type entrained-flow oxygen-blow gasifier, operating at 44.9 bar and 1309°C . High-

temperature syngas (160 kg/s at 900°C) leaving the gasifier is cooled down (497°C) in a convective syngas cooler: hot raw syngas flows inside the tubes which are immersed in water. Saturated steam at 145 bar is generated in the gasifier vessel and in the syngas cooler. Syngas is re-circulated from the convective cooler exit back to the gasifier vessel to reduce syngas exit temperature. Particles are removed through a wet scrubber. Incoming syngas (76 kg/s) enters the scrubber where it comes into direct contact with water. The water traps the particles, which are collected in the pool at the bottom of the vessel. Particle-free syngas, which has been moisturized in the process, leaves the scrubber through demisters that collect water droplets to prevent carry-over. Syngas is then routed to the water-gas shift (WGS) section with a temperature of 178°C. The sour shift process converts CO and H₂O to CO₂ and H₂ to a large extent. Steam, extracted from the steam cycle at an intermediate pressure level (52 bar), is added to the syngas in order to enhance and sustain the reaction (with a consequent energy penalty in the steam turbine). A H₂O/CO ratio of 2 was assumed. The process achieves a 96% CO conversion and a 98% COS conversion (COS hydrolysis is directly carried out in the WGS avoiding a dedicated reactor and thermal swing). The heat of reaction is partially recovered by producing high pressure saturated steam (40.5 kg/s at 145 bar). The shifted syngas leaves the WGS unit at a relatively high temperature (235°C) and is cooled down (47°C) to undergo the cold gas cleaning processes operating at low temperature. It is first cooled against a H₂-rich fuel gas going to the gas turbine (which is by this preheated to 200°C). The remaining cooling duty is provided by cooling water. The syngas coolers total pressure drop was set to 10%. During these cooling steps, a large fraction of water present in the shifted syngas condenses and is knocked out of the syngas stream. Water removal down to trace-level is fundamental for the following PSA process, since water competitively adsorbs onto the solid bed when dealing with common adsorbents. Given the high operating pressure, water removal is particularly effective (water content down to ≈ 0.6% vol.) and the final water content entering the PSA unit is rather low (≈ 0.03% vol. after the acid gas removal unit). Acid gas (H₂S) has to be removed from the shifted syngas in order to comply with SO_x emissions limits and to reduce potential for corrosion in the power island equipment. The acid gas removal (AGR) unit involves a single stage absorption process. *THERMOFLEX* computes the acid gas removal rate based on the input H₂S removal efficiency (99.9%). A fraction of CO₂ is removed along with the H₂S. The energy input specifications simulate a physical solvent, namely Selexol. In particular, the heat requirement for the reboiler was set to 21.0 MJ/kg_{H₂S}. This heat duty is provided by condensing steam at low pressure (5 bar). The power consumption (for pumps etc.) computed by the AGR model results to be 2.1 MJ/kg_{H₂S}. The sulfur-free syngas is then routed to the PSA unit.

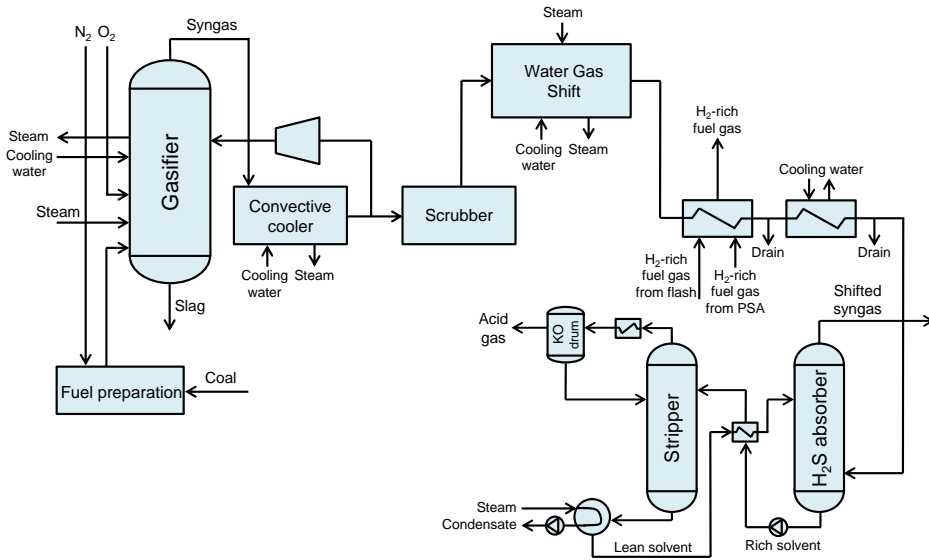


Figure 17. Detailed flowsheet of the gasification and syngas treatment section of the IGCC plant.

3.3.3 CO_2 separation and H_2 production

The gas separation technology adopted for CO_2 separation (and for ultrapure H_2 production when applies) is PSA. The PSA unit can include one or more PSA stages. The gas stream entering the PSA unit is that leaving the AGR unit, which pressure is 38.8 bar (the temperature has been varied in the thesis between 55 and 95°C). The volumetric composition is the following: 37.9% CO_2 , 53.5% H_2 , 1.5% CO , 0.06% CH_4 , 6.7% N_2 , 0.3% Ar and 0.04% other components. The gas streams leaving the PSA unit are: a CO_2 -rich gas stream (at 1 bar in the base case), which is sent to the CO_2 compression unit; a H_2 -rich gas stream (at 24 bar), which is sent to gas turbines as fuel. When the IGCC coproduction framework applies, a third outlet gas stream, made of ultrapure H_2 , leaves the PSA unit (at 38.8 bar). The exact design of the PSA depends on the plant configuration considered. The different instances studied are defined in the section 3.4.3. Some fans have to be considered in the PSA unit, in order to overcome the pressure drop in the adsorption columns. The energy consumption of these fans was calculated discounting the ideal compression work by an isentropic efficiency of 85%.

3.3.4 CO₂ compression and purification

The CO₂-rich gas stream leaving the PSA unit (at 1 bar in the base case) is cooled down to 28°C and sent to the CO₂ compression and purification unit, where it is compressed to an appropriate pressure for transport. This pressure was assumed to be 110 bar. *Figure 18* shows the CO₂ compression and purification section in detail. The compression arrangement includes multiple intercooled stages. The intercooled compressor model is the same as that described in section 3.2.5. Since the CO₂ purity obtained by the PSA process was not matching the specification established (i.e. $\geq 90\%$ vol.), a further purification process was implemented. It consists of impurities removal by means of two flash separators integrated in the CO₂ compression section. The model was developed in *Aspen HYSYS*. Such approach has already been suggested for removing a selection of non-CO₂ gases from oxy-combustion power plants [72,73]. The CO₂-rich gas stream is first partially compressed (up to 30 bar in the base case, by means of 4 intercooled stages) and the water is removed. The dehydrated gas stream enters a system of two multi-stream heat exchangers (MSHE), each followed by a flash separator (see *Figure 18*). An appropriate temperature is set at the outlet of each heat exchanger (-30°C and -54.5°C , values taken from [73]), in order to allow to collect CO₂ in liquid phase. As a result two gas streams are obtained: a CO₂-rich stream, matching the requested purity specification (final CO₂ purity $\approx 99\%$ vol.), which completes the compression process; a CO₂-lean stream, rich in H₂, which is added to the syngas injected as fuel in the gas turbine. The cooling duty is provided by the throttling of the CO₂-rich gas streams. The purification process increases the compression power requested (0.50 MJ/kg_{CO2}), due to the additional pressure ratio to be provided by the compressors in response to the CO₂-rich gas stream throttling. However, the additional H₂ recovered in the flash separators and sent to the gas turbine counterbalances this effect to a large extent.

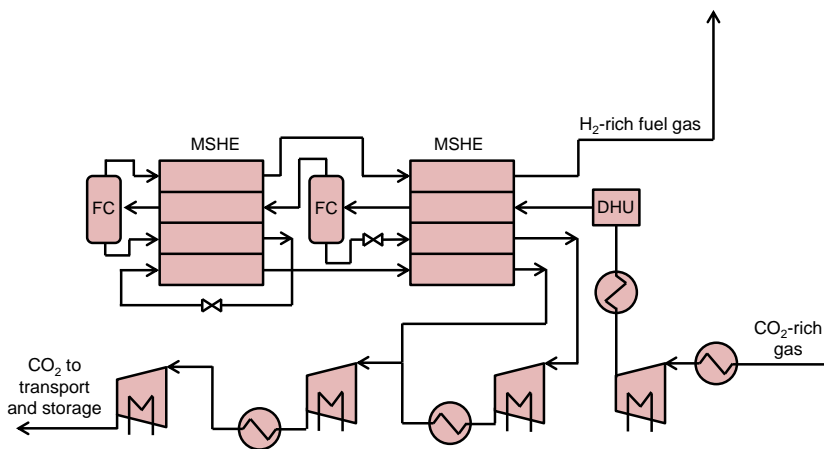


Figure 18. Detailed flowsheet of the compression and purification section of the IGCC plant.

3.3.5 Power island

The power island is responsible for syngas energy conversion into electricity. A combined cycle is adopted for the purpose, consisting of a gas turbine and a steam bottoming cycle. *Figure 19* shows the power island section in detail. The gas stream fueling the gas turbine is composed by the H₂-rich gas stream leaving the PSA unit plus the additional H₂ recovered in the flash processes. This gas stream is preheated to 200°C before being fed to the gas turbine combustor. A dilution with N₂ coming from the ASU is included for NO_x formation control. As a rule-of-thumb, the N₂ dilution has been adjusted in the different cases proposed so to retain similar Wobbe index as for the base case [67]. The gas turbine (GT) considered is a Siemens SGT5-4000F, a large-scale “F class” 50 Hz selected from the *ThermoFlow* library of gas turbine engines. The simulation of the GT is based on a reverse-engineered, detailed, physical engine model developed by *THERMOFLEX*. A compressor map is constructed to relate compressor efficiency to pressure ratio and corrected inlet flow. Turbine cooling air and process air extraction from the compressor at user-defined locations is taken into account. The turbine cooling air is larger (≈ 53 kg/s) in comparison to typical values for gas turbine running on natural gas, due to the significant presence of water in the flue gas. The model modifies compressor behavior dependent upon the location and quantity of extracted air. The combustion model is a generalized equilibrium calculation modified by an efficiency to account for the non-ideal process. The calculation procedure accounts for combustor pressure loss, fuel dilution and fuel delivery temperature. NO_x, CO and unburned hydrocarbon emissions have to be set by the user. A simplified turbine map is constructed to relate turbine efficiency to pressure ratio and corrected flow. Pressure drops are estimated throughout the GT cycle and are taken into account by the model. The part load operation includes the utilization of variable IGV. The GT operates with a pressure ratio of ≈ 17.5 and a TIT (stagnation temperature at first rotor inlet) of $\approx 1300^\circ\text{C}$, giving an efficiency of about 40% (electric generator output per fuel LHV). The process air extracted from the compressor, to be sent to the ASU, is expanded (from 17.5 bar to 10.5 bar) in order to recover part of the compression work. The flue gas from the turbine is discharged at $\approx 580^\circ\text{C}$ and its remaining energy content is used to produce steam at three different pressure levels, respectively 138 bar, 47 bar and 5 bar, in a HRSG. The design of the HRSG is optimised by *THERMOFLEX*. The heat transfer duty for each heat exchanger is determined by its water/steam side inputs and the program computes the corresponding heat transfer rate, exit state of the flue gas stream and heat transfer ability UA. The minimum temperature difference allowed in the economizers was set to 5°C, the pinch point in the evaporators to 10°C and the minimum temperature difference allowed in the superheaters to 5°C. The heat loss, expressed as percentage of the energy transferred to water/steam, was set to 0.5%. The steam produced by the HRSG is expanded in a steam turbine (ST), providing an additional power output. The ST is divided in HP, IP and LP section. The design was

tuned in accordance with HRSG pressure levels. Steam extraction points were selected based on gasifier, reboiler and other process needs. Dry step efficiencies are defined for each turbine group and the same correction principles apply as those outlined in section 3.2.2. The overall isentropic efficiencies results to be about 90%, 93% and 88%, respectively for the HP, IP and LP group. A water-cooled condenser is used to condense the turbine exhaust steam, operating at a design pressure of 0.048 bar. The total gross power output, considering all H₂ used for power generation, is about 460 MW: GT gross power output 288 MW, ST gross power output 167 MW and air expander gross power output 5 MW.

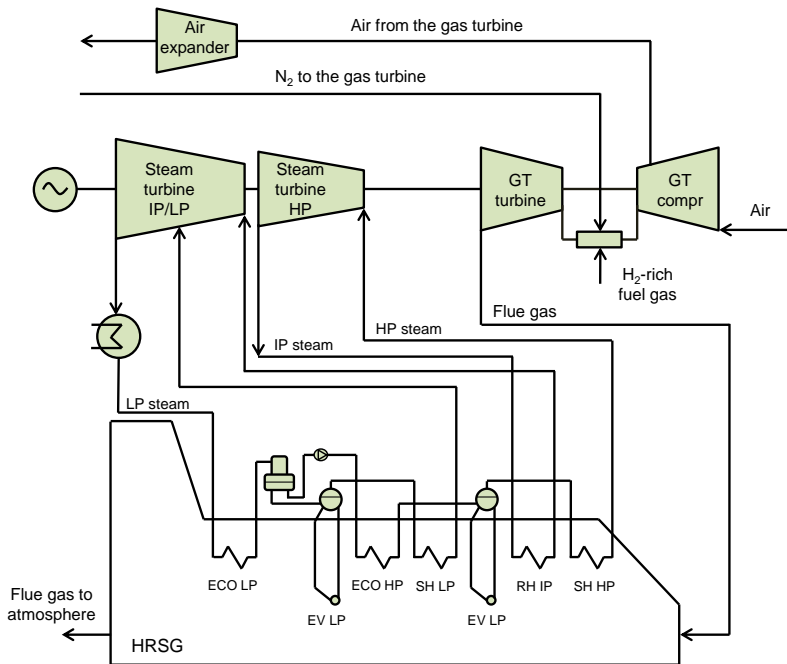


Figure 19. Detailed flowsheet of the power island section of the IGCC plant.

3.4 Process design and modeling of PSA process

Adsorptive gas separation processes are carried out in fixed-bed adsorbers which contain porous adsorbent particles. The following sub-sections provide an overview of the developed model to simulate the PSA unit. The mathematical model for describing the adsorption bed dynamics is first outlined alongside with boundary and initial conditions. Following, the PSA process configurations are established, according to the

specific objectives. The definition of a PSA configuration entails to determine the number of columns working in parallel, the PSA cycle and the adsorbent material. In the last sub-section the approach for the numerical solution of the PSA model is discussed.

3.4.1 Governing equations

In order to simulate the behavior of the PSA unit, a model of a fixed-bed column was developed. The model must be able to describe the dynamics of adsorption/desorption on the porous adsorbent selected during the PSA cycle. The mathematical description of the process relies on material, energy and momentum balances as well as the adsorption isotherm. The complete model results in a complex set of partial differential and algebraic equations (PDAEs), whose solution would be tedious and time-consuming. Therefore, several simplifications have been suggested in the literature, especially with regard to the kinetics of the adsorption process. The model adopted in this thesis relies on some of these simplifications. The guiding criterion for the selection of the degree of complexity was to develop a model as simple as possible but still able to satisfactorily predict the gas separation performance of the unit. It is worth to stress that the proposed work aims to be an analysis of complex systems (i.e. coal-fired power plants), of which the PSA unit constitutes an integrated sub-section. An in-depth representation of the adsorption mechanisms was believed to be out of the scope of the thesis.

The overview of the governing equations for the adsorption column was structured as following. First the complete equations are presented in order to provide a sound theoretical basis. Then the simplifications applied are introduced and explained, leading to the modeling framework used in PSA process simulation. Before analyzing the equations, some modeling assumptions are listed:

- The gas in the bulk phase is considered to follow the ideal gas law.
- The bed is assumed uniform. Constant bulk density and bed porosity.
- The radial diffusion effects are ignored.
- The heat of adsorption is independent of temperature and adsorbed phase loading.

Material balance and mass transfer rate – Assuming an axially dispersed plug flow pattern in the fixed bed adsorption column, the transient component material balance for the bulk gas phase is given by:

$$\varepsilon \frac{\partial C_i}{\partial t} = -\frac{\partial(u_s C_i)}{\partial z} + \frac{\partial}{\partial z} \left(\varepsilon D_{ax,i} \frac{\partial C_i}{\partial z} \right) - \rho_p (1 - \varepsilon) \frac{\partial \hat{q}_i}{\partial t} \quad (3.1)$$

where ε is the bed porosity, C_i is the gas phase concentration of component i (mol/m³), u_s is the gas superficial velocity (m/s), $D_{ax,i}$ is the axial dispersion coefficient of component i (m²/s), ρ_p is the volumetric mass density of the particle (m³/kg), \hat{q}_i is the

average concentration of component i in the adsorbent particle (mol/kg) and z is the distance in the axial direction (m). The axial dispersion coefficient lumps together the mechanisms which contribute to axial mixing and can be estimated through one of the following correlations [29,74]:

$$D_{ax,i} = (0.45 + 0.55\varepsilon)D_{g,i}^m + 0.35\frac{d_p}{2}|u_s| \quad (3.2)$$

$$\frac{\varepsilon D_{ax,i}}{D_{g,i}^m} = 20 + 0.5Sc Re \quad (3.3)$$

where $D_{g,i}^m$ is the multicomponent molecular diffusivity of component i (m^2/s), d_p is the adsorbent particle diameter (m), Sc is the Schmidt number and Re is the Reynolds number.

The overall material balance can be expressed similarly like:

$$\varepsilon \frac{\partial C_{tot}}{\partial t} = -\frac{\partial(u_s C_{tot})}{\partial z} - \rho_p(1-\varepsilon) \sum_i^{NC} \frac{\partial \hat{q}_i}{\partial t} \quad (3.4)$$

where C_{tot} is the total gas phase concentration (mol/m^3).

The overall rate of mass transfer term ($\partial \hat{q}_i / \partial t$) is coupling the material balance in the bulk gas phase with the material balance in the adsorbent particle. Given the bi-disperse structure of the adsorbents considered (i.e. population of macro and micropores), two additional equations are needed: a material balance in the macropores and one in the micropores. In order to model the mass transfer from one phase to the other, the effects of the mass transfer resistances between the fluid and the particle and within the particle have to be taken into account. At the microscopic level, an adsorption process involves the following steps in sequence (desorption step follows these steps in reverse) [75]:

- The adsorbate diffuses from the bulk fluid phase to the external surface of the adsorbent pellet.
- From the external surface, adsorbate diffuses into and through the macropores.
- Adsorbate diffuses further in the micropores before getting adsorbed.

Accordingly, three main mass transfer resistances can be defined:

- External film resistance
- Macropore diffusional resistance
- Micropore diffusional resistance

The *external film transfer resistance* assumes that the rate of mass transport between a solid surface and a flowing fluid is limited by a film adjacent to the surface. Considering

steady-state conditions at the fluid-solid interface, the mass transfer rate across the external film is supposed to be equal to the diffusive flux at the particle surface:

$$\frac{\partial \hat{q}_i}{\partial t} = a_p k_{f,i} (C_i - C_{por,i}^s) = a_p \varepsilon_p D_{p,i} \left. \frac{\partial C_{por,i}}{\partial t} \right|_{R=R_p} \quad (3.5)$$

where a_p is the particle surface area per unit volume (m^2/m^3), $k_{f,i}$ is the external mass transfer coefficient of component i (m/s), $C_{por,i}^s$ is the concentration in the macropore of component i at the particle surface (mol/m^3), ε_p is the particle porosity, $D_{p,i}$ is the macropore diffusivity of component i (m^2/s), $C_{por,i}$ is the concentration in the macropore of component i (mol/m^3), R is the distance along the macroparticle radius (m) and R_p is the macroparticle radius (m). The external mass transfer coefficient ($k_{f,i}$) depends on the flow conditions and actually differs from one point to another on the same particle. In practice, however, an average value for the film coefficient is used and can be characterized by using the system's Sherwood, Reynolds and Schmidt number [76]:

$$Sh = \frac{2k_{f,i}R_p}{D_{g,i}^m} = 2 + 1.1Sc^{1/3} Re^{0.6} \quad (3.6)$$

The bulk gas phase material balance can be rewritten as following:

$$\varepsilon \frac{\partial C_i}{\partial t} = -\frac{\partial (u_s C_i)}{\partial z} + \frac{\partial}{\partial z} \left(\varepsilon D_{ax,i} \frac{\partial C_i}{\partial z} \right) - \rho_p (1-\varepsilon) a_p k_{f,i} (C_i - C_{por,i}^s) \quad (3.7)$$

The *macropore diffusional resistance* may be the result of different contributions, depending on the relative magnitude of the pore diameter and the mean free path of the adsorbate under the operating conditions in the pore. When the pore diameter is much greater than the mean free path, molecular diffusion dominates the transport. In this case the diffusion resistance mainly arises from collision between diffusing molecules. The multicomponent molecular diffusivity can be estimated by Wilke correlation [51,74]:

$$D_{g,i}^m = \frac{1 - y_i}{\sum_{j \neq i} \frac{y_j}{D_{g,ij}}} \quad (3.8)$$

where y_i is the mole fraction of component i , $D_{g,ij}$ is the binary diffusion coefficient of the ij system (m^2/s). The binary molecular diffusivities can be calculated through the Fuller empirical correlation [77,78]:

$$D_{g,ij} = \frac{10^{-3}T^{1.75} \left[\frac{1}{MW_i} + \frac{1}{MW_j} \right]^{-1/2}}{(P/101325) \left[\left(\sum_i \xi_i \right)^{1/3} + \left(\sum_j \xi_j \right)^{1/3} \right]^2} \quad (3.9)$$

where T is the gas temperature (K), MW_i is the molecular weight of component i (g/mol), P is the pressure (Pa) and ξ_i is the diffusion parameter for component i. Alternatively, the Chapman and Enskog equation can be utilized [74,78]:

$$D_{g,ij} = \frac{3f_D}{16n\sigma_{ij}^2\Omega_D} \left[\frac{4kT}{\pi} \left(\frac{1}{MW_i} + \frac{1}{MW_j} \right) \right]^{1/2} \quad (3.10)$$

where f_D is a correction term, σ_{ij} is the characteristic length of the intermolecular force law (\AA), Ω_D is the collision integral for diffusion and k is the Boltzmann constant. When the pore diameter is small compared to the molecular mean free path, Knudsen diffusion dominates the mass transfer mechanism. The resistance to mass transfer is mainly due to the particles collisions against the pore wall. The Knudsen diffusivity can be defined as [29]:

$$D_{K,i} = 9700R_p \sqrt{\frac{T}{MW_i}} \quad (3.11)$$

where $D_{K,i}$ is the Knudsen diffusivity for component i (m^2/s). When both mechanisms (molecular and Knudsen diffusivity) significantly influence the mass transfer, the effective macropore diffusivity can be estimated by the Bosanquet equation [29]:

$$\frac{1}{D_{p,i}} = \tau \left(\frac{1}{D_{g,i}^m} + \frac{1}{D_{K,i}} \right) \quad (3.12)$$

where τ is the tortuosity factor.

Once defined the mass transfer mechanism in the macropore, the material balance can be expressed as:

$$\varepsilon_p \frac{\partial C_{\text{por},i}}{\partial t} = \frac{1}{R^2} \frac{\partial}{\partial R} \left(R^2 \varepsilon_p D_{p,i} \frac{\partial C_{\text{por},i}}{\partial R} \right) - \rho_p \frac{\partial \bar{q}_i}{\partial t} \quad (3.13)$$

where \bar{q}_i is the averaged adsorbed concentration of component i (mol/kg). The boundary

conditions for the macropore balance are as follows:

$$\left. \frac{\partial C_{\text{por},i}}{\partial R} \right|_{R=0} = 0 \quad (3.14)$$

$$k_{f,i} (C_i - C_{\text{por},i}^s) = \varepsilon_p D_{p,i} \left. \frac{\partial C_{\text{por},i}}{\partial t} \right|_{R=R_p} \quad (3.15)$$

The *micropore diffusional resistance* involves a different mass transfer mechanism compared to those previously described. Since the pore diameter is in the order of magnitude of the molecular diameter, the adsorbate cannot escape the force field of the adsorbent surface. The transport of mass occurs by an activated process involving jumps between adsorption sites [79]. The resulting micropore diffusivity follows an Arrhenius type correlation [29]:

$$D_{c,i} = D_{c,i}^0 \exp\left(-\frac{E_{a,i}}{R_g T}\right) \quad (3.16)$$

where $D_{c,i}$ is the micropore diffusivity of component i (m^2/s), $D_{c,i}^0$ is the limiting micropore diffusivity at infinite temperature of component i (m^2/s), $E_{a,i}$ is the activation energy of component i (J/mol) and R_g is the universal gas constant (J/mol K). The material balance equation in the micropore is:

$$\frac{\partial \bar{q}_i}{\partial t} = \frac{1}{r^2} \frac{\partial}{\partial r} \left(r^2 D_{c,i} \frac{\partial q_i}{\partial r} \right) \quad (3.17)$$

where q_i is the distributed adsorbate concentration of component i in the micropore (mol/kg) and r is the distance along the micropore radius (m). The boundary conditions for the micropore balance are as follows:

$$\left. \frac{\partial q_i}{\partial r} \right|_{r=0} = 0 \quad (3.18)$$

$$q_i(t, r_c) = q_i^* \quad (3.19)$$

where q_i^* is the equilibrium adsorbed concentration of component i (mol/kg) and r_c is the micropore radius (m).

That outlined is the complete set of equations for describing the material balance during

an adsorption process in a fixed-bed. Although the results would be closer to reality, the mathematical complexity associated with such equations suggests the utilization of simpler rate expressions. The most-frequently applied rate-law simplification is called linear driving force (LDF) approximation [80]. The LDF model assumes that the adsorption rate is proportional to the linear difference between the equilibrium adsorbed concentration and an average adsorbed concentration within the particle:

$$\frac{\partial \bar{q}_i}{\partial t} = k_{\text{LDF},i} (q_i^* - \bar{q}_i) \quad (3.20)$$

The LDF coefficient (k_{LDF}) accounts for the overall mass transfer resistance. Its definition depends on the mass transfer mechanisms considered. The characteristics of the adsorbents selected for this work, namely two zeolites 5A [81,82] and an activated carbon [82], allowed a further simplification. This simplification is based on the evaluation of the mass transfer resistances and it assumes the limiting case where diffusion in the micropores is the controlling mass transfer mechanism. Accordingly, the other mass transfer resistances have been neglected (i.e., macropore and film diffusion). Such approach is supported by previous studies [82,83] and has been already successfully applied by other works simulating the behavior of PSA units [41,49]. With this assumption, the macropore concentration is equal to the gas phase concentration and therefore the macropore mass balance is eliminated from the model. Since micropore diffusivity is the only mass transfer resistance considered, the LDF coefficient can be defined as:

$$k_{\text{LDF},i} = \chi_{\text{LDF}}^c \frac{D_{c,i}}{r_c^2} \quad (3.21)$$

where χ_{LDF}^c is the linear driving force geometrical factor. The simplifications introduced lead to this new equation accounting for the component material balance in the bulk gas phase and in the macropores:

$$\frac{\partial C_i}{\partial t} [\varepsilon + \varepsilon_p (1 - \varepsilon)] = -\frac{\partial (u_s C_i)}{\partial z} + \frac{\partial}{\partial z} \left(\varepsilon D_{\text{ax},i} \frac{\partial C_i}{\partial z} \right) - \rho_p (1 - \varepsilon) \frac{\partial \bar{q}_i}{\partial t} \quad (3.22)$$

While overall material balance is now expressed as:

$$\frac{\partial C_{\text{tot}}}{\partial t} [\varepsilon + \varepsilon_p (1 - \varepsilon)] = -\frac{\partial (u_s C_{\text{tot}})}{\partial z} - \rho_p (1 - \varepsilon) \sum_i^{\text{NC}} \frac{\partial \bar{q}_i}{\partial t} \quad (3.23)$$

Equation (3.20), (3.22) and (3.23) constitute the reduced model for the material balance

which has been used in the thesis.

Adsorption isotherm – An adsorbent in contact with the surrounding gaseous mixture for a sufficiently long time eventually attains equilibrium. For a given gas-solid system, the amount adsorbed at equilibrium is described by:

$$q^* = f(P, T) \quad (3.24)$$

At a fixed temperature, q^* is only a function of pressure and the relation is called an adsorption isotherm (see *Figure 20*).

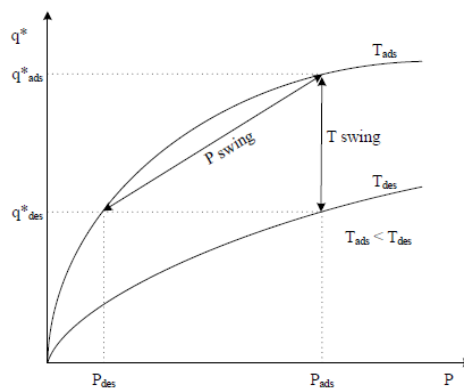


Figure 20. Adsorption isotherms.

Figure 20 also shows how adsorption/desorption is facilitated by changing total pressure or temperature of the system. The most common approach to predict an adsorption isotherm, for both physical and chemical adsorption, is the *Langmuir approach*. The theoretical basis relies on the concept of dynamic equilibrium between the rates of condensation (adsorption) and evaporation (desorption). The *Langmuir model* is the simplest, yet very useful, model derived by the *Langmuir approach*. Other models based on the *Langmuir approach* include *Freundlich model*, *Langmuir-Freundlich model*, *BET model*, *Sips model* and *Toth model*. Other models have been developed based on different approaches than the *Langmuir* (e.g., the *Gibbs approach*, the *potential theory*).

In its usual form, the following assumptions apply in the *Langmuir model*:

- The adsorbed molecule or atom is held at definite, localized sites.
- Each site can accommodate one and only one molecule or atom.
- The energy of adsorption is a constant over all sites, and there is no interaction between neighboring adsorbates.

The resulting multicomponent adsorption isotherm is:

$$q_i^* = \frac{q_{m,i} k_i P_i}{1 + \sum_j^{NC} k_j P_j} \quad (3.25)$$

where $q_{m,i}$ is the specific saturation adsorption capacity of component i (mol/kg), k_i is the equilibrium constant of component i (Pa^{-1}) and P_i is the partial pressure (Pa). In the thesis, two models have been utilized, derived from the basic *Langmuir model*. Both assume that a molecule can occupy more than one site on the solid surface and demonstrated to interpret accurately the adsorption capacity of the adsorbents selected [54,81,82].

The dual-site Langmuir model:

$$q_i^* = \frac{q_{m,i}^1 k_i^1 P_i}{1 + \sum_j^{NC} k_j^1 P_j} + \frac{q_{m,i}^2 k_i^2 P_i}{1 + \sum_j^{NC} k_j^2 P_j} \quad (3.26)$$

The multi-site Langmuir model:

$$\frac{q_i^*}{q_{m,i}} = a_i k_i P_i \left[1 - \sum_i^{NC} \left(\frac{q_i^*}{q_{m,i}} \right) \right]^{a_i} \quad (3.27)$$

where a_i is the number of neighboring sites occupied by adsorbate molecule for component i .

Energy balance – Adsorption is an exothermic process (while desorption is endothermic) and temperature changes influence the adsorption equilibrium behavior and, possibly, the adsorption rates. Thus, accounting for heat generation and transfer in adsorbent beds is essential for accurate modeling of adsorption processes. A complete model must consider the energy balance in the bulk gas phase, in the solid phase and in the column wall. The energy balance in the bulk gas phase is given by:

$$C_{v,G} C_{tot} \frac{\partial T}{\partial t} - R_g T \frac{\partial C_{tot}}{\partial t} + \frac{u_s}{\varepsilon} C_{p,G} C_{tot} \frac{\partial T}{\partial z} = + \frac{1}{\varepsilon} \frac{\partial}{\partial z} \left(\lambda_{ax} \frac{\partial T}{\partial z} \right) + \frac{(1-\varepsilon)}{\varepsilon} a_p h_f (T - T_s^s) + \frac{4 h_w}{\varepsilon d_w} (T - T_w) \quad (3.28)$$

where $C_{v,G}$ is the gas specific heat at constant volume (J/mol K), $C_{p,G}$ is the gas specific heat at constant pressure (J/mol K), λ_{ax} is the axial thermal dispersion coefficient (J/m s K), h_f is the film heat transfer coefficient between the gas and particle ($\text{J/m}^2 \text{s K}$), T_s^s is the temperature at the particle surface (K), h_w is the wall heat transfer coefficient ($\text{J/m}^2 \text{s K}$)

K) and T_w is the wall temperature (K). The axial thermal dispersion coefficient can be estimated with the following correlation [51,84]:

$$\frac{\lambda_{ax}}{k_g} = 7 + 0.5 \text{Pr Re} \quad (3.29)$$

where k_g is the thermal conductivity of the gas phase (J/m s K). The film heat transfer coefficient between the gas and the adsorbent can be estimated through the Chilton-Colburn analogy. In particular, the following correlation can be applied [76]:

$$Nu = \frac{2h_f R_p}{k_g} = 2 + 1.1 Sc^{1/3} \text{Re}^{0.6} \quad (3.30)$$

The solid phase energy balance is expressed by the following equation:

$$\left[\varepsilon_p (1-\varepsilon) C_{v,G} C_{por} + (1-\varepsilon) C_s \rho_p + (1-\varepsilon) \rho_p \sum_i^{NC} C_{ads,i} \bar{q}_i \right] \frac{\partial T_s}{\partial t} - \varepsilon_p (1-\varepsilon) R T_s \frac{\partial C_{por}}{\partial t} = \quad (3.31)$$

$$+ \rho_p (1-\varepsilon) \sum_i^{NC} (-\Delta H_{r,i}) \frac{\partial \bar{q}_i}{\partial t} + (1-\varepsilon) a_p h_f (T - T_s^s)$$

where T_s is the temperature in solid phase (K), C_s is the particle specific heat (J/kg K), $C_{ads,i}$ is the specific heat of component i in the adsorbed phase (J/mol K) and $\Delta H_{r,i}$ is the heat of adsorption of component i (J/mol). The conductivity of the particle has been neglected in the energy balance.

The last energy balance is the one for the wall of the column. It is given by:

$$\rho_w C_w \frac{\partial T_w}{\partial t} = a_w h_w (T - T_w) - a_u U (T_w - T_\infty) \quad (3.32)$$

where ρ_w is the volumetric mass density of the wall (kg/m³), C_w is the wall specific heat (J/kg K), a_w is the ratio of the internal surface area to the volume of the column wall (m²/m³), a_u is the ratio of the external surface area to the volume of the column wall (m²/m³) and U is the overall heat transfer coefficient (J/m² s K). Different approaches can be used to estimate the wall heat transfer coefficient, for instance Leva's correlation [85]:

$$Nu = \frac{2h_w R_{w,i}}{k_g} = 0.813 \text{Re}^{0.9} \exp(-6R_p / R_{w,i}) \quad (3.33)$$

where $R_{w,i}$ is the internal radius of the column (m). The overall heat transfer coefficient

between the wall and the environment can be estimated as [86]:

$$\frac{1}{U} = \frac{1}{h_u} + \frac{R_{w,e}}{k_w} \ln \left(\frac{R_{w,e}}{R_{w,i}} \right) \quad (3.34)$$

where $R_{w,e}$ is the external radius of the column (m), k_w is the wall conductivity (J/m s K) and h_u is the external convective heat transfer coefficient (J/m² s K). The external convective heat transfer coefficient can be estimated through the following correlation [86]:

$$\frac{h_u L}{k_{g,e}} = 0.68 + \frac{0.67 Ra^{1/4}}{\left[1 + (0.492 / Pr)^{9/16} \right]^{4/9}} \quad (3.35)$$

where L is the length of the column (m), $k_{g,e}$ is the thermal conductivity of the external air (J/m s K) and Ra is the Rayleigh number.

A frequently used model simplification suggests to assume thermal equilibrium between the gas and solid phases. Such approach is very often applied in the literature and allows defining a single equation for the energy balance in the gas and solid phase. An additional simplification assumes adiabatic operation of the adsorption column. In industrial-scale processes, like those analysed in the thesis, it is reasonable to consider the heat loss through the wall and the heat accumulated in the wall to be negligible in comparison to the amount of heat caused by the heat of adsorption. Thus, the energy balance in the wall can be safely disregarded. Once applied those simplifications, the reduced energy balance, utilized in the thesis, is given by a single equation:

$$\left[C_{v,G} C_{tot} + \frac{\varepsilon_p (1-\varepsilon)}{\varepsilon} C_{v,G} C_{tot} + \frac{(1-\varepsilon)}{\varepsilon} C_{s,p} + \frac{(1-\varepsilon)}{\varepsilon} \rho_p \sum_i^{NC} C_{ads,i} \bar{q}_i \right] \frac{\partial T}{\partial t} - \frac{\varepsilon + \varepsilon_p (1-\varepsilon)}{\varepsilon} RT \frac{\partial C_{tot}}{\partial t} + \frac{u_s}{\varepsilon} C_{p,G} C_{tot} \frac{\partial T}{\partial z} = + \frac{1}{\varepsilon} \frac{\partial}{\partial z} \left(\lambda_{ax} \frac{\partial T}{\partial z} \right) + \rho_p \frac{(1-\varepsilon)}{\varepsilon} \sum_i^{NC} (-\Delta H_{r,i}) \frac{\partial \bar{q}_i}{\partial t} \quad (3.36)$$

Momentum balance – As the bulk fluid flows through the void spaces between adsorbent particles, it experiences a pressure drop due to viscous energy losses and drop in kinetic energy. The momentum balance considers the terms of pressure drop and velocity changes across the packed bed and relates them through the following correlation:

$$\frac{\partial P}{\partial z} = -K_D u_s - K_V u_s |u_s| \quad (3.37)$$

where K_D and K_V are parameters corresponding to the viscous and kinetic pressure loss terms, respectively. Ergun derived semi-empirical relationships for them [87]:

$$K_D = \frac{150 (1-\varepsilon)^2}{d_p^2 \varepsilon^3} \mu \quad (3.38)$$

$$K_V = \frac{1.75 (1-\varepsilon)}{d_p \varepsilon^3} \rho_G \quad (3.39)$$

where μ is the dynamic viscosity (Pa s) and ρ_g is the gas volumetric mass density (kg/m^3). The resulting equation is the *Ergun equation* and has been used in the thesis to describe the pressure drop along the bed length:

$$\frac{\partial P}{\partial z} = - \left[\frac{150 (1-\varepsilon)^2}{d_p^2 \varepsilon^3} \mu u_s + \frac{1.75 (1-\varepsilon)}{d_p \varepsilon^3} \rho_G u_s |u_s| \right] \quad (3.40)$$

3.4.2 Boundary and initial conditions

The Danckwerts boundary conditions (BCs) apply, assuming no dispersion or radial variation in concentration or temperature either upstream or downstream of the reaction section. Different BCs define the PSA process steps. The PSA steps, described in section 2.3.2, can be divided in three groups with regard to the BCs implemented. *Figure 21* schematically represents these three instances.

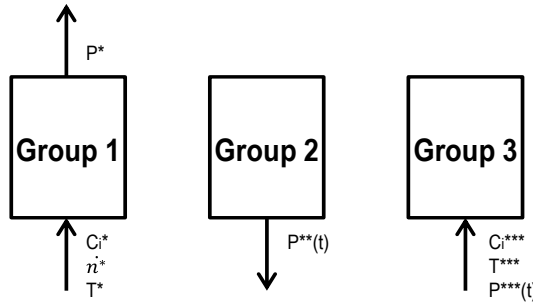


Figure 21. Schematics of the three groups in which the PSA steps are divided with regard to the BCs.

The BCs of the first group define a column which is fed with a gas stream at constant pressure. Both sides of the column are open and the gas is left to flow through. The PSA steps which belong to this group are *feed/adsorption*, *heavy reflux/rinse* and *purge*. For the side of the column where the gas stream flows in, the following BCs apply:

$$\varepsilon D_{ax,i} \frac{\partial C_i}{\partial z} = -u_s (C_i^* - C_i) \quad (3.41)$$

$$\lambda_{ax} \frac{\partial T}{\partial z} = -u_s C_{p,G} C_{tot} (T^* - T) \quad (3.42)$$

$$\dot{n} = \dot{n}^* \quad (3.43)$$

For the side of the column where the gas stream flows out, the following BCs apply:

$$\frac{\partial C_i}{\partial z} = 0 \quad (3.44)$$

$$P = P^* \quad (3.45)$$

$$\frac{\partial T}{\partial z} = 0 \quad (3.46)$$

C_i^* , T^* , \dot{n}^* are known characteristics of the specific gas stream fed to the column, while P^* is the constant pressure of the system.

The BCs of the second group define a column closed on one side, while the pressure is decreased down to a given level. The pressure gradient makes a fraction of the gas accumulated in the column to leave from the open side. The PSA steps which belong to this group are *blowdown* and *pressure equalization - depressurization*. For the side of the column which is closed, the following BCs apply:

$$\frac{\partial C_i}{\partial z} = 0 \quad (3.47)$$

$$\dot{n} = 0 \quad (3.48)$$

$$\frac{\partial T}{\partial z} = 0 \quad (3.49)$$

For the side of the column where the gas stream flows out, the following BCs apply:

$$\frac{\partial C_i}{\partial z} = 0 \quad (3.50)$$

$$P = P^{**}(t) \quad (3.51)$$

$$\frac{\partial T}{\partial z} = 0 \quad (3.52)$$

$P^{**}(t)$ is the defined time profile of the column pressure, which decreases during the step. Alternatively the velocity at the open end of the bed could be specified but the computational time would increase. Specifying the pressure history is a convenient approach for reducing the calculation load and has been utilized in several studies [88–91]. Pressure during *blowdown* step has been defined to vary with time according to the following relationship:

$$P_{BD}^{**}(t) = P_2 + (P_1 - P_2)\exp(-\chi t) \quad (3.53)$$

where P_1 and P_2 are the initial and final pressures, χ is an arbitrary parameter defined according to the literature and t is the time. Pressure during *pressure equalization - depressurization* step has been defined to vary linearly with time:

$$P_{PEQ-D}^{**}(t) = P_1 - \frac{(P_1 - P_2)}{t_{PEQ}} t \quad (3.54)$$

where P_1 and P_2 are the initial and final pressures, t_{PEQ} is the time length of the pressure equalization step and t is the time.

The BCs of the third group define a column which is fed with a gas stream while its opposite side is closed. As a result the pressure increases. The PSA steps which belong to this group are *feed pressurization*, *light product pressurization* and *pressure equalization - pressurization*. For the side of the column where the gas stream flows in, the following BCs apply:

$$\varepsilon D_{ax,i} \frac{\partial C_i}{\partial z} = -u_s (C_i^{***} - C_i) \quad (3.55)$$

$$\lambda_{ax} \frac{\partial T}{\partial z} = -u_s C_{p,G} C_{tot} (T^{***} - T) \quad (3.56)$$

$$P = P^{***}(t) \quad (3.57)$$

For the side of the column which is closed, the following BCs apply:

$$\frac{\partial C_i}{\partial z} = 0 \quad (3.58)$$

$$\dot{n} = 0 \quad (3.59)$$

$$\frac{\partial T}{\partial z} = 0 \quad (3.60)$$

C_i^{***} and T^{***} are known characteristics of the specific gas stream fed to the column. $P^{***}(t)$ is the defined time profile of the column pressure, which increases during the step. The same reasoning behind the specification of the pressure history holds as the one discussed for the BCs of the second group. Pressure during *feed pressurization*, *light product pressurization* and *pressure equalization - pressurization* steps has been defined to vary linearly with time:

$$P^{***}(t) = P_1 + \frac{(P_2 - P_1)}{t_{\text{step}}} t \quad (3.61)$$

where P_1 and P_2 are the initial and final pressures, t_{step} is the time length of the step considered and t is the time.

The adsorption columns simulated are considered to be initially filled with a light gas, which could be N_2 or H_2 depending on the system studied.

3.4.3 PSA configuration

The operating conditions in which the PSA process is supposed to perform and the applications it is designed for, necessarily led to different PSA configurations for the cases considered. The configurations differ in terms of number of columns, type of steps and scheduling of the cycle. The guiding criterion, for the selection of the optimum process design, was the necessity of meeting the key performance objectives dictated by the specific application, within the constraints of the system. For example, PSA processes for CO_2 separation were requested to approach levels of CO_2 recovery and purity demanded by a CCS application (i.e., CO_2 recovery $\geq 90\%$ and purity $\geq 95\%$). When the main goal was ultrapure H_2 production, the target was obtaining a product gas stream with a H_2 purity of 99.99+% vol. A multitude of different process configurations exists and may be used. Given the large number of variables to consider, there is not a well-defined framework to pinpoint the most suitable alternative. In the thesis, it was

decided to rely, as starting point, on cycle configurations successfully employed in the literature [36,41,54]. Some modifications were then implemented with respect to those cycles, in order to deal with the specific process framework considered. The PSA processes presented are the result of an optimization process taking into account several parameters and targeting the briefly mentioned performance objectives. The resulting processes are believed to represent the state-of-the-art for PSA-based gas separation, in line with the scope of the thesis to provide an overview of the actual status of this technology. However, other configurations are possible and may lead to similar performances.

The first PSA process configuration had to perform CO₂ separation in a post-combustion case (i.e. ASC plant with CO₂ capture). A two-stage PSA process was selected, with columns of both stages packed with a zeolite 5A. The first PSA stage consists of a 3-bed 5-step cycle, while the second stage consists of a 2-bed 5-step cycle. The sequence of different steps undergone by a column is shown in *Figure 22*, while the cycle scheduling is shown in *Table 2*. In accordance with the literature review, two stages were adopted because a single stage does not seem to be able to achieve the requested performance in terms of CO₂ recovery and purity. Since no flue gas compression is implemented upstream the PSA unit, the flue gas enters at about atmospheric pressure. The aim of the first stage is to achieve the highest possible CO₂ recovery. As a tradeoff, it is not possible to achieve very high CO₂ purity. CO₂ from the flue gas gets adsorbed during the adsorption step. The regeneration process is carried out by decreasing the pressure and is completed by sending a fraction of the adsorption off-gas as purging gas stream. A rinse step is also designed in order to displace part of the light gas filling the column before the regeneration starts. The CO₂-rich gas leaving from the blowdown and purge steps is then collected and sent to the second PSA stage, where it is further purified. In order to enhance the second PSA process performance, a compression of the gas stream is implemented between the PSA stages. In the second stage no recirculation streams are present (i.e. there is no purge or rinse step). The adsorbent regeneration is ensured by a blowdown step and the separation process is aided by a pressure equalization step. The gas stream leaving during the blowdown step is the CO₂-rich gas stream to undergo further compression and conditioning processes for transport and storage.

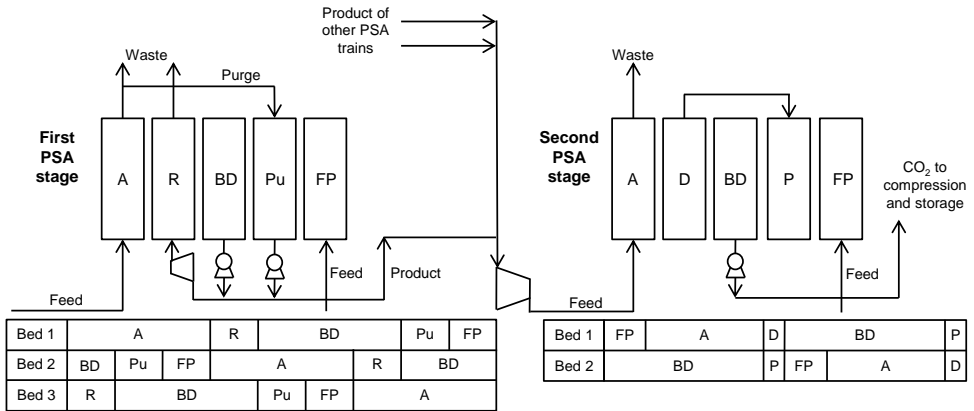


Figure 22. Schematic of the first PSA configuration. Both PSA stages are represented. The sequence of the steps undergone by a single column of each train is reported. The steps considered are: adsorption (A), pressure equalization - depressurization (D), rinse (R), blowdown (BD), purge (Pu), pressure equalization - pressurization (P), feed pressurization (FP).

Table 2. Scheduling of the first PSA configuration.

Stage	Step time (s)							TOT
	A	R	D	BD	Pu	P	FP	
1	$t_{\text{cycle1}}/3$	$t_{\text{cycle1}}/9$	-	$t_{\text{cycle1}}/3$	$t_{\text{cycle1}}/9$	-	$t_{\text{cycle1}}/9$	t_{cycle1}
2	t_{A2}	-	t_{PEQ2}	$t_{A2}+t_{\text{FP2}}$	-	t_{PEQ2}	t_{FP2}	t_{cycle2}

The second PSA process configuration had to remove CO₂ from a shifted syngas in a pre-combustion case (i.e. IGCC plant with CO₂ capture). A single stage 7-bed 12-step PSA process was selected, with all columns packed with an activated carbon. The sequence of different steps undergone by a column is shown in Figure 23, while the cycle scheduling is shown in Table 3. The PSA process is supposed to be able to process the shifted syngas and return two product gas streams: a CO₂-rich stream to be sent to compression and transport; a H₂-rich stream to be fed to the gas turbine as fuel. The PSA configuration is more complex than the previous one, as it includes a larger number of columns and steps. During the adsorption step, CO₂ is adsorbed onto the surface of the adsorbent, while H₂ flows through the column, being the main constituent of the gas stream released during this step (i.e. the H₂-rich gas stream). Other gas components are partially adsorbed in the packed bed. The extent of their adsorption depends on the affinity of the adsorbent towards the specific gas component and on the adsorption dynamics in the bed. The regeneration is again carried out through a blowdown and a purge step (using a fraction of the H₂-rich gas as purging stream), where CO₂ is desorbed and concentrated in a CO₂-rich gas stream. In its basic design, 4 consecutive pressure equalization steps are implemented. Further, in order to meet

constraints in the cycle scheduling (i.e. ensuring continuous operation and the correct interaction between different columns), 4 idle steps needed to be included, negatively affecting the process productivity. *Papers II and III* demanded for some changes in this PSA process configuration, whether to test the impact of process modifications on the system or because an additional product stream aimed to be obtained (i.e. ultrapure H₂). Given that the basic structure of the PSA cycle remained the one outlined, the specific designs are not reported in this section. However, the relative papers include a detailed definition of those cycles, pinpointing the differences in comparison to this base case.

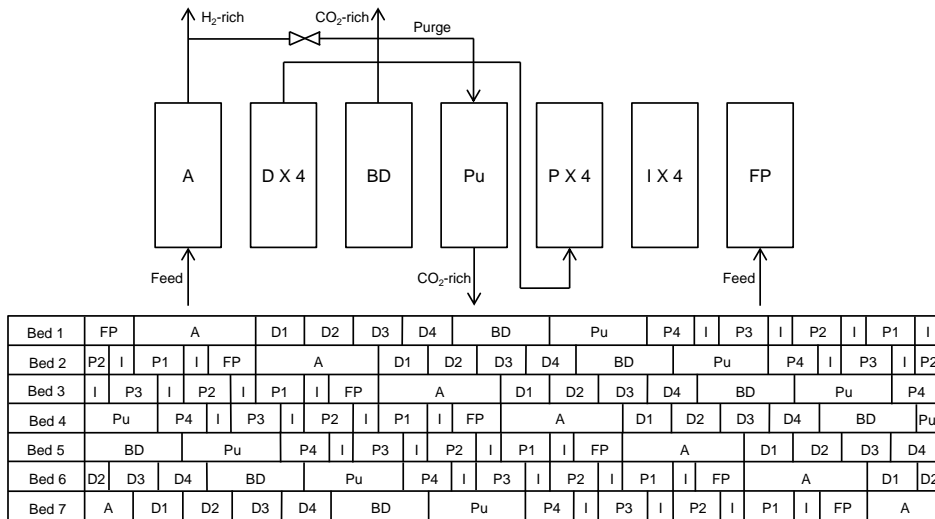


Figure 23. Schematic of the second PSA configuration. The sequence of the steps undergone by a single column of each train is reported. The steps considered are: adsorption (A), pressure equalization – depressurization (D), blowdown (BD), purge (Pu), pressure equalization - pressurization (P), Idle (I), feed pressurization (FP).

Table 3. Scheduling of the second PSA configuration.

Step time (s)							
A	D X 4	BD	Pu	P X 4	I X 4	FP	TOT
t_A	t_{PEQ}	t_{BD}	$2t_A - t_{PEQ} - t_{BD}$	t_{PEQ}	$t_A - 2t_{PEQ}$	t_{PEQ}	t_{cycle}

The third PSA process configuration had to purify a H₂-rich gas stream in order to produce ultrapure H₂. A single stage 6-bed 11-step PSA process was selected, with all columns packed with a zeolite 5A. The sequence of different steps undergone by a column is shown in *Figure 24*, while the cycle scheduling is shown in *Table 4*. The main objective of the PSA process is to concentrate H₂ to high purity levels ($\geq 99.99\%$ vol.). Thus, all the gas components other than H₂ needs to be adsorbed onto the zeolite

during the adsorption step, allowing the off-gas to reach the requested H₂ concentration. The bed needs to be extensively regenerated in order to avoid the breakthrough of any gas components during adsorption step. The regeneration is initiated through a pressure swing in the blowdown step. Following a gas stream rich in light components, H₂ in the first instance, is sent to the top of the column to complete the bed regeneration (i.e. purge step). The purging gas stream is provided by a tailor-made depressurization step, called *depressurization providing purge (DPu)*. The gas leaving the column during the regeneration steps, blowdown and purge, is called tail gas. Three pressure equalization steps are also designed, which are fundamental to keep the adsorption bed, especially the upper part, cleaned from impurities. For the same reason, the column pressurization is implemented by feeding counter-currently a fraction of the ultrapure H₂ gas stream rather than using the feed gas stream like in all other PSA configurations discussed.

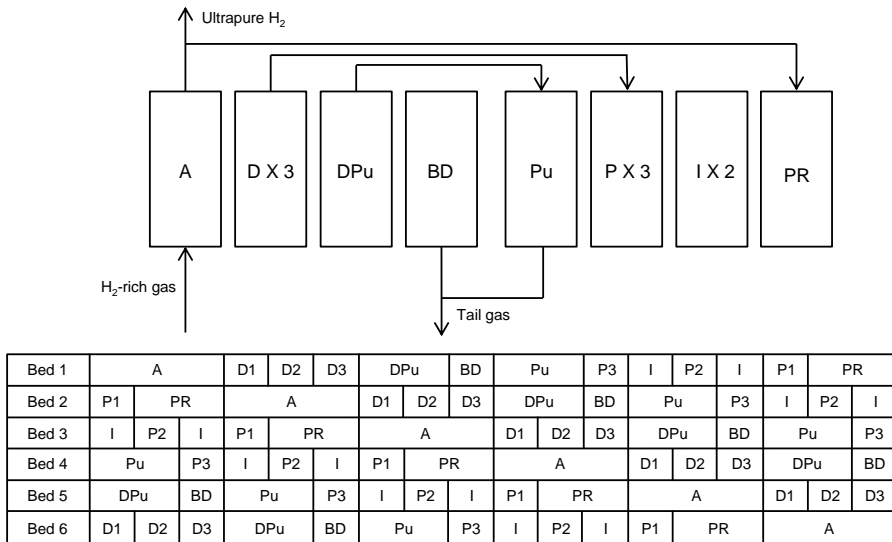


Figure 24. Schematic of the third PSA configuration. The sequence of the steps undergone by a single column of each train is reported. The steps considered are: adsorption (A), pressure equalization - depressurization (D), depressurization providing purge (DPu), blowdown (BD), purge (Pu), pressure equalization - pressurization (P), Idle (I), light product pressurization (PR).

Table 4. Scheduling of the third PSA configuration.

Step time (s)								
A	D X 3	Dpu	BD	Pu	P X 3	I X 2	PR	TOT
$t_{\text{cycle}}/6$	$t_{\text{cycle}}/18$	$t_{\text{cycle}}/9$	$t_{\text{cycle}}/18$	$t_{\text{cycle}}/9$	$t_{\text{cycle}}/18$	$t_{\text{cycle}}/18$	$t_{\text{cycle}}/9$	t_{cycle}

3.4.4 Solution of the PSA model

The one-dimensional dynamic PSA model developed results in a set of partial differential and algebraic equations (PDAEs). Such set of modeling equation was implemented in gPROMS environment [70]. A considerable computational effort is required in order to solve the dynamic model. One way to reduce the computational time was to use an unibed approach. This modeling strategy consists of simulating a single column of the PSA train, instead of all columns [41,50,91,92]. The cyclic behaviour of the PSA process allows for this simplification, i.e. all the columns undergo the same steps cyclically. The interactions between different columns were accounted for by virtual gas streams which were defined through the information stored in the previous cycles. Because only a limited amount of information was stored, some precision was lost. Anyway, the accuracy obtained demonstrated to be satisfactory. A virtual gas stream had to be defined for the following steps: *heavy reflux/rinse, purge, pressure equalization - pressurization, light product pressurization*. Using the unibed approach, it is essential to ensure that the material balances are always closed. Specific attention must be paid in the simulation of the *pressure equalization* steps. Given the BCs implemented, which specify the pressure history, an appropriate value of the equalization pressure needs to be set in order to avoid inconsistencies in the material balance. An iterative process to determine the correct pressure value at the end of the pressure equalization steps was implemented, in accordance with the procedure outlined in [41]. The final pressure was the one ensuring that the number of moles flowing out from one bed was balanced to the flow into the other bed, under the assumption that the pressure changes linearly with time.

Physical properties of the gas were evaluated in all the points of the bed through an external physical property package (i.e., Multiflash-Infochem ComputerServices Ltd.) interfaced with gPROMS.

The discretization algorithm applied for the numerical solution of the model is the Centered Finite Difference Method (CFDM). The spatial domain was discretized in 150 intervals, unless otherwise specified. The simulations were run until the cycle steady state (CSS) arose. Even though its inherent dynamic nature, PSA reaches a condition in which the transient behavior of the entire cycle remains constant and repeats itself invariably from cycle to cycle. This condition is termed CSS. CSS occurrence allows connecting the inherently dynamic PSA process to the rest of the plant, which is working in a steady-state mode, though some simplifications of the off-gas streams characteristics needed to be implemented anyway.

3.5 Definition of efficiencies and performance indicators

The performance of the systems investigated were analysed on three different levels in order to get a comprehensive overview.

3.5.1 Energy performance

Since the focus is on the energy sector, the energy performance of the plants is of primary importance. The main indicator used to measure the efficiency of energy conversion is the *net electric efficiency* (η_{el}), referred to the lower heating value of the fuel:

$$\eta_{el} = \frac{\text{Net electric output}}{\text{Coal energy}_{LHV}} \quad (3.62)$$

η_{el} defines how much of the coal energy input is converted to electricity to be exported out of the plant. The net electric output is defined as following:

$$\text{Net electric output} = (\dot{W}_T - \dot{W}_C)\eta_m\eta_g + \dot{W}_{ST}\eta_m\eta_g + \dot{W}_{AE}\eta_m\eta_g - (\dot{W}_{IC} + \dot{W}_P)\eta_m\eta_{drive} - \dot{W}_{aux} \quad (3.63)$$

where \dot{w}_T is GT turbine power (kW), \dot{w}_C is GT compressor power (kW), \dot{w}_{ST} is steam turbine power (kW), \dot{w}_{AE} is air expander power (kW), \dot{w}_{IC} is total power consumption of the intercooled compressors (kW), \dot{w}_P is total power consumption of the pumps (kW), \dot{w}_{aux} is auxiliary power consumption (kW), η_m is the mechanical efficiency, η_g is the generator efficiency and η_{drive} is the efficiency of the drives for the different compressors and pumps. The coal energy (on LHV basis) is defined as following:

$$\text{Coal energy}_{LHV} = \dot{m}_f LHV_f \quad (3.64)$$

where \dot{m}_f is the coal mass flow rate (kg/s) and LHV_f is the coal lower heating value (kJ/kg). This single indicator is sufficient when electricity is the only plant product. The thesis deals also with IGCC plants where ultrapure H_2 is produced together with electricity. In such case the assessment of the plant energy performance is not straightforward and requires setting an analysis framework to compare different energy products. A first additional indicator introduced was the H_2 efficiency (η_{H_2}):

$$\eta_{H_2} = \frac{\text{Ultrapure } H_2 \text{ energy}_{LHV}}{\text{Coal energy}_{LHV}} \quad (3.65)$$

The ultrapure H₂ energy (on LHV basis) is defined as following:

$$\text{Ultrapure H}_2 \text{ energy}_{LHV} = \dot{m}_{H_2} LHV_{H_2} \quad (3.66)$$

where \dot{m}_{H_2} is the ultrapure H₂ mass flow rate (kg/s) and LHV_{H₂} is the ultrapure H₂ lower heating value (kJ/kg). η_{H_2} defines how much of the coal energy input is stored in the ultrapure H₂. The direct comparison of η_{el} and η_{H_2} would put on the same thermodynamic level two different forms of energy (electricity and chemical energy). In order to deal with the issue and define an overall efficiency term which allows an immediate comparison of different systems performances, the energy content of H₂ has been discounted with two different factors. A first approach suggests to assign a thermal efficiency of 0.6 for the conversion of the ultrapure H₂ energy beforehand the comparison with power. This value has been chosen referring to a previous work [93] and can be thought to represent the efficiency of a combined cycle for electricity production. Accordingly, a first *cumulative energy efficiency* ($\eta_{tot\ 60}$) can be defined:

$$\eta_{tot\ 60} = \eta_{el} + 0.6 \cdot \eta_{H_2} \quad (3.67)$$

Despite the arbitrary choice of the multiplying factor, the so defined cumulative efficiency can be a useful way to compare results from different sources. The second approach proposed discounts the H₂ efficiency term with a *power production efficiency* ($\eta_{el\ prod}$):

$$\eta_{el\ prod} = \frac{\text{Gross electric output}}{\text{Syngas energy input in the gas turbine}_{LHV}} \quad (3.68)$$

The gross electric output is defined as following:

$$\text{Gross electric output} = (\dot{W}_T - \dot{W}_C) \eta_m \eta_g + \dot{W}_{ST} \eta_m \eta_g + \dot{W}_{AE} \eta_m \eta_g \quad (3.69)$$

The syngas energy input (on LHV basis) is defined as following:

$$\text{Syngas energy input in the gas turbine}_{LHV} = \dot{m}_s LHV_s \quad (3.70)$$

where \dot{m}_s is the syngas mass flow rate (kg/s) and LHV_s is the syngas lower heating value (kJ/kg). $\eta_{el\ prod}$ takes into account how much of the shifted syngas energy content is converted to power within the system configuration under investigation. A second *cumulative energy efficiency* (η_{tot}^*) is, thus, defined:

$$\eta_{tot}^* = \eta_{el} + \eta_{el\ prod} \cdot \eta_{H_2} \quad (3.71)$$

This second approach allows evaluating how much power could be obtained from ultrapure H₂ if the same efficiency for the energy conversion applies (or other way around, how much power was not produced in order to obtain ultrapure H₂). The drawback is that there is not always enough available information to calculate $\eta_{el\ prod}$.

3.5.2 Gas separation performance

The plants evaluated implement CO₂ capture by PSA technology, thus a key criterion to assess their effectiveness must be related to their CO₂ separation performance. In this sense, some indicators are defined. The gas separation unit must be able to concentrate CO₂ to the levels requested for transport and storage. The *CO₂ purity* (Y_{CO_2}) measures the degree of CO₂ concentration. Y_{CO_2} is defined as the volumetric fraction of CO₂ in the product stream sent to the CO₂ compression unit. An efficient gas separation technology must also be able to capture the largest possible extent of CO₂ processed. The *CO₂ recovery* (R_{CO_2}) is defined as the fraction of the formed CO₂ which is captured and subsequently transported for final storage. The CO₂ formed may originate from various form of carbon in the fuel. R_{CO_2} has the significant drawback that it does not take into account the additional CO₂ formed when a CO₂ capture process is implemented, due to the associated energy penalty. A more accurate indicator should consider the CO₂ actually avoided from being emitted. With regard to that, an additional indicator is introduced, namely the *CO₂ capture efficiency* (η_{CO_2}). η_{CO_2} is the real measure to what extent the CO₂ is captured from a power plant, relatively to a reference plant without CO₂ capture. It can be defined as following:

$$\eta_{CO_2} = 1 - \frac{\eta_{el\ for\ the\ reference\ plant\ without\ CO_2\ capture}}{\eta_{el\ for\ the\ plant\ implementing\ CO_2\ capture}} (1 - R_{CO_2}) \quad (3.72)$$

When evaluating the aforementioned separation performance indicators, it is important to clearly define the system boundaries. If not specified otherwise, the entire plant is considered. However, another possibility limits the analysis to the PSA unit only. In such case, some differences may arise, either in terms of CO₂ concentration in the product stream and CO₂ captured (e.g. an additional purification process is implemented downstream PSA) or in terms of CO₂ formed (e.g. further conversion of carbon-containing compounds to CO₂ downstream the PSA).

H₂ has a primary role in pre-combustion cases. Similar indicators to those relative to CO₂, can be defined. The *H₂ purity* (Y_{H_2}) is the volumetric fraction of H₂ in the product gas stream considered (to avoid misunderstandings the considered product gas stream needs to be clearly specified). The *H₂ recovery* (R_{H_2}) is the fraction of the total H₂

formed which is recovered in a useful product gas stream. The useful product gas streams can be the H₂-rich syngas fueling the gas turbine or the ultrapure H₂ produced by a PSA process. The H₂ formed may originate from gasification and shift processes upstream the separation unit.

3.5.3 *Footprint of the gas separation technology*

One last level to evaluate the effectiveness of the systems under investigation, is to consider the footprint of the gas separation technology used. A large footprint, apart from introducing issues of space availability, may translate in high capital costs. When estimations are provided in the thesis, the footprint of the CO₂ separation technology has been evaluated in terms of size and number of columns necessary for the CO₂ separation process. A more thorough analysis, including all the equipment relative to the separation process, would be needed in order to obtain more reliable outputs, suitable for economic analyses. However, it has been considered beyond the scope of this work.

3.6 Specifications and constraints of the systems

The specifications applying to the different gas streams have been defined in accordance with recommendations from the literature [94,95].

The CO₂-rich gas stream is requested to have a CO₂ volumetric concentration above 95%. Maximum allowable concentrations of impurities are also recommended for safe transport in pipelines. The issues considered are safety and toxicity limits, compression work, hydrate formation, corrosion and free water formation. The desired CO₂ recovery was set to 90%. However, this is a target to approach more than an actual process specification (in some instance it was not possible to reach such recovery level). The final pressure and temperature of the CO₂-rich gas stream after the CO₂ compression process have been set to 110 bar and 28°C, respectively. These conditions allow transporting CO₂ as a dense phase.

Stringent specifications commonly apply for the production of ultrapure H₂. It is normally the end application which sets the requirements for the H₂ purity and other impurities allowed, even though in some cases transport and/or intermediate storage actually puts higher restrictions. Proton Exchange Membrane (PEM) fuel cells set the strictest requirements both on H₂ purity (99.99+% vol.) and on the impurities content. Other applications have more relaxed requirements. When possible, PEM fuel cell specifications were used in the thesis, in order to have the maximum flexibility for the utilization of the H₂ gas stream. Possible additional conditioning processes for the delivery of H₂ have not been taken into account and the ultrapure H₂ is made available at the pressure and temperature at which it leaves the PSA process.

Chapter 4 Results and discussions

This chapter provides a summary of the selected papers, which contain the results achieved. The main outcomes and contributions are reported and discussed for each paper, in a dedicated sub-section. For a more complete overview, the whole papers are enclosed at the end of the thesis.

The order in which papers are presented follows the progression of the thesis work. Alongside the description of the contents, the motivations that led to deal with the specific analysis are outlined. The aim is to shed some light also on the development path of the thesis, pointing out why certain topics were considered more relevant than others and thus were addressed first.

4.1 Paper I - Evaluating Pressure Swing Adsorption as a CO₂ separation technique in coal-fired power plants

In line with the main goal of the thesis, *Paper I* provides with a first assessment on the viability of PSA as a valid option for CCS in coal-fired power plants. The composite models developed were used to evaluate the post- and pre-combustion CO₂ capture cases defined, namely the ASC plant and the IGCC plant integrating a PSA unit for CO₂ separation. The objective was to investigate the competitiveness of PSA with respect to the benchmark technology for CCS in power plants (i.e. absorption). Full-plant analyses were developed, with the performance of the system evaluated in terms of energy efficiency, CO₂ separation performance and footprint of the technology.

The PSA unit into the ASC plant was placed downstream the flue gas treatment processes and had a limited influence on the other units of the plant. The flue gas enters the PSA unit at atmospheric pressure (upstream flue gas compression was evaluated unfeasible for the large power consumption involved). In order to meet the CO₂ separation requirements (i.e. $\geq 90\%$ CO₂ recovery and $\geq 95\%$ CO₂ purity), a two-stage PSA process was necessary. The regeneration of the adsorption columns was carried out at an under-atmospheric pressure (0.1 bar). The resulting CO₂ separation performances were 90.2% CO₂ recovery and 95.1% CO₂ purity. The auxiliary energy consumption of the plant demonstrated to be to large extent due to direct electrical power requirements

for vacuum pumps and compressors. A comparison with chemical absorption technology showed a different energy consumption pattern. The most energy-demanding sub-process in chemical absorption is the regeneration of the solvent, typically using steam in a reboiler. No thermal duty is needed for a PSA process. Despite the substantial difference in the types of energy required, the total energy penalty is similar. The PSA-based case returned a net electric efficiency of 34.8% while the absorption-based case returned 34.2% (the reference plant without CO₂ capture was evaluated to have an efficiency of 45.1%). A serious obstacle to PSA applicability within this framework comes from the analysis of the estimated footprint. In accordance with some key design criteria, taking into account maximum pressure drop and superficial velocity in the adsorption column, the PSA unit would need 265 columns to process the whole flue gas flow rate. Given that the columns were sized to have 8 m diameter and 10 m length, the outcome did not appear acceptable.

Adding a PSA unit into the IGCC plant is more challenging, given the higher level of integration required. The PSA unit, constituted of a single PSA stage, was placed downstream the syngas treatment section and upstream the power island. The high pressure at which the gas stream enters the PSA unit (38.8 bar) avoids the need of under-atmospheric pressure for adsorbent regeneration purposes. The regeneration pressure of the PSA process was set to 1 bar. Since the PSA process was hardly succeeding in fully meeting the established CO₂ separation requirements, an additional purification process was integrated in the CO₂ compression unit. This was a flash separation process able to collect highly concentrated CO₂ in liquid phase. The final CO₂ separation performances were 86.1% CO₂ recovery and 98.9% CO₂ purity. The recovery level was slightly lower than the target. The main energy consumptions are connected to the steam extraction for the WGS process and to the CO₂ compression. A comparative analysis with a plant using physical absorption as CO₂ capture technology was developed. Whilst WGS gave similar energy penalties in both cases, the energy required for CO₂ compression was larger in the PSA case. The CO₂-rich gas stream leaving the PSA unit has to be compressed from 1 bar to 110 bar, whereas the regeneration strategy in the absorption unit releases CO₂-rich streams at three pressure levels (12.7, 7.5 and 1.1 bar). However, the absorption unit introduces other types of energy consumption (i.e. solvent pumping and refrigeration). The energy efficiencies were ultimately similar, even though absorption displayed an advantage (36.2% for the PSA-based plant and 37.1% for the absorption-based plant, while the reference plant without CO₂ capture had 47.3%). The footprint of the PSA unit is significantly less compared to the post-combustion case. A single PSA train (7 columns of 6.6 m diameter and 10 m length) was able to process the entire flow rate of syngas.

The main results achieved with the system analyses for the post- and pre-combustion cases are summarized in *Table 5*.

Table 5. Main outputs of the system analyses for the post- and pre-combustion case.

Plant summary	Post-combustion (ASC)			Pre-combustion (IGCC)		
	No Capture	Absorption	PSA	No Capture	Absorption	PSA
Power input						
Coal flow rate (kg/s)	66,2	66,2	66,2	33,3	38,5	38,5
Coal LHV (MJ/kg)	25,2	25,2	25,2	25,2	25,2	25,2
Net fuel input (MW _{th})	1666	1666	1666	837	968	968
Power output						
Gross electric output (MW)	828	715	827	450	461	460
Net electric output (MW)	751	570	579	396	358	350
Plant performance						
Net electric efficiency (%)	45,1 %	34,2 %	34,8 %	47,3 %	37,1 %	36,2 %
CO ₂ purity (%)	-	100,0 %	95,1 %	-	100,0 %	98,9 %
CO ₂ recovery (%)	-	90,0 %	90,2 %	-	90,6 %	86,1 %
CO ₂ capture efficiency (%)	-	86,8 %	87,3 %	-	88,1 %	81,8 %
Footprint analysis						
Column diameter (m)	-	20,7	8	-	2,2	6,6
Number of columns	-	2	265	-	2	7
Footprint (m ²)	-	674	13285	-	8	239

4.2 Paper II - Comprehensive analysis on the performance of an IGCC plant with a PSA process integrated for CO₂ capture

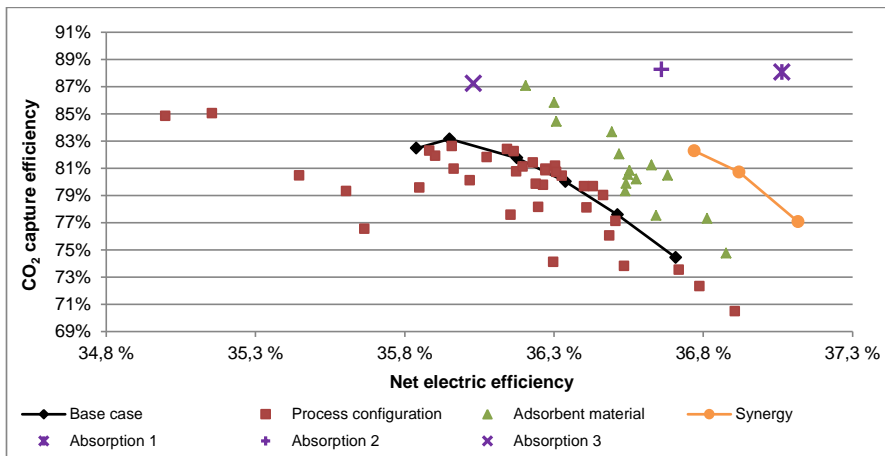
According to the outcome of *Paper I*, the following papers deal with the pre-combustion case. Despite the energy and CO₂ separation performance resulting from the post-combustion analysis was competitive, the footprint issue was considered an obstacle hard to overcome. Even though a different design approach may reduce the number of columns necessary (although with a negative influence on other aspects, e.g. the energy performance) and other strategies are in development (e.g. structured adsorbents [96–98]), the issue appeared difficult to be solved within the considered process framework. Therefore, the choice was to focus on the IGCC plant implementing CO₂ capture through PSA for further analyses.

Paper II provides a comprehensive overview on the performance and the potentials of such system. Physical absorption was again considered the benchmark CO₂ capture technology. The plant performance obtained was evaluated mainly in terms of net electric efficiency and CO₂ capture efficiency. The possible range of performances was investigated by taking into consideration two domains, which were thought to have a significant influence: the process configuration and the adsorbent material.

Several process configurations and operating conditions were tested. Well-thought modifications demonstrated the capability to increase the performance of the plant with regard to a specific performance indicator but, generally, to the detriment of another one. For example, competitive energy penalties could be obtained, at the expense of substantial reduction of the CO₂ capture efficiency.

An analysis on the adsorbent material was also carried out. Given a known activated carbon as starting point, a selected group of properties were varied in a targeted way, in order to simulate advanced adsorbents. Improving the properties of the adsorbent demonstrated to have a significant effect, not only on the CO₂ separation performance but also on the performance of the entire plant. The modification of certain adsorbent material properties demonstrated to have a stronger positive impact (e.g. the heat of adsorption because of its influence on the saturation capacity at different pressures). In accordance to this analysis, some recommendations for the development of improved adsorbents were suggested. Ultimately, the potential performance improvements connected to advancements in material science were established.

Nor modifications in the process or in the adsorbent material were able to fully close the performance gap with absorption, as can be noted in *Figure 25*, which displays all the cases simulated in terms of net electric efficiency and CO₂ capture efficiency.



tailor-made on a given process configuration was defined. The outcome of the process simulations was promising. Net electric efficiencies competitive with the reference absorption values could be obtained. The corresponding CO₂ capture efficiencies, albeit not as high as with absorption, were on acceptable levels (see *Figure 25*). A synergy of process engineering and material science demonstrated to be a key issue for enhancing PSA competitiveness.

4.3 Paper III - Pressure swing adsorption for coproduction of power and ultrapure H₂ in an IGCC plant with CO₂ capture

Paper II showed potentials and limits of PSA as CO₂ capture technology in a pre-combustion framework. Overall, the outcome seems to suggest absorption to have an advantage in the context investigated. On the other hand, the analysis undertaken helped to point out some interesting characteristics of PSA. The complexity of PSA cycles, normally seen as a drawback, allows tuning the process to a large extent and according to specific requirements. A well-thought sequence of steps could be able to produce H₂ with extremely high purity. This has been seen as an opportunity and was investigated in *Paper III*.

The paper analyses an IGCC plant coproducing power and H₂ with CO₂ capture. A variable power-to-hydrogen output, if obtained retaining good plant efficiency, offers advantages in terms of flexible operation, enabling the plant to follow the fluctuations in power demand. In this sense, two novel plant configurations were presented, entirely based on PSA technology. The first configuration relies on two PSA trains in series (*Two-train PSA*). While the main goal of the first train is CO₂ removal from the shifted syngas, the second train further processes part of the H₂-rich off-gas in order to increase the H₂ purity and produce ultrapure H₂. The second configuration assessed relies on a single PSA train (*One-train PSA*). The relative PSA process is able to concentrate CO₂ from the shifted syngas, while producing two different H₂-rich gas streams (an ultrapure H₂ stream and a fuel-grade H₂ stream).

Process simulations showed that both the configurations proposed were able to shift between the two energy products without compromising the plant energy efficiency, while processing a constant coal input. Within the cases analysed, a load variation of about 13% (net power output reduced from 346 MW to 300 MW) was obtained by increasing the ultrapure H₂ throughput (up to a maximum of 163 MW). Further load reductions are considered feasible, as PSA can be designed to handle a rather large range of operating conditions without significant losses in efficiency. Some limitations

arose in the capability of the *One-train PSA* configuration to meet the ultrapure H₂ specifications (H₂ purity of 99.99+% vol.) at different operating conditions. If more relaxed specifications apply, no other issues appeared to limit the flexibility of the PSA process. The cumulative energy efficiency of the plant – defined by properly taking into account the two different products, i.e. electricity and ultrapure H₂ – was rather stable for both configurations tested (between 36.9% and 37.3%) at different output ratios, an essential requirement to realize overall plant flexibility. The CO₂ recovery was also retained on acceptable levels (> 83%). The *Two-train PSA* configuration displayed a small advantage over the *One-train PSA* configuration in terms of cumulative energy efficiency and H₂ purity achieved. On the other hand, the *One-train PSA* configuration relies on a single separation stage, which results in an advantage in terms of footprint.

The common design for an IGCC coproduction system entails an absorption unit for removing CO₂ from a high pressure syngas followed by a PSA unit for purifying a fraction of the resulting H₂-rich gas stream. In this absorption-based configuration, it is common practice to compress the PSA tail gas and feed it to the gas turbine, in order to recover the energy available in the residual H₂ content. The PSA-based configurations allow avoiding this PSA tail gas compression with potential benefits in terms of energy performance. A comparative analysis with absorption-based plants from the literature seems to confirm the effectiveness of the novel configurations proposed, as can be argued by analysing the performances shown in *Table 6*.

Table 6. Main outputs of the system analyses for the IGCC power and H₂ coproduction plants with CO₂ capture based either on PSA or absorption. For the sake of comparison also the performances of the corresponding plants producing only power are reported. The absorption-based cases were taken from the literature.

	Coal input MW	CO ₂ capture technology	R _{CO2} %	Y _{H2} %	η _{H2} %	η _{el} %	η _{tot60} %
Only power PSA	971	PSA	84,6	-	-	36,2	36,2
Two-train PSA	1095	PSA	85,2	99,998	8,4	31,5	36,9
One-train PSA	1088	PSA	85,7	99,983	8,8	31,3	36,6
Only power Abs [99]	1167	Selexol	92,4	-	-	36,0	36,0
Coproduction Abs [99]	1167	Selexol	92,4	99,950	8,6	31,1	36,2

Chapter 5 Conclusions and further work

5.1 Conclusions

Two process designs, involving the integration of a PSA unit for CO₂ capture into coal-fired power plants, were successfully developed. The plants considered were an advanced supercritical pulverized coal (ASC) plant and an integrated gasification combined cycle (IGCC) plant. Full-plant analyses were developed, based on a composite model of the plant, in order to study the competitiveness of the defined systems. The basis for comparison was set to be the same type of plant integrating a more mature technology for CO₂ capture (i.e. chemical or physical absorption).

The post-combustion case analysed (i.e. ASC with CO₂ capture) showed that PSA can be competitive with regard to the separation and the energy performance. PSA was able to match the CO₂ separation requirements (i.e., $Y_{\text{CO}_2} \geq 95\%$ and $R_{\text{CO}_2} \geq 90\%$) and the relative energy penalty was slightly lower than that resulting from an amine-absorption process (a drop in efficiency of 10.3% against 10.9%). However, the footprint of the PSA unit (over 260 adsorption columns needed) demonstrated to be way larger than that related to absorption and unlikely acceptable, neither practically nor economically.

Regarding the pre-combustion case, the PSA-based system performance approached that of the physical absorption counterpart, both in terms of CO₂ separation and plant energy efficiency, albeit not matching it. The obtained CO₂ recovery ($R_{\text{CO}_2} = 86.1\%$) was slightly lower compared to the level aimed (i.e., 90%). The energy penalty due to the integration of the PSA unit was 11.1%, about 0.9% higher compared to the value relative to absorption. The footprint, even though larger than with absorption, appeared to be reasonable for actual implementation.

Overall, the energy and CO₂ separation performances demonstrated to be competitive, especially in the post-combustion case. However, the large footprint is a considerable obstacle to the actual applicability of PSA in that framework. Pre-combustion analysis returned slightly lower performance and a performance gap with regard to absorption was noted, but the footprint was reasonable. Therefore, the integration of PSA in an

IGCC plant was studied more in detailed. A thorough evaluation on the performances achievable in the pre-combustion case was provided. Several process configurations and operating conditions were tested. Tradeoffs between net electric efficiency and CO₂ capture efficiency were observed. The impact on the plant performance of adsorbent material properties modifications was also studied. The most influencing properties were pinpointed and guidelines for future adsorbent materials development were suggested. The potential performance improvements were evaluated. None of the cases studied, either modifying the process or the adsorbent material, returned a performance matching absorption both in terms of net electric efficiency and CO₂ capture efficiency. An additional approach was then outlined to fully realize the potential of the PSA-based pre-combustion system. Tuning adsorbent material properties according to a specific process configuration demonstrated to be critical in order to enhance the plant energy performance on the same level as the absorption-based counterpart, albeit the achieved CO₂ recovery could not meet the 90% target.

The possibility of using PSA to coproduce power and ultrapure H₂ within an IGCC plant with CO₂ capture was also assessed. Two novel plant configurations were defined, able to provide a flexible power-to-hydrogen output ratio. The first configuration proposed relies on two PSA trains in series (*Two-train PSA*), while the second configuration succeeds to carry out both CO₂ separation and H₂ purification within a single PSA stage (*One-train PSA*). Simulations of these systems successfully shifted between the two plant products, at constant coal input and retaining good plant efficiency. The net power output could be reduced from 346 MW to 300 MW by increasing the ultrapure H₂ throughput. Larger load variations are evaluated realistically achievable given a minimum redesign of the PSA processes. The *Two-train PSA* configuration achieved higher performance in terms of energy efficiency and H₂ purity. The *One-train PSA* configuration returned lower but still good performance, while its design includes a gas single separation stage instead of two. The novel PSA-based configurations were also assessed in comparison with the common coproduction layout, consisting of an absorption unit for CO₂ capture and a PSA unit for H₂ purification. Using PSA as the only gas separation technology appeared advantageous on an energy efficiency point of view and higher cumulative energy efficiencies could be achieved (36.9% and 36.6% versus 36.2%).

5.2 Further work

In accordance with the overall goal, the thesis work provides an evaluation on PSA as CO₂ capture technology in different coal-based power generation systems. Being a first assessment, it does not demand completeness but rather to give a reliable indication on the current state-of-the-art and on future prospects. Common adsorbent materials and

processes were considered in the analyses. The set of outcomes obtained can constitute the starting point for further work, as it can provide guidelines on which process frameworks are worth of analysis and on which issues need to be addressed.

In the post-combustion case, PSA clearly shows its limitations with regard to the capability to process large flue gas volumes with reasonable footprints. Therefore, further work is suggested to investigate new options to deal with this issue. It would be interesting to assess the advantages coming along with the utilization of structured adsorbents. In particular to verify if this group of adsorbents would be able to provide a substantial benefit on the process footprint without decreasing the CO₂ separation performance. Otherwise, different process frameworks are probably to be considered (e.g. moving bed adsorption reactors). Other analyses are also possible, for instance the utilization of different adsorbents or the attempt to carry out the separation process within one PSA stage, but their investigation should be subject to the solution of the footprint issue.

Regarding the pre-combustion case, some additional analyses can be recommended. It would be interesting to evaluate the performance of adsorbents developed following the guidelines suggested in the thesis, with properties tuned on specific process configurations. The expertise acquired on the integration of adsorption systems into power plants can be utilized for the optimization of sorption enhanced processes (e.g. sorption enhanced water-gas shift), which already demonstrated to be rather promising. The coproduction process framework is also worth additional analyses. The absolute novelty of the process designs defined leaves doors open for improvements. Optimized PSA processes can be investigated and the mechanisms to switch between power and ultrapure H₂ as well. It would be of importance to evaluate the actual degree of flexibility which can be achieved within those configurations, i.e. evaluate to what extent the load of the plant can be decreased while retaining good plant efficiency.

In order to complete the evaluation of PSA processes for CO₂ capture, some additional suggestions are provided. The comparative analyses with other decarbonization processes were often carried out referring to results taken from the literature, for instance in the coproduction framework. The literature-based cases were selected to match to a large extent the set of fundamental assumptions used in the thesis, so to ensure fair comparisons. However, some differences were necessarily present. An improvement of the work could be developing accurate modeling frameworks for all the cases analysed (with or without a PSA unit), based on common modeling assumptions. The standardization process could also involve the models already developed, which could be improved according to new guidelines. This would enhance the reliability of the comparisons. Additionally, a techno-economic analysis would increase the value of the overall evaluation. Some estimates showing the absolute level and the proportion of

the capital and operating costs would provide elements of importance in the analysis of the approaches proposed.

Further, the developed system analysis framework applies some simplifying assumptions and overlooks some aspects which may need to be looked into more in depth. An example is the integration between the inherently dynamic PSA process and the other units of the system. A proper scheduling of the PSA cycle was considered in order to ensure continuous operation. However, some simplifications apply with regard to the gas streams leaving the PSA unit. Possible fluctuations of the characteristics (e.g. composition, flow rate, etc.) of these gas streams were not taken into account whereas properly averaged values were used. On the other hand, irregular feeding can be problematic for some equipment, like gas turbine or compressors. An evaluation of the effect on turbomachinery equipment should be provided and methodologies to smooth out those variations (e.g. buffer tanks or special scheduling) should be subject of analysis. This necessity is even more stressed for off-design modes of operation, like those applying when a varying power-to-hydrogen output ratio is requested.

References

- [1] Working group III of the IPCC. IPCC special report on carbon dioxide capture and storage. vol. 2. New York: Cambridge University Press; 2005.
- [2] Herzog H, Meldon J, Hatton A. Advanced Post-Combustion CO₂ Capture. 2009.
- [3] Jansen D, Gazzani M, Manzolini G, Dijk E Van, Carbo M. Pre-combustion CO₂ capture. *Int J Greenh Gas Control* 2015;40:167–87.
- [4] Shafeeyan MS, Daud WMAW, Houshmand A, Arami-Niya A. Ammonia modification of activated carbon to enhance carbon dioxide adsorption: Effect of pre-oxidation. *Appl Surf Sci* 2011;257:3936–42.
- [5] Gray ML, Soong Y, Champagne KJ, Pennline H, Baltrus JP, Stevens RW, et al. Improved immobilized carbon dioxide capture sorbents. *Fuel Process Technol* 2005;86:1449–55.
- [6] Ko D, Siriwardane R, Biegler LT. Optimization of a pressure-swing adsorption process using zeolite 13X for CO₂ sequestration. *Ind Eng Chem Res* 2003;42:339–48.
- [7] Ho MT, Allinson GW, Wiley DE. Reducing the Cost of CO₂ Capture from Flue Gases Using Pressure Swing Adsorption. *Ind Eng Chem Res* 2008;47:4883–90.
- [8] Glier JC, Rubin ES. Assessment of solid sorbents as a competitive post-combustion CO₂ capture technology. *Energy Procedia* 2013;37:65–72.
- [9] National Academy of Sciences & The Royal Society. Climate Change Evidence & Causes. Retrieved from: <http://nas-sites.org/americasclimatechoices/events/a-discussion-on-climate-change-evidence-and-causes/>. 2014.
- [10] IPCC. Climate Change 2014: Synthesis Report. Contribution of Working Groups I, II and III to the Fifth Assessment Report of the Intergovernmental Panel on Climate Change. Retrieved from: <http://www.ipcc.ch/report/ar5/syr/>. 2014.
- [11] IEA. World Energy Outlook Special Report 2015: Energy and climate change. Retrieved from: <http://www.worldenergyoutlook.org/>. 2015.
- [12] IEA. Technology Roadmap - Carbon capture and storage. Retrieved from: <http://www.iea.org/publications/freepublications/publication/technology-roadmap-carbon-capture-and-storage-2013.html>. 2013.
- [13] IEA. Energy Technology Perspectives 2012 - Pathways to a Clean Energy System. Retrieved from: <http://www.iea.org/etp/>. 2012.
- [14] Global CCS Institute. The Global Status of CCS: 2014. Retrieved from: <http://www.globalccsinstitute.com/in-focus/global-status-ccs-2014>. 2014.
- [15] IEA Greenhouse Gas R&D Programme, Stork Engineering Consultancy. Leading options for the capture of CO₂ emissions at power stations. Report Number PH3/14. 2000.
- [16] Abu-Zahra M, Abbas Z, Singh P, Feron P. Carbon Dioxide Post-Combustion Capture: Solvent Technologies Overview, Status and Future Directions. Mater.

- Process. energy Commun. Curr. Res. Technol. Dev., 2013.
- [17] Stanger R, Wall T, Spörl R, Paneru M, Grathwohl S, Weidmann M, et al. Oxyfuel combustion for CO₂ capture in power plants. *Int J Greenh Gas Control* 2015;40:55–125.
 - [18] Geankoplis CJ. *Transport Processes and Unit Operations (includes unit operations)*. Prentice Hall Press 2003:905.
 - [19] Choi S, Drese JH, Jones CW. Adsorbent materials for carbon dioxide capture from large anthropogenic point sources. *ChemSusChem* 2009;2:796–854.
 - [20] Hedin N, Chen L, Laaksonen A. Sorbents for CO₂ capture from flue gas aspects from materials and theoretical chemistry. *Nanoscale* 2010;2:1819–41.
 - [21] Hedin N, Andersson L, Bergström L, Yan J. Adsorbents for the post-combustion capture of CO₂ using rapid temperature swing or vacuum swing adsorption. *Appl Energy* 2013;104:418–33.
 - [22] Samanta A, Zhao A, Shimizu GKH, Sarkar P, Gupta R. Post-Combustion CO₂ Capture Using Solid Sorbents: A Review. *Ind Eng Chem Res* 2012;51:1438–63.
 - [23] Siriwardane R V., Shen MS, Fisher EP, Poston JA. Adsorption of CO₂ on molecular sieves and activated carbon. *Energy and Fuels* 2001;15:279–84.
 - [24] Yaghi OM, O’Keeffe M, Ockwig NW, Chae HK, Eddaoudi M, Kim J. Reticular synthesis and the design of new materials. *Nature* 2003;423:705–14.
 - [25] Férey G. Hybrid porous solids: past, present, future. *Chem Soc Rev* 2008;37:191–214.
 - [26] Tafipolsky M, Amirjalayer S, Schmid R. Atomistic theoretical models for nanoporous hybrid materials. *Microporous Mesoporous Mater* 2010;129:304–18.
 - [27] Sumida K, Rogow DL, Mason JA, McDonald TM, Bloch ED, Herm ZR, et al. Carbon Dioxide Capture in Metal-Organic Frameworks. *Chem Rev* 2012;112:724–81.
 - [28] Casas N, Schell J, Blom R, Mazzotti M. MOF and UiO-67/MCM-41 adsorbents for pre-combustion CO₂ capture by PSA: Breakthrough experiments and process design. *Sep Purif Technol* 2013;112:34–48.
 - [29] Yang RT. *Gas Separation by Adsorption Processes*. London: London Imperial College Press; 1997.
 - [30] Agarwal A, Biegler LT, Zitney SE. A Superstructure-Based Optimal Synthesis of PSA Cycles for Post-Combustion CO₂ Capture. *Aiche J* 2010;56:1813–28.
 - [31] Mehrotra A, Ebner AD, Ritter JA, Ebner AD, Mehrotra A, Ebner AD, et al. Arithmetic approach for complex PSA cycle scheduling. *Adsorpt - J Int Adsorpt Soc* 2010;16:113–26.
 - [32] Reynolds S, Ebner A, Ritter J. Stripping PSA cycles for CO₂ recovery from flue gas at high temperature using a hydrotalcite-like adsorbent. *Ind Eng Chem Res* 2006;42:78–94.
 - [33] Zhang J, Webley P, Xiao P. Effect of process parameters on power requirements of vacuum swing adsorption technology for CO₂ capture from flue gas. *Energy*

- Convers Manag 2008;49:346–56.
- [34] Xiao P, Zhang J, Webley P, Li G, Singh R, Todd R. Capture of CO₂ from flue gas streams with zeolite 13X by vacuum-pressure swing adsorption. *Adsorption* 2008;14:575–82.
- [35] Delgado JA, Uguina MA, Sotelo JL, Águeda VI, Sanz A, Gómez P. Numerical analysis of CO₂ concentration and recovery from flue gas by a novel vacuum swing adsorption cycle. *Comput Chem Eng* 2011;35:1010–9.
- [36] Liu Z, Grande CA, Li P, Yu J, Rodrigues AE. Multi-bed vacuum pressure swing adsorption for carbon dioxide capture from flue gas. *Sep Purif Technol* 2011;81:307–17.
- [37] Shen C, Liu Z, Li P, Yu J. Two-stage VPSA process for CO₂ capture from flue gas using activated carbon beads. *Ind Eng Chem Res* 2012;51:5011–21.
- [38] Haghpanah R, Majumder A, Nilam R, Rajendran A, Farooq S, Karimi IA, et al. Multiobjective optimization of a four-step adsorption process for postcombustion CO₂ capture via finite volume simulation. *Ind Eng Chem Res* 2013;52:4249–65.
- [39] Haghpanah R, Nilam R, Rajendran A, Farooq S, Karimi IA. Cycle Synthesis and Optimization of a VSA Process for Postcombustion CO₂ Capture. *Aiche J* 2013;59:4735–48.
- [40] Krishnamurthy S, Rao VR, Guntuka S, Sharratt P, Haghpanah R, Rajendran A, et al. CO₂ capture from dry flue gas by Vacuum Swing Adsorption: a pilot plant study. *AIChE J* 2014;60:1830–42.
- [41] Casas N, Schell J, Joss L, Mazzotti M. A parametric study of a PSA process for pre-combustion CO₂ capture. *Sep Purif Technol* 2013;104:183–92.
- [42] García S, Gil M V., Pis JJ, Rubiera F, Pevida C. Cyclic operation of a fixed-bed pressure and temperature swing process for CO₂ capture: Experimental and statistical analysis. *Int J Greenh Gas Control* 2013;12:35–43.
- [43] Abanades JC, Arias B, Lyngfelt A, Mattisson T, Wiley DE, Li H, et al. Emerging CO₂ capture systems. *Int J Greenh Gas Control* 2015.
- [44] Ebner AD, Ritter JA. State-of-the-art Adsorption and Membrane Separation Processes for Carbon Dioxide Production from Carbon Dioxide Emitting Industries. vol. 44. 2009.
- [45] Park J-H, Kim J-N, Cho S-H, Kim J-D, Yang RT. Adsorber dynamics and optimal design of layered beds for multicomponent gas adsorption. *Chem Eng Sci* 1998;53:3951–63.
- [46] Yang J, Lee C. Adsorption dynamics of a layered bed PSA for H₂ recovery from coke oven gas. *AIChE J* 1998;44:1325–34.
- [47] Ahn H, Yang J, Lee C-H. Effects of Feed Composition of Coke Oven Gas on a Layered Bed H₂ PSA Process. *Adsorption* 2001;7:339–56.
- [48] Sircar S, Golden TC. Purification of Hydrogen by Pressure Swing Adsorption. *Sep Sci Technol* 2000;35:667–87.
- [49] Ribeiro AM, Grande CA, Lopes FVS, Loureiro JM, Rodrigues AE. A parametric

- study of layered bed PSA for hydrogen purification. *Chem Eng Sci* 2008;63:5258–73.
- [50] Ribeiro AM, Grande CA, Lopes FVS, Loureiro JM, Rodrigues AE. Four beds pressure swing adsorption for hydrogen purification: Case of humid feed and activated carbon beds. *AIChE J* 2009;55:2292–302.
- [51] Lopes FVS, Grande CA, Ribeiro AM, Oliveira ELG, Loureiro JM, Rodrigues AE. Enhancing capacity of activated carbons for hydrogen purification. *Ind Eng Chem Res* 2009;48:3978–90.
- [52] Lopes FVS, Grande CA, Rodrigues AE. Activated carbon for hydrogen purification by pressure swing adsorption: Multicomponent breakthrough curves and PSA performance. *Chem Eng Sci* 2011;66:303–17.
- [53] Ahn S, You YW, Lee DG, Kim KH, Oh M, Lee CH. Layered two- and four-bed PSA processes for H₂ recovery from coal gas. *Chem Eng Sci* 2012;68:413–23.
- [54] Luberti M, Friedrich D, Brandani S, Ahn H. Design of a H₂ PSA for cogeneration of ultrapure hydrogen and power at an advanced integrated gasification combined cycle with pre-combustion capture. *Adsorption* 2014;20:511–24.
- [55] Sircar S, Kratz WC. Simultaneous Production of Hydrogen and Carbon Dioxide from Steam Reformer Off-Gas by Pressure Swing Adsorption. *Sep Sci Technol* 1988;23:2397–415.
- [56] Krishnamurthy R, Malik VA, Stokley AG. Hydrogen and carbon dioxide coproduction, 1990.
- [57] Couche MR. Hydrogen generation process. US005669960A, 1997.
- [58] Federal Institute for Geoscience and Natural Resources (BGR). Energy study 2014. Reserves, Resources and Availability of Energy Resources. Hannover: 2014.
- [59] Massachusetts Institute of Technology. The Future of Coal - An interdisciplinary MIT study. Retrieved from: <http://web.mit.edu/coal/>. 2007.
- [60] NETL. Cost and Performance Baseline for Fossil Energy Plants Volume 1a: Bituminous Coal (PC) and Natural Gas to Electricity. DOE/NETL-2015/1723. 2015.
- [61] ECOFYS. International comparison of fossil power efficiency and CO₂ intensity - Update 2014. Final report. Project number: CESNL15173. 2014.
- [62] Miller BG. Coal Energy Systems. Elsevier Academic Press; 2005.
- [63] Maurstad O. An Overview of Coal based Integrated Gasification Combined Cycle (IGCC) Technology. Massachusetts Institute of Technology - Laboratory for Energy and the Environment. Publication No. LFEE 2005-002 WP. 2005.
- [64] NETL. Cost and Performance Baseline for Fossil Energy Plants Volume 1b: Bituminous Coal (IGCC) to Electricity. Revision 2b – Year Dollar Update. DOE/NETL-2015/1727. 2015.
- [65] Botero C, Field RP, Herzog HJ, Ghoniem AF. The Phase Inversion-based Coal-CO₂ Slurry (PHICCOS) feeding system: Technoeconomic assessment using

- coupled multiscale analysis. *Int J Greenh Gas Control* 2013;18:150–64.
- [66] Gazzani M, Macchi E, Manzolini G. CO₂ capture in integrated gasification combined cycle with SEWGS - Part A: Thermodynamic performances. *Fuel* 2013;105:206–19.
- [67] EBTF. DECARBit: Enabling advanced pre-combustion capture techniques and plants. European best practice guidelines for assessment of CO₂ capture technologies. Project FP7 - ENERGY.2007.5.1.1. 2011.
- [68] Bolland O. CO₂ Capture in power plants - Compendium. 2013.
- [69] Thermoflow Inc. Thermoflow Version 24.0 2014.
- [70] Process System Enterprise Limited. gPROMS 4.1.0 2015.
- [71] Aspen Technology Inc. Aspen HYSYS V7.3 2012.
- [72] Pipitone G, Bolland O. Power generation with CO₂ capture: Technology for CO₂ purification. *Int J Greenh Gas Control* 2009;3:528–34.
- [73] Posch S, Haider M. Optimization of CO₂ compression and purification units (CO₂CPU) for CCS power plants. *Fuel* 2012;101:254–63.
- [74] Ruthven DM. Principle of adsorption and adsorption processes. John Wiley & Sons; 1984.
- [75] Agarwal A. Advanced Strategies for Optimal Design and Operation of Pressure Swing Adsorption Processes. Carnegie Mellon University, 2010.
- [76] Wakao N, Funazkri T. Effect of fluid dispersion coefficients on particle-to-fluid mass transfer coefficients in packed beds. *Chem Eng Sci* 1978;33:1375–84.
- [77] Fuller EN, Schettler PD, Giddings JC. A new method for prediction of binary gas-phase diffusion coefficients. *Ind Eng Chem* 1966;16:551.
- [78] Poling BE, Prausnitz JM, O'Connell JP. The Properties of Gases and Liquids. 5th editio. McGraw - Hill; 2001.
- [79] Shafeeyan MS, Wan Daud WMA, Shamiri A. A review of mathematical modeling of fixed-bed columns for carbon dioxide adsorption. *Chem Eng Res Des* 2014;92:961–88.
- [80] Glueckauf E, Coates JI. Theory of Chromatography. Part IV. The Influence of Incomplete Equilibrium on the Front Boundary of Chromatograms and on the Effectiveness of Separation. *J Chem Soc* 1947.
- [81] Liu Z, Grande CA, Li P, Yu J, Rodrigues AE. Adsorption and Desorption of Carbon Dioxide and Nitrogen on Zeolite 5A. *Sep Sci Technol* 2011;46:434–51.
- [82] Lopes FVS, Grande CA, Ribeiro AM, Loureiro JM, Evaggelos O, Nikolakis V, et al. Adsorption of H₂, CO₂, CH₄, CO, N₂ and H₂O in activated carbon and zeolite for hydrogen production. *Sep Sci Technol* 2009;44:1045–73.
- [83] Yuçel H, Ruthven DM. Diffusion of CO₂ in 4A and 5A zeolite crystals. *J Colloid Interface Sci* 1980;74:186–95.
- [84] Wakao N, Kaguei S. Heat and mass transfer in packed beds. Gordon and Breach Science Publishers; 1982.
- [85] Leva M. Heat Transfer to Gases through Packed Tubes. *Ind Eng Chem* 1947.

- [86] Incropera FP, DeWitt DP, Bergman TL, Lavine AS. *Fundamentals of Heat and Mass Transfer*. vol. 6th. John Wiley & Sons; 2007.
- [87] Froment GF, Bischoff KB, De Wilde J. *Chemical Reactor Analysis and Design*. 3rd ed. John Wiley & Sons; 2011.
- [88] Schell J, Casas N, Marx D, Mazzotti M. Precombustion CO₂ Capture by Pressure Swing Adsorption (PSA): Comparison of Laboratory PSA Experiments and Simulations. *Ind Eng Chem Res* 2013;52:8311–22.
- [89] Cen P, Yang RT. Separation of a Five-Component Gas Mixture by Pressure Swing Adsorption. *Sep Sci Technol* 1985;20:725–47.
- [90] Yang RT, Doong SJ. Gas Separation by Pressure Swing Adsorption: A Pore-Diffusion Model for Bulk Separation. *AIChE J* 1985;31:1829–985.
- [91] Park J-H, Kim J-N, Cho S-H. Performance Analysis of Four-Bed H₂ PSA Process Using Layered Beds. *AIChE J* 2000;46:790–802.
- [92] Jiang L, Fox VG, Biegler LT. Simulation and optimal design of multiple-bed pressure swing adsorption systems. *AIChE J* 2004;50:2904–17.
- [93] Li M, Rao AD, Scott Samuelsen G. Performance and costs of advanced sustainable central power plants with CCS and H₂ co-production. *Appl Energy* 2012;91:43–50.
- [94] DYNAMIS. *Towards Hydrogen and Electricity Production with Carbon Dioxide Capture and Storage*. 2007.
- [95] de Visser E, Hendriks C, Barrio M, Mølnvik MJ, de Koeijer G, Liljemark S, et al. Dynamis CO₂ quality recommendations. *Int J Greenh Gas Control* 2008;2:478–84.
- [96] Rezaei F, Mosca A, Webley P, Hedlund J, Xiao P. Comparison of traditional and structured adsorbents for CO₂ separation by vacuum-swing adsorption. *Ind Eng Chem Res* 2010;49:4832–41.
- [97] Thiruvenkatachari R, Su S, Yu XX, Jin Y. A site trial demonstration of CO₂ capture from real flue gas by novel carbon fibre composite monolith adsorbents. *Int J Greenh Gas Control* 2015;42:415–23.
- [98] Brandani F, Rouse A, Brandani S, Ruthven DM. Adsorption Kinetics and Dynamic Behavior of a Carbon Monolith. *Adsorption* 2004;10:99–109.
- [99] Cormos CC. Assessment of hydrogen and electricity co-production schemes based on gasification process with carbon capture and storage. *Int J Hydrogen Energy* 2009;34:6065–77.

Papers

Paper I

Evaluating Pressure Swing Adsorption as a CO₂ separation technique in coal-fired power plants

Luca Riboldi, Olav Bolland

International Journal of Greenhouse Gas Control 139, 1-16 (2015)



Evaluating Pressure Swing Adsorption as a CO₂ separation technique in coal-fired power plants



Luca Riboldi*, Olav Bolland

Energy and Process Engineering Department, The Norwegian University of Science and Technology, NO-7491 Trondheim, Norway

ARTICLE INFO

Article history:

Received 2 December 2014

Received in revised form 28 January 2015

Accepted 4 February 2015

Keywords:

CO₂ capture

Process simulations

Coal-fired power plants

Pressure Swing Adsorption

Efficiency penalty

ABSTRACT

The paper provides with a first assessment on the suitability of Pressure Swing Adsorption (PSA) as a valid option for Carbon Capture and Storage (CCS) in coal-fired power plants. A full-plant analysis of an Advanced SuperCritical (ASC) pulverized coal plant and of an Integrated Gasification Combined Cycle (IGCC) plant, operating with a PSA unit, is presented. The systems selected aim to represent the most diffused options for coal-based power generation, respectively in a post- and pre-combustion application of CO₂ separation. The definition of the PSA process is tailored for the two different scenarios considered, starting from the adsorbent selected (zeolite 5A and activated carbon, respectively for post- and pre-combustion). The objective is to investigate the competitiveness of PSA with respect to the benchmark technology for CCS, namely absorption. In order to consider the different aspects measuring the effectiveness of a CO₂ separation technique, the performance of the power plants is evaluated in terms of CO₂ separation performance, energy efficiency and footprint of the technology. The post-combustion scenario analysis shows that PSA can be competitive with regard to the separation and the energy performance. PSA is able to match the CO₂ separation requirements, and the relative energy penalty is slightly lower than that resulting from amine-absorption. Despite that, the footprint of the PSA unit demonstrates to be way larger than that related to absorption and unlikely acceptable. PSA in the pre-combustion scenario returns more encouraging results, approaching the outcomes achieved with absorption both in terms of CO₂ separation performance and plant energy efficiency. The footprint, even though significantly larger than with absorption, appears to be reasonable for actual implementation.

© 2015 Elsevier Ltd. All rights reserved.

1. Introduction

The atmospheric concentration of carbon dioxide (CO₂) has increased by 40% since pre-industrial times, and recently passed the 400 ppm milestone. CO₂ is regarded as the main responsible for the atmospheric greenhouse effect, which is producing the warming of the climate system. It is extremely likely that human influence has been the dominant cause of the observed warming (IPCC, 2013). One possible mitigation action for stabilizing the atmospheric CO₂ concentration, while continuing exploiting fossil fuel resources, is Carbon dioxide Capture and Storage (CCS). CCS consists in separating CO₂ from large anthropogenic point sources, such as thermal power plants, compressing it for transportation and permanently storing it in underground geological formation. There are different types of CO₂ capture systems: post-combustion,

pre-combustion and oxyfuel combustion (IPCC, 2005). Many different techniques have been proposed for capturing CO₂. These includes: chemical or physical absorption, adsorption, reactive solids, membranes, cryogenic processes (Ebner and Ritter, 2009). To date, all commercial CO₂ capture plants are based on absorption for separating CO₂ (Herzog et al., 2009), as it is the most mature and well understood technology. However, its large scale deployment is hindered by the large power consumption, which negatively affects the energy efficiency of the plant. That, summed to other concerns related to the solvent toxicity and to the potentially high corrosion rate, makes advisable to investigate alternatives. In the current work, Pressure Swing Adsorption (PSA) process is analyzed as an option for post- and pre-combustion CO₂ capture. PSA is a cyclic process. During the adsorption step, the CO₂ present in the feed gas stream is fixed on the surface of the selected adsorbent. Following, the regeneration of the bed is carried out by a pressure swing operation. The potential advantage connected to this process is the absence of any thermal energy duty during the regeneration step. Adsorption processes have been successfully employed for CO₂ removal from synthesis gas for hydrogen production

* Corresponding author at: Kolbjørn Hejes vei 1a, NO-7491 Trondheim, Norway. Tel.: +47 735 93559.

E-mail address: luca.riboldi@ntnu.no (L. Riboldi).

Nomenclature

a_i	number of neighboring sites occupied by adsorbate molecule for species i
C_i	gas concentration of species i , mol/m ³
C_p	specific heat at constant pressure, MJ/(kg K)
$C_{p,ads}$	adsorbed phase specific heat at constant pressure, J/(kg K)
$C_{p,g}$	gas specific heat at constant pressure, J/(mol K)
$C_{p,s}$	particle specific heat at constant pressure, J/(kg K)
C_{tot}	total gas concentration, mol/m ³
$D_{ax,i}$	axial dispersion coefficient of species i , m ² /s
$D_{c,i}$	micropore diffusivity of species i , m ² /s
$D_{0c,i}$	limiting micropore diffusivity at infinite temperature of species i , m ² /s
$D_{mg,i}$	multicomponent diffusion coefficient of species i , m ² /s
$D_{g,ij}$	binary diffusion coefficient of the ij system, m ² /s
d_p	particle diameter, m
$E_{a,i}$	activation energy of species i , J/mol
$\Delta H_{r,i}$	heat of adsorption of species i , J/mol
k_f	gas conductivity, J/(s m K)
k_i	equilibrium constant of species i , Pa ⁻¹
$k_{\infty,i}$	adsorption constant at infinite temperature of species i , Pa ⁻¹
$k_{LDF,i}$	linear driving force coefficient, s ⁻¹
\dot{m}	mass flow rate, kg/s
\dot{n}	mole flow rate, mol/s
P	pressure, Pa
P_{CO_2}	CO ₂ purity
Pr	Prandtl number
q_i^*	equilibrium adsorbed concentration of species i , mol/kg
\bar{q}_i	averaged adsorbed concentration of species i , mol/kg
$q_{m,i}$	specific saturation adsorption capacity of species i , mol/kg
R	universal gas constant, Pa m ³ /(mol K)
R_{CO_2}	CO ₂ recovery
R_{H_2}	H ₂ recovery
Re	Reynolds number
r_c	crystal radius, m
T	temperature, K
u_s	superficial velocity, m/s
y_i	mole fraction of species i
z	axial direction, m

Greek letters

γ	specific heat ratio
ε	bed porosity
ε_p	particle porosity
η_{CO_2}	CO ₂ capture efficiency
η_{is}	isentropic efficiency
η_{net}	net electric efficiency
λ_{ax}	axial thermal dispersion coefficient, J/(s m K)
μ	dynamic viscosity, Pa s
ξ_i	diffusion parameter for species i
ρ_g	gas volumetric mass density, kg/m ³
ρ_p	volumetric mass density of the particle, kg/m ³
χ_{LDF}	linear driving force geometrical factor (15 for zeolite 5A, 3 for activated carbon)

Acronyms

ASC	advanced supercritical
C	compressor
CCS	carbon capture and storage
DHU	dehydration unit
FS	flash separator
IC	inter-cooler
IGCC	integrated gasification combined cycle
LHV	lower heating value
LDF	linear driving force
MSHE	multi stream heat exchanger
PSA	pressure swing adsorption
TV	throttling valve
WGS	water gas shift

Subscripts

i	species
-----	---------

Superscripts

NC	number of components
----	----------------------

(Cen and Yang, 1986; Ribeiro et al., 2008, 2009; Yang and Lee, 1998; Yang et al., 1997). With regard to CCS applications, PSA process suitability has to be proven yet. A large number of studies have been done in order to assess PSA processes operating in the condition typical of post- (Agarwal et al., 2010; Choi et al., 2003; Chou and Chen, 2004; Ishibashi et al., 1996; Kikkinides et al., 1993; Ko et al., 2005; Liu et al., 2011a; Mehrotra et al., 2010; Na et al., 2001, 2002; Nikolic et al., 2008; Plaza et al., 2010; Reynolds et al., 2006; Takamura et al., 2001; Tlili et al., 2009) and pre-combustion (Casas et al., 2013; Schell et al., 2013) applications. A significant lack was found in the analysis of more comprehensive systems (The Future of Coal, 2007), where the PSA process is integrated with the rest of the plant. Few works deal with the understanding of such complex arrangements. In post-combustion applications, only preliminary studies have been carried out, whose results can be considered partial (Panowski et al., 2010) and/or focusing on a particular side of the topic (e.g., economic considerations) (Ho et al., 2008). In pre-combustion applications, more thorough analyses have been performed. Liu and Green (2014) evaluated the applicability of PSA as CO₂ removal technology in an Integrated Gasification Combined Cycle (IGCC). They simulated a warm PSA process based on a tailored adsorbent, able to perform at elevated temperature. The results achieved are in line with those of a Selexol absorption process. Other studies investigated the performance of Sorption Enhanced Water Gas Shift (SEWGS), an innovative CO₂ capture process for pre-combustion applications, applied to both IGCC (Gazzani et al., 2013) and Natural Gas Combined Cycle (NGCC) (Manzolini et al., 2011). In either case the outcome appears to be extremely promising. The objective of this paper is to provide a full-plant analysis of coal-fired plants implementing CO₂ capture by a cold PSA process, meaning that the process takes place at temperature levels suitable for many of the most common adsorbents. Coal was selected as fuel because of its higher emission index (higher CO₂ emission per unit of energy released). Further, coal utilization is predicted to increase in the future, under any foreseeable scenario (The Future of Coal, 2007). Thus, CCS will become a critical tool in order to enable a sustainable exploitation of coal. Two plant configurations were considered, respectively to account for a post- and a pre-combustion scenario. Post-combustion CO₂ capture is implemented by integrating a PSA process into an Advanced SuperCritical (ASC) pulverized coal plant. Pre-combustion CO₂ capture is implemented by integrating a PSA process into an Integrated

Gasification Combined Cycle (IGCC) plant. First, the layout of the thermal power plant, to be coupled with the CO₂ capture unit, is defined and modeled. Following, the modeling of the PSA process is presented resulting in a dynamic computational model. The procedure for the choice of the optimal PSA process configuration is outlined. A full-plant analysis is then provided for both the scenarios. Simulations were also implemented for the reference case without CO₂ capture and for the case with CO₂ capture based on an absorption process. A plant-level comparison is carried out, returning the competitiveness of PSA process with regard to another technique of decarbonization (i.e., state-of-the-art absorption processes). The performance of the system is evaluated on three levels, namely CO₂ separation performance, energy efficiency and footprint of the technology.

2. Modeling of the power plant

The model of the power plant was developed by ThermoFlow Inc. products: STEAM PRO, GT PRO and THERMOFLEX. The focus is on coal-fired power plants, since combustion of coal produces high specific emission of CO₂ per unit of electricity generated. Accordingly, two thermal power plant layouts were selected to represent the most common systems for coal-based power generation. These systems are an Advanced SuperCritical (ASC) pulverized coal plant and an Integrated Gasification Combined Cycle (IGCC) plant, respectively constituting the basis for the post- and pre-combustion CO₂ capture scenario.

First, a baseline case without CO₂ capture was modeled. The purpose was to benchmark the coal-fired power plant, in order to have a reference case for comparisons. However, the object of the study is to assess the plant performance when CO₂ capture is implemented. Therefore, the mentioned plants were equipped with a CO₂ capture unit. A mature technology for separating CO₂ from the gas stream already exists (i.e., absorption). For the sake of fair comparisons between different CO₂ capture technologies, models were developed for the plants with state-of-the-art absorption CO₂ capture processes. For the post-combustion scenario, a MEA-based chemical absorption process was considered. For the pre-combustion scenario, a Selexol-based two-stage absorption process was considered. Finally, the same power plants coupled to a PSA process for CO₂ capture were modeled, as this constitutes the core of the current work. Six cases were, hence, simulated:

1. ASC plant without CO₂ capture
2. ASC plant with CO₂ capture by absorption
3. ASC plant with CO₂ capture by PSA
4. IGCC plant without CO₂ capture
5. IGCC plant with CO₂ capture by absorption
6. IGCC plant with CO₂ capture by PSA

All the cases discussed were based on the European Benchmarking Task Force (EBTF) recommendations (DECARBit, 2011). The purpose was to define a common set of assumptions and parameters for the different simulations, in order to guarantee the consistency of the comparisons. A description of the reference coal-fired power plants and of the same plants implementing CO₂ capture by absorption can be found in the EBTF report (DECARBit, 2011). In the present work, only the definition of the additional units in the plant layout integrating a PSA process is reported, as this constitutes the novelty of the analysis.

2.1. ASC plant with CO₂ capture by PSA

The integration of a PSA unit in the ASC plant is not affecting much the general layout. The additional units are

all downstream the flue gas treatment units, and consist in a water removal section, a PSA process and a compression stage for CO₂ transport. The plant upstream remains basically unchanged. The resultant plant layout is represented in Fig. 1. The characteristics of the most relevant streams are given in Table 1.

The water removal unit is added because water is known to hinder the CO₂ adsorption process. An equilibrium separation is carried out. The flue gas stream is cooled down to approximately 20 °C and fed to a flash separator. This simple process can only lower the water content down to about 2%. It would be advisable to reach water contents much lower than that, but it would require a different dehydration strategy. This has not been included in the simulation. For a deeper insight regarding the water presence issue, refer to the dedicated Section 3.3. The partially dehydrated flue gas stream is entering the PSA unit, where CO₂ is separated from the other components in a two stages PSA process. The necessity of two PSA stages will be illustrated later. The pressure of the CO₂-rich gas stream leaving the PSA unit needs to be raised to an appropriate level for transportation and storage. A target pressure of 110 bar was assumed. The CO₂-rich stream undergoes a compression process in a five-stage intercooled compressor. The CO₂-lean stream resulting from the PSA process is vented to the atmosphere.

2.2. IGCC plant with CO₂ capture by PSA

The addition of a PSA unit to the IGCC plant requires a higher degree of integration compared to the post-combustion scenario. A major difference is that the CO₂-lean gas stream leaving the PSA process (i.e., the H₂-rich gas stream) is further processed in the plant, constituting the fuel for the gas turbine. The additional units, with respect to the reference IGCC plant (DECARBit, 2011), consist in a water-gas shift section, a PSA process and a compression stage for CO₂ transport. The plant layout is represented in Fig. 2. The characteristics of the most relevant streams are given in Table 2.

The Water-Gas Shift (WGS) converts CO and H₂O into CO₂ and H₂, providing a beneficial effect on the following CO₂ separation due to the increase in the CO₂ partial pressure. COS hydrolysis is also carried out in the WGS process. The syngas is then cooled down. During the cooling process, condensing water is removed. Thanks to the relatively high pressure, water presence is drastically decreased (≈0.6%). The syngas stream at an appropriate temperature is fed to the H₂S removal unit and successively to the PSA unit. The outputs of the PSA process are a CO₂-rich stream and a H₂-rich stream. The latter is the fuel for the gas turbine cycle and is preheated by the syngas leaving the WGS process. Since the CO₂-rich gas stream does not achieve the requirements for being processed and transported, a further purification step is implemented. It consists in the removal of impurities by means of two flash separators integrated in the CO₂ compression section (see Fig. 3). This approach has already been suggested for removing a selection of non-CO₂ gases from oxy-combustion power plants (Pipitone and Bolland, 2009; Posch and Haider, 2012). After a first partial compression (up to 30 bar) and a dehydration process, the CO₂-rich gas stream enters a system of two multi-stream heat exchangers, each followed by a flash separator. The appropriately set temperature levels (−30 °C and −54.5 °C (Posch and Haider, 2012)) allow to separate two different streams: a CO₂-rich stream, matching the requested purity specifications, which completes the compression process; a CO₂-lean stream, rich in H₂, which can be added to the syngas injected as fuel in the gas turbine. The CO₂-rich stream is further compressed to 110 bar in an intercooled-compressor. An air expander is also present, providing an additional power output. It partially expands the air extracted

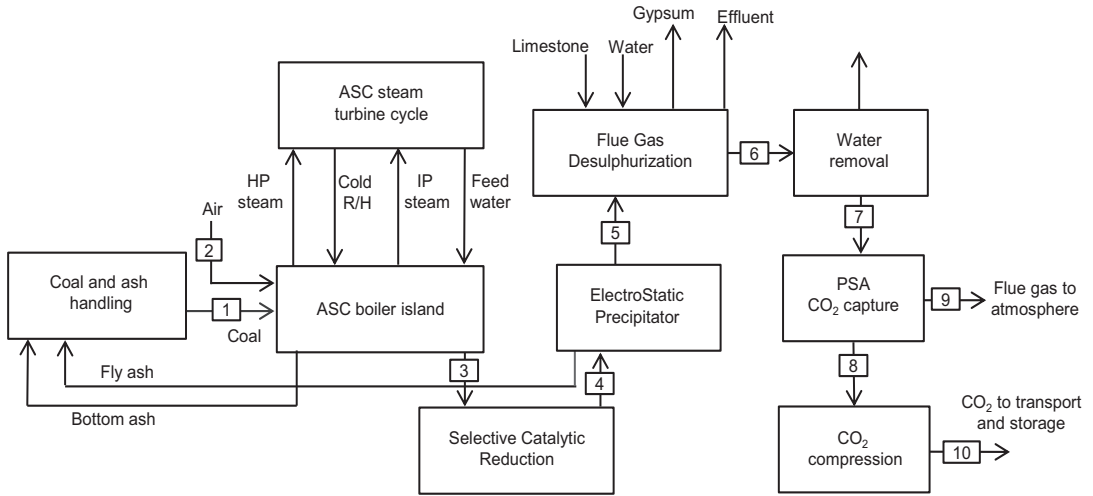


Fig. 1. ASC plant with integrated a PSA unit for CO₂ capture and a CO₂ compression unit.

Table 1
Stream table of the ASC plant integrated with a PSA unit for CO₂ capture and a CO₂ compression unit.

Stream	in (kg/s)	T (°C)	P (bar)	MW (g/mol)	Composition (% mol.)					
					CO ₂	N ₂	O ₂	Ar	SO ₂	H ₂ O
1	66.2	66.2	1.0	–	–	–	–	–	–	–
2	744.2	744.2	1.0	28.9	0.03	77.3	20.7	0.9	–	1.0
3	735.7	735.7	1.0	29.9	14.9	74.1	2.9	0.9	0.04	7.2
4	800.8	800.8	1.0	29.8	13.6	74.4	4.4	0.9	0.04	6.7
5	800.8	800.8	1.0	29.8	13.6	74.4	4.4	0.9	0.04	6.7
6	823.3	823.3	1.0	29.3	13.1	71.3	4.2	0.9	0.002	10.5
7	781.1	781.1	1.0	30.4	14.3	77.8	4.6	0.94	0.002	2.3
8	150.4	150.4	1.0	43.2	95.1	4.6	0.3	0.02	–	–
9	619.7	619.7	1.0	28.6	1.7	91.8	5.4	1.1	–	–
10	150.4	150.4	110.0	43.2	95.1	4.6	0.3	0.02	–	–

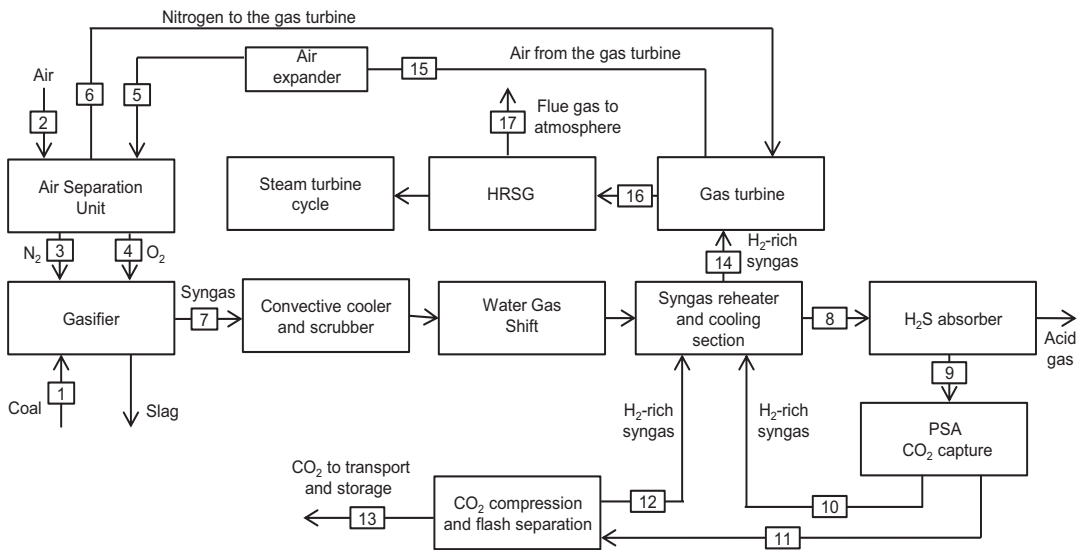


Fig. 2. IGCC plant with integrated a PSA unit for CO₂ capture and a CO₂ compression unit.

Table 2Stream table of the IGCC plant integrated with a PSA unit for CO₂ capture and a CO₂ compression unit.

Stream	\dot{m} (kg/s)	T (°C)	P (bar)	MW (g/mol)	Composition (% mol.)									
					H ₂	CO ₂	CO	CH ₄	N ₂	O ₂	Ar	H ₂ S	H ₂ O	
1	38.5	25.0	1.0	7.7	-	-	-	-	-	-	-	-	-	-
2	64.6	15.0	1.0	28.9	-	0.03	-	-	-	77.3	20.7	0.9	-	1.0
3	8.5	82.5	1.0	8.5	-	0	-	-	-	100	-	-	-	-
4	31.2	123.9	44.9	32.0	-	0	-	-	-	3.5	95.0	1.5	-	-
5	64.6	351.8	10.6	28.9	-	0.03	-	-	-	77.3	20.7	0.9	-	1.0
6	87.5	116.2	24.1	28.0	-	0	-	-	-	100	-	-	-	-
7	76.3	497.1	43.1	21.3	26.2	3.1	55.7	-	10.0	-	-	0.4	0.2	4.3
8	108.7	47.2	39.4	20.2	53.1	37.7	1.5	0.06	6.7	-	-	0.3	0.1	0.6
9	107.6	64.0	38.8	20.2	53.5	37.9	1.5	0.06	6.7	-	-	0.3	0.0001	0.03
10	19.1	62.5	38.8	6.5	84.7	2.6	2.0	0.1	10.1	-	-	0.5	-	-
11	88.6	38.6	1.0	37.2	14.8	81.6	0.9	0.03	2.5	-	-	-	-	0.06
12	8.2	17.6	27.7	15.1	63.5	22.8	3.5	0.1	10.0	-	-	-	-	-
13	80.4	28.0	110.0	43.7	0.6	98.9	0.1	0.01	0.4	-	-	-	-	-
14	27.2	230.0	24.1	7.8	81.5	5.7	2.2	0.08	10.1	-	-	0.4	-	-
15	64.6	432.3	17.6	28.9	-	0.03	-	-	77.3	20.7	0.9	-	-	1.0
16	656.1	579.5	1.0	27.4	-	1.2	-	-	75.1	10.1	0.8	-	-	12.7
17	656.1	113.8	1.0	27.4	-	1.2	-	-	75.1	10.1	0.8	-	-	12.7
18	88.5	28.0	30.0	37.2	14.8	81.7	0.9	0.03	2.6	-	-	-	-	-
19	88.5	-30.0	30.0	37.2	14.8	81.7	0.9	0.03	2.6	-	-	-	-	-
20	24.5	-54.5	28.8	26.9	37.7	54.0	2.2	0.07	6.1	-	-	-	-	-
21	16.4	17.7	7.2	43.7	0.6	98.8	0.2	0.01	0.5	-	-	-	-	-
22	64.0	17.7	17.4	43.7	0.6	99.0	0.1	0.01	0.3	-	-	-	-	-

from the gas turbine compressor and fed to the ASU, in order to recover part of the compression work.

3. Modeling of the PSA unit

3.1. Adsorption bed model

The mathematical model for the dynamic simulation of an adsorption bed relies on material, energy and momentum balances. The adsorbents are considered to have a bi-disperse structure (i.e., a population of macro and micropores). Three material balances would be theoretically necessary, one for the bulk gas phase, one for the macropores and one for the micropores. In order to reduce the computational time requested to solve the set of equations, a simplification was introduced. This simplification is based on the evaluation of the mass transfer resistances, and it assumes

the limiting case where one mass transfer mechanism is controlling, namely the diffusion in the micropores. Accordingly, the other mass transfer resistances have been neglected (i.e., macropore and film diffusion). This simplification have been supported by previous studies (Lopes et al., 2009a; Ruthven et al., 1980; Yucel and Ruthven, 1980) and have been already successfully applied by other works simulating the behavior of PSA units (Ribeiro et al., 2008; Casas et al., 2013). The kinetic of the mass transfer process is accounted for the Linear Driving Force (LDF) approximation (Yang, 1997; Azevedo and Rodrigues, 1999; Rodrigues and Dias, 1998; Sircar and Hufton, 2000). Its application is in line with the material balance simplifications above-mentioned. Similarly the energy balances have been simplified assuming thermal equilibrium between the gas and solid phases, reducing to one the equation needed (Ribeiro et al., 2008). An energy balance with the wall and the environment should be considered. It is common practice to describe the heat transfer with

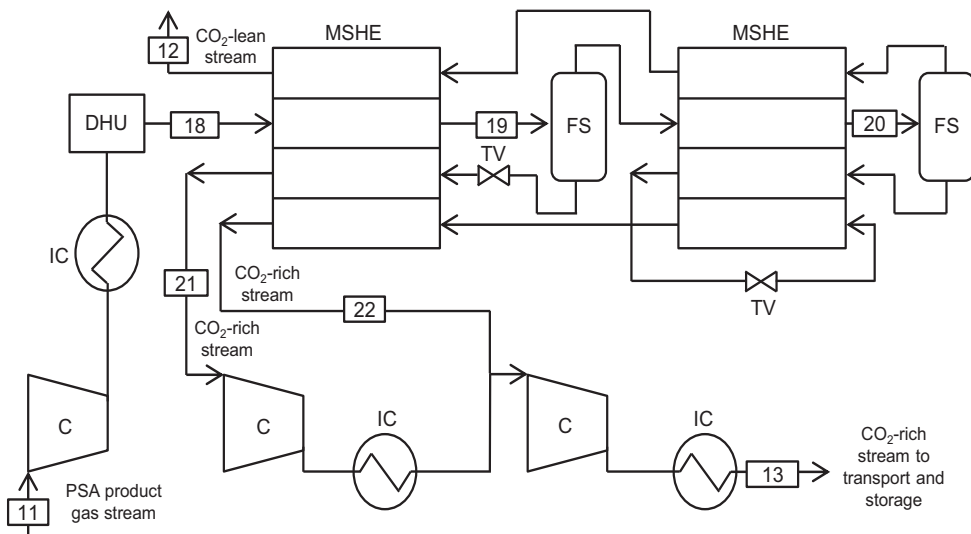


Fig. 3. CO₂ compression unit integrated with a double flash separation process.

the wall and the environment by average heat transfer coefficients. However, the influence of these terms is decreasing with the size of the unit. Given that the novelty of this work is to evaluate the PSA unit performance in actual operating arrangements (large diameter reactors), the reactors have been considered to be adiabatic. This approach seems to provide satisfactory predicting capabilities and it simplifies the model. The additional assumptions adopted in the model are listed below:

- The gas in the bulk phase is considered to follow the ideal gas law.
- The bed is assumed uniform throughout all its length (10 m). Constant bulk density (735 kg/m³ for the zeolite 5A and 522 kg/m³ for the activated carbon) and bed porosity (0.32 for the zeolite 5A and 0.38 for the activated carbon).
- The flow pattern is described by the axially dispersed plug flow.
- The radial diffusion effects are ignored.
- The momentum balance is described by the use of the well-known Ergun equation (Froment et al., 2010).
- The heat of adsorption is independent of temperature and adsorbed phase loading.

Based on these assumptions, the governing equations utilized are the following.

Component mass balance:

$$\frac{\partial C_i}{\partial t} [\varepsilon + \varepsilon_p(1 - \varepsilon)] = -\frac{\partial(u_s C_i)}{\partial z} + \frac{\partial}{\partial z} \left(\varepsilon D_{ax,i} C_{tot} \frac{\partial y_i}{\partial z} \right) - \rho_p(1 - \varepsilon) \frac{\partial \bar{q}_i}{\partial t} \quad (1)$$

LDF model:

$$\frac{\partial \bar{q}_i}{\partial t} = k_{LDF,i} (q_i^* - \bar{q}_i) \quad \text{with } k_{LDF,i} = \chi_{LDF} \frac{D_{C,i}}{r_c^2} \quad (2)$$

Overall mass balance:

$$\frac{\partial C_{tot}}{\partial t} [\varepsilon + \varepsilon_p(1 - \varepsilon)] = -\frac{\partial(u_s C_{tot})}{\partial z} - \rho_p(1 - \varepsilon) \sum_i^{NC} \frac{\partial \bar{q}_i}{\partial t} \quad (3)$$

Energy balance:

$$\left[\varepsilon C_{p,G} C_{tot} + \varepsilon_p(1 - \varepsilon) C_{p,G} C_{tot} + (1 - \varepsilon) C_{p,S} \rho_p \right. \\ \left. + (1 - \varepsilon) \rho_p \sum_i^{NC} C_{p,ads,i} \bar{q}_i \right] \frac{\partial T}{\partial t} = -u_s C_{p,G} C_{tot} \frac{\partial T}{\partial z} + \frac{\partial}{\partial z} \left(\lambda_{ax} \frac{\partial T}{\partial z} \right) \\ + \rho_p(1 - \varepsilon) \sum_i^{NC} (-\Delta H_{r,i}) \frac{\partial \bar{q}_i}{\partial t} \quad (4)$$

Momentum balance:

$$\frac{\partial P}{\partial z} = - \left[\frac{150(1 - \varepsilon)^2}{d_p^2 \varepsilon^3} \mu u_s + \frac{1.75(1 - \varepsilon)}{d_p} \rho_G u_s |u_s| \right] \quad (5)$$

The transport parameters are evaluated through frequently used correlations (see Table A.1 in Appendix A). Averaged values were successively used for the simulations. Physical properties of the gas were evaluated in all the points of the bed through an external physical property package (i.e., Multiflash–Infochem Computer Services Ltd.) interfaced with the main simulation tool.

The adsorbent selected for the post-combustion scenario is a zeolite 5A (Liu et al., 2011b). Zeolites are well studied CO₂ adsorbents, which proved to perform well in the conditions typical of post-combustion applications (i.e., very low CO₂ partial pressure)

(Siriwardane et al., 2001, 2005; Harlick and Tezel, 2004). Even though zeolites 13X are normally regarded as the most effective zeolites for CO₂ adsorption processes, a zeolite 5A was considered. This choice was driven by the availability of data and comparative results (Liu et al., 2011a). Bearing in mind that the simulation outputs would possibly be slightly superior with a zeolite 13X, it is opinion of the authors that the key outcomes presented afterwards are still valid. The same considerations can be applied discussing the possibility of utilizing two different adsorbents in the two PSA stages. Tailored adsorbents can suit better the specific operating conditions providing a performance enhancement but hardly significant.

The uptake capacity of the adsorbent is described by an extended multi-site Langmuir model:

$$\frac{q_i^*}{q_{m,i}} = a_i k_i P_i \left[1 - \sum_i^{NC} \left(\frac{q_i^*}{q_{m,i}} \right) \right]^{a_i}, \quad \text{with } k_i = k_{\infty,i} \exp \left(-\frac{\Delta H_{r,i}}{RT} \right) \quad (6)$$

Data were available just for CO₂ and N₂, the main constituents of the flue gas to process. The fraction of O₂ has been included with N₂. This approximation has been suggested by the similar selectivity of CO₂ with regard to N₂ and O₂ (Choi et al., 2003; Siriwardane et al., 2001) and it is therefore thought not to meaningfully affect the results.

The adsorbent selected for the pre-combustion scenario is an activated carbon (Lopes et al., 2009a). Activated carbons demonstrated to outperform zeolites when overpassing a certain threshold (≈ 7 bar) of CO₂ partial pressure (Siriwardane et al., 2001). Thus, in the typical pre-combustion operating conditions (e.g., $P_{CO_2} = 14.7$ bar) activated carbon has been considered to be the most suitable option. The adsorption isotherm was again described by an extended multi-site Langmuir model, represented by Eq. (6). Even though equilibrium data were available also for CH₄, the syngas components given as an input in the PSA model were just CO₂, H₂, CO and N₂. The small mole fraction of methane would not really influence the performance of the whole unit. Nevertheless, adding another component resulted in less stability of the model and additional computational efforts. Thus, the fraction of CH₄ has been included with CO.

The physical properties, the kinetic and the equilibrium data of the adsorbents are reported in Table 3.

3.2. PSA process

PSA is a gas separation process in which the adsorbent is regenerated by rapidly reducing the partial pressure of the adsorbed component, either by lowering the total pressure or by using a purge gas. The process is inherently discontinuous, since during the regeneration step the gas feed to a column has necessarily to be interrupted. Thus, different columns working in tandem are requested in order to enable the processing of a continuous feed. A coordinated group of columns is defined as PSA train. If different trains are present, the process gas stream is equally split between them. The columns of a train cyclically undergo a series of steps in an asynchronous manner. Some of these steps are closely interconnected, implying restrictions to the scheduling of the cycle. The steps that have been considered for the PSA process are:

- Feed (F): the feed gas is co-currently injected at the bottom of the column. The components of the gas stream starts to be selectively adsorbed on the surface of the adsorbent.
- Rinse (R): before starting the regeneration of the bed, part of the product gas is fed to the column. This gas, rich in CO₂, displaces the inert bulk gas remained in the column after the feed step.

Table 3

Bed characteristics, physical properties, kinetic data equilibrium data of the adsorbents.

Physical properties						
		d_p (mm)	ε_p	ρ_p (kg/m ³)	$C_{p,s}$ (J/(kg K))	
Zeolite 5A (Liu et al., 2011b)						
		2.70	0.30	1083	920	
Activated carbon (Lopes et al., 2009a)						
		2.34	0.57	842	709	
Equilibrium and kinetic parameters						
	α	k_{oc} (Pa ⁻¹)	q_m (mol/kg)	ΔH_r (kJ/mol)	D_{oc}/r_c^2 (s ⁻¹)	E_a (kJ/mol)
Zeolite 5A (Liu et al., 2011b)						
CO ₂	2.1	1.47E-11	3.92	-37.9	14.8	26.3
N ₂	2.5	3.79E-11	3.28	-19.4	0.1	6.3
Activated carbon (Lopes et al., 2009a)						
CO ₂	3.0	2.13E-11	7.86	-29.1	17.5	15.8
N ₂	4.0	2.34E-10	5.89	-16.3	1.0	7.0
H ₂	1.0	7.69E-11	23.57	-12.8	14.8	10.4
CO	2.6	2.68E-11	9.06	-22.6	59.2	17.5

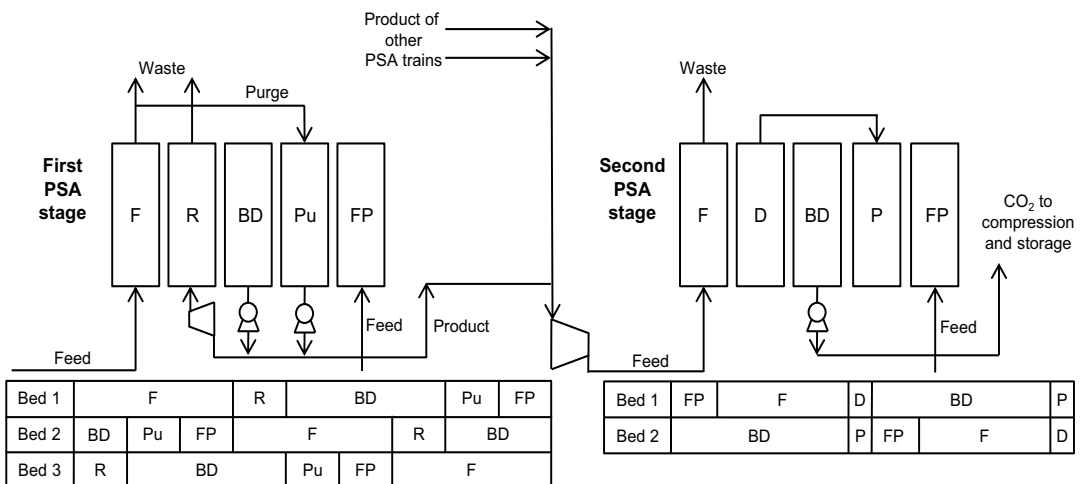
- Depressurization (D): the pressure is reduced by putting in contact the column with another at a lower pressure level.
- Blowdown (BD): the pressure is reduced to the lowest level in order to regenerate the bed. A stream of CO₂-rich gas is leaving the column during this step.
- Purge (Pu): the regeneration is completed by injecting a purging gas into the column, normally counter-currently. This step is again carried out at the lowest pressure of the system and produces a CO₂-rich gas stream.
- Pressurization (P): the pressure is increased by putting in contact the column with another at a higher pressure level.
- Null (N): the column is left idle.
- Feed Pressurization (FP): part of the feed gas is used to pressurize the column to the highest pressure level necessary for the adsorption process.

The different operating conditions in which the PSA process is supposed to perform in post- and pre-combustions scenarios, necessarily led to different configurations, in terms of number of beds and type of steps. The guiding criterion, for the selection of the process layout, was the necessity of approaching values of CO₂ recovery and purity sufficient for a CCS application (i.e., CO₂ recovery \approx 90% and purity \approx 95%). A multitude of different process configurations exists and may be employed. Given the large number of variables to consider (i.e., type and number of steps, duration

of the cycle, adsorbent material, etc.) there is not a well-defined framework to pinpoint the most suitable alternative. In the present work, it was decided to refer to cycle configurations successfully employed in the literature (Liu et al., 2011a; Casas et al., 2013). Minor changes have been done with respect to those cycles, in order to deal with the slightly different operating conditions considered. However, other configurations are possible and may lead to similar good performance. For the post-combustion scenario, a first PSA stage consists in a three-bed five-step cycle, while a second stage consists in a two-bed five-step cycle. The sequence of different steps undergone by a column is shown in Fig. 4. For the pre-combustion scenario, the PSA configuration adopted in the present work is a seven-bed twelve-step cycle, where the sequence of different steps undergone by a column is shown in Fig. 5.

Different boundary conditions have to be established for each step of the PSA cycle. The Danckwerts boundary conditions are applied. They assume no dispersion or radial variation in concentration or temperature either upstream or downstream of the reaction section. Table B.1 in Appendix B reports those boundary conditions.

The energy consumption directly related to the PSA process consists in the power necessary to a fan to overcome the pressure drops and the power necessary to the vacuum pump to create an under-atmospheric pressure (when requested from the regeneration strategy). If a rinse step is implemented, a fan is necessary for feeding the rinse flow rate into the column and overcoming the

**Fig. 4.** PSA processes for the post-combustion scenario. Representation of the sequence of steps undergone by a single column in the first and second PSA stage.

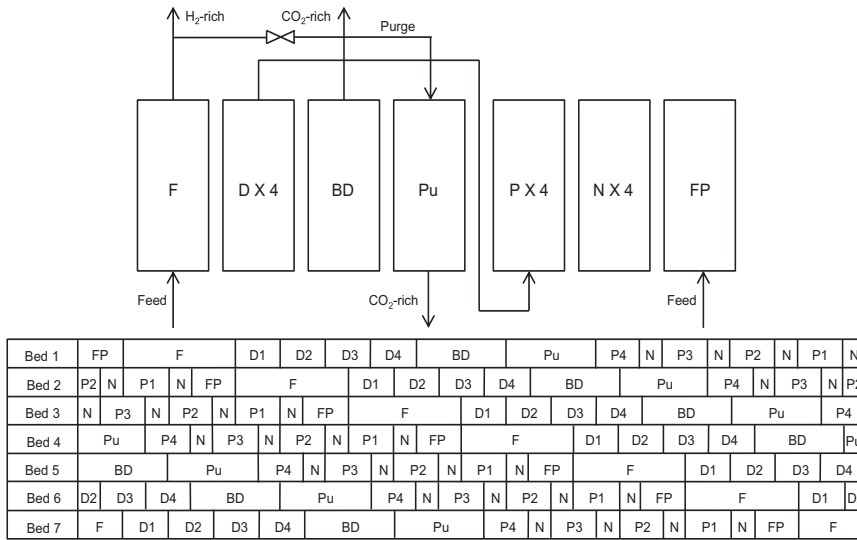


Fig. 5. PSA process for the pre-combustion scenario. Representation of the sequence of steps undergone by a single column.

pressure drops. Furthermore, a gas compression may be applied, with the relative compression power duty. These energy consumptions were evaluated within the PSA model as following:

$$\text{Fan power} = \frac{1}{\eta_{is}} \frac{\gamma_{fan}}{\gamma_{fan} - 1} RT_{in} \left[\left(\frac{P_{in}}{P_{out}} \right)^{(\gamma_{fan}-1)/\gamma_{fan}} - 1 \right] \dot{n}_{in} \quad (7)$$

Compressor power

$$= \frac{1}{\eta_{is}} \frac{\gamma_{compr}}{\gamma_{compr} - 1} RT_{in} \left[\left(\frac{P_{in}}{P_{out}} \right)^{(\gamma_{compr}-1)/\gamma_{compr}} - 1 \right] \dot{n}_{in} \quad (8)$$

Vacuum power

$$= \frac{1}{\eta_{is}} \frac{\gamma_{vacuum}}{\gamma_{vacuum} - 1} RT_{in} \left[\left(\frac{P_{atm}}{P_{vacuum}} \right)^{(\gamma_{vacuum}-1)/\gamma_{vacuum}} - 1 \right] \dot{n}_{in} \quad (9)$$

3.3. Water and adsorption

Presence of water is often troublesome in PSA processes. Water competitively adsorb on the solid sorbents and tend to accumulate since classical pressure swing operation may be not sufficient to desorb it. Both zeolites and activated carbons have demonstrated to experience this negative effect (zeolites appears to be more sensible to water presence). Few studies really dealt with this issue in detail when analyzing the suitability of CO₂ capture through PSA processes. Some experimental studies have been conducted both with zeolites (Brandani and Ruthven, 2004; Gallei and Stumpf, 1976; Li et al., 2011) and with activated carbons (Lopes et al., 2009a; Adams et al., 1988; Wang et al., 2008). However, not much has been done regarding modeling. This can be considered as a big gap, especially when considering post-combustion application where significant amount of water is present in the flue gas. The common approach suggested in the literature is to remove water prior the CO₂ capture unit by means of a separate PSA unit or a pre-layer of selective adsorbents like activated alumina or silica gel desiccants (Liu et al., 2011a; Chue et al., 1995). These methods have to prove to perform satisfactorily integrated in the complex arrangement of a power plant with CO₂ capture systems. Further, they will result in additional power consumption.

In the post-combustion simulation proposed, water is removed to as large extent as possible by condensation, and the remaining

water is neglected in the PSA process due to lack of modeling data. The effect of this approximation could not be evaluated and would need to be investigated. For pre-combustion applications the content of water in the syngas entering the PSA unit is down to trace level (0.03%). As long as a more efficient regeneration procedure (e.g., heating of the bed) is planned after a certain number of cycles, in order to avoid water accumulation, the performance should not be significantly affected (Ribeiro et al., 2009). Thus, the water content was neglected in the present work without further concerns.

3.4. Solution of the PSA model

The described modeling framework for the PSA process results in a set of partial differential and algebraic equations (PDAEs). The solution was obtained implementing the modeling equations in gPROMS environment (Process System Enterprise, London, UK). The set of PDAEs requires a considerable computational effort in order to be solved. One way to simplify the model, thus to reduce the computational time, was to adopt a one-column approach. This modeling strategy consists in simulating just one of the columns of the whole train (Ribeiro et al., 2009; Casas et al., 2013; Jiang et al., 2004; Park et al., 2000). The interactions between different columns are accounted for by virtual gas streams which are defined through the information stored in the previous cycles. The rinse, purge and pressure equalization-pressurization steps rely on this modeling technique. Adopting this simplification, it is essential to assure that the mass balances are always closed. This is rather straightforward for the rinse and purge steps, while the pressure equalization steps requires an additional effort. In fact, an appropriate value of the equalization pressure needs to be set, in order to avoid inconsistency in the mass balances. The procedure outlined by Casas et al. (2013) was applied to determine this pressure level.

The discretization algorithm applied for the numerical solution of the model is the Centered Finite Difference Method (CFDM). The spatial domain was discretized in 150 intervals. A higher number of discretization points was not used, because it would have significantly increased the computational time, without increasing in a similar manner the accuracy of the simulation.

The columns are considered to be initially filled with nitrogen and hydrogen, respectively in the post and pre-combustion scenario. The simulation is stopped when the Cycle Steady State (CSS)

arises. At CSS the process repeats itself invariably, meaning that the conditions at the end of each cycle are the same as those at the beginning. Whilst the operation of a single column remains batchwise, the process reaches a steady condition. All the results presented refer to the cycles at CSS.

4. Results and discussion

4.1. Definition of the performance parameters

The CO₂ separation performance is primarily evaluated in terms of CO₂ recovery (R_{CO_2}) and purity (P_{CO_2}). In the pre-combustion scenario it is also useful to define the H₂ recovery (R_{H_2}), giving that H₂ is fuelling the downstream gas turbine cycle. The CO₂ recovery may be misleading when large energy penalties result from the CO₂ separation process. For this reason, an additional parameter was introduced, namely the CO₂ capture efficiency (η_{CO_2}). The CO₂ capture efficiency is the real measure to what extent the CO₂ is captured from a power plant, relatively to a reference plant without CO₂ capture. The aforementioned parameters are defined as following:

$$R_{CO_2} = \frac{\dot{m} \text{ of CO}_2 \text{ in the product stream}}{\dot{m} \text{ of CO}_2 \text{ formed}} \quad (10)$$

$$P_{CO_2} = \text{CO}_2 \text{ volumetric concentration in the product stream} \quad (11)$$

$$R_{H_2} = \frac{\dot{m} \text{ of H}_2 \text{ entering the gas turbine as fuel}}{\dot{m} \text{ of H}_2 \text{ entering the CO}_2 \text{ separation unit}} \quad (12)$$

$$\eta_{CO_2} = 1 - \frac{\eta_{net} \text{ for the reference plant without CO}_2 \text{ capture}}{\eta_{net} \text{ for the plant implementing CO}_2 \text{ capture}} (1 - R_{CO_2}) \quad (13)$$

The energy efficiency of the plant is evaluated through the net electric efficiency (η_{net}), referred to the LHV:

$$\eta_{net} = \frac{\text{Net electric output}}{\text{Net fuel input}} \quad (14)$$

The footprint of the CO₂ separation technology is evaluated in terms of square meters occupied by the relative unit. The preliminary analysis carried out considers the size and the number of columns necessary for the CO₂ separation process. A more thorough analysis, including all the equipment relative to the separation process, would be needed in order to obtain more reliable outputs. However, it has been considered beyond the sake of the present work, which aims to give a first assessment on the possible dimensions of the units and on the difference between the separation techniques.

4.2. Post-combustion PSA process

Liu et al. (2011a) demonstrated that, in order to achieve the requested performance in terms of CO₂ recovery and purity, the flue gas resulting from the combustion of coal needs to undergo a two-stage PSA process. The first stage considered in the current work consists in a three-bed and five-step cycle (Fig. 4). Since no flue gas compression is implemented upstream the PSA unit, the flue gas enters at about atmospheric pressure. The aim of the first stage is to achieve the highest possible CO₂ recovery. As a tradeoff, it is not possible to achieve very high CO₂ purity. The regeneration process is carried out by decreasing the pressure to 0.1 bar. This pressure value has been suggested in many studies (Kikkinides et al., 1993; Liu et al., 2011a; Na et al., 2001, 2002; Takamura et al., 2001). The regeneration pressure to be applied is dependent on the shape

of the adsorbent isotherm and on the degree of vacuum to reach in order to guarantee proper bed regeneration. 0.1 bar seemed to balance the different requirements. Other values may have been considered but the advantages in terms of energy savings obtained with a higher regeneration pressure would be counterbalanced by lower separation performance. As an example, some simulations were implemented with the vacuum level set to 0.2 bar. Whilst the energy penalty could be effectively reduced of about 0.5%, the overall CO₂ recovery dropped under the target value (86.8 %). The CO₂ enriched-gas leaving from the blowdown and purge steps are then collected and sent to the second PSA stage, a two-bed five-step cycle (two-bed six-step if purge is implemented), where it is further purified. In order to enhance the second PSA process performance, a compression of the gas stream is implemented between the PSA stages. The gas is brought up to 2 bar before undergoing the second adsorption process. Fig. 6 shows the overall levels of CO₂ recovery and CO₂ purity obtained in the PSA process (after the two PSA stages) by varying the Purge-to-Feed mole flow rate ratio (P/F) of the second PSA stage. It is clear from the figure that there is a tradeoff between CO₂ recovery and purity. The highlighted point in Fig. 6 ($P_{CO_2} = 95.1\%$ and $R_{CO_2} = 90.2\%$) represents the PSA operating conditions selected for the process to be matched with the power plant. It refers to a PSA process in which the purge step has not been implemented, hence with a P/F ratio equal to zero. This configuration was chosen because it is able to contemporary fulfill the specification of CO₂ recovery and purity. Additionally, the absence of a purge step simplifies the process configuration. The resultant characteristics of the two PSA stages, which were selected to be integrated in the ASC plant, are reported in Table 4.

The PSA columns were initially sized in order to be able to process the entire flow rate. Since an excessively large diameter would have been required, a maximum size of 8 m was stated. A limitation to the superficial velocity was also introduced (0.15 m/s), in order to maintain the pressure drop in the column within a certain threshold (≈ 0.1 bar). The superficial velocity adopted was also verified to be lower than the minimum fluidization velocity. These design considerations implied the need for splitting the total flow rate in a number of trains, respectively 73 and 23 for the first and second PSA stage. Fewer trains are needed in the second PSA stage because large part of the undesired components has already been separated in the first PSA stage.

4.3. Post-combustion scenario analysis

Table 5 summarizes the outcome of the full-plant analysis carried out on the three cases considered for the post-combustion

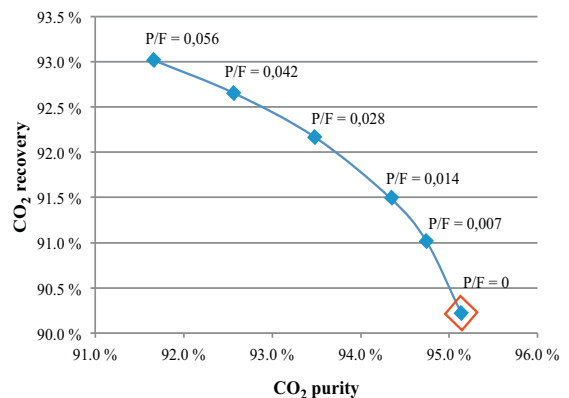


Fig. 6. CO₂ separation performance of the PSA process in the post-combustion scenario. Results reported refer to different Purge-to-Feed ratio (P/F) of the mole flow rates in the second PSA stage.

Table 4
Scheduling, characteristics and performance of the PSA process in the post-combustion scenario.

Stage	Step time (s)							Mole flow rate (mol/s)			CO ₂ (%)	
	F	R	D	BD	Pu	P	FP	Feed	Purge	Rinse	Purity	Recovery
1	702	234	0	702	234	–	234	304.3	91.3	91.3	49.7	93.8
2	650	–	50	830	–	50	180	360.0	–	–	95.1	96.1

scenario. The plant without CO₂ capture facilities and the plant with a state-of-the-art absorption unit were defined in compliance with the framework determined in the EBTF project (DECARBit, 2011). They are meant to be the basis for comparison with the ASC plant integrated with PSA, defined in this work. All the simulations were carried out with the same net fuel input.

4.3.1. Separation performance

The CO₂ separation performance of the PSA process succeeds to meet the required specifications ($R_{CO_2} = 90.2\%$ and $P_{CO_2} = 95.1\%$). If necessary, those values can be further increased at the expense of a higher energy consumption. As an example, a flue gas compression can be implemented before the PSA unit. The resulting increase in the flue gas total pressure would imply an increase of the CO₂ partial pressure, positively affecting the adsorption process. A simulation was run to evaluate this option, considering a flue gas compression from 1 bar to 1.5 bar. The outputs fully met the CO₂-rich stream specifications ($R_{CO_2} = 90.85\%$ and $P_{CO_2} = 95.42\%$) even applying a lower pressure at the entrance of the second PSA unit (i.e., 1.5 bar instead of 2 bar). However, the compression of the flue gas would be an energy demanding process and the impact on the energy balance of the system is evaluated later. The general outcome is that the CO₂ separation performance of the PSA unit, defined including two following PSA stages, is able to reach the target levels of CO₂ recovery and purity, and to return a CO₂ efficiency even slightly higher than absorption. Moreover, by playing with the PSA process configuration, it is possible to further raise or lower down the separation performance with a consistent impact on the energy penalty: the highest the desired separation performance, the highest is the expected energy penalty.

4.3.2. Energy performance

PSA demonstrates to be competitive with absorption when looking at the energy analysis. The attained net electric efficiency is

Table 5
Main outputs of the full-plant analysis in the post-combustion scenario.

Plant summary	No capture	Absorption	PSA
Power inputs			
Coal flow rate (kg/s)	66.2	66.2	66.2
Coal LHV (MJ/kg)	25.2	25.2	25.2
Net fuel input (MW _{th})	1665.5	1665.5	1665.6
Power outputs			
Steam turbine output (MW)	828.1	714.6	827.3
Gross electric output (MW)	828.1	714.6	827.3
CO ₂ separation power consumption (MW)	–	10.4	102.8
Flue gas compression power consumption (MW)	–	0.0	15.4
CO ₂ compression power consumption (MW)	–	47.5	52.8
Miscellaneous auxiliaries (MW)	77.4	87.0	77.5
Total auxiliary power consumption (MW)	77.4	144.8	248.4
Net electric output (MW)	750.7	569.7	578.9
Plant performance			
Net electric efficiency (%)	45.1	34.2	34.8
CO ₂ purity (%)	–	100.0	95.1
CO ₂ recovery (%)	–	90.0	90.2
CO ₂ capture efficiency (%)	–	86.8	87.3

slightly higher to that associated with the absorption-based plant. The reference ASC plant without CO₂ capture displayed a η_{net} of 45.1%. It drops to 34.2% and 34.8%, respectively with CO₂ capture by absorption and PSA. Before it was mentioned the possibility of carrying out a flue gas compression (up to 1.5 bar) upstream the PSA process, attaining enhanced CO₂ separation performance. The energy spent for the compression would have a significant impact on the energy balance of the plant, lowering the final η_{net} down to 33.6%. A reason that may justify such a procedure is the benefit that would be obtained in terms of sizes and footprint of the separation unit. Thus, the possibility will be still mentioned in the footprint section, but, otherwise, this option does not appear to be worth of further analyses. The most significant power consumptions, contributing to reduce the η_{net} of the plant in the presence of CO₂ capture processes, are shown in Fig. 7. It is worthwhile to mention that, in order to be able to compare the difference sources of power losses, the power consumption connected to steam extractions needs to be defined (while all the others are direct electric power consumptions). In fact, the reduction in power output is less than the heat content of the steam. It was evaluated considering the missing expansion of the steam between the extraction point and the downstream condenser, the steam condition at the extraction point and the steam turbine efficiency. Eq. (15) shows the methodology adopted:

Power consumption due to steam extraction

$$= \eta_{is,st} \dot{m}_{steam} c_p T_1 \left[1 - \left(\frac{P_2}{P_1} \right)^{(\gamma-1)/\gamma} \right] \quad (15)$$

The total power consumption is slightly lower for the PSA case, as was easily predictable given the higher η_{net} . When applying an absorption process for capturing CO₂, the largest share of power consumption is connected to the reboiler heating duty for the regeneration of the solvent. In order to comply with this energy demand, steam is extracted from the turbine. This procedure results in a decrease of the gross power output of the plant of about 113.6 MW. The other significant power consumption is related to the compression of the CO₂-rich stream. A five-stage intercooled compressor is used to raise the pressure from 1.7 bar to 110 bar for transport (47.5 MW). In the PSA case the process is not demanding for any steam extraction. However, other sources of power consumptions are present. They are related to the pressure modifications undergone by the flue gas, necessary to carry out the adsorption-desorption process. The term defined as CO₂ separation power consumption includes in the PSA case: the power requested by the vacuum pumps to establish the vacuum for the regeneration of the bed (95.5 MW); the power supplied to the fan to overcome the pressure drops during the feed, feed pressurization and rinse step (7.3 MW). The CO₂ separation power consumption results to be the largest source of power loss (102.8 MW), while in the absorption case it has a limited impact (10.4 MW mainly due to the consumption of the pumps for the solvent circulation). The flue gas compression occurring between the two PSA stages has a non-negligible impact on the energy balance, accounting for 15.4 MW. In the PSA case the CO₂-rich stream compression displays a power consumption of 52.8 MW. The compression power duty is larger than in the absorption case mainly because of the higher pressure ratio to provide. The CO₂-rich stream leaves the PSA process at a

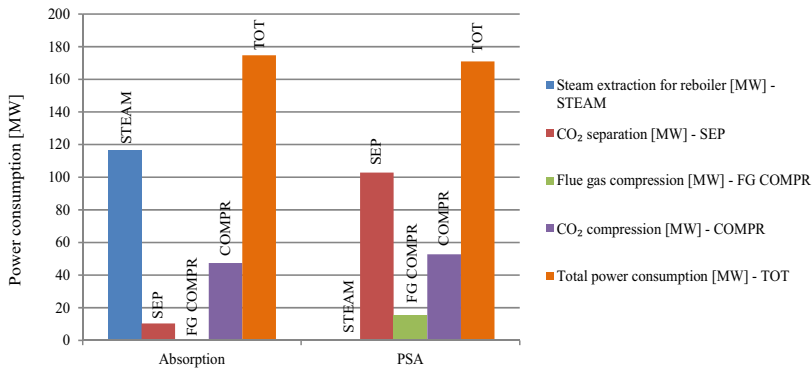


Fig. 7. Power consumptions related to the CO₂ capture and compression process for the post-combustion scenario.

lower pressure level (1 bar) compared to that resulting from the absorption process (1.7 bar). In conclusion, capturing CO₂ in a PSA process displays the big advantage of not requiring any steam, leaving untouched the steam turbine cycle. The implementation of a PSA process introduces new sources of power consumptions connected to the pressure swing processes necessary to comply with the requested CO₂ separation performance. However, the overall balance seems positive under an energy point of view. It is worth to mention that the pumps and compressors simulated have been considered to operate at steady state. This is a strong simplification given the inherent dynamic behavior of a PSA process. It is not known to what extent a discontinuous feed to those devices can negatively affect their performance.

4.3.3. Footprint

The mole flow rate entering a single PSA train cannot be further increased, compared to the level reported in Table 4, for limitations related to the pressure drop and the minimum fluidization velocity. Treating the total flue gas volume, the plant needs a large number of PSA trains (i.e., about 73 and 23 trains for the first and second PSA stage). Each PSA train is constituted by 3 and 2 columns, respectively in the first and second PSA stage, and the diameter of a column was set to 8 m. Table 6 shows an estimation of the footprints of the two separation techniques considered. The absorption column diameter was calculated by defining a reasonable superficial velocity of the flue gas entering the column (i.e., 2 m/s). It becomes clear that the total footprint of the PSA-based CO₂ capture unit is excessive to be considered feasible. A way to partially reduce the footprint could be to introduce a flue gas compression before the PSA unit. Compressing the flue gas up to 1.5 bar demonstrated to lead to a reduction in the number of necessary PSA trains of about 9 units. It was already verified that this operation would also be beneficial for the CO₂ separation process. However, the final footprint would still be much larger than that of the absorption-counterpart. Not to mention the additional power consumption introduced which would severely affect the process competitiveness under an energy efficiency point of view.

Table 6
Footprint analysis for the post-combustion scenario.

	Absorption	PSA
Column diameter (m)	20.7	8.0
Number of columns	2	264
Footprint (m ²)	674	13285

4.4. Pre-combustion PSA process

The PSA process is supposed to be able to process the syngas and return two streams: a CO₂-rich stream to be sent to compression and transportation; and a CO₂-lean stream, rich in H₂, to be fed to the gas turbine as fuel. Both streams request some purity characteristics to be fulfilled, namely CO₂ and/or H₂ purity and recovery. Previous studies (Casas et al., 2013) suggested that a single PSA stage would have been able to fulfill these requirements in conditions typical for a pre-combustion application. However, Casas et al. (2013) simulated a gas stream which contains only H₂ and CO₂. When applying a realistic syngas composition, the results of the simulations became different from those expected. The PSA layout adopted in the present work is a seven-bed and twelve-step cycle and the regeneration pressure was set to 1 bar. Some demonstrative simulations were run to assess the effectiveness of the selected regeneration pressure. Higher regeneration pressure levels can bring an improvement on an energy point of view, although the reduced purity could partially even out the expected reduction in compression power consumption. Conversely, the separation performance decreases according to the less effective regeneration process. 1 bar appeared to be the regeneration pressure which was closer to meet both separation and energy specifications. Fig. 8 shows the levels of CO₂ recovery and CO₂ purity obtained in the assessed PSA process by varying the Purge-to-Feed ratio (P/F). The values reported in the figure refer only to the PSA unit. The overall plant CO₂ purity and recovery will be different since an additional flash separation process is implemented after the PSA process. Fig. 8

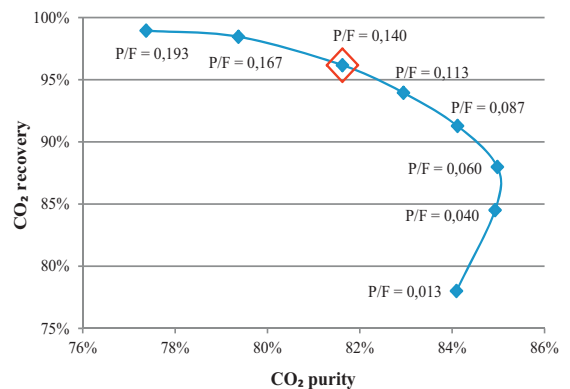


Fig. 8. CO₂ separation performance of the PSA process in the pre-combustion scenario. Results reported refer to different Purge-to-Feed ratio (P/F) of the mole flow rates.

Table 7
Scheduling, characteristics and performance of the PSA process in the pre-combustion scenario.

	Step time (s)							Mole flow rate (mol/s)		CO ₂ (%)	
	F	D × 4	BD	Pu	P × 4	N × 4	FP	Feed	Purge	Purity	Recovery
PSA	90	41	80	59	41	8	41	3771.6	525.0	81.6	96.2
PSA + flash	–	–	–	–	–	–	–	–	–	98.9	89.8

makes clear that the PSA process is not quite able to match the specifications. Whilst the CO₂ recovery can be pushed easily over the target value of 90%, the CO₂ purity hardly reaches values around 85%. A further increase of the CO₂ purity appears difficult to achieve and would come at the expense of the CO₂ recovery, which would drastically decrease. Realizing the impossibility to reach the desired output streams characteristics within the PSA unit, the strategy was modified. A solution could have been to introduce an additional PSA stage (likewise post-combustion scenario) or better to apply a dual PSA process (Grande and Blom, 2012). Considerations mainly regarding the possible footprint related to a second PSA train lead us to choose a different option. Nevertheless, the dual PSA process could result competitive and should be matter of further investigations. To comply with the selected alternative, the CO₂ recovery target was set to the highest possible level, while a relatively lower value of purity was accepted. It was then introduced a further CO₂ purification process downstream of the PSA unit. It consists of a double flash separation integrated in the CO₂ compression process (Fig. 3). Referring to Posch and Haider (2012), the temperatures selected at the outlet of each heat exchanger were set respectively to –30 °C and –54.5 °C. The gas stream is compressed up to 30 bar before entering the flash separation unit. Implementing this additional separation step, the final result in terms of CO₂ purity ($P_{CO_2} = 98.9\%$) and recovery ($R_{CO_2} = 89.8\%$) basically fulfilled the requirements. The H₂ recovery ($R_{H_2} = 99.6\%$) was satisfactory as well. The operating conditions selected for the full-plant analysis are those represented by the highlighted point in Fig. 8 (i.e., $P/F = 0.140$). This configuration was chosen because it provides a good balance between separation and energy performances. Table 7 displays the relative PSA characteristics, together with the separation performance obtained. The overall separation performance, resulting from the integration of the flash separation unit, is also reported.

The criteria adopted for the design of the pre-combustion PSA unit are similar to those discussed in the post-combustion scenario.

Table 8
Main outputs of the full-plant analysis in the pre-combustion scenario.

Plant summary	No capture	Absorption	PSA + flash
Power inputs			
Coal flow rate (kg/s)	33.3	38.5	38.5
Coal LHV (MJ/kg)	25.2	25.2	25.2
Net fuel input (MW _{th})	837.3	968.1	968.2
Power outputs			
Gas turbine output (MW)	253.1	287.9	287.1
Steam turbine output (MW)	192.6	167.6	167.4
Air expander output (MW)	4.5	5.7	5.4
Gross electric output (MW)	450.2	461.1	459.9
CO ₂ separation power consumption (MW)	–	16.5	0.0
CO ₂ compression power consumption (MW)	–	18.7	41.3
ASU power consumption (MW)	38.9	51.5	51.6
Miscellaneous auxiliaries (MW)	15.5	16.3	16.7
Total auxiliary power consumption (MW)	54.3	103.0	109.6
Net electric output (MW)	395.8	358.1	350.2
Plant performance			
Net electric efficiency (%)	47.3	37.1	36.2
CO ₂ purity (%)	–	100.0	98.9
CO ₂ recovery–separation technology (%)	–	94.6	89.8
CO ₂ recovery–overall plant (%)	–	90.6	86.1
H ₂ recovery (%)	–	100.0	99.6
CO ₂ capture efficiency (%)	–	88.1	81.8

A less stringent limitation was imposed to the maximum pressure drop (≈ 0.15 bar) and a lower superficial velocity had to be utilized (0.08 m/s) in order to make up for the higher operating pressure (as can be inferred from the Ergun equation, the higher the operating pressure, the larger the pressure drop). However, a single PSA train was evaluated as able to process the entire syngas flow rate. Accordingly, the columns diameter was set to 6.6 m.

4.5. Pre-combustion scenario analysis

Table 8 summarizes the outcome of the full-plant analysis carried out on the three cases considered for the pre-combustion scenario. The plant without CO₂ capture facilities and the plant with a state-of-the-art absorption unit were defined in compliance with the framework determined in the EBTF project (DECARBit, 2011). They are meant to be the basis for comparison with the IGCC plant integrated with PSA, defined in this work. The simulations were run such as to obtain similar exhaust gas flow rates at the gas turbine outlet. This assumption meant to support following comparisons of the results by allowing same size gas turbines to be used for the simulations. The typology of gas turbine considered is large-scale “F class” 50 Hz.

4.5.1. Separation performance

When evaluating the CO₂ separation performance, PSA and double flash process seems to match the requirements. The P_{CO_2} is above 95% and R_{CO_2} is slightly lower than the target, with a value of 89.8% (at least when considering the CO₂ recovery only for the separation technology). It is important to achieve a high value of P_{CO_2} (98.9%), because this is strictly related to the H₂ recovery, which is, in fact, very high as well ($R_{H_2} = 99.6\%$). Recovering large part of H₂ is essential in order to guarantee good energy performance of the system. However, the syngas fuelling the gas turbine contains traces of CO and CH₄, products of the gasification process. Their combustion results in the formation of additional CO₂ which has to

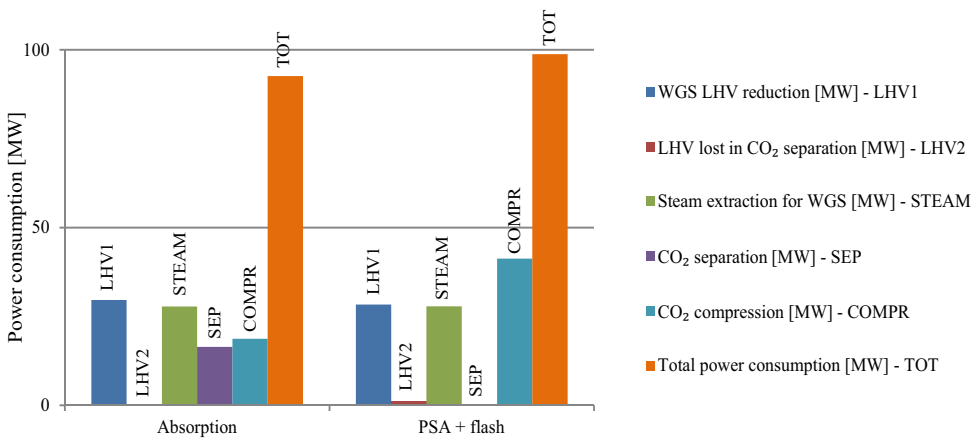


Fig. 9. Power consumptions related to the CO₂ capture and compression process for the pre-combustion scenario.

be taken into account in the CO₂ balance of the overall plant. For this reason, there is an additional CO₂ recovery parameter, which is considering the total CO₂ formed. The R_{CO_2} for the PSA case drops then to 86.1% which is not fully fulfilling the requirement. Conversely, absorption as decarbonization technique succeeds to reach the suggested target values, attaining P_{CO_2} , overall R_{CO_2} and R_{H_2} of 100%, 90.5% and 100% respectively. The CO₂ capture efficiency well summarizes the discussed picture. η_{CO_2} for the PSA-based plant is 81.8%, a value that can be considered acceptable, although lower than that achieved with absorption (88.1%).

4.5.2. Energy performance

The energy analysis of the pre-combustion scenario reveals that absorption is not clearly outperforming PSA. The reference IGCC plant without CO₂ capture attains a η_{net} of 47.3%. Introducing an absorption unit or a PSA unit for CO₂ capture drops the η_{net} down to 37.1% and 36.2% respectively. The difference between the two cases is rather small (0.9%). A breakdown analysis of the power consumption, related to the integration of a CO₂ capture unit, highlights some differences (see Fig. 9). Since some power consumptions are characteristic of a pre-combustion application, they are described hereafter (the calculation of the equivalent power consumption is also explained, if the term reported is not a direct electric power consumption):

- WGS LHV reduction: the WGS process produces a reduction of the syngas LHV (partially balanced by a higher mass flow rate). The reduction in the fuel energy is converted into power consumption by considering the net efficiency of the plant.
- LHV lost in CO₂ separation: since traces of hydrogen and carbon monoxide are leaving with the CO₂-rich stream, their heating value is wasted. The reduction in the fuel energy is converted into power consumption considering the net efficiency of the plant.
- Steam extraction for WGS: some steam need to be extracted by the steam turbine in order to be fed to the WGS process. The missing expansion of that steam causes a reduction in the steam turbine power output. The power consumption is calculated as described in the post-combustion scenario for steam extractions.

The PSA unit does not directly require much energy. The CO₂ separation power consumption is very small (≈ 0.05 MW) and mainly due to the fans for overcoming the pressure drop in the bed. Since the regeneration pressure is atmospheric, no vacuum pumps need to be installed. The avoidance of a rinse step in the PSA process configuration is also contributing to limit the power

consumption. In the absorption case the CO₂ separation power consumption is larger. The required 16.5 MW are mostly supplied to the pumps for the solvent circulation. However, the particular configuration of the absorption/regeneration process is favorable when considering the power for the compression of the CO₂-rich stream. The regeneration process for the absorption case is occurring at three different pressure levels (12.7, 7.5 and 1.1 bar). In the PSA process the CO₂-rich stream leaves the unit at 1 bar, meaning that the pressure ratio that the compressor has to provide is, on average, larger. Moreover, in the double flash separation process, the CO₂-rich streams leaving the flashes are partially expanded in adiabatic throttles, since by entering counter-currently the heat exchangers they assure the necessary cooling potential. Hence, the CO₂ compression duty is further increased. The CO₂ compression power consumption results to be 41.3 MW for the PSA case, while for the absorption case is 18.7 MW. It can be argued that the power saved in the separation process, adopting PSA, is more than balanced by the additional power demand for CO₂ compression. The other power consumptions evaluated are very similar in both cases, so they do not modify the picture outlined. Summing up, the CO₂ capture through a PSA unit shifts the power consumption from the capture process to the CO₂ compression, while all the other power loss contributions remain almost unchanged. However, the increase in the compression power results to prevail. Accordingly the energy efficiency penalty relative to the PSA case is slightly higher than that relative to the absorption case.

4.5.3. Footprint

Given the high pressure at which the syngas enters the PSA unit (38.8 bar), resulting in a relatively low volumetric flow rate, it was possible to design the PSA unit in a way that all the syngas is processed by a single PSA train. The superficial velocity adopted is able to maintain the pressure drop within acceptable limits (≈ 0.15 bar). The value was also verified not to overpass the minimum fluidization velocity at the operating conditions considered. Established the velocity and knowing the volumetric flow rate, the cross sectional area was evaluated and, hence, the diameter of the column. It resulted to be 6.6 m. Even though a PSA train is formed by 7 columns working in parallel, the footprint of the PSA unit appears to be acceptable. However, the footprint of an absorption unit would be much smaller. Table 9 compares the estimations of the two footprints, highlighting the remarks of the analysis. The absorption column diameter was calculated by defining a reasonable superficial velocity of the flue gas entering the column (i.e., 1 m/s).

Table 9
Footprint analysis for the pre-combustion scenario.

	Absorption	PSA
Column diameter (m)	2.2	6.6
Number of columns	2	7
Footprint (m ²)	8	239

5. Conclusions

In the current work, the suitability of PSA process for CO₂ capture in coal-fired power plants has been assessed. The effectiveness of PSA is evaluated on three different levels: CO₂ separation performance, energy efficiency and footprint of the technology. A post- and a pre-combustion scenario have been considered.

In the post-combustion scenario a PSA process is integrated with an Advanced SuperCritical (ASC) pulverized coal plant. The outputs of the full-plant analysis were compared to those of a similar plant implementing a state-of-the-art absorption process for capturing CO₂. A two stage PSA process is necessary in order to achieve satisfactory characteristics of the CO₂-rich stream to be transported and stored. The first PSA stage is a three-bed five-step cycle, the second is a two-bed five-step cycle. The resulting CO₂ purity ($P_{CO_2} = 95.1\%$) and recovery ($R_{CO_2} = 90.2\%$) fulfill the target levels established (i.e., $P_{CO_2} \approx 95\%$ and $R_{CO_2} \approx 90\%$). The utilization of a PSA process shifts the power consumption related to CO₂ capture from a thermal duty for regenerating the solvent (i.e., amine absorption) to direct electrical power for vacuum pumps and compressors. The resultant energy penalty is competitive with that of the benchmark absorption-based plant, as it was possible to obtain a net electric efficiency slightly higher. The main obstacle for the suitability of PSA in post-combustion application is related to its footprint. The flue gas flow rate has to be split in a large number of PSA trains (about 73 and 23 for first and second PSA stage) to be processed. Given the diameter (8 m) of each of the columns constituting a train, the footprint of the PSA unit is much larger compared to the reference absorption unit. Modifications in the process configuration may bring an improvement in this sense, at the expense of other performance indicators. However, the gap is so large that is difficult to imagine filling it within the considered process framework.

The application of a PSA process in a pre-combustion scenario returns more promising results. The PSA process is integrated in an Integrated Gasification Combined Cycle (IGCC) plant. The outputs of the full-plant analysis were compared to those of a similar plant implementing a state-of-the-art absorption process for capturing CO₂. The PSA process considered was a seven-bed and twelve-step cycle. In order to comply with the separation performance specifications, an additional double flash separation process was integrated in the CO₂ compression unit. The obtained purity ($P_{CO_2} = 98.9\%$) of the CO₂-rich stream fulfills the requirement. The overall CO₂ recovery ($R_{CO_2} = 86.1\%$) is slightly lower compared to the level aimed (i.e., 90%). However, a rearrangement of the process could be able to trade off part of the purity for a higher recovery,

so that the process meets both the requirements. The absorption process fully complies with the target values. The energy analysis of the simulated PSA-based plant yields a η_{net} of 36.2%. The η_{net} of the reference IGCC plant without CO₂ capture is 47.3%, while integrating an absorption process for CO₂ capture drops it to 37.1%. The difference of energy efficiency between the two cases studied is lower than 1%. The footprint of the PSA unit is not problematic, since a single PSA train (7 columns of 6.6 m diameter) is able to process the volumetric flow rate of the syngas. In conclusion, PSA process has the chance to become competitive in a pre-combustion scenario for CO₂ capture. The general performance obtained is slightly lower compared to that relative to a plant implementing an absorption process. On the other hand, PSA is a less mature technology for CO₂ capture applications. Therefore, substantial improvements are likely achievable. For instance, the layout of the whole process may be further optimized. Advancements in material technology may also introduce adsorbents with increased uptake capacity and selectivity, and possibly with higher thermal resistance. Such an accomplishment would make possible better separation performance and a higher degree of process integration. Hence, there is reason to believe that PSA can become a suitable alternative to absorption for pre-combustion CO₂ capture.

Acknowledgement

The authors gratefully acknowledge the financial support provided through the “EnPe – NORAD’s Programme within the energy and petroleum sector”.

Appendix A. Calculation of the transport parameters

Table A.1
Transport parameters equations.

Axial dispersion (Ruthven, 1984)

$$(16) D_{ax,i} = (0.45 + 0.55\varepsilon)D_{g,i}^m + 0.35 \frac{d_p}{\tau} |u_s|$$

Wilke model for a single-phase mixture of gases (Fuller et al., 1966; Poling et al., 2000)

$$(17) D_{g,i}^m = \frac{1-y_i}{\sum_{i' \neq i} (y_{i'}/D_{g,i'})}$$

$$(18) D_{g,i'} = \frac{10^{-3} r^{1.75} [(1/M_i) + (1/M_{i'})]^{1/2}}{(\rho_g/101325) \left[\left(\sum_i \xi_i \right)^{1/3} + \left(\sum_{i'} \xi_{i'} \right)^{1/3} \right]^2}$$

Micropore diffusivity (Ruthven, 1984)

$$(19) \frac{D_{e,i}}{r_c^2} = \frac{D_{e,i}^0}{r_c^2} \exp\left(-\frac{E_{a,i}}{RT}\right)$$

Axial thermal dispersion coefficient (Lopes et al., 2009b)

$$(20) \frac{\lambda_{ax}}{k_f} = 7 + 0.5PrRe$$

Appendix B. Boundary conditions for the PSA processes

Table B.1

Boundary conditions adopted for the PSA processes. The co-current blowdown and co-current pressure equalization boundary conditions are the same as the counter-current counterpart applied inverted at the extremities of the column.

<p><u>Feed: $z = 0$</u></p> $\varepsilon D_{ax,i} \frac{\partial C_i}{\partial z} = -u_s(C_{F,i} - C_i)$ $\dot{n} = \dot{n}_F$ $\lambda_{ax} \frac{\partial T}{\partial z} = -u_s C_p C_{tot}(T_F - T)$	<p>$z = L$</p> $\frac{\partial C_i}{\partial z} = 0$ $P = P_F$ $\frac{\partial T}{\partial z} = 0$	
<p><u>Rinse: $z = 0$</u></p> $\varepsilon D_{ax,i} \frac{\partial C_i}{\partial z} = -u_s(C_{R,i} - C_i)$ $\dot{n} = \dot{n}_R$ $\lambda_{ax} \frac{\partial T}{\partial z} = -u_s C_p C_{tot}(T_R - T)$	<p>$z = L$</p> $\frac{\partial C_i}{\partial z} = 0$ $P = P_F$ $\frac{\partial T}{\partial z} = 0$	
<p><u>Pressure equalization–depressurization: $z = 0$</u></p> $\frac{\partial C_i}{\partial z} = 0$ $\dot{n} = 0$ $\frac{\partial T}{\partial z} = 0$	<p>$z = L$</p> $\frac{\partial C_i}{\partial z} = 0$ $P = P_{eq}$ $\frac{\partial T}{\partial z} = 0$	
<p><u>Counter-current blowdown: $z = 0$</u></p> $\frac{\partial C_i}{\partial z} = 0$ $P = P_{BD}$ $\frac{\partial T}{\partial z} = 0$	<p>$z = L$</p> $\frac{\partial C_i}{\partial z} = 0$ $\dot{n} = 0$ $\frac{\partial T}{\partial z} = 0$	
<p><u>Purge: $z = 0$</u></p> $\frac{\partial C_i}{\partial z} = 0$ $P = P_{BD}$ $\frac{\partial T}{\partial z} = 0$	<p>$z = L$</p> $\varepsilon D_{ax,i} \frac{\partial C_i}{\partial z} = -u_s(C_{Pu,i} - C_i)$ $\dot{n} = \dot{n}_{Pu}$ $\lambda_{ax} \frac{\partial T}{\partial z} = -u_s C_p C_{tot}(T_{Pu} - T)$	
<p><u>Counter-current pressure equalization–pressurization: $z = 0$</u></p> $\frac{\partial C_i}{\partial z} = 0$ $\dot{n} = 0$ $\frac{\partial T}{\partial z} = 0$	<p>$z = L$</p> $\varepsilon D_{ax,i} \frac{\partial C_i}{\partial z} = -u_s(C_{eq,i} - C_i)$ $\dot{n} = \dot{n}_{eq}$ $\lambda_{ax} \frac{\partial T}{\partial z} = -u_s C_p C_{tot}(T_{eq} - T)$	
<p><u>Feed pressurization: $z = 0$</u></p> $\frac{\partial C_i}{\partial z} = 0$ $\dot{n} = 0$ $\frac{\partial T}{\partial z} = 0$	<p>$z = L$</p> $\varepsilon D_{ax,i} \frac{\partial C_i}{\partial z} = -u_s(C_{FP,i} - C_i)$ $P = P_{FP}$ $\lambda_{ax} \frac{\partial T}{\partial z} = -u_s C_p C_{tot}(T_{FP} - T)$	

References

- Adams, L.B., et al., 1988. An examination of how exposure to humid air can result in changes in the adsorption properties of activated carbons. *Carbon* 26 (4), 451–459.
- Agarwal, A., Biegler, L.T., Zitney, S.E., 2010. A superstructure-based optimal synthesis of PSA cycles for post-combustion CO₂ capture. *AIChE J.* 56 (7), 1813–1828.
- Azevedo, D.C.S., Rodrigues, A.E., 1999. Bilinear driving force approximation in the modeling of a simulated moving bed using bidisperse adsorbents. *Ind. Eng. Chem. Res.* 38 (9), 3519–3529.
- Brandani, F., Ruthven, D.M., 2004. The effect of water on the adsorption of CO₂ and C₃H₈ on type X zeolites. *Ind. Eng. Chem. Res.* 43 (26), 8339–8344.
- Casas, N., et al., 2013. A parametric study of a PSA process for pre-combustion CO₂ capture. *Sep. Purif. Technol.* 104 (0), 183–192.
- Cen, P., Yang, R.T., 1986. Bulk gas separation by pressure swing adsorption. *Ind. Eng. Chem. Fundam.* 25 (4), 758–767.
- Choi, W.-K., et al., 2003. Optimal operation of the pressure swing adsorption (PSA) process for CO₂ recovery. *Korean J. Chem. Eng.* 20 (4), 617–623.
- Chou, C.-T., Chen, C.-Y., 2004. Carbon dioxide recovery by vacuum swing adsorption. *Sep. Purif. Technol.* 39 (1–2), 51–65.
- Chue, K.T., et al., 1995. Comparison of activated carbon and zeolite 13X for CO₂ recovery from flue gas by pressure swing adsorption. *Ind. Eng. Chem. Res.* 34 (2), 591–598.

- DECARBit, 2011. Enabling advanced pre-combustion capture techniques and plants. European best practice guidelines for assessment of CO₂ capture technologies. European Benchmarking Task Force.
- Ebner, A.D., Ritter, J.A., 2009. State-of-the-art adsorption and membrane separation processes for carbon dioxide production from carbon dioxide emitting industries. *Sep. Sci. Technol.* 44 (6), 1273–1421.
- Froment, G.F., Bischoff, K.B., De Wilde, J., 2010. *Chemical Reactor Analysis and Design*, 3rd edition. John Wiley & Sons, Inc.
- Fuller, E.N., Schettler, P.D., Giddings, J.C., 1966. New method for prediction of binary gas-phase diffusion coefficients. *Ind. Eng. Chem.* 58 (5), 18–27.
- Gallei, E., Stumpf, G., 1976. Infrared spectroscopic studies of the adsorption of carbon dioxide and the coadsorption of carbon dioxide and water on CaY- and NiY-zeolites. *J. Colloid Interface Sci.* 55 (2), 415–420.
- Gazzani, M., Macchi, E., Manzolini, G., 2013. CO₂ capture in integrated gasification combined cycle with SEWGS – Part A: Thermodynamic performances. *Fuel* 105, 206–219.
- Grande, C.A., Blom, R., 2012. Dual pressure swing adsorption units for gas separation and purification. *Ind. Eng. Chem. Res.* 51 (25), 8695–8699.
- Harlick, P.J.E., Tezel, F.H., 2004. An experimental adsorbent screening study for CO₂ removal from N₂. *Microporous Mesoporous Mater.* 76 (1–3), 71–79.
- Herzog, H., Meldon, J., Hatton, A., 2009. Advanced Post-Combustion CO₂ Capture.
- Ho, M.T., Allinson, G.W., Wiley, D.E., 2008. Reducing the cost of CO₂ capture from flue gases using pressure swing adsorption. *Ind. Eng. Chem. Res.* 47 (14), 4883–4890.
- IPCC, 2005. In: Metz, B., Davidson, O., de Coninck, H.C., Loos, M., Meyer, L.A. (Eds.), IPCC Special Report on Carbon Dioxide Capture and Storage. Prepared by Working Group III of the Intergovernmental Panel on Climate Change. Cambridge University Press, Cambridge, United Kingdom/New York, NY, USA, 442 pp.
- IPCC, 2013. In: Stocker, T.F., Qin, D., Plattner, G.-K., Tignor, M., Allen, S.K., Boschung, J., Nauels, A., Xia, Y., Bex, V., Midgley, P.M. (Eds.), *Climate Change 2013: The Physical Science Basis Contribution of Working Group I to the Fifth Assessment Report of the Intergovernmental Panel on Climate Change*. Cambridge University Press, Cambridge, United Kingdom/New York, NY, USA, 1535 pp.
- Ishibashi, M., et al., 1996. Technology for removing carbon dioxide from power plant flue gas by the physical adsorption method. *Energy Convers. Manag.* 37 (6–8), 929–933.
- Jiang, L., Fox, V.G., Biegler, L.T., 2004. Simulation and optimal design of multiple-bed pressure swing adsorption systems. *AIChE J.* 50 (11), 2904–2917.
- Kikkinides, E.S., Yang, R.T., Cho, S.H., 1993. Concentration and recovery of carbon dioxide from flue gas by pressure swing adsorption. *Ind. Eng. Chem. Res.* 32 (11), 2714–2720.
- Ko, D., Siriwardane, R., Biegler, L.T., 2005. Optimization of pressure swing adsorption and fractionated vacuum pressure swing adsorption processes for CO₂ capture. *Ind. Eng. Chem. Res.* 44 (21), 8084–8094.
- Li, G., et al., 2011. Dual mode roll-up effect in multicomponent non-isothermal adsorption processes with multilayered bed packing. *Chem. Eng. Sci.* 66 (9), 1825–1834.
- Liu, Z., Green, W.H., 2014. Analysis of adsorbent-based warm CO₂ capture technology for integrated gasification combined cycle (IGCC) power plants. *Ind. Eng. Chem. Res.* 53 (27), 11145–11158.
- Liu, Z., et al., 2011a. Multi-bed vacuum pressure swing adsorption for carbon dioxide capture from flue gas. *Sep. Purif. Technol.* 81 (3), 307–317.
- Liu, Z., et al., 2011b. Adsorption and desorption of carbon dioxide and nitrogen on zeolite 5A. *Sep. Sci. Technol.* 46 (3), 434–451.
- Lopes, F.V.S., et al., 2009a. Adsorption of H₂: CO₂, CH₄, CO, N₂ and H₂O in activated carbon and zeolite for hydrogen production. *Sep. Sci. Technol.* 44 (5), 1045–1073.
- Lopes, F.V.S., et al., 2009b. Enhancing capacity of activated carbons for hydrogen purification. *Ind. Eng. Chem. Res.* 48 (8), 3978–3990.
- Manzolini, G., et al., 2011. Integration of SEWGS for carbon capture in natural gas combined cycle. Part A: Thermodynamic performances. *Int. J. Greenh. Gas Control* 5 (2), 200–213.
- Mehrotra, A., Ebner, A., Ritter, J., 2010. Arithmetic approach for complex PSA cycle scheduling. *Adsorption* 16 (3), 113–126.
- Na, B.-K., et al., 2001. CO₂ recovery from flue gas by PSA process using activated carbon. *Korean J. Chem. Eng.* 18 (2), 220–227.
- Na, B.-K., et al., 2002. Effect of rinse and recycle methods on the pressure swing adsorption process to recover CO₂ from power plant flue gas using activated carbon. *Ind. Eng. Chem. Res.* 41 (22), 5498–5503.
- Nikolic, D., et al., 2008. Generic modeling framework for gas separations using multibed pressure swing adsorption processes. *Ind. Eng. Chem. Res.* 47 (9), 3156–3169.
- Panowski, M., Klainy, R., Sztelder, K., 2010. Modelling of CO₂ adsorption from exhaust gases. In: Yue, G., et al. (Eds.), *Proceedings of the 20th International Conference on Fluidized Bed Combustion*. Springer, Berlin/Heidelberg, pp. 889–894.
- Park, J.-H., Kim, J.-N., Cho, S.-H., 2000. Performance analysis of four-bed H₂ PSA process using layered beds. *AIChE J.* 46 (4), 790–802.
- Pipitone, G., Bolland, O., 2009. Power generation with CO₂ capture: technology for CO₂ purification. *Int. J. Greenh. Gas Control* 3 (5), 528–534.
- Plaza, M.G., et al., 2010. Post-combustion CO₂ capture with a commercial activated carbon: comparison of different regeneration strategies. *Chem. Eng. J.* 163 (1–2), 41–47.
- Poling, B., Prausnitz, J., Connell, J.O., 2000. *The Properties of Gases and Liquids*. McGraw-Hill Education.
- Posch, S., Haider, M., 2012. Optimization of CO₂ compression and purification units (CO₂CPU) for CCS power plants. *Fuel* 101, 254–263.
- Reynolds, S.P., Ebner, A.D., Ritter, J.A., 2006. Stripping PSA cycles for CO₂ recovery from flue gas at high temperature using a hydrocalcite-like adsorbent. *Ind. Eng. Chem. Res.* 45 (12), 4278–4294.
- Ribeiro, A.M., et al., 2008. A parametric study of layered bed PSA for hydrogen purification. *Chem. Eng. Sci.* 63 (21), 5258–5273.
- Ribeiro, A.M., et al., 2009. Four beds pressure swing adsorption for hydrogen purification: case of humid feed and activated carbon beds. *AIChE J.* 55 (9), 2292–2302.
- Rodrigues, A.R.E., Dias, M.M., 1998. Linear driving force approximation in cyclic adsorption processes: simple results from system dynamics based on frequency response analysis. *Chem. Eng. Process. Process Intensif.* 37 (6), 489–502.
- Ruthven, D.M., 1984. *Principle of Adsorption and Adsorption Processes*.
- Ruthven, D.M., Lee, L.-K., Yucel, H., 1980. Kinetics of non-isothermal sorption in molecular sieve crystals. *AIChE J.* 26 (1), 16–23.
- Schell, J., et al., 2013. Precombustion CO₂ capture by pressure swing adsorption (PSA): comparison of laboratory PSA experiments and simulations. *Ind. Eng. Chem. Res.* 52 (24), 8311–8322.
- Sircar, S., Hufton, J.R., 2000. Why does the linear driving force model for adsorption kinetics work? *Adsorption* 6 (2), 137–147.
- Siriwardane, R., et al., 2001. Adsorption and desorption of CO₂ on solid sorbents. *J. Energy Environ. Res.* 19–31.
- Siriwardane, R.V., et al., 2005. Adsorption of CO₂ on zeolites at moderate temperatures. *Energy Fuels* 19 (3), 1153–1159.
- Takamura, Y., et al., 2001. Evaluation of dual-bed pressure swing adsorption for CO₂ recovery from boiler exhaust gas. *Sep. Purif. Technol.* 24 (3), 519–528.
- The Future of Coal. Massachusetts Institute of Technology, 2007.
- Tlili, N., Grévillet, G., Vallières, C., 2009. Carbon dioxide capture and recovery by means of TSA and/or VSA. *Int. J. Greenh. Gas Control* 3 (5), 519–527.
- Wang, Y., et al., 2008. Comparative studies of CO₂ and CH₄ sorption on activated carbon in presence of water. *Colloids Surf. A: Physicochem. Eng. Asp.* 322 (1–3), 14–18.
- Yang, R.T., 1997. *Gas Separation By Adsorption Processes*.
- Yang, J., Lee, C.-H., 1998. Adsorption dynamics of a layered bed PSA for H₂ recovery from coke oven gas. *AIChE J.* 44 (6), 1325–1334.
- Yang, J., Lee, C.-H., Chang, J.-W., 1997. Separation of hydrogen mixtures by a two-bed pressure swing adsorption process using zeolite 5A. *Ind. Eng. Chem. Res.* 36 (7), 2789–2798.
- Yucel, H., Ruthven, D.M., 1980. Diffusion of CO₂ in 4A and 5A zeolite crystals. *J. Colloid Interface Sci.* 74 (1), 186–195.

Correction of Table 1

In the *Table 1* published in *Paper I*, there is an inaccuracy. The column of the temperatures reports values of the mass flow rate of the relative streams. The following is the correct version of that table.

Table 1

Stream table of the ASC plant integrated with a PSA unit for CO₂ capture and a CO₂ compression unit.

Stream	ṁ (kg/s)	T (°C)	P (bar)	MW (g/mol)	Composition (% mol.)					
					CO ₂	N ₂	O ₂	Ar	SO ₂	H ₂ O
1	66.2	25.0	1.0	-	-	-	-	-	-	-
2	744.2	15.0	1.0	28.9	0.03	77.3	20.7	0.9	-	1.0
3	735.7	338.9	1.0	29.9	14.9	74.1	2.9	0.9	0.04	7.2
4	800.8	117.0	1.0	29.8	13.6	74.4	4.4	0.9	0.04	6.7
5	800.8	127.1	1.0	29.8	13.6	74.4	4.4	0.9	0.04	6.7
6	823.3	62.5	1.0	29.3	13.1	71.3	4.2	0.9	0.002	10.5
7	781.1	20.0	1.0	30.4	14.3	77.8	4.6	0.94	0.002	2.3
8	150.4	15.4	1.0	43.2	95.1	4.6	0.3	0.02	-	-
9	619.7	35.2	1.0	28.6	1.7	91.8	5.4	1.1	-	-
10	150.4	28.0	110.0	43.2	95.1	4.6	0.3	0.02	-	-

Paper II

Comprehensive analysis on the performance of an IGCC plant with a PSA process integrated for CO₂ capture

Luca Riboldi, Olav Bolland

International Journal of Greenhouse Gas Control 143, 57-69 (2015)



ELSEVIER

Contents lists available at ScienceDirect

International Journal of Greenhouse Gas Control

journal homepage: www.elsevier.com/locate/ijggc

Comprehensive analysis on the performance of an IGCC plant with a PSA process integrated for CO₂ capture



Luca Riboldi*, Olav Bolland

Energy and Process Engineering Department, the Norwegian University of Science and Technology, NO-7491 Trondheim, Norway

ARTICLE INFO

Article history:

Received 14 July 2015

Received in revised form 9 October 2015

Accepted 15 October 2015

Keywords:

CO₂ capture

PSA

IGCC

Process simulations

ABSTRACT

The main goal of this paper is to provide a comprehensive overview on the performance of an integrated gasification combined cycle (IGCC) implementing CO₂ capture through a pressure swing adsorption (PSA) process. The methodology for integrating a PSA process into the IGCC plant is first defined and then a full-plant model is developed. A reference case is outlined both for the PSA-based plant and for an absorption-based plant. Physical absorption is considered the benchmark technology for the application investigated. The full-plant model allowed an assessment of the potentials of PSA in this framework. The plant performance obtained was evaluated mainly in terms of energy penalty and CO₂ capture efficiency. Several process configurations and operating conditions were tested. The results of these simulations demonstrated the influence of the PSA process on the overall performance and the possibility to shape it according to specific requirements. A sensitivity analysis on the adsorbent material was also carried out, aiming to establish the possible performance enhancements connected to advancements in the material. Improving the properties of the adsorbent demonstrated to have a strong impact not only on the CO₂ separation process but also on the performance of the entire plant. However, nor modifications in the process or in the material were able to fully close the gap with absorption. In this sense a synergetic approach for addressing further performance enhancements is outlined, based on the close collaboration between process engineering and material science.

© 2015 Elsevier Ltd. All rights reserved.

1. Introduction

The world is at a critical juncture in its efforts to contrast climate change. A comprehensive strategy is an impelling issue as further postponements would increase significantly the cost and the difficulty to meet the 2 °C limit for the temperature increase. Greenhouse-gas emissions from the energy sector represent roughly two-thirds of all anthropogenic greenhouse-gas emissions. Effective action in the energy sector is, consequentially, essential to tackling the climate change problem (IEA, 2015). Many scenarios published by independent institutions show that a long-term decarbonisation path cannot do without Carbon Capture and Storage (CCS). CCS enables a strong reduction of net CO₂ emissions from fossil-fueled power plants and industrial processes, providing a protection strategy for power plants that cannot be thought to be completely dismantled in a realistic scenario of a carbon-constrained world (IEA, 2013). The estimated cost of not including CCS in the toolbox would be prohibitive. An important milestone was recently achieved when the first commercial-scale CCS power

plant came online in Canada (SaskPower Boundary Dam Unit 3). Globally, there are other 13 large-scale CCS projects in operation, with a further nine under construction (Global CCS Institute, 2015). The outlook on the strategic role of CCS highlights the importance of investigating more and more efficient technologies for capturing CO₂ from various sources. Among other options, this paper focuses on pressure swing adsorption (PSA) as a methodology for separating CO₂ from a gas mixture in the power sector. PSA is a cyclic process based on the ability of some solid adsorbents to selectively attract and fix CO₂ molecules on their surface. Before the adsorbent bed gets completely saturated, the feed is stopped and a regeneration process is carried out. When the regeneration of the adsorbent is performed by reducing the total pressure of the system, the process is termed PSA. PSA has been considered for its potential low energy requirements. Especially in pre-combustion applications, where the pressure is not reduced below atmospheric conditions, the main energy consumption is caused by the CO₂ compression. Thermal energy duty is generally avoided. Furthermore, a relatively low environmental impact has been predicted in the literature (Khoo and Tan, 2006). The technology can be adopted for several industrial applications, including CCS (Abanades et al., 2015; Ebner and Ritter, 2009), and an extensive literature can be found regarding processes (Reynolds et al., 2006) and materials

* Corresponding author at: Kolbjørn Hejes vei 1a, 7491 Trondheim, Norway.
E-mail address: luca.riboldi@ntnu.no (L. Riboldi).

Nomenclature

a_i	number of neighboring sites occupied by adsorbate molecule for species i
$C_{p,s}$	particle specific heat at constant pressure, J/(kg K)
$D_{0c,i}$	limiting micropore diffusivity at infinite temperature of species i , m^2/s
d_p	particle diameter, m
$E_{a,i}$	activation energy of species i , J/mol
$\Delta H_{r,i}$	isosteric heat of adsorption of species i , J/mol
k_i	equilibrium constant of species i , Pa^{-1}
$k_{\infty,i}$	adsorption constant at infinite temperature of species i , Pa^{-1}
P	pressure, Pa
P_{flash}	pressure at the entrance of the flash column, bar
P_{reg}	regeneration pressure for the PSA process, bar
q_i	equilibrium adsorbed concentration of species i , mol/kg
$q_{m,i}$	maximum adsorption capacity of species i , mol/kg
R	universal gas constant, $Pa\ m^3/(mol\ K)$
R_{CO_2}	CO ₂ recovery
R_{H_2}	H ₂ recovery
t	step time, s
T	temperature, K
T_{feed}	temperature at the entrance of the PSA column, K
Y_{CO_2}	CO ₂ purity

Greek letters

ε	bed void fraction
ε_p	particle void fraction
η_{CO_2}	CO ₂ capture efficiency
η_{el}	net electric efficiency
ρ_p	volumetric mass density of the particle, kg/m^3

Acronyms

CCS	carbon capture and storage
CSS	cyclic steady state
DHU	dehydration unit
FS	flash separator
HRSG	heat recovery steam generator
IGCC	integrated gasification combined cycle
LHV	lower heating value
NC	number of components
PEQ	pressure equalization
P/F	purge-to-feed ratio
PSA	pressure swing adsorption
SEWGS	sorption enhanced water gas shift
WGS	water gas shift

adopted (Choi et al., 2009). In a previous work, we provided with a first assessment on the feasibility of large scale PSA process for removing and concentrating CO₂ in coal-fired power plants, both in a post- and pre-combustion scenario (Riboldi and Bolland, 2015). PSA showed to have the opportunity to become competitive with absorption, the most mature technology currently available, on an energy and CO₂ separation point of view. However, the large plant footprint estimated for the post-combustion case appeared to be a significant obstacle to further developments for that application. Pre-combustion case did not face such problem, so a detailed analysis of an IGCC plant integrating a PSA process is carried out in this paper. PSA demonstrated to be a promising option for removing CO₂ from the syngas of an IGCC plant if the separation process occurs at high temperature levels (Liu and Green, 2014). Also when combined with the shift process, a concept called

Sorption Enhanced Water Gas Shift (SEWGS), PSA performs efficiently (Gazzani et al., 2013), albeit needs to address some challenges relative to the operability of the systems (Najmi et al., 2015). The same challenges apply to any system configuration involving a PSA process in pre-combustion applications. The current paper analyses the range of performances achievable by implementing a cold PSA separation (i.e., the syngas is cooled down after the Water Gas Shift section to proper temperature for the gas removal processes). In line with a previous work (Riboldi and Bolland, 2015), the process arrangement adopted is to consider a single PSA train. A dual PSA system may allow obtaining higher separation performance. On the other hand, it would imply an increase of the footprint and consequently of the capital costs. The additional PSA train can become more attractive when pure H₂ has to be produced. An interesting example is the demonstration project located within the Valero refinery in Port Arthur (Texas) (Baade et al., 2012), where the syngas from two steam-methane reformers is processed in a dual PSA system to produce H₂ and capture CO₂.

Within the framework considered in this work, a composite model has been developed which allows simulating the IGCC-PSA plant defined. Two main domains were considered for the performance investigation, namely the process configuration and the adsorption material. Modifications in the process layout and in the operating conditions were proposed and studied at a system level by means of the full-plant model developed. The impact of advancements in the adsorbent material was also studied. A sensitivity analysis on some targeted material properties was carried out and the effect evaluated on the separation process and on the overall plant. The outputs of all the process simulations were evaluated through a series of performance indicators defined to represent the energy and CO₂ capture efficiency of the plant. The basis for comparison was set to be an IGCC integrated with a physical absorption unit for CO₂ removal.

2. The IGCC plant integrating a PSA process

2.1. Plant model and layout

In order to model the IGCC-PSA plant two different simulation tools have been used. The gasification and gas treatment section, the power station, and the CO₂ compression unit have been modeled in Thermoflex (Thermoflow Inc.). PSA is a batchwise process, thus a dynamic model needed to be defined. A dynamic 1-dimensional model was developed in gPROMS (Process System Enterprise) (gPROMS, 2012). It is constituted by a set of partial differential and algebraic equations (PDAEs), representing material, energy and momentum balances in the packed bed. A more detailed description of the model and of the solution of it can be found in Riboldi and Bolland (2015). The two models described were connected through a common interface in order to exchange information. Even though the PSA process is inherently dynamic, it reaches something defined as cyclic steady state (CSS). CSS occurs when the conditions at the end of the cycle are exactly the same observed at the beginning. The occurrence of CSS and the utilization of several columns working in parallel assure the operating continuity of the system: the PSA can be connected to the rest of the plant which is working in a steady-state mode. The layout of the whole IGCC-PSA plant is represented in Fig. 1. For a detailed description of the various units and of the integrating principles reference can be made to Riboldi and Bolland (2015), DECARBIT (2011). The gasification takes place in an entrained flow dry-fed gasifier with convective gas cooler. Coal used is a Douglas Premium Bituminous Coal. The gasification pressure is set to 44.9 bar and the temperature to 1550 °C. The syngas undergoes a shift process and acid gases are removed by a single-stage Selexol process. The PSA

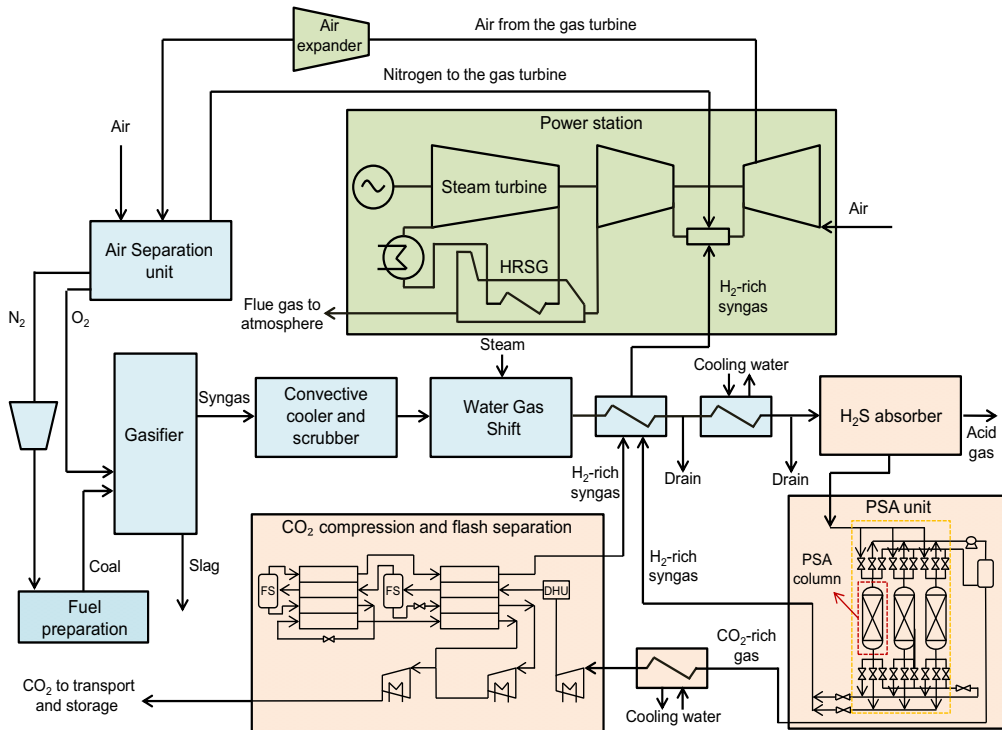


Fig. 1. Flowsheet of the IGCC plant integrating a PSA unit for CO₂ capture.

process separates CO₂ from the shifted syngas which is fueling the power island. A combined cycle is producing a gross power output of about 460 MW. The gas turbine is a F class type. The bottom steam cycle features 3 pressure levels with reheat. The CO₂-rich stream is sent to the compression station, where it is further purified by means of a two-steps flash separation and it is delivered at 110 bar for transportation.

2.2. Base case process conditions and specifications

In order to be able to carry out a thorough performance analysis on the defined IGCC plant with CO₂ capture, a base case needs to be defined. The choice of this base case is arbitrary and is necessary to understand the influence of different modifications introduced. The selection has been based on a previous work (Riboldi and Bolland, 2015). The instance selected demonstrated to return a good balance between separation and energy performances, and takes into consideration the operating constraints given by the integration of PSA into the IGCC plant. Most of the operating parameters are taken from EBTf (DECARBit, 2011), in order to set a defined framework for fair comparisons of the results. The pressure, the mass flow rate and the composition entering the PSA unit are dictated by the process upstream. The CO₂-rich gas stream leaving PSA needs to be compressed to 110 bar for transportation, with a CO₂ volumetric concentration above 95% (de Visser et al., 2008). The second product stream leaving PSA is rich in H₂. It has to be fed to the combustor of the gas turbine, thus it needs to fulfill specifications in terms of pressure (with a lower limit of 24.12 bar) and temperature (as high as 230 °C in accordance with the syngas pre-heating system). Within the mentioned constraints, the operating conditions of the PSA process and of the CO₂ compression process could be freely chosen. Table 1 shows the values of the most significant ones. The PSA process relies on a 7-bed 12-step cycle and it was defined in order to fulfill the specifications of the two

Table 1

Operating parameters and characteristics of the base case selected.

CO ₂ compression and flash separation	
Flash pressure (bar)	30
Delivery pressure (bar)	110
T flash 1 ^a (K)	243.2
T flash 2 ^a (K)	218.7
PSA	
Adsorption pressure (bar)	38.8
Regeneration pressure (bar)	1
Syngas composition (% vol.) (CO ₂ -H ₂ -CO-N ₂)	0.380–0.537–0.016–0.067
Syngas temperature (K)	338
Syngas flow rate (mol/s)	5331.7
P/F ratio	0.10
PSA cycle time (s)	630
t _{feed} (s)	90
t _{pressure equalization} (s)	41
t _{blowdown} (s)	80
t _{purge} (s)	59
t _{null} (s)	8
t _{feed pressurization} (s)	41
PSA column characteristics	
Bed length (m)	10
Bed diameter (m)	6.6
Bed porosity	0.38
Solid density (kg/m ³)	1939

^a T flash is the temperature of the gas stream entering the flash separators.

product streams in the most effective way. Fig. 2 shows the sequence of steps undergone by each column of the PSA unit and the scheduling of the cycle. More on the definition of the PSA cycle and on its optimization can be found in a previous work (Riboldi and Bolland, 2015). The adsorbent material selected is a commercial activated carbon (Lopes et al., 2009).

The performance of the defined base case is shown in Table 2. The performance indicators utilized aims to give an assessment of the energy and CO₂ separation efficiency of the system. They include the net electric efficiency (η_{el}), the H₂ recovery (R_{H_2}), the

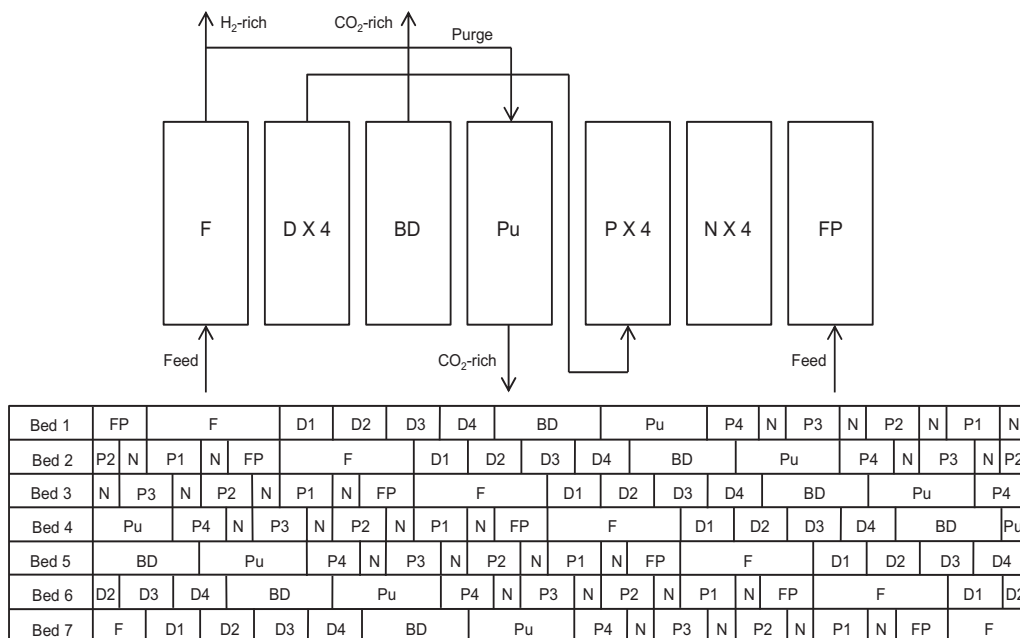


Fig. 2. Scheduling of steps undergone by a column in the PSA cycle. The steps considered are: feed pressurization (FP), feed (F), pressure equalization – depressurization (D), blowdown (BD), purge (Pu), pressure equalization – pressurization (P), null (N).

Table 2

Overview of the performance of an IGCC plant with and without CO₂ capture.

	No capture	Absorption 1	Absorption 2 (DECARBit, 2011)	Absorption 3 (Gazzani et al., 2013)	PSA
η_{net} (%)	47.3%	37.1%	36.7%	36.0%	36.2%
R_{H_2} (%)	–	100.0%	99.3%	99.7%	99.6%
Y_{CO_2} (%)	–	100.0%	98.2%	99.0%	98.9%
R_{CO_2} (%)	–	90.6%	90.9%	90.3%	86.1%
η_{CO_2} (%)	–	88.1%	88.3%	87.2%	81.8%
Footprint (m ²)	–	8	–	–	239

CO₂ recovery (R_{CO_2}), the CO₂ purity (Y_{CO_2}) and the CO₂ capture efficiency (η_{CO_2}). These quantities are defined as following:

$$\eta_{el} = \frac{\text{Net electric output}}{\text{Thermal power input}_{LHV}} \quad (1)$$

$$R_{H_2} = \frac{\dot{m} \text{ of } H_2 \text{ entering the gas turbine as fuel}}{\dot{m} \text{ of } H_2 \text{ entering the } CO_2 \text{ separation unit}} \quad (2)$$

$$R_{CO_2} = \frac{\dot{m} \text{ of } CO_2 \text{ in the product stream}}{\dot{m} \text{ of } CO_2 \text{ formed}} \quad (3)$$

$$Y_{CO_2} = y_{CO_2} \text{ in the product stream} \quad (4)$$

$$\eta_{CO_2} = 1 - \frac{\eta_{net} \text{ for the reference plant without } CO_2 \text{ capture}}{\eta_{net} \text{ for the plant implementing } CO_2 \text{ capture}} (1 - R_{CO_2}) \quad (5)$$

When the recovery and the purity are referring only to the PSA process, thus not including the flash separation, the performance indicator is reported with the prefix PSA (e.g., PSA- R_{CO_2}).

Considerations on the footprint of the separation unit are also present, taking into account the dimensions of the columns used for the different CO₂ separation technologies (the footprint values reported are simply the total square meters occupied by the separation columns).

Table 2 shows also results for an IGCC plant not implementing CO₂ capture and compression (simulated in Thermoflex) and for an IGCC plant integrating a two-stage Selexol process, which is considered to be the most common commercial technology for removing CO₂ and H₂S (Field and Brasington, 2011). The description of these systems can be easily found in the literature (DECARBit, 2011; NETL, 2013). Three cases for the absorption method are reported. A first one is the result of Thermoflex modeling and simulation. The utilization of the same modeling tool assures that identical assumptions for the IGCC plant in the PSA and absorption cases are applied. Nevertheless, Thermoflex assumes a constant value for the CO₂ purity in the absorption unit, equal to 100%. The value is overestimated as typical values range around 99%. This led to a consequent overestimation of the energy performance, since no H₂ is leaving with the CO₂-rich stream to be compressed. For this reason, two additional sets of results were taken from the literature, in order to get a more thorough overview of the state-of-the-art of absorption for CO₂ separation in this pre-combustion application.

3. Process configuration and operating conditions

In this section the performance of the IGCC-PSA plant is analyzed by investigating different process configurations and operating conditions. The results will be shown in terms of η_{net} and η_{CO_2} for the overall plant. Although many of the modifications regard the PSA process, the output is studied at the system level.

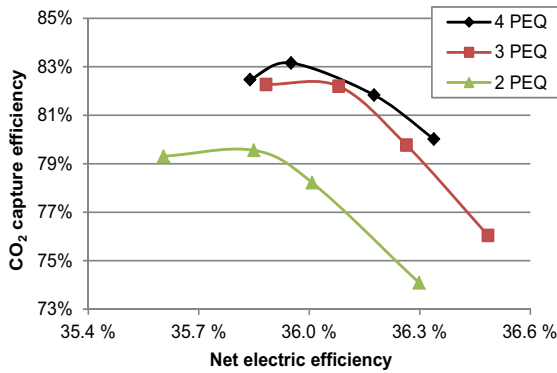


Fig. 3. Plant performance with different PEQ steps in the PSA process.

Previous studies investigated the optimum operating configuration for the separation unit alone (Casas et al., 2013a). However, the plant is highly integrated and modifications in the separation unit affect significantly the other units. The full-plant model developed allows to analyze these effects.

In the following sub-sections alternative process configurations or operating conditions are suggested. The resulting outputs are described and analyzed. Most of the time, a set of results is graphically shown for each case studied. It refers to the system operating within the outlined conditions, but with different purge-to-feed (P/F) mole flow rate ratio of the PSA process. An increase of P/F causes a decrease of $PSA-Y_{CO_2}$ and an increase of $PSA-R_{CO_2}$. The effect on the whole system is a reduction of η_{net} . This indication can be utilized to understand in which direction P/F is changing in the figures proposed. By taking into account the tradeoff between $PSA-Y_{CO_2}$ and $PSA-R_{CO_2}$ obtained through modification of the purge mole flow rate, this representation aims to show the range of possible results within the same process framework.

3.1. Number of pressure equalization steps

The cycle adopted in the PSA unit is rather complex. It involves several steps which a single column undergoes and some of these steps imply two different columns to interact. A typical example is the pressure equalization (PEQ) step, where two columns at different pressure levels are put in contact. By means of the pressure gradient, the high pressure column releases part of its bulk gas to pressurize the other. The pressure of the two columns equalizes to a value in the middle between the starting ones. The larger the number of PEQ steps, the larger is the number of columns working in parallel and the more complex becomes the systems. On the other hand, the PEQ steps actively contribute to an efficient separation process, displacing, before regeneration starts, a fraction of the bulk gas that would otherwise leave with CO_2 . The correlation between number of PEQ steps, energy and separation performance was studied by running several full-plant simulations. PSA cycles with 4, 3 and 2 PEQ steps were considered, while the general structure of the cycle remains identical. An additional adjustment was introduced to the bed length. Decreasing the number of PEQ steps implies a lower pressure at the beginning of the feed pressurization step and, thereby, a larger amount of gas to pressurize the column. Since the incoming syngas to process is constant, the feed flow rate during the adsorption step would be reduced. For the sake of fair comparisons, we wanted to keep the feed flow rate as stable as possible in the different instances considered. For this reason the length of the column was decreased, down to 9 m and 8 m respectively for the 3PEQ and the 2PEQ case, since this reduces the gas necessary for the column pressurization. Fig. 3 shows the

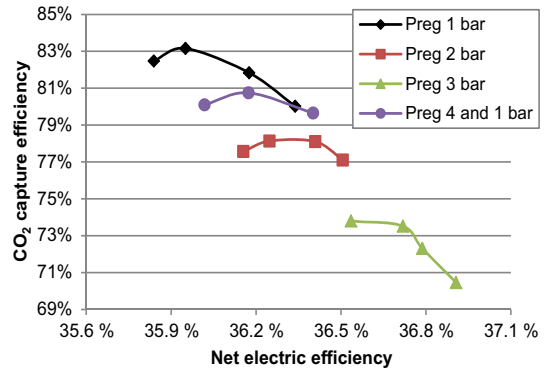


Fig. 4. Plant performance with different regeneration strategies.

outputs of the simulations implemented. Reducing the number of PEQ steps translates in a decrease of the PSA separation performance, which eventually leads to a decreased η_{CO_2} . The η_{el} does not display a clear trend. Its changes result from the balance of CO_2 purity ($PSA-Y_{CO_2}$) and CO_2 recovery ($PSA-R_{CO_2}$) in the PSA process, which both affect the off-gas mass flow rate to be compressed. The number of columns constituting a train and, hence, the footprint of the system is decreasing in accordance with the decrease of the number of PEQ steps implemented. As a general rule, the number of columns needed in the selected process framework is:

$$\text{No. columns} = \text{PEQ steps} + 3 \quad (6)$$

3.2. Regeneration strategy

The modification of the regeneration pressure (P_{reg}) of the PSA process has a direct impact both on the separation and energy performance. The lower the P_{reg} the better is the capacity of the adsorption bed to efficiently desorb CO_2 . This translates in higher values of $PSA-Y_{CO_2}$ and $PSA-R_{CO_2}$. Conversely, increasing P_{reg} results in a lower effectiveness of the separation process. On an energy point of view, increasing P_{reg} implies a lower pressure ratio for the CO_2 compressor and, hence, a decrease in the power consumption is expected. The system performance was investigated increasing P_{reg} from 1 bar up to 2 and 3 bar. It was decided not to study the effect of P_{reg} lower than 1 bar because that would require the utilization of vacuum pumps, increasing the power consumption and the complexity of the system. Following the same procedure previously outlined, the bed length was adjusted in order to deal with the constraint of processing a fixed syngas flow rate. A higher P_{reg} means that less gas is needed to pressurize the column. Accordingly, the bed length was properly increased to 11 m and 12 m respectively for the P_{reg} 2 and 3 bar case. Fig. 4 shows that an augmented P_{reg} is indeed increasing the η_{el} , as a consequence of the decrease in the CO_2 compressor power consumption. On the other hand the effectiveness of the separation process necessarily decreases and in particular lower $PSA-Y_{CO_2}$ values are obtained. The lower the $PSA-Y_{CO_2}$, the higher is the mass flow rate to be compressed. The increased mass flow rate partially counterbalances the reduced pressure ratio in the compressors. However, also the final R_{CO_2} (after the flash separation) is decreasing with the increase of P_{reg} , reducing again the mass flow rate to be processed in the final stage of the compression. The overall separation performance is negatively influenced by higher P_{reg} . Whilst the Y_{CO_2} remains stable, thanks to the flash separation process, the same is not happening with the R_{CO_2} . The increased amount of gas entering the multi-flash unit, due to the lower $PSA-Y_{CO_2}$, makes the flash separation more challenging, resulting in a larger quantity of CO_2 leaving with the H_2 -rich gas stream.

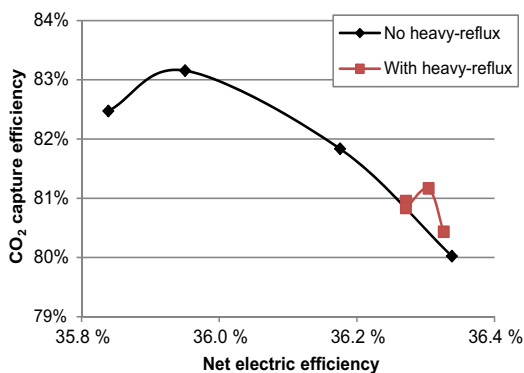


Fig. 5. Plant performance with and without a heavy-reflux step in the PSA process.

In the attempt of limiting the negative effects on the separation efficiency, another regeneration strategy was also tested. It consists in carrying out the regeneration step at different pressure levels. The regeneration pressure (P_{reg}) could be initially fixed to a higher value (e.g., 4 bar) and afterwards to a final atmospheric value. The effectiveness of the bed regeneration should not be heavily influenced by the new process configuration, while the fraction of CO_2 -rich gas recovered in the first part of the blowdown would need a lower pressure ratio. Simulations of the PSA process were run with the proposed multi-pressure regeneration step. The pressure levels were set to 4 bar and 1 bar. The PSA process was modified in order to suit the new regeneration procedure (3PEQ steps and different steps time) and the length of the column was set to 11 m. The results of the simulations are shown in Fig. 4. The new regeneration strategy produced a benefit in terms of reduced compressor power consumption in one single case. This is due to the lower PSA- Y_{CO_2} we were able to obtain which translated in a larger mass flow rate to be compressed. The maximum energy efficiency achieved (36.4%) is slightly higher than the base case, but to the detriment of the separation performance. The removal of one pressure equalization step is the main reason behind the reduced CO_2 capture efficiency but it is necessary in order to enable a first regeneration step at 4 bar.

3.3. Introduction of a heavy-reflux step

A well-documented option to increase the PSA- Y_{CO_2} is to introduce a heavy-reflux step (also called rinse step) in the PSA cycle (Liu et al., 2011; Na et al., 2002). It consists in feeding a CO_2 -rich stream to the column before blowdown. By means of that, the light-gas, mainly H_2 , in the bed void space can be partially displaced. The gas stream utilized to displace the void gas is the product gas obtained from the regeneration process, hence, rich in CO_2 . In order to implement the heavy-reflux, the PSA process was redesigned in order to accommodate the new step. It was chosen to set it just before the blowdown, so that it was not needed a significant compression of the product gas to be rinsed. The simulations demonstrate that the addition of a heavy-reflux step is not providing with significant advantages, as can be noticed from Fig. 5. The obtained increase in the PSA- Y_{CO_2} is limited to about 1%. An analysis of the results suggests that the utilization of the rinse gas stream is able to just partially displace the H_2 from the void space of the column. A more complete displacement would require a too large rinse flow rate, which would drastically decrease R_{CO_2} . In order to limit the decrease of R_{CO_2} , the gas stream leaving the column during the heavy-reflux step is sent to the compression and flash separation unit instead of being vented. The resulting separation performance is on average lower than the base case, while the energy performance registered is on similar levels.

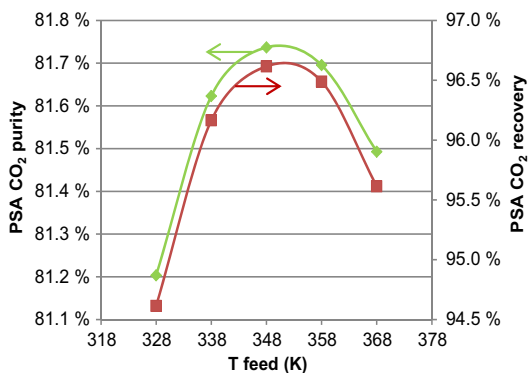


Fig. 6. PSA performance with different T_{feed} .

3.4. Feed temperature

The temperature adopted at the entrance of the PSA unit (T_{feed}) has an impact on the plant performance. This effect has been evaluated by simulating the plant behavior at different T_{feed} : 328 K, 338 K (base case), 348 K, 358 K and 368 K. In the first instance, it is interesting to notice the effect on the separation unit (see Fig. 6). One would expect the PSA process to perform better at the lowest temperature tested, in accordance with the exothermic nature of adsorption. Conversely, the actual trend is showing a maximum in the separation performance (CO_2 purity and recovery for the PSA process) when the T_{feed} is set to 348 K. In order to explain this trend, the whole cycle needs to be taken into consideration. Whilst low temperatures are beneficial for adsorption (exothermic process), they are detrimental for desorption (endothermic process and because the adsorbent saturate at lower pressures). In the PSA process investigated, no temperature swing is implemented. Thus, the lower is the temperature at the beginning of the cycle, the lower will likely be during the regeneration steps. The working capacity, defined as the difference between the equilibrium capacity during adsorption and desorption, constitutes the real measure of the effectiveness of the separation process. It reached a maximum when the syngas is introduced at 348 K. It has been shown before that not always the optimum for the PSA unit corresponds to the optimum for the overall plant. The full-plant model allowed the investigation of the T_{feed} effect also at a system level. The base case with a P/F ratio of 0.14 was selected as starting point and the different T_{feed} were tested. The outputs of the simulations are shown in Fig. 7. The best cases on a CO_2 separation point of view (T_{feed} 348 K and 358 K) display a small decrease in the η_{net} . This is

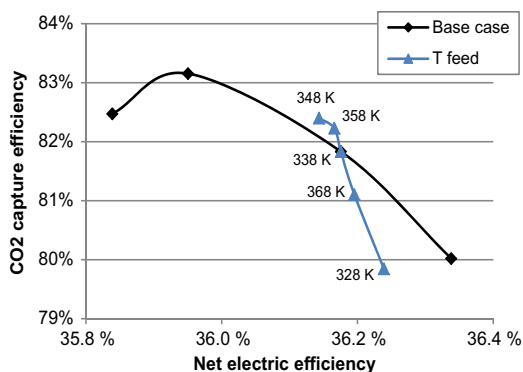


Fig. 7. Plant performance with different T_{feed} .

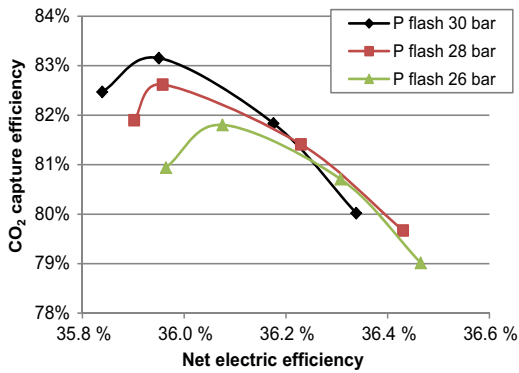


Fig. 8. Plant performance with different P_{flash} .

due to two main factors: the higher CO₂ recovery, which implies a larger gas stream to be compressed, thereby increased power to the compressors (even though also the CO₂ purity is increasing, partially counterbalancing that); the slight less efficient H₂ recovery in the flash separation unit and the consequent decrease of the gross power output. In spite of that, they are more effective than the other cases assessed (T_{feed} 328 K and 368 K) which achieve slightly lower energy penalty at the expense of more significant reduction of the CO₂ capture efficiency.

3.5. Flash pressure

The CO₂-rich product stream which is leaving the PSA unit is sent to the CO₂ compression and flash separation unit. There a first compression process increases the pressure before the gas stream enters two multi-stream heat exchangers and two flash separators. The operating parameters were set according to previous studies and taking into account thermodynamic constraints to the system (Darde et al., 2009; Pipitone and Bolland, 2009; Posch and Haider, 2012). This section wants to investigate the impact of modification of the flash pressure P_{flash} (i.e., the pressure after the first compression, at which the gas stream enters the first flash column). The base case sets it to 30 bar. Two additional pressure levels were considered, namely 28 bar and 26 bar. Lower pressures were not considered because the H₂ recovered in this process is sent to the gas turbine and needs to have a pressure of about 24 bar. Considering the pressure drops in the unit, the P_{flash} cannot be set lower than 26 bar, unless a recompression is planned. The outputs of the simulations are shown in Fig. 8. The general trend is that decreasing P_{flash} has a negative effect on the separation performance. The separation in the flash columns becomes less effective and the CO₂ recovery decreases (hence also η_{CO_2}). However, a large fraction of H₂ is still recovered (more diluted with CO₂) and the overall compression power decreases. Thus, the η_{net} is slightly lifted up.

3.6. CO₂ recirculation

A way to improve the CO₂ separation process is to recirculate part of the product CO₂-rich stream and increasing the CO₂ partial pressure entering the PSA unit. This possibility is analyzed by utilizing CO₂ as fuel preparation gas (an option already proposed in the literature (Botero et al., 2013)). The coal feeding system is normally designed to utilize 0.02207 kg N₂ per kg coal, with the pure N₂ taken from the ASU. If CO₂ has to be used, the gas flow rate required is double than the flow rate of N₂ and the operating conditions need to be adjusted (DECARBit, 2011). The CO₂ used

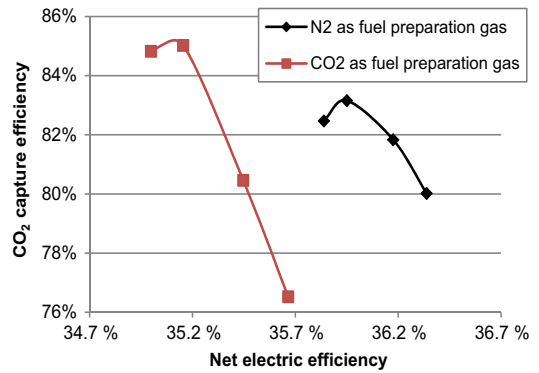


Fig. 9. Plant performance with and without CO₂ recirculation.

in the fuel feeding system is extracted from the CO₂ compression section at a pressure of 50 bar, as requested by the specifications. Fig. 9 shows the results obtained by the full-plant simulations. Better separation performance was obtained. With a sufficiently high P/F ratio the R_{CO_2} reaches the desired level of 90%, while the Y_{CO_2} remains on high levels (>99%). The increase in η_{CO_2} is more limited as it reaches a maximum value of 85%. In fact, the enhanced separation performance is counterbalanced by an increase in the energy penalty. Since the amount of the gas stream needed for transporting the coal is double than the N₂-based counterpart, the amount of gas to be processed is increased. This translates into augmented power consumption for the compressors which have to compress a larger mass flow rate. Another modification observed is that the steam turbine power output slightly decreases because a larger quantitative of steam needs to be extracted to be fed to the WGS process, due to the larger fraction of CO in the syngas. These two effects outbalance the power consumption reduction in the ASU, due to the missing N₂ compression for fuel preparation purposes. The overall outcome is that the energy efficiency is reduced to values between 35.0% and 35.7%.

3.7. Remarks on the process configuration and operating conditions analysis

Fig. 10 shows the performance of the base case defined, all the simulation outputs of alternative process configurations and the reference results for absorption. It is interesting to look at the overall trend represented in the figure. The base case is an acceptable compromise between energy and separation efficiency. Enhancements can be achieved by modifications of the process configuration or of its operating parameters. However, most of the times, an improvement in the energy efficiency results in a decrease of the CO₂ capture efficiency (e.g., increasing P_{reg}) or vice versa (e.g., CO₂ recirculation). Consequently, it is difficult to state what is the optimum process configuration or set of operating parameters. Those are dependent on the specific requirements the plant needs to fulfill. So, for example, if a CO₂ recovery of about 80% was considered acceptable, some of the configurations studied would return η_{el} on the level of the absorption counterpart. A certain flexibility in the range of performances achievable is to be noted. However, Fig. 10 clearly shows that modifications to the process may fill the gap with absorption only in relation to a specific performance indicator. When the effectiveness of the separation technologies is analyzed as a whole (energy, separation and footprint), absorption is still displaying an advantage over PSA.

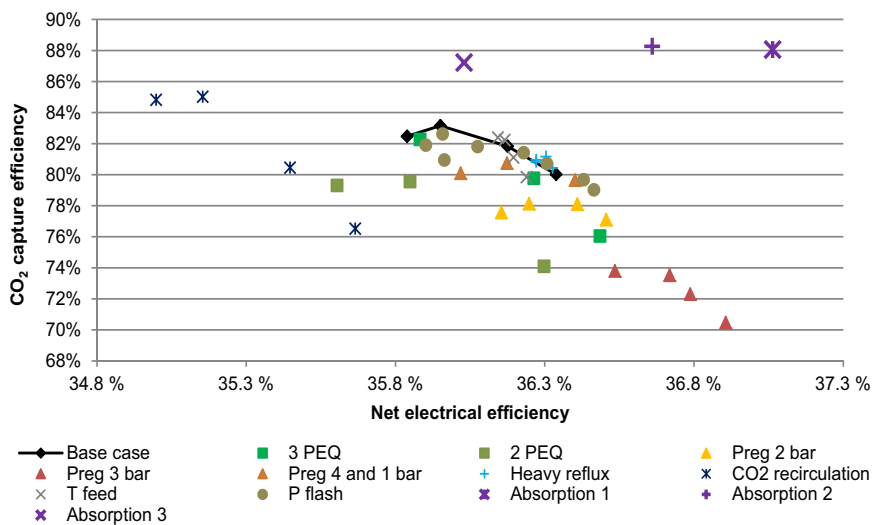


Fig. 10. Overview of plant performances achievable by modifications of the process.

4. Adsorbent material

The characteristics of the adsorbent material have a strong impact on the effectiveness of the CO₂ separation process. One of the firsts and more important decisions when it comes to design a PSA process is the choice of the proper adsorbent. In the previous analyses the adsorbent considered is a commercial activated carbon (Lopes et al., 2009). Activated carbon demonstrates to outperform zeolites (which are normally considered to be the benchmark for CO₂ separation) when the adsorption process occurs at relatively high CO₂ partial pressure (Siriwardane et al., 2001). This is the case for a pre-combustion application. Other advantages of activated carbons over zeolites are the lower costs (Choi et al., 2009) and the higher resistance to water presence in the gas mixture (Choi et al., 2009; Li et al., 2008; Ribeiro et al., 2009). Material science is very active in the research of new adsorbents with enhanced characteristics for CO₂ separation (Arstad et al., 2008; Casas et al., 2013b; Hedin et al., 2010; Lu et al., 2008). Much effort is put in the laboratory tests to develop adsorbents with remarkable performance. In this section a different approach has been adopted for the study of adsorbent material influence. Instead of testing specific adsorbents, which would require the availability of a large amount of modeling data, we tried to define the optimum characteristics of an adsorbent to perform efficiently in the framework under investigation. Taking as reference the activated carbon, a sensitivity analysis on some meaningful properties was carried out. The original values of the properties were varied in targeted ways in order to evaluate how those variations affect the process performance, and to pinpoint the most influential properties. The output variables carefully monitored were those related to the effectiveness of the adsorbent. It was taken track of the effects on the CO₂ recovery, purity and on the selectivity at which the material is able to separate CO₂. The full-plant model enabled then to assess the impact on the overall system. Being aware of the limitations of such analysis, it was thought to be useful for providing an indication on the performance enhancements realistically achievable by advancements in the adsorbent materials. Furthermore, it can be a source of inputs and guidelines to the material scientists in order to address future developments.

Table 3

Adsorption and physical properties of the reference activated carbon.

Activated carbon and adsorbent bed – Physical properties						
d_p (mm)	ε_p	ρ_p (kg/m ³)	$C_{p,s}$ (J/kg/K)	ε		
2.34	0.57	842	709	0.38		
Activated carbon – Equilibrium and kinetic parameters						
a (-)	k_{∞} (Pa ⁻¹)	q_m (mol/kg)	ΔH_r (kJ/mol)	D_{0e}/r_c^2 (s ⁻¹)	E_a (kJ/mol)	
CO ₂	3.0	2.128E-11	7.855	-29.1	17.5	15.8
N ₂	4.0	2.343E-10	5.891	-16.3	1.0	7.0
H ₂	1.0	7.690E-11	23.570	-12.8	14.8	10.4
CO	2.6	2.680E-11	9.063	-22.6	59.2	17.5

4.1. Sensitivity analysis

The equilibrium behavior of the activated carbon is described by a multi-site Langmuir isotherm (Nitta et al., 1984):

$$\frac{q_i^*}{q_{m,i}} = a_i k_i P_i \left[1 - \sum_i^{NC} \left(\frac{q_i^*}{q_{m,i}} \right) \right]^{a_i}, \quad \text{with } k_i = k_{\infty,i} \exp \left(-\frac{\Delta H_{r,i}}{RT} \right) \quad (7)$$

The values of the properties have been taken from the literature (Lopes et al., 2009) and they are shown in Table 3.

An ideal adsorbent selectively retains CO₂ on its surface while the other components are flowing through. However, in a real process a fraction of all the non-CO₂ components is also fixed on the solid surface. An adsorbent can be improved according to two different strategies: its ability of fixing CO₂ can be increased or the undesired uptake of the other gas components can be decreased. Accordingly, the properties have been divided into two groups: the CO₂-related properties on one side, the properties of non-CO₂ components (i.e., H₂, CO and N₂) on the other. When the impact of one CO₂ property (e.g., q_{m,CO_2}) had to be evaluated, its value was increased in fixed percentages (+1%, 5%, 10%, 20%, 30%), while the values of all the other properties were kept constant. Conversely, when the impact of a non-CO₂ property was investigated (e.g., $q_{m,non-CO_2}$), only the values of that property referring to the non-CO₂ components were decreased to the same extent (-1%, 5%, 10%, 20%, 30%). The properties selected for the study are:

- the *maximum adsorption capacity* q_m , indicating the maximum amount of the specific component that can be adsorbed per kg of adsorbent.
- the *adsorption equilibrium constant at infinite temperature* k_∞ , necessary for calculating the adsorption equilibrium constant k .
- the *isosteric heat of adsorption* ΔH_r , measuring the strength of adsorption of the specific component to the adsorbent.

The material and packing characteristics were also taken into account in the analysis, in the form of void fractions. They were expected to have a significant influence on the performance of the adsorption process. In the first instance because they affect the volume based adsorption capacity of the bed. Furthermore, it was noticed that a significant fraction of the impurities leaving with CO_2 rather than being adsorbed onto the solid – and released during bed regeneration – are accumulated in the void spaces of the bed as bulk phase. Thus, reducing the void space is expected to reduce the accumulation of impurities in the bed. The void fraction was considered at two levels, which were decreased in –1%, 5%, 10%, 20%:

- the *particle void fraction* ε_p , measuring the void space in the particle due to its porous structure.
- the *bed void fraction* ε , measuring the void space in the bed due to the characteristic of the packing.

An example can be useful to clarify the procedure. Assuming that q_{m,CO_2} is the property to be investigated, its original value 7.885 mol/kg is increased in the mentioned percentages. The physical meaning of this is that a kilo of the adsorbent can accommodate at equilibrium a larger amount of CO_2 . The value of the all the other properties is unvaried. When the same analysis is to be done on the $q_{m,\text{non-CO}_2}$, the maximum capacity of H_2 , CO and N_2 are decreased according to the selected percentages (meaning that a kilo of adsorbent can accommodate at equilibrium a lower amount of those components). The other properties are at the reference value, included q_{m,CO_2} . The same procedure was utilized to study all the properties. This methodology allows evaluating the influence of each single property studied, given that any variation in the performance can be uniquely ascribed to the implemented modification.

4.2. Effect on the PSA process

The effect of the sensitivity analysis was first evaluated on the separation effectiveness of the PSA process. The output is graphically shown in Figs. 11–14. The horizontal axis indicates the extent of the modification implemented on the single property, while on the vertical axis the CO_2 purity or recovery obtained by means of that modification is reported. As we described, the CO_2 properties were increased in fixed percentages, while the non- CO_2 properties were decreased to the same extent. A base case performance is reported, where the characteristics of the PSA cycle are those previously outlined (cf. Section 2.2). Since the purity appeared to be the most critical factor, it was chosen to use as starting point for the sensitivity analysis one with a low P/F ratio (i.e., $P/F=0.06$) which returns the following results: $\text{PSA-}Y_{\text{CO}_2} = 85.3\%$ and $\text{PSA-}R_{\text{CO}_2} = 88.7\%$. Such choice was taken in order to be able to ascribe any further increase of the purity to the material modification and not to the trade-off of some percentage points of the recovery.

All the modifications proposed tend to increase both CO_2 recovery and purity. This was expected since the way to vary the properties was meant to improve the adsorbent material. Different properties show different influences on the separation efficiency. ΔH_r seems to display the strongest one. An increase of $\Delta H_{r,\text{CO}_2}$

brings a positive effect on the isotherm at high pressure. Contemporarily the adsorption isotherm becomes steeper in the low pressure region, thus it becomes more and more difficult to desorb CO_2 from the bed. For small increases of $\Delta H_{r,\text{CO}_2}$ the overall effect is positive (the working capacity is augmented). For higher values of $\Delta H_{r,\text{CO}_2}$, the reduced effectiveness of the regeneration process starts to prevail. Accordingly, the positive effect reaches a maximum when the value is increased of about 10%; after that, the benefits on the performance indicators tend to diminish. When the decrease of $\Delta H_{r,\text{non-CO}_2}$ is considered, the uptake capacity for non- CO_2 components at high pressure is reduced; hence a lower amount of those gases is retained on the material during adsorption step and a higher amount of CO_2 can be fixed, with a consequent benefit on $\text{PSA-}R_{\text{CO}_2}$. Furthermore, decreasing the strength of the adsorption bond for the non- CO_2 components (i.e., reducing $\Delta H_{r,\text{non-CO}_2}$) makes their regeneration easier. A large fraction of them can be desorbed during the PEQ steps, which become extremely effective and avoid a drastic reduction of $\text{PSA-}Y_{\text{CO}_2}$ that would occur if those gases were flowing out during the regeneration steps (i.e., blowdown and purge).

Also q_{m,CO_2} has a strong impact on the separation process. An increase of q_{m,CO_2} results in a remarkable increase of $\text{PSA-}R_{\text{CO}_2}$ (on the same level attained with modification of ΔH_r) because of the increased uptake capacity of the adsorbent. On the other hand, the $\text{PSA-}Y_{\text{CO}_2}$, after an initial increase, drops to values lower than the base case. This is due to the CO_2 adsorption wavefront getting steeper for the higher driving force exercised by the adsorption bed. Accordingly, the part of the bed not saturated with CO_2 adsorbs a higher amount of the other components, whose adsorption wavefronts travel quicker through the column. Those components are then released during desorption producing the reduction of $\text{PSA-}Y_{\text{CO}_2}$.

The other properties examined (i.e., $q_{m,\text{non-CO}_2}$ and k_{∞,CO_2} and $k_{\infty,\text{non-CO}_2}$) display a similar, more limited, effect. The performance indicators increase in an almost linear way but more slowly than the previous cases. Reducing $q_{m,\text{non-CO}_2}$ increases the active sites available for CO_2 uptake and the reduction of the non- CO_2 components adsorbed is also beneficial for the regeneration process. Modifications in k_∞ – whether increasing k_{∞,CO_2} or decreasing $k_{\infty,\text{non-CO}_2}$ – act as correspondent modifications in the partial pressure. Thereby, they have a steady positive effect increasing with the extent of the modification.

The last parameters analyzed were ε_p and ε . Their trend is similar even though ε_p displays a stronger impact, both positive and negative, on the separation performance. The implemented reduction of the void fractions has as primary effect the increase of the adsorbent and bulk density. A larger quantity of adsorbent can be accommodated per volume of bed, thus more CO_2 can be fixed. This explains the remarkable increase in the $\text{PSA-}R_{\text{CO}_2}$. A diminished void fraction reduces also the amount of bulk gas accumulated in the bed. Given that such bulk gas is mainly constituted by the lighter components, H_2 in the first instance, and that they are released during the regeneration steps, an initial increase of $\text{PSA-}Y_{\text{CO}_2}$ can be verified. However, when the decrease of the void fractions exceeds certain levels, the amount of non- CO_2 components retained onto the adsorbent augments so much, due to the increased adsorbent and bulk densities, to overcome the reduction of impurities present as bulk phase. The $\text{PSA-}Y_{\text{CO}_2}$ starts then to decrease significantly.

4.3. Effect on the overall plant

In order to evaluate the overall effect on the plant, the most significant cases were extrapolated by the previous analysis (highlighted in the previous figures) and utilized in the full-plant model. It was chosen to select one example for each type of property

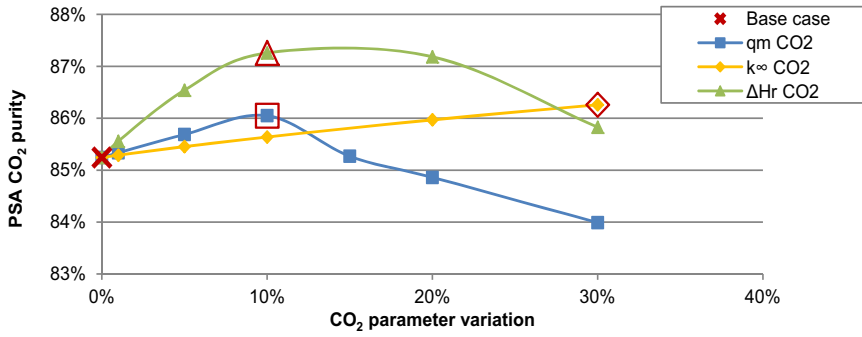


Fig. 11. Effect on the PSA CO₂ purity of the sensitivity analysis on the CO₂ related properties.

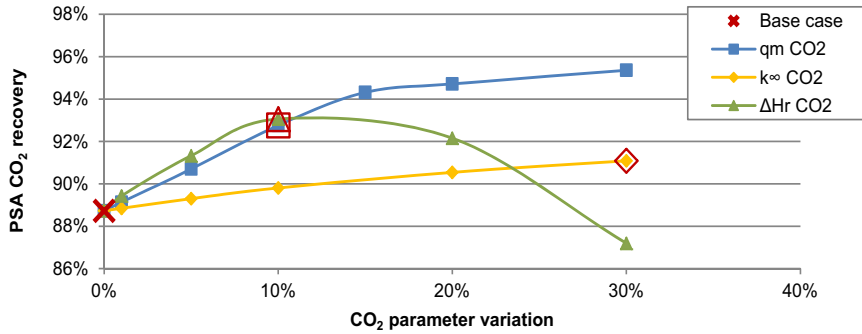


Fig. 12. Effect on the PSA CO₂ recovery of the sensitivity analysis on the CO₂ related properties.

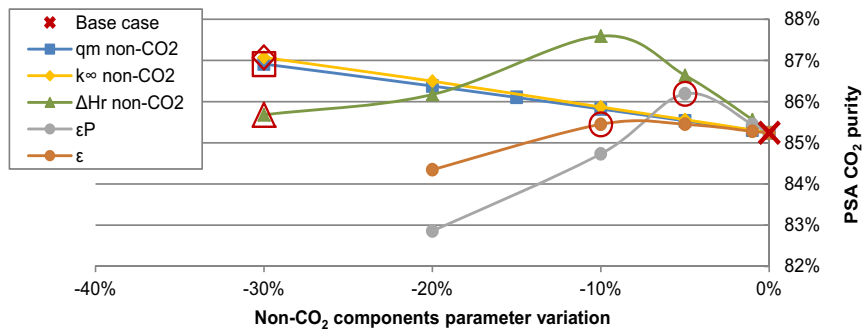


Fig. 13. Effect on the PSA CO₂ purity of the sensitivity analysis on the non-CO₂ related properties.

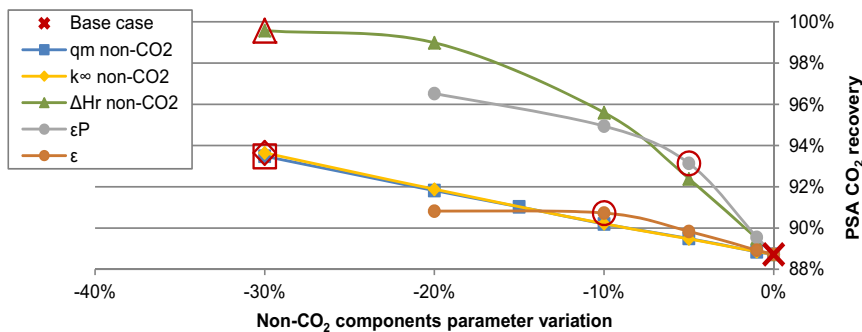


Fig. 14. Effect on the PSA CO₂ recovery of the sensitivity analysis on the non-CO₂ related properties.

variation studied. The instances selected are listed hereafter and can be thought as fictitious adsorbents with improved characteristics:

- $q_{m,CO_2} + 10\%$
- $q_{m,non-CO_2} - 30\%$
- $k_{\infty,CO_2} + 30\%$
- $k_{\infty,non-CO_2} - 30\%$
- $\Delta H_{r,CO_2} + 10\%$
- $\Delta H_{r,non-CO_2} - 30\%$
- $\varepsilon_p - 5\%$
- $\varepsilon_p - 10\%$

Two additional cases are also proposed. They consider the contemporary modification of a group of properties, rather than of a single one. The aim was to verify if the positive effects of the implemented modifications could be combined. The two cases studied refer to fictitious adsorbents with the following characteristics:

- Combined 5: $q_{m,CO_2} + 10\%$, $k_{\infty,CO_2} + 10\%$, $\Delta H_{r,CO_2} + 10\%$.
- Combined 6: $q_{m,non-CO_2} - 10\%$, $k_{\infty,non-CO_2} - 10\%$, $\Delta H_{r,non-CO_2} - 10\%$.

The output of the simulations, in terms of CO₂ capture efficiency and net electric efficiency, are shown in Fig. 15. The absorption-based results are also included. Likewise the process analysis, the base case is represented as a line and not as a single point. The line is drawn by connecting different base case points. Those instances refer to the unmodified activated carbon material with different P/F ratios in the PSA process. This representation is useful because it helps to point out the performance improvements effectively ascribable to the material. A process modification as simple as increasing the purge flow rate in the PSA process is able to tradeoff part of the PSA- Y_{CO_2} for a higher PSA- R_{CO_2} , with consequences on the full-plant performance. The base case line takes into account this effect and sets the benchmark for our analysis. If a simulation output produces a point which lies above the base case line, the correspondent case can claim to bring an actual performance improvement, regardless the process influence. All the cases reported fall in this category. Also the simulations referring to combined property modifications were run for different P/F ratios.

4.4. Remarks on the adsorbent material analysis

It has been demonstrated that proper modifications of adsorbent specific properties can bring significant performance improvements. Some of these material properties displayed a stronger impact on the separation process and, consequently, on the overall process. This is the case of the heat of reaction of non-CO₂ components ($\Delta H_{r,non-CO_2}$). Its reduction demonstrated to bring significant benefits, standing out among the other results obtained. The case simulated (i.e., $\Delta H_{r,non-CO_2} - 30\%$) achieves a η_{CO_2} (87.1%) which is comparable to that of an absorption-based plant, even though the η_{el} still ranks slightly lower. A higher value for η_{el} can be obtained by exploiting the influence of the process. An example is reported, where the same modified adsorbent ($\Delta H_{r,non-CO_2} - 30\%$) is used adopting a lower P/F ratio ($P/F=0.007$) in the PSA process. The empty diamond in Fig. 15 is showing the relative full-plant simulation output. It can be noted that, whilst the η_{CO_2} decreases down to 80.5%, the η_{el} can be lifted up to 36.7%, a value which is competitive with absorption. Similar results are obtained by combined modifications of the properties, especially for the case involving all the non-CO₂ properties reduced of 10% (i.e., Combined 6). This is leading to another interesting remark. The properties modifications which reduce the material affinity for non-CO₂ components

seem to be more effective than those increasing the CO₂ adsorption properties. This can be verified both on the single property modification (diamonds are generally located over triangles in Fig. 15) and in the two combined modification examples (Combined 6 performs better than Combined 5). This trend highlights the importance to focus not only on the CO₂ adsorption characteristics when developing an adsorption material. In order to guarantee a good selectivity for the gas separation process, it is fundamental also to assure that the uptake of the non-desired gases is limited. Summing up, tailored advancements in the adsorbent material demonstrated to be potentially very important to increase the competitiveness of PSA. The cases analyzed, even though based on arbitrary property modifications, shows that the development of improved adsorbents may substantially reduce the gap with absorption. Even though some criteria are indicated in order to guide this development, it is beyond the scope of this work to define how to pursue them. What can be mentioned is that a variety of activated carbons can be produced, allowing tailoring of their adsorptive properties. Even more promising is the utilization of Metal Organic Frameworks (MOFs). Their structure and chemical composition can be easily tuned in order to obtain desired properties. It must be also pointed out that the analysis carried out covers only the adsorbents with a Langmuir-like shape isotherm. This family of adsorbents encompasses, among others, activated carbons and some MOFs. Other MOFs display a sigmoidal shape which could lead to different performances. However, additional research efforts need to be carried out to guarantee the actual applicability of MOFs. The main issues yet to be addressed are related to the effect of impurities, the practical aspects of employing a PSA process (Sumida et al., 2012), the stability over multiple adsorption/desorption cycles (Choi et al., 2009), the material formulation and mechanical stability (Casas et al., 2013b).

5. Synergies between process and adsorbent material

In the previous sections advancements of the process and of the material were investigated in order to enhance the overall plant performance. However, the approach adopted is to some extent inaccurate. It considers the two domains as separated issues, while they have a strong influence on each other. It should be good practice to deal with the plant optimization problem as a whole. Such way of proceeding complicates the analysis but reveals synergies that can be very beneficial. Therefore an attempt in this sense was made by trying to define an optimal adsorbent for a specific process configuration.

The PSA process taken into account was meant to return a good performance under an energy point of view. Utilizing the knowledge acquired, the process configuration was designed with the following changes compared to the base case:

- P_{reg} 2 bar.
- T_{feed} 358 K.
- P_{flash} 26 bar.

The following step was to determine the adsorbent properties modifications which would make the adsorbent to perform efficiently in this new set of operating conditions. The exact definition of the most suitable properties values is not an easy task, as the PSA process is influenced by a large number of parameters. The methodology to determine which properties to modify, how and to what extent was based on the experience gained with the previous analysis on the material adsorbent. However, it also relied to some degree on a trial and error procedure. The outcome was a modified adsorbent with the following characteristics:

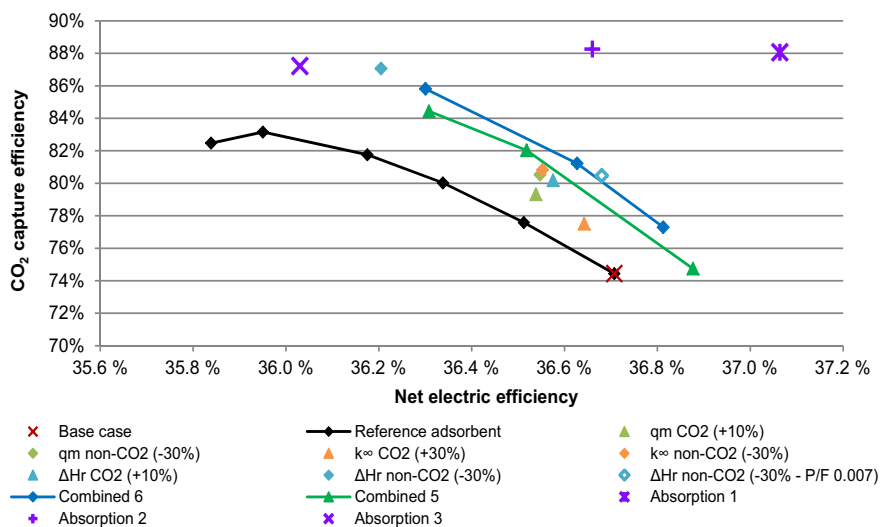


Fig. 15. Overview of plant performances achievable by modifications of the material.

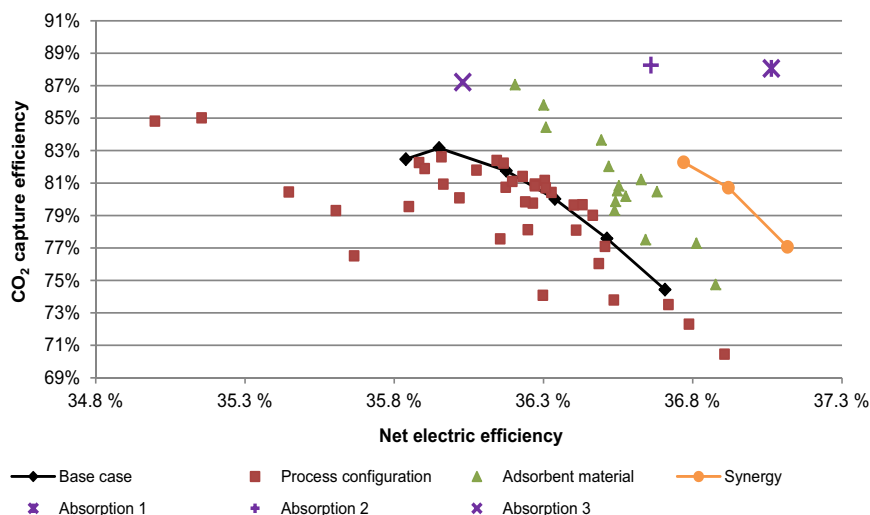


Fig. 16. Plant performance achieved through a synergetic approach of process and material modifications. All the performances achieved by modifications of the process or the material are also reported.

- q_{m,CO_2} and $k_{\infty,CO_2} + 10\%$
- $\Delta H_{r,CO_2} - 10\%$
- $q_{m,non-CO_2}$ and $k_{\infty,non-CO_2}$ and $\Delta H_{r,non-CO_2} - 30\%$

The CO₂ heat of adsorption was decreased of 10%. The explanation for that should be searched in the effect of ΔH_r on the slope of the adsorption isotherm. In order for the regeneration process to be effective at a higher pressure (i.e., P_{reg} 2 bar), the slope of the adsorption isotherm needs to be gentler in the low pressure region. A decrease of ΔH_r works in that way. Without further changes, the decrease of ΔH_r would also reduce the CO₂ uptake at high pressures, hindering the adsorption process. Thereby, q_{m,CO_2} and k_{∞,CO_2} were increased to restore the adsorption capacity during the adsorption step. This increase was limited to 10% because further increases demonstrated to be ultimately ineffective. Additionally, all the properties relative to the non-CO₂ components were decreased of 30% as it demonstrated to be beneficial (cf. Section 4.2).

The new defined scenario, involving a material with tailor-made characteristics for the chosen process configuration, was named *Synergy* and it was simulated for three different P/F ratios. The outputs are displayed in Fig. 16. The obtained energy performance are extremely competitive (with values between 36.8% and 37.1%) and on average higher than those achievable with absorption. The CO₂ capture efficiency still ranks lower than the absorption-based counterpart, as it ranges between 76% and 82%, but it was not dramatically reduced. Fig. 16 shows also all the outputs obtained by process modifications (squares) or material modifications (triangles) and discussed in previous sections. It is worthwhile to notice that the approach adopted seems to add together the benefits achieved by the two domains subject of our analyses. This example demonstrates how the close collaboration between process engineering and material science is of paramount importance in order to develop effectively the studied system. Even though the proposed case is based on a fictitious adsorbent material, the general remark could be that there is room for

improvements and for approaching competitiveness in the pre-combustion scenario.

6. Conclusions

An analysis on the feasibility and competitiveness of PSA in a pre-combustion CO₂ capture application has been carried out. The system considered for the analysis is an IGCC plant. The plant integrating a PSA unit has been defined and a composite model has been built in order to simulate its functioning. The performance obtained, evaluated in terms of energy and CO₂ capture efficiency, is compared to state-of-the-art absorption-based plants. The range of performances and the potential of the IGCC-PSA system were investigated by taking into consideration two domains, which were thought to have a significant influence: the process configuration and the adsorbent material.

Different process configurations and operating conditions were studied through process simulations. Such analysis improved the understanding of the system, enabling a correct evaluation of the available options for boosting the plant performance according to specific requirements. A tradeoff between energy efficiency and CO₂ capture efficiency was observed. Competitive energy penalty could be obtained, at the expense of substantial reduction of the CO₂ capture efficiency. The optimum plant configuration is difficult to be defined without establishing which performance indicator to prioritize and which performance levels are acceptable. None of the options studied could fully fill the performance gap with regard to absorption.

The influence of the adsorbent material on the overall plant performance was studied through a sensitivity analysis. Given an activated carbon as reference adsorbent, the impact of improved adsorption properties was studied by varying them in a targeted manner and, thus, simulating advancements in the material. The objective was to establish the most influencing properties, to assess the possible performance enhancements and to provide guidelines for future material development. The effects were first evaluated on the separation process. The effects on the final CO₂ recovery, purity and on the selectivity at which the material is able to separate CO₂ were monitored. The most significant cases resulting from this analysis were implemented in the full-plant model, in order to assess the impact on the overall plant. The material modifications proposed demonstrated to enhance the system performance, albeit not on the level of absorption. Some adsorbent properties showed a stronger impact than others, in particular the heat of reaction. It was also noticed that decreasing the adsorbent affinity for non-CO₂ components seems slightly more effective than increase its affinity toward CO₂. Overall, proper advancements in the adsorbent materials have the chance to give an important contribution to boost PSA competitiveness.

The last analysis proposed aims to combine the positive effects obtained by modifications in the process and in the adsorbent material. An attempt was made in order to exploit possible synergies, utilizing the knowledge acquired in the previous analyses. A material tailor-made on a specific process configuration was defined. The performance resulting from the process simulation was extremely promising. A net electric efficiency slightly higher than the reference absorption value could be obtained, without large reduction in the CO₂ capture efficiency. A synergy of process engineering and material science demonstrated to be a key issue for enhancing PSA competitiveness.

Acknowledgements

The authors gratefully acknowledge the financial support provided through the “EnPe – NORAD’s Programme within the energy and petroleum sector”.

References

- Abanades, J.C., et al., 2015. Emerging CO₂ capture systems. *Int. J. Greenh. Gas Control* 40, 126–166.
- Arstad, B., et al., 2008. Amine functionalised metal organic frameworks (MOFs) as adsorbents for carbon dioxide. *Adsorption* 14 (6), 755–762.
- Baade, W., et al., 2012. CO₂ capture from SMRs: A demonstration project. In: *Hydrocarbon Processing*, pp. 63–68.
- Botero, C., et al., 2013. The phase inversion-based coal-CO₂ slurry (PHICCOS) feeding system: techno-economic assessment using coupled multiscale analysis. *Int. J. Greenh. Gas Control* 18 (0), 150–164.
- Casas, N., et al., 2013a. A parametric study of a PSA process for pre-combustion CO₂ capture. *Sep. Purif. Technol.* 104 (0), 183–192.
- Casas, N., et al., 2013b. MOF and UiO-67/MCM-41 adsorbents for pre-combustion CO₂ capture by PSA: breakthrough experiments and process design. *Sep. Purif. Technol.* 112 (0), 34–48.
- Choi, S., Drese, J.H., Jones, C.W., 2009. Adsorbent materials for carbon dioxide capture from large anthropogenic point sources. *ChemSusChem* 2 (9), 796–854.
- Darde, A., et al., 2009. Air separation and flue gas compression and purification units for oxy-coal combustion systems. *Energy Proc.* 1 (1), 527–534.
- de Visser, E., et al., 2008. Dynamis CO₂ quality recommendations. *Int. J. Greenh. Gas Control* 2 (4), 478–484.
- DECARBit, 2011. Enabling advanced pre-combustion capture techniques and plants, European best practice guidelines for assessment of CO₂ capture technologies. European Benchmarking Task Force.
- Ebner, A.D., Ritter, J.A., 2009. State-of-the-art adsorption and membrane separation processes for carbon dioxide production from carbon dioxide emitting industries. *Sep. Sci. Technol.* 44 (6), 1273–1421.
- Field, R.P., Brasington, R., 2011. Baseline flowsheet model for IGCC with carbon capture. *Ind. Eng. Chem. Res.* 50 (19), 11306–11312.
- Gazzani, M., Macchi, E., Manzolini, G., 2013. CO₂ capture in integrated gasification combined cycle with SEWGS – Part A: Thermodynamic performances. *Fuel* 105 (0), 206–219.
- Global CCS Institute, 2015. *The Global Status of CCS: 2014*.
- gPROMS, 2012. *Process System Enterprise Limited*.
- Hedin, N., Chen, L., Laaksonen, A., 2010. Sorbents for CO₂ capture from flue gas – aspects from materials and theoretical chemistry. *Nanoscale* 2 (10), 1819–1841.
- IEA, 2013. *Technology Roadmap – Carbon capture and storage*.
- IEA, 2015. *Energy and Climate Change – World Energy Outlook Special Report*.
- Khoo, H.H., Tan, R.B.H., 2006. Life cycle investigation of CO₂ recovery and sequestration. *Environ. Sci. Technol.* 40 (12), 4016–4024.
- Li, G., et al., 2008. Capture of CO₂ from high humidity flue gas by vacuum swing adsorption with zeolite 13X. *Adsorption* 14 (2–3), 415–422.
- Liu, Z., Green, W.H., 2014. Analysis of adsorbent-based warm CO₂ capture technology for integrated gasification combined cycle (IGCC) power plants. *Ind. Eng. Chem. Res.* 53 (27), 11145–11158.
- Liu, Z., et al., 2011. Multi-bed vacuum pressure swing adsorption for carbon dioxide capture from flue gas. *Sep. Purif. Technol.* 81 (3), 307–317.
- Lopes, F.V.S., et al., 2009. Adsorption of H₂, CO₂, CH₄, CO, N₂ and H₂O in activated carbon and zeolite for hydrogen production. *Sep. Sci. Technol.* 44 (5), 1045–1073.
- Lu, C., et al., 2008. Comparative study of CO₂ capture by carbon nanotubes, activated carbons, and zeolites. *Energy Fuels* 22 (5), 3050–3056.
- Na, B.-K., et al., 2002. Effect of rinse and recycle methods on the pressure swing adsorption process to recover CO₂ from power plant flue gas using activated carbon. *Ind. Eng. Chem. Res.* 41 (22), 5498–5503.
- Najmi, B., Bolland, O., Colombo, K.E., 2015. Load-following performance of IGCC with integrated CO₂ capture using SEWGS pre-combustion technology. *Int. J. Greenh. Gas Control* 35 (0), 30–46.
- NETL, 2013. *Cost and Performance Baseline for Fossil Energy Plants. Vol. 1: Bituminous Coal and Natural Gas to Electricity*.
- Nitta, T., et al., 1984. An adsorption isotherm of multi-site occupancy model for homogeneous surface. *J. Chem. Eng. Jpn.* 17 (1), 39–45.
- Pipitone, G., Bolland, O., 2009. Power generation with CO₂ capture: technology for CO₂ purification. *Int. J. Greenh. Gas Control* 3 (5), 528–534.
- Posch, S., Haider, M., 2012. Optimization of CO₂ compression and purification units (CO₂ CPU) for CCS power plants. *Fuel* 101 (0), 254–263.
- Reynolds, S.P., Ebner, A.D., Ritter, J.A., 2006. Stripping PSA cycles for CO₂ recovery from flue gas at high temperature using a hydrotalcite-like adsorbent. *Ind. Eng. Chem. Res.* 45 (12), 4278–4294.
- Ribeiro, A.M., et al., 2009. Four beds pressure swing adsorption for hydrogen purification: case of humid feed and activated carbon beds. *AIChE J.* 55 (9), 2292–2302.
- Riboldi, L., Bolland, O., 2015. Evaluating pressure swing adsorption as a CO₂ separation technique in coal-fired power plants. *Int. J. Greenh. Gas Control* 39 (0), 1–16.
- Siriwardane, R.V., et al., 2001. Adsorption of CO₂ on molecular sieves and activated carbon. *Energy Fuels* 15 (2), 279–284.
- Sumida, K., et al., 2012. Carbon dioxide capture in metal-organic frameworks. *Chem. Rev.* 112 (2), 724–781.
- Thermoflex, 2014. *Thermoflex Version 24.0.1*. Thermoflow Inc.

Paper III

Pressure swing adsorption for coproduction of power and ultrapure H₂ in an IGCC plant with CO₂ capture

Luca Riboldi, Olav Bolland

International Journal of Hydrogen Energy In Press (2016)

Available online at www.sciencedirect.com

ScienceDirect

journal homepage: www.elsevier.com/locate/hydro

Pressure swing adsorption for coproduction of power and ultrapure H₂ in an IGCC plant with CO₂ capture

Luca Riboldi*, Olav Bolland

Energy and Process Engineering Department, NTNU, Norwegian University of Science and Technology, NO-7491 Trondheim, Norway

ARTICLE INFO

Article history:

Received 29 January 2016
Received in revised form
13 April 2016
Accepted 14 April 2016
Available online xxx

Keywords:

IGCC
Adsorption
Flexibility
CO₂ capture
H₂ production
Process simulation

ABSTRACT

The coproduction of power and ultrapure H₂ within an Integrated Gasification Combined Cycle (IGCC) plant implementing CO₂ capture offers advantages in terms of flexible operation while retaining good efficiency. The common design includes an absorption unit for removing CO₂ from a high pressure syngas followed by a Pressure Swing Adsorption (PSA) unit for purifying a part of the resulting H₂-rich gas stream. A drawback of this design consists in the necessity for compression of the PSA tail gas in order to recover the energy available in the residual H₂ content. This paper presents two novel configurations for power and H₂ coproduction with CO₂ capture, entirely based on PSA technology. The first relies on two PSA trains in series (*Two-train PSA*), while the other is able to carry out CO₂ separation and H₂ purification within a single PSA train (*One-train PSA*). The two systems were defined and simulated through a composite model of the whole plant. The process simulation results showed that both the configurations proposed are able to shift between the two energy products without compromising the performance of the plant. The load of the plant could be decreased by increasing the ultrapure H₂ throughput, while maintaining a constant feed of coal to the gasifier. The *Two-train PSA* configuration achieved higher performance in terms of energy efficiency and H₂ purity. The *One-train PSA* configuration returned slightly lower but still good performance, while its design includes a single separation stage instead of two. Additionally, both configurations enable the avoidance of PSA tail gas compression giving an advantage against the absorption-based design. A comparative analysis with results taken from the literature seems to confirm this assertion.

© 2016 Hydrogen Energy Publications LLC. Published by Elsevier Ltd. All rights reserved.

Introduction

Two fundamental characteristics for thermal power plants in the near future are the capability of capturing CO₂ in the most efficient way and the possibility to be operated in a flexible

manner. For what concerns the CO₂ emissions, the latest IPCC report clearly pointed out that a strong and immediate commitment is needed if we want to limit the potentially devastating effects of global warming [1]. The energy sector is responsible for a large fraction of anthropogenic greenhouse gas emissions [2]. An intervention in this sector has to be

* Corresponding author. Kolbjørn Hejes vei 1a, 7491 Trondheim, Norway. Tel.: +47 735 93559.

E-mail address: luca.riboldi@ntnu.no (L. Riboldi).

<http://dx.doi.org/10.1016/j.ijhydene.2016.04.089>

0360-3199/© 2016 Hydrogen Energy Publications LLC. Published by Elsevier Ltd. All rights reserved.

undertaken and cannot disregard Carbon Capture and Storage (CCS) [3]. The deployment of other low-carbon energy technologies is also critical, a portfolio of renewable energy sources in the first instance. However, the utilization of fossil fuels is predicted to keep on covering a large share of the power generation in the next decades. CCS allows the exploitation of fossil fuels, while reducing their carbon footprint. Thereby, CCS is an indispensable technology in a reasonable roadmap towards a carbon constrained world, allowing a smooth transition to a long-term scenario dominated by renewable energies. In this context, the concept of flexible operability becomes of primary importance. With the progressive penetration of renewable energy sources into the energy sector, continuous base load operation mode of fossil fuel power plants will become more and more unlikely [4,5]. The intermittent nature of some renewable energy sources (e.g. solar and wind) will deeply modify the energy market and, accordingly, the capacity of efficient operation at part-load will become essential for thermal power plants.

Integrated Gasification Combined Cycle (IGCC) seems to be attractive for capturing CO₂ [6]. The high pressure at which the CO₂ separation can be carried out helps limiting the energy penalty. On the other hand, an IGCC plant is not generally suitable for part-load operation. Operating at reduced loads introduces challenges due to the inertia of the process units (mainly air separation unit and gasifier) and to the elevated auxiliary power demand. One way to deal with that could be the coproduction of hydrogen besides power [5,7]. With the term flexibility in this paper we mean the ability of the plant to shift between two different energy products (i.e. electricity and H₂), resulting from the conversion of a constant coal input, while retaining acceptable efficiency. An IGCC plant which has a variable power-to-hydrogen output may be able, to some extent, to follow the fluctuations in power demand. During low power demand periods, the hydrogen production can be increased to the detriment of the power output. This allows the gasifier and other processing units retaining a working mode close to the design point. The produced ultrapure H₂ can be stored or exported outside the plant. Hydrogen, with certain specifications, is a valuable product for the chemical sector and, possibly, for the transport sector. In this sense, a hydrogen market is predicted to emerge [7,8].

The common IGCC configuration for hydrogen and power coproduction with CO₂ capture found in the literature consists

of: coal gasification, low temperature gas clean-up, sour water-gas shift process, CO₂ removal through an absorption process (normally based on a physical solvent, e.g. Selexol), purification (H₂ purity > 99.9%) of a H₂-rich gas fraction via PSA while the remaining part is fed to a gas turbine. The tail gas from the PSA is compressed and added to the fuel gas stream, given its residual H₂ content. Fig. 1 gives a simplified representation of such system. The fraction of the H₂-rich gas stream depends on the established power-to-hydrogen ratio. The performance attainable by the outlined basic configuration, relying on commercially ready technology, has been extensively analyzed in the literature [9–12], also from an economic point of view [8]. Other studies investigated the potential advantages of employing advanced technologies [13,14] and the possibility of differentiating the fuel mixture to be gasified [13–16]. All the mentioned studies rely on PSA technology for the production of ultrapure H₂. Several PSA designs have been proposed in this sense [17–21]. The main objective of an effective PSA design is to maximize the H₂ recovery, while meeting the required purity specifications. A large amount of PSA tail gas would otherwise need to be compressed in order to be fed to the gas turbine and not to waste its energy content. This fuel compression is a complex and energy intensive process. The research for high H₂ recovery has led to increasing complexity of the PSA arrangement. Luberti et al. [22] showed the tradeoff between H₂ recovery and system complexity (productivity accordingly). The aim of the current paper is to address the issue in a different way, which allows for the avoidance of tail gas compression. The idea is to utilize PSA both for the CO₂ separation and for the ultrapure H₂ production. The adoption of the same technology discloses integration opportunities, possibly leading to an efficiency improvement. PSA may be a feasible option for CO₂ capture in coal-fired power plants [23], although absorption seems to generally offer higher overall performance [24]. PSA has also been assessed in a warm gas cleanup arrangement [25] and in sorption enhanced processes [26,27]. The relative outputs were promising but those PSA systems require tailor-made adsorbent materials and composite processes, whereas this work aims to evaluate common technologies. Provided that, the investigation of possible configurations of PSA-based IGCC plants implementing CO₂ capture while coproducing power and hydrogen is a relatively unexplored topic. A demonstration project at the Valero

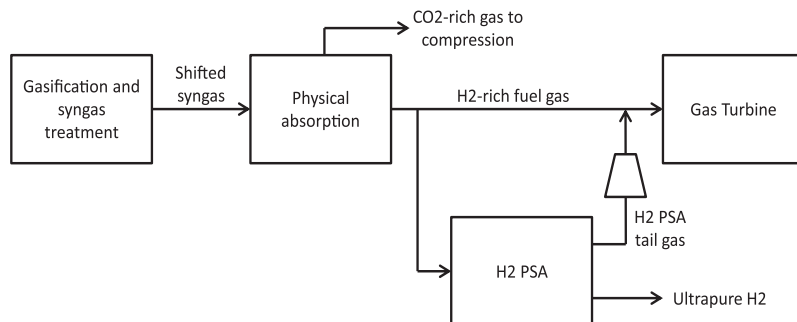


Fig. 1 – Block flow diagram of an IGCC plant with CO₂ separation by absorption and coproduction of H₂ by PSA.

refinery in Port Arthur (Texas) [28] applies a dual PSA system, where the main objective is H_2 production with low CO_2 emissions. The produced H_2 is utilized in the manufacturing of petrochemicals and as clean transportation fuel by refinery customers, while the purified and compressed CO_2 is used for Enhanced Oil Recovery (EOR) projects. The PSA system is based on a patented PSA process for simultaneous production of pure H_2 and CO_2 from steam methane reforming syngas [29]. It involves the utilization of two PSA trains consisting of 6 and 3 columns respectively, and the utilization of rotating machinery (i.e., vacuum pumps and CO_2 recycle compressors), which makes it an energy intensive process. A system which is close to what we suggest in the current work has been studied by Chen et al. [13]. The paper discusses the conceptual design and the performance of an advanced IGCC plant using a fixed-bed sorption technology for CO_2 separation [30,31], while the ultrapure H_2 is produced by a common PSA process. Due to the proprietary nature of the process, not much has been published about it.

In this work we investigate, on a system level, two possible configurations for coproduction of power and ultrapure H_2 in an IGCC plant with CO_2 capture. The first one relies on two integrated PSA trains in series: one PSA train with the primary goal of removing and concentrating CO_2 from the shifted syngas, while producing a fuel-grade H_2 -rich gas stream; the other PSA train further purifies part of the H_2 -rich gas stream in order to meet the specification requirements for being commercialized. The second configuration is based on a single PSA train which is able to separate CO_2 , while releasing two H_2 -rich gas streams with different H_2 concentrations. Both configurations studied have been designed with a significant

ultrapure H_2 throughput (i.e. up to 15% of the coal lower heating value). The production of ultrapure H_2 was chosen in order to allow comparison with similar works in the literature. However, a design entailing a different throughput would have been likewise possible. Composite models of the defined systems have been built for the process simulations. The composite model includes a dynamic model for the PSA processes and a steady-state model for the other process units (ASU, gasifier, CO_2 compression station, etc.) and for the power island (gas turbine and steam cycle).

IGCC plant design and modeling

The analyses of the novel IGCC system configurations are based on process simulations of the entire plant. To enable this approach, a composite model has been build encompassing all the different units constituting the plant. These units can be grouped in the following sections:

- Air separation
- Gasification and syngas treatment
- CO_2 separation and ultrapure H_2 production
- CO_2 compression and flash separation
- Power island

The general layout of the IGCC plant is shown in Fig. 2. The differences between the two novel configurations proposed are located in the CO_2 separation and ultrapure H_2 production unit. The other sections are common to all the system configurations studied. A description of this common

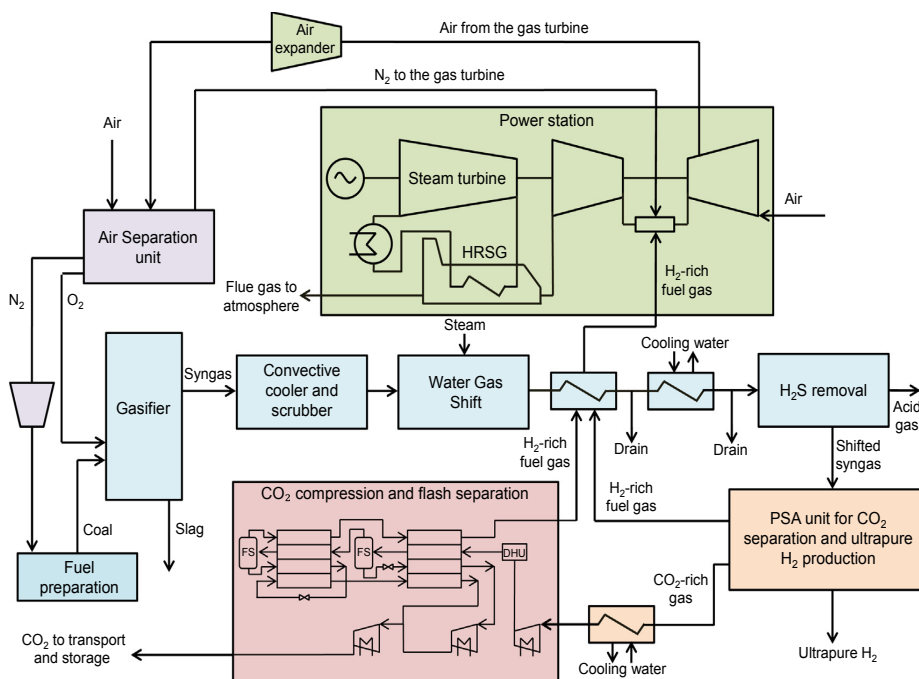


Fig. 2 – General flowsheet of an IGCC plant coproducing power and ultrapure H_2 with CO_2 capture through PSA.

framework is given in the following. When possible, it was based on the set of assumptions defined by the European Benchmarking Task Force (EBTF) [32]. A bituminous Douglas Premium Coal is fed to the gasifier using N_2 as fuel preparation gas. Coal gasification occurs in a Shell-type entrained-flow oxygen-blow gasifier, at a pressure of 44.9 bar. Steam is generated in the gasifier and in the following syngas cooler. The O_2 to be utilized in the gasifier is produced in a cryogenic Air Separation Unit (ASU). The distillation column is operated at 10 bar, producing a 95% pure O_2 gas stream. The ASU is integrated with other units. For instance, 50% of the compressed air entering the ASU is taken from the compressor of the gas turbine. As a byproduct also rather pure N_2 is made available. The surplus N_2 is compressed and used both to convey gas to the gasifier and to dilute the H_2 -rich fuel gas to the combustor of the gas turbine. The high temperature syngas (900 °C) leaving the gasifier is cooled down (497 °C) in a convective syngas cooler and particles removed through wet scrubbers. Syngas is then routed to the Water Gas Shift (WGS) section with a temperature of 178 °C. The sour shift process takes place in two consecutive reactors, in order to convert CO to CO_2 and H_2 to the highest possible extent. Steam, coming from the steam cycle, is added to the syngas (with a H_2O/CO ratio of 2) in order to enhance the reaction. The heat of reaction is partially recovered by producing high pressure saturated steam. Alongside the shift process, COS hydrolysis occurs in the WGS reactors. The shifted syngas leaves the WGS section at 235 °C and needs to be cooled down to undergo the gas cleaning treatment. It is first cooled against the H_2 -rich fuel gas which goes to the gas turbine. The remaining cooling duty is provided by cooling water. During these cooling steps, a large fraction of water still present in the shifted syngas condenses and is extracted. The sulfur compounds have to be removed from the shifted syngas. A single stage Selexol process is applied for H_2S removal. The physical solvent, a dimethyl ether of polyethylene glycol, selectively absorbs H_2S , which is then released during the solvent regeneration. The sulfur-free syngas is routed to the PSA unit. The gas conditions at the entrance of this unit were set to be 38.8 bar and 64 °C. PSA is a process based on the utilization of solid adsorbents to selectively retain CO_2 (and, in some instances, other components) from a gas mixture. The regeneration of the column is carried out through a pressure swing operation. In order to assure the operating continuity, a number of columns are set to work in parallel. Each column undergoes the same cycle, which is constituted by a number of proper steps, in a synchronised manner. The exact design of the PSA depends on the configuration considered. Its definition is discussed in dedicated sections of the paper. Three gas streams leave the PSA unit: a CO_2 -rich gas stream, an ultrapure H_2 gas stream and a H_2 -rich gas stream. The CO_2 -rich gas stream is cooled down and sent to the CO_2 compression and flash separation unit, where it is compressed to an appropriate pressure for transportation, i.e. 110 bar. The compression arrangement includes multiple intercooled stages. Since the CO_2 purity obtained by the PSA process is not matching the specification established, a further purification process is implemented and integrated in the CO_2 compression unit. The design of the unit is

described in another work [23] along with the advantages and disadvantages of implementing the flash separation [33]. The ultrapure H_2 can be whether commercialized or stocked in order to enhance the flexibility of the plant. Further conditioning processes may be necessary for the delivery of ultrapure H_2 but this has not been considered here. The last product stream from the PSA unit is the H_2 -rich gas stream which, after being heated up to about 200 °C, is fueling the gas turbine. A dilution with N_2 coming from the ASU is done, mainly in order to be able to use the normal gas turbine combustor designed for natural gas. As rule-of-thumb the N_2 dilution has been adjusted in the different cases proposed so to retain the same Wobbe index. The gas turbine considered is a large scale F-class, common for all the system configurations studied. The compressed air bled from the compressor is expanded before being sent to the ASU. The air expander increases the total power output by recovering part of the compression work. The flue gas from the turbine is discharged at about 585 °C and its remaining energy content is used to produce steam at three different pressure levels in a Heat Recovery Steam Generator (HRSG). Accordingly, the steam bottoming cycle features three pressure levels with reheat, respectively 138 bar, 47 bar and 5 bar. The total gross power output is about 460 MW, considering all H_2 for power.

The air separation, gasification and syngas treatment, CO_2 compression and power island were modeled in Thermoflex (ThermoFlow Inc.) [34]. The PSA unit was modeled with gPROMS [35] and a description of the model is provided in the next section. The flash separation process was modeled in Aspen HYSYS [36]. The simulation platforms were set to exchange information through a common Microsoft Excel interface so that an efficient process simulation of the overall plant was made possible.

PSA model

The dynamic behavior of the adsorption beds constituting a PSA train is described by a 1-dimensional mathematical model with proper boundary conditions for each step of the cycle. The model relies on a set of Partial Differential and Algebraic Equations (PDAEs) representing material, energy and momentum balances. For a detailed description of the model, including all the equations adopted, the assumptions introduced and the boundary conditions implemented, reference is made to [23].

Assuming an axially dispersed plug flow, micropore diffusion to be the dominating mass transfer resistance and Linear Driving Force (LDF) approximation to apply, the component and overall material balance equations are, respectively:

$$\frac{\partial C_i}{\partial t} [\varepsilon + \varepsilon_p(1 - \varepsilon)] = -\frac{\partial(u_s C_i)}{\partial z} + \frac{\partial}{\partial z} \left(\varepsilon D_{ax,i} \frac{\partial C_i}{\partial z} \right) - \rho_p(1 - \varepsilon) \frac{\partial \bar{q}_i}{\partial t} \quad (1)$$

$$\frac{\partial C_{tot}}{\partial t} [\varepsilon + \varepsilon_p(1 - \varepsilon)] = -\frac{\partial(u_s C_{tot})}{\partial z} - \rho_p(1 - \varepsilon) \sum_i^{NC} \frac{\partial \bar{q}_i}{\partial t} \quad (2)$$

The LDF equation for the adsorption rate is:

$$\frac{\partial \bar{q}_i}{\partial t} = k_{LDF,i} (q_i^* - \bar{q}_i) \quad (3)$$

The columns are considered to be adiabatic and thermal equilibrium is assumed between the gas and solid phases. The resulting energy balance equation is:

$$\begin{aligned} & \left[C_{v,G}C_{tot} + \frac{\varepsilon_p(1-\varepsilon)}{\varepsilon}C_{v,G}C_{tot} + \frac{(1-\varepsilon)}{\varepsilon}C_{p,S}\rho_p \right. \\ & \left. + \frac{(1-\varepsilon)}{\varepsilon}\rho_p \sum_i^{NC} C_{ads,i}\bar{q}_i \right] \frac{\partial T}{\partial t} - \frac{\varepsilon + \varepsilon_p(1-\varepsilon)}{\varepsilon}RT \frac{\partial C_{tot}}{\partial t} + \frac{u_s}{\varepsilon}C_{p,G}C_{tot} \frac{\partial T}{\partial z} \\ & = +\frac{1}{\varepsilon} \frac{\partial}{\partial z} \left(\lambda_{ax} \frac{\partial T}{\partial z} \right) + \rho_p \frac{(1-\varepsilon)}{\varepsilon} \sum_i^{NC} (-\Delta H_{r,i}) \frac{\partial \bar{q}_i}{\partial t} \end{aligned} \quad (4)$$

The Ergun equation applies for the momentum balance:

$$\frac{\partial P}{\partial z} = - \left[\frac{150}{d_p^2} \frac{(1-\varepsilon)^2}{\varepsilon^3} \mu u_s + \frac{1.75}{d_p} \frac{(1-\varepsilon)}{\varepsilon^3} \rho_G u_s |u_s| \right] \quad (5)$$

Two adsorbent materials are utilized in the system analyses, with equilibrium parameters and physical properties taken from literature (see Table 1), namely an activated carbon [37] and a zeolite 5A [22]. The adsorption equilibrium of different gas components on the activated carbon is described by a multi-site Langmuir model. The equilibria of CO₂, H₂, CH₄, CO and N₂ have been taken into account.

$$\frac{q_i^*}{q_{m,i}} = a_i k_i P_i \left[1 - \sum_i^{NC} \left(\frac{q_i^*}{q_{m,i}} \right) \right]^{a_i}, \quad \text{with } k_i = k_{\infty,i} \exp \left(-\frac{\Delta H_{r,i}}{RT} \right) \quad (6)$$

For what concerns the zeolite 5A, a dual-site Langmuir model was utilized in order to be consistent with the referenced literature. In this case the gases considered were CO₂, H₂, Ar, CO and N₂.

$$q_i^* = \frac{q_{m,i}^1 k_i^1 P_i}{1 + \sum_j^{NC} k_j^1 P_j} + \frac{q_{m,i}^2 k_i^2 P_i}{1 + \sum_j^{NC} k_j^2 P_j}, \quad \text{with } k_i^k = k_{\infty,i}^k \exp \left(-\frac{\Delta H_{r,i}^k}{RT} \right) \quad (7)$$

One can notice that while for the activated carbon the CH₄ equilibrium capacity is taken into account, for the zeolite 5A

the Ar equilibrium capacity is considered instead. This different approach can be explained by the availability of modeling data and can be justified looking in which part of the system the two adsorbents are applied. Activated carbon is used to process the shifted syngas, where traces of CH₄ are still present. Zeolite is used for the production of ultrapure H₂. In this case the input gas has normally already been purified and the presence of CH₄ is negligible. On the other hand traces of Ar, even though small, can negatively affect the final H₂ purity. Whenever the adsorption equilibria of CH₄ or Ar are not taken into account, their fractions have been included with CO and N₂, respectively.

Different boundary conditions to the column enable to describe the steps of a PSA process. A single-column approach has been adopted. It consists of modeling a single column of a train, instead of all columns. The cyclic behavior of the PSA process allows this simplification, i.e. all the columns undergoes the same steps cyclically. When two columns of the same train interact, the single-column model relies on the information stored previously during the cycle to describe such interaction. This modeling strategy allows significantly reducing the computational time, without excessive loss in accuracy.

The set of PDAEs was implemented in gPROMS [35]. The Centered Finite Difference Method (CFDM) was used as discretization algorithm for the numerical solution of the model.

Even though its inherent dynamic nature, PSA reaches a condition in which the transient behavior of the entire cycle remains constant and repeats itself invariably from cycle to cycle. This condition is termed Cyclic Steady State (CSS). All the results reported refer to the process at CSS condition.

Performance indicators and gas stream specifications

This section gives an overview on the performance indicators utilized and on the constraints and specifications considered.

On an energy point of view the assessment of the plant performance is not straightforward, given that two different products have to be considered, i.e. electricity and H₂. Some standards and protocols suggest that different energy

Table 1 – Equilibrium parameters and physical properties of the adsorbents used.

Isotherm parameters							
Activated carbon	a	k _∞ (bar ⁻¹)	q _m (mol/kg)	ΔH _r (kJ/mol)			
CO ₂	3.0	2.13E-06	7.86	-29.1			
H ₂	1.0	7.69E-06	23.57	-12.8			
CO	2.6	2.68E-06	9.06	-22.6			
N ₂	4.0	2.34E-05	5.89	-16.3			
CH ₄	3.5	7.92E-06	6.73	-22.7			
Zeolite 5A	k _∞ ¹ (bar ⁻¹)	k _∞ ² (bar ⁻¹)	q _m ¹ (mol/kg)	q _m ² (mol/kg)	ΔH _r ¹ (kJ/mol)	ΔH _r ² (kJ/mol)	
CO ₂	1.08E-07	1.23E-04	0.71	3.71	-38.3	-29.8	
H ₂	4.23E-07	1.33E-04	0.71	3.71	-19.7	-9.3	
CO	2.43E-08	2.32E-05	0.71	3.71	-47.7	-21.0	
N ₂	2.14E-06	8.99E-05	0.71	3.71	-31.3	-15.0	
Ar	1.40E-09	4.90E-04	0.71	3.71	-50.2	-11.2	
Physical properties							
	d _p (mm)	ε _p	ρ _p (kg/m ³)	C _{p,s} (J/kg/K)			
Activated carbon	2.34	0.57	842	709			
Zeolite 5A	1.70	0.50	1126	920			

products generation efficiencies should be calculated and each referred to the total energy input [38].

$$\eta_{el} = \frac{\text{Net electric output}}{\text{Coal energy}_{LHV}} \quad (8)$$

$$\eta_{H_2} = \frac{\text{Ultrapure H}_2 \text{ energy}_{LHV}}{\text{Coal energy}_{LHV}} \quad (9)$$

However, we want to define an overall efficiency term which allows an immediate comparison of different systems performances. A first approach suggests to assign a thermal efficiency of 0.6 for the conversion of the exported H₂ beforehand the comparison with power. This value has been chosen referring to a previous work [14] and can be thought to represent the efficiency of a combined cycle for electricity production.

$$\eta_{tot\ 60} = \eta_{el} + 0.6 \cdot \eta_{H_2} \quad (10)$$

Despite the arbitrary choice of the multiplying factor, the so defined cumulative efficiency can be a useful way to compare results from different sources. What we believe to be the most appropriate method of analysis is to discount the H₂ efficiency term with a power production efficiency. This factor takes into account how much of the shifted syngas energy content is converted to power within the same plant configuration under investigation.

$$\eta_{el\ prod} = \frac{\text{Gross electric output}}{\text{Syngas energy input in the gas turbine}_{LHV}} \quad (11)$$

$$\eta_{tot}^* = \eta_{el} + \eta_{el\ prod} \cdot \eta_{H_2} \quad (12)$$

In this way it is evaluated how much power could be actually obtained from H₂ if the same efficiency for the energy conversion applies (or other way around, how much power was not produced in order to obtain H₂). The underlying assumption of this indicator is that the combined cycle (gas turbine and bottoming steam cycle) efficiency would remain constant if all the H₂ was sent to the GT. This is an approximation but it gives reasonable values. The drawback is that there is not always enough information in the literature to calculate the power production efficiency. η_{tot}^* has been computed for all the cases simulated in the current study. For most of the other studies reported there were not enough data available, thus the general comparison between different systems relies on $\eta_{tot\ 60}$ as a performance indicator.

The separation performance of all the cases studied considers both the CO₂ and H₂ balance of the system. The effectiveness of CO₂ removal from the syngas is measured in terms of CO₂ recovery, defined as:

$$R_{CO_2} = \frac{\dot{m} \text{ of CO}_2 \text{ compressed for transportation}}{\dot{m} \text{ of CO}_2 \text{ formed throughout the IGCC plant}} \quad (13)$$

In order to better analyze the system, it may be useful to introduce an additional indicator, which still represent CO₂ recovery but taking into consideration only the PSA process. The difference with respect to that above outlined lies in the fact that the processes downstream the PSA are not considered, neither in terms of further CO₂ removal (i.e. the flash separation process) nor in terms of additional CO₂ formed (i.e. the combustion of CO and CH₄ in the gas turbine).

$$PSA - R_{CO_2} = \frac{\dot{m} \text{ of CO}_2 \text{ captured in the PSA process}}{\dot{m} \text{ of CO}_2 \text{ formed upstream the PSA process}} \quad (14)$$

The specifications applying to the different gas streams have been taken from the literature [7,39]. It must be pointed out that the end application sets the standards for the ultrapure H₂ purity ($Y_{H_2}^*$) and other impurities allowed (in some cases transport and/or intermediate storage actually puts the highest restrictions on H₂ purity but we did not consider this possibility). Proton Exchange Membrane (PEM) fuel cells set the strictest requirements both on H₂ purity (99.99+% vol.) and on the impurities content (to avoid catalyst poisoning). Other applications have more relaxed requirements. When possible we tried to match PEM fuel cell specifications, in order to have the maximum flexibility for the utilization of the H₂ gas stream.

In this work, possible additional conditioning processes for the delivery of H₂ have not been taken into account and the H₂ is made available at the pressure and temperature at which it leaves the PSA process.

Two-train PSA configuration

Power and ultrapure H₂ are to be coproduced in an IGCC plant by means of PSA. The most obvious way is to take the benchmark configuration as starting point and substitute the absorption unit with a PSA unit. Thereby, the new configuration consists of two PSA trains in series. The motivation behind the investigation of this novel system lies in the integration opportunities that arise from the utilization of the same technology for the CO₂ separation and ultrapure H₂ production. The next section describes the PSA cycles adopted, pinpointing the integration opportunities and explaining how they can be beneficial. The performance of a plant implementing the defined system is following reported and discussed.

The adsorption material selected for the packing of the beds differs between the first and the second train. The first PSA train utilizes activated carbon [37], which demonstrated to provide good CO₂ separation performance at high inlet CO₂ partial pressure [40]. In the second PSA train the focus is no longer on the CO₂ separation but on the H₂ production. Multi-layer structures are often adopted, resulting in an activated carbon layer at the bottom-end of the column and a zeolite layer over it. While the activated carbon is mainly responsible for the uptake of CO₂ and CH₄, the zeolite takes care of the remaining traces of CO and N₂. Ahn et al. [41] demonstrated that gas mixtures rich in N₂ and poor in CO₂ require zeolite-rich beds. Since this is the case in our analysis, a bed completely filled with zeolites has been used. This allows a simplification of the model while the performance is believed to be competitive with the multi-layer counterpart. The zeolite has been selected in the literature [22,37]. The equilibrium and physical properties of the two adsorbents are reported in Table 1.

PSA cycles

The first PSA stage is based on the same cycle already applied in other works [23] for CO₂ separation purposes. It is a 7-bed

12-step cycle operating between a high pressure level of 38.8 bar and a low pressure level of 1 bar. A H₂-rich gas stream is withdrawn at high pressure (38.8 bar) during the adsorption step, whereas a CO₂-rich gas stream is released during the low pressure (1 bar) regeneration steps (i.e. blowdown and purge). The H₂-rich gas stream is then split in two parts: a fraction is fed to the gas turbine combustor; the remaining part is sent to the second PSA for further purification. The second PSA stage is based on a 6-bed 11-step cycle. It has been defined in accordance with the study by Luberti et al. [22], where different advanced PSA cycles to be applied in IGCC plant are defined. The cycle selected for our study is meant to be a compromise between separation performance and complexity of the system. In this second PSA process, whilst the high pressure level is again 38.8 bar at which the ultrapure H₂ is produced, the pressure for bed regeneration is set to 1.8 bar. This has to do with the system integration implemented: the low pressure tail gas of the second PSA process is utilized as purge gas for the first PSA process. Delivering it with a pressure slightly higher than atmospheric allows feeding it to the column of the first PSA train without any compression. Differently than typical system configurations, the tail gas is not utilized as fuel to the gas turbine. The consequent avoidance of tail gas compression is a clear advantage and is made possible by the utilization of PSA as the only gas separation technology. Further, the amount of H₂-rich gas from the second PSA train, which is not sent as fuel to the gas turbine (because is used for purging purposes), is balanced by the additional amount of H₂-rich gas that can be obtained from the first PSA. In fact, the gas stream leaving the adsorption step of the first PSA train is now used only as gas turbine fuel or for producing ultrapure H₂; no fractions of it are any longer recirculated within the cycle as purge gas. The whole system configuration of the *Two-train PSA*, with the different steps undertaken and the scheduling of the cycles, is shown in Fig. 3. The characteristics of the cycles and of the adsorption reactors have been selected in order to comply with the requirements of the system in the most efficient way possible. Those characteristics are reported in Table 2.

Two-train PSA results

Table 3 summarizes the main outputs of the process simulations. All the cases analyzed refer to a common framework with the same coal input to the plant. The gradual shift from power to ultrapure H₂ as outputs of the process has been obtained by modifications of the second PSA cycle. The parameters involved are the scheduling of the cycle (i.e. cycle time steps – t_{cycle}) and the ratio of H₂-rich syngas sent to the second PSA process out of the total H₂-rich syngas produced by the first PSA process (H₂/Prod). The cases have been termed after the ratio of net electric output and H₂ energy output (PW/H₂). Alternative modifications could have been considered to achieve the same effect, e.g. the purge gas flow rate. Changing the share between power and ultrapure H₂ within this system configuration is rather straightforward. High flexibility can be easily achievable without major modifications of the system. According to the cases reported, the load of the plant was varied of about 13% with the process units (ASU, gasification, etc.) working at their design point. Further load changes were

not tested but are realistically achievable. The PSA process could be easily designed to deal with a large range of operating conditions, for example accepting lower productivity levels compared to the design proposed here. Thus, PSA does not appear to pose constraints in terms of flexibility. The limiting factor may eventually become the ability of the gas turbine to work at part-load retaining good efficiencies. However, the cases discussed in this section could be handled by the part-load operation strategy of the gas turbine without significant drop in its efficiency.

For what concerns the energy performance of the new system configuration, some considerations can be argued from the simulations results. Augmenting the throughput of ultrapure H₂ decreases the net electric efficiency. This was expected since a fraction of the coal energy input is stored as chemical energy in the H₂ and, hence, not used for producing power. The energy accumulated in the ultrapure H₂ is accounted for in the H₂ efficiency. The higher the throughput of ultrapure H₂, the higher is that efficiency term. What can be thought to be the real criterion for comparisons for all the cases is one of the cumulative efficiency terms defined. A detailed analysis of the energy balance shows that the system configuration leads to a slight increase of the auxiliary power consumption when the ultrapure H₂ production is increased. This is the result of two opposite effects connected with the two main power consumptions varying in the cases reported:

- The CO₂ compression power.
- The compression power for the N₂ to dilute the fuel in the gas turbine.

For the present configuration and the way to shift from one power product to the other, an increase of ultrapure H₂ throughput implies an increase of CO₂ recovery (PSA-R_{CO₂}) and a decrease of CO₂ purity (PSA-Y_{CO₂}) in the PSA process. This results in a larger CO₂-rich stream mass flow rate to be compressed and, hence, in more power required. Conversely, when more ultrapure H₂ is produced, necessarily a lower H₂ amount is used as fuel to the gas turbine. The dilution with N₂ is reduced in accordance with the Wobbe index and the power to compress that N₂ stream decreases. The overall effect is a slight increase of the auxiliary power consumption with higher ultrapure H₂ throughput. If the energy content of H₂ is discounted by a factor of 0.6, the outlined situation causes the $\eta_{\text{tot } 60}$ to decrease when shifting the production on ultrapure H₂. Even if the discounting factor considered is $\eta_{\text{el prod}}$, which is calculated to be slightly lower than 0.65, the cumulative efficiency decreases with the ultrapure H₂ throughput. The multiplying factor to approximately equalize the energy performance for all the cases reported would be as high as ≈ 0.69 . The design point of the plant would preferably be one with a low ultrapure H₂ throughput. Whether the described trend holds for larger variations of the plant products has not been investigated. Additional issues may arise (e.g. performance of the gas turbine at reduced loads).

The performance related to CO₂ separation is not heavily influenced by modifications in the split between power and ultrapure H₂. As previously mentioned, a larger ultrapure H₂ throughput would cause PSA-R_{CO₂} to increase and PSA-Y_{CO₂} to decrease. On a plant perspective the final Y_{CO₂} is rather stable,

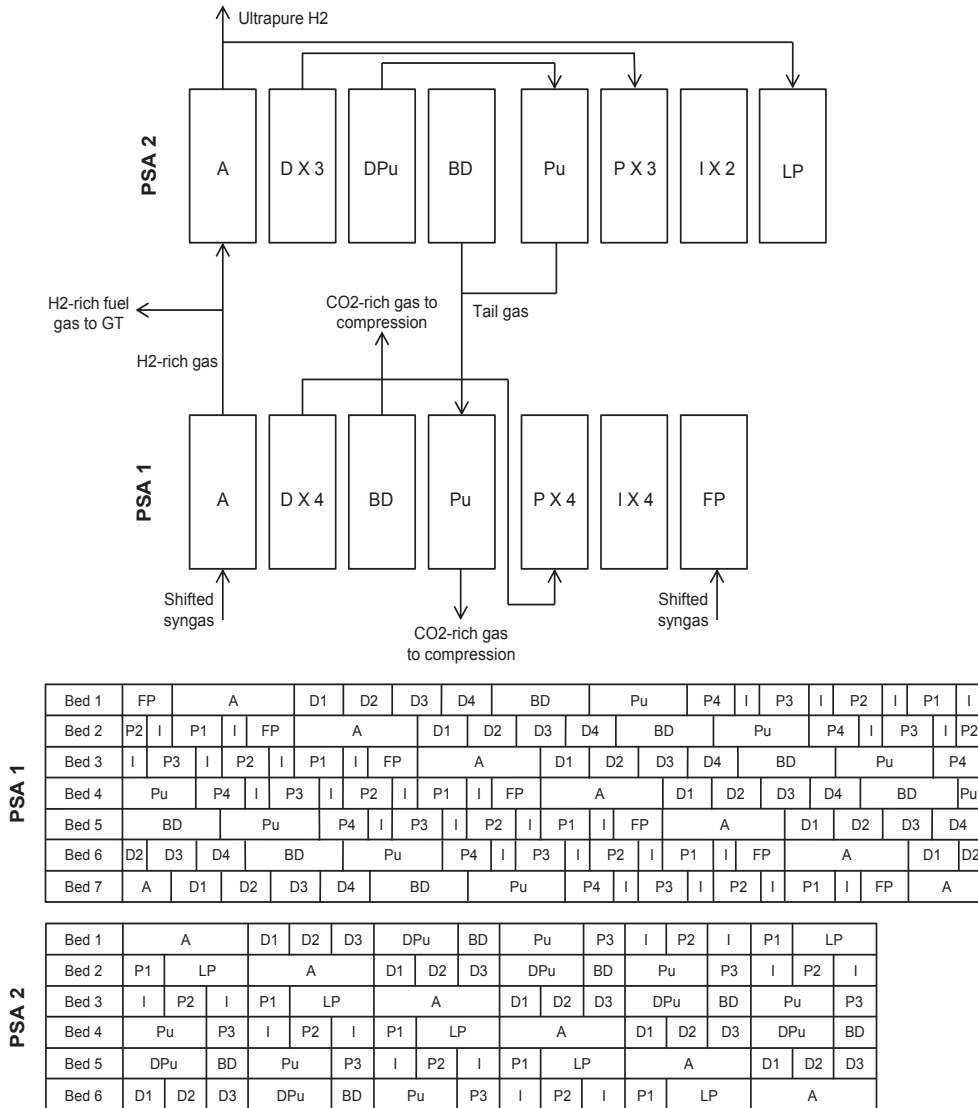


Fig. 3 – Schematics of the two PSA processes in series. The sequence of the steps undergone by a single column of each train is reported alongside with the scheduling of the cycle. The steps considered are: Adsorption or Feed (A), Pressure equalization – Depressurization (D), Depressurization providing Purge (DPu), Blowdown (BD), Purge (Pu), Pressure equalization – Pressurization (P), Feed Pressurization (FP), Light product Pressurization (LP), Idle (I).

Table 2 – Characteristics of the two PSA processes in series and of the adsorption columns.

		Step time (s)								Mole flow rate (mol/s)	
PSA 1	A	D X 4	DPu	BD	Pu	P X 4	I	FP	TOT	Feed	Purge
	90	41	–	80	59	41	32	41	384	4400	From PSA 2
PSA 2	A	D X 3	DPu	BD	Pu	P X 3	I	LP	TOT	Feed	Purge
	$t_{\text{cycle2}}/6$	$t_{\text{cycle2}}/18$	$t_{\text{cycle2}}/9$	$t_{\text{cycle2}}/18$	$t_{\text{cycle2}}/9$	$t_{\text{cycle2}}/18$	$t_{\text{cycle2}}/9$	$t_{\text{cycle2}}/9$	t_{cycle2}	n_{feed2}	200
Bed characteristics											
L (m)				D (m)				ϵ			
PSA 1	11			7.1			0.38				
PSA 2	10			2.8			0.38				

Table 3 – Performance of the IGCC plant implementing the Two-train PSA configuration.

Two-train PSA	PW/H ₂ 1.8 H ₂ /Prod 0.299 t _{cycle2} 342 s	PW/H ₂ 2.5 H ₂ /Prod 0.244 t _{cycle2} 378 s	PW/H ₂ 2.9 H ₂ /Prod 0.221 t _{cycle2} 396 s	PW/H ₂ 3.1 H ₂ /Prod 0.208 t _{cycle2} 414 s	PW/H ₂ 3.6 H ₂ /Prod 0.187 t _{cycle2} 450 s
Coal flow rate (kg/s)	44	44	44	44	44
Coal thermal input (MW)	1095	1095	1095	1095	1095
Gas turbine output (MW)	244	262	270	274	280
Steam turbine output (MW)	165	169	171	172	174
Air expander output (MW)	5	6	6	6	6
Gross electric output (MW)	415	437	448	453	460
Total power consumption (MW)	115	115	115	115	114
Net electric output (MW)	300	322	333	338	346
Net electric efficiency – η_{el} (%)	27.35%	29.39%	30.37%	30.83%	31.54%
Power gen. efficiency – $\eta_{el\ prod}$ (%)	64.43%	64.59%	64.71%	64.76%	64.78%
CCS					
CO ₂ purity – Y_{CO_2} (%)	98.8%	98.8%	98.8%	98.8%	98.8%
CO ₂ recovery – R_{CO_2} (%)	86.8%	85.9%	85.6%	85.2%	84.7%
Ultrapure H₂					
H ₂ throughput (kg/s)	1.36	1.09	0.96	0.90	0.81
H ₂ purity – Y_{H_2} (%)	99.999%	99.998%	99.998%	99.998%	99.991%
H ₂ thermal power (MW)	163	131	115	108	97
H ₂ efficiency – η_{H_2} (%)	14.90%	11.93%	10.48%	9.83%	8.86%
Overall plant					
Cumulative efficiency ₆₀ – η_{tot60} (%)	36.29%	36.55%	36.66%	36.73%	36.86%
Cumulative efficiency* – η_{tot}^* (%)	36.95%	37.09%	37.15%	37.20%	37.28%

due to the flash separation process, while R_{CO_2} increases slightly mainly due to the higher PSA- R_{CO_2} .

One-train PSA configuration

This section investigates the possibility of producing ultrapure H₂ as a secondary product stream from a single PSA process, which retains its ability to separate and concentrate CO₂ from a shifted syngas stream. The general design of the novel PSA process is based on a previous work [23]. Some modifications are introduced in the PSA arrangement in order to enable the additional production of ultrapure H₂. No additional separation stages for CO₂ separation and H₂ production have to be included in the system configuration. The bed is assumed to be filled with the same activated carbon used in the Two-train PSA configuration [37]. The following sections outline the design of the gas separation unit and analyze the performance of the resulting system.

Modified PSA cycle

The PSA process consists of a 7-bed 13-step cycle operating between a high pressure level of 38.8 bar and a low pressure level of 1 bar. The H₂-rich products are obtained at high pressure (38.8 bar) during the adsorption step. The regeneration is carried out by lowering the pressure down to 1 bar and allows for extracting a CO₂-rich gas stream. The main modification introduced with regard the original cycle is to split the adsorption step into two parts. During the first part (A1) the off-gas will be constituted by ultrapure H₂, while during the second part (A2) it will be the H₂-rich fuel for the gas turbine. For both the steps the feed is the shifted syngas. If the column is sufficiently regenerated, when the syngas is first introduced

all the gases other than H₂ get adsorbed in the first part of the bed. Thus, a very high-purity stream of H₂ is leaving the column. Such high H₂ purity for the off-gas stream cannot be kept for long, since soon some impurities begin to breakthrough. When that is the case, the second part of the adsorption step takes over and the off-gas is used as gas turbine fuel. Fig. 4 and Table 4 give an overview of the modified cycle configuration, showing the sequence of steps undergone by a single column of a train, the cycle scheduling and the characteristics of the adsorption column. Apart from splitting the adsorption step into two parts, other modifications needed to be introduced in comparison to the reference PSA cycle. In the first instance, the continuous and possibly stable feed to the gas turbine had to be ensured. This translates in one of the 7 columns of the train always undergoing the second part of the adsorption step (A2). In order to comply with that, the time length of the first depressurization step (D1) was decreased to allow accommodating the step A1 in the scheduling of the cycle. This countermeasure allowed the A2 steps of the different columns to follow one another in a continuous pattern (see Fig. 4) and to ensure the continuous feed of the gas turbine. The decrease of the D1 step time implied an equal decrease of the relative pressurization step (P1). One more modification of the PSA cycle is the nature of the purge gas stream. In the cases analyzed, part of the ultrapure H₂ is adopted, instead of the H₂-rich gas for the gas turbine. The utilization of ultrapure H₂ was made necessary by the necessity of a significant regeneration of the column, which needs to be free from impurities when the A1 step begins.

One-train PSA results

Table 5 summarizes the main outputs of the system simulations with coproduction of power and H₂ through a single PSA

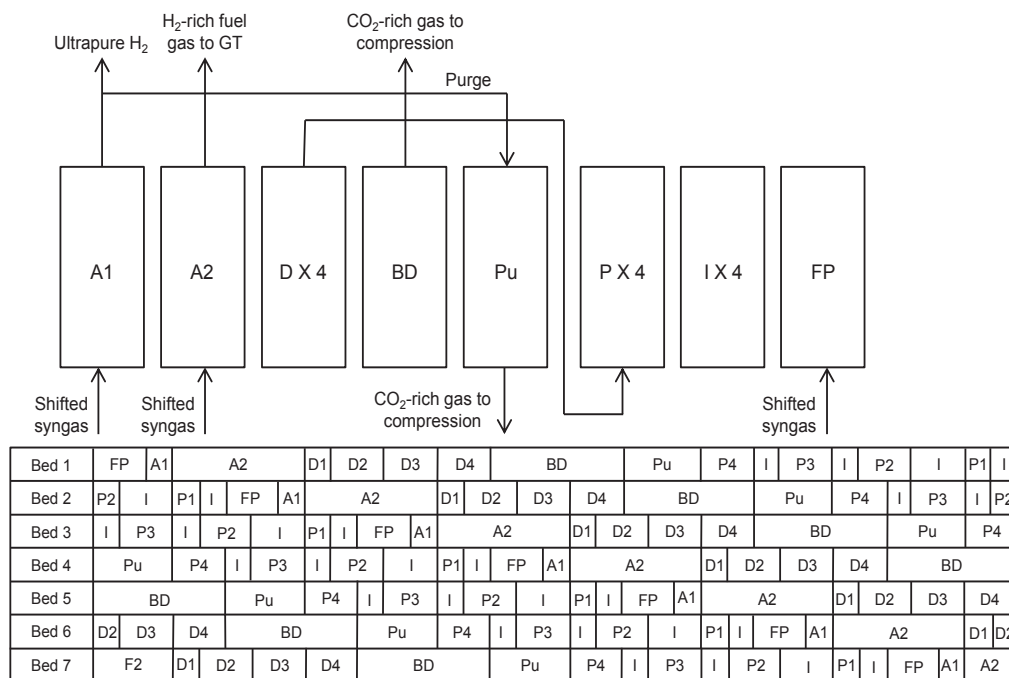


Fig. 4 – Schematic of the single PSA process. The sequence of the steps undergone by a single column of the train is reported alongside with the scheduling of the cycle. The steps considered are: Adsorption or Feed with ultrapure H₂ production (A1), Adsorption or Feed with fuel-grade H₂ production (A2), Pressure equalization – Depressurization (D), Blowdown (BD), Purge (Pu), Pressure equalization – Pressurization (P), Feed Pressurization (FP), Idle (I).

Table 4 – Characteristics of the single PSA process and of the adsorption column.

PSA	Step time (s)											Mole flow rate (mol/s)		
	A1	A2	D1	D X 3	BD	Pu	P X 3	P1	I	FP	TOT	Feed	Purge	
	25	90	16	41	80	59	41	16	57	41	630	3490.3	3490.3 P/F	
Bed characteristics														
L (m)				D (m)				ε						
PSA	12				6.8				0.38					

train. The cases refer to different purge-to-feed (P/F) mole flow ratio in the PSA process, while the coal input is constant. Modifying the P/F ratio translates in modifications of the purge flow rate applied (since the feed flow rate is kept constant). Such basic procedure enables different splits between power and ultrapure H₂ production. The cases have been termed after the ratio of net electric output and H₂ energy output (PW/H₂).

It has to be pointed out that only one case of those reported matched the set H₂ purity specification, i.e. 99.99+% vol, and this constitutes the biggest drawback of the *One-train* PSA configuration. The case matching the purity specification is that with a P/F ratio of 0.18. Some measures could be taken in the other cases in order to increase the ultrapure H₂ purity, though those would involve a reduction of ultrapure H₂ throughput. The general remark is that there is a trade-off between the ultrapure H₂ purity and throughput. The stricter are the constraints on ultrapure H₂ purity, the less flexible is

the operation. If PEM fuel cells are considered as end-application for the produced H₂, this configuration may not be able to cover a large range of power output variations. On the other hand, assuming that lower H₂ purities are acceptable (H₂ used for other end applications or simply stored for allowing flexible operations), a certain degree of flexibility in the power production is possible with minimal modifications in the system, i.e. simply increasing/decreasing the P/F ratio of the PSA process.

Assuming a relaxed specification on H₂ purity applies, the load of the plant was varied of about 10%. The change in the modes of operation did not involve any significant variation in the process units upstream the PSA. Higher load changes are feasible in accordance with reduced H₂ purity requirements and with the capability of the gas turbine to work off-design. A worth-to-mention advantage of this system configuration is that it is designed with a single separation stage for CO₂ separation and H₂ production. Both the benchmark arrangement

Table 5 – Performance of the IGCC plant implementing the One-train PSA configuration.

One-train PSA	PW/H ₂ 2.2	PW/H ₂ 2.6	PW/H ₂ 3.0	PW/H ₂ 3.5	PW/H ₂ 4.3
	P/F 0.09	P/F 0.12	P/F 0.15	P/F 0.18	P/F 0.21
Coal flow rate (kg/s)	43	43	43	43	43
Coal thermal input (MW)	1088	1088	1088	1088	1088
Gas turbine output (MW)	252	261	270	278	287
Steam turbine output (MW)	167	169	171	173	175
Air expander output (MW)	6	6	6	6	6
Gross electric output (MW)	425	436	447	458	468
Total power consumption (MW)	111	113	115	117	119
Net electric output (MW)	314	323	331	340	349
Net electric efficiency – η_{el} (%)	28.85%	29.66%	30.46%	31.28%	32.07%
Power gen. efficiency – $\eta_{el prod}$ (%)	64.36%	64.53%	64.68%	64.85%	64.94%
CCS					
CO ₂ purity – Y_{CO_2} (%)	98.9%	98.9%	99.0%	99.0%	99.0%
CO ₂ recovery – R_{CO_2} (%)	83.2%	84.3%	85.1%	85.7%	86.1%
Ultrapure H₂					
H ₂ throughput (kg/s)	1.21	1.06	0.93	0.80	0.68
H ₂ purity – Y_{H_2} (%)	99.842%	99.933%	99.968%	99.983%	99.990%
H ₂ thermal power (MW)	142	126	111	96	81
H ₂ efficiency- η_{H_2} (%)	13.01%	11.62%	10.22%	8.84%	7.46%
Overall plant					
Cumulative efficiency ₆₀ – η_{tot60} (%)	36.66%	36.63%	36.60%	36.58%	36.55%
Cumulative efficiency* – η_{tot}^* (%)	37.23%	37.15%	37.08%	37.01%	36.91%

(absorption unit and PSA unit) and the first configuration studied in this paper (two PSA trains) necessitate two different separation stages. A single stage translates in reduced footprint and, possibly, capital costs.

From an energy performance perspective, the coproduction of ultrapure H₂ decreases the net electric efficiency and increases the H₂ efficiency. Similarly to the Two-train PSA configuration, the two power consumptions undergoing significant variations in the cases analyzed are the CO₂ compression power and the compression power for the N₂ to dilute the fuel in the gas turbine. The latter retains the same behavior previously outlined. Higher ultrapure H₂ throughput means lower H₂ to the gas turbine and lower N₂ dilution needed, which results in decreased compression power. The CO₂ compression power is influenced in a different manner compared to what we discussed before. To increase the ultrapure H₂ throughput the P/F ratio needs to be reduced. Consequently, the purge flow rate diminishes leading to a lower PSA-R_{CO₂} and a higher PSA-Y_{CO₂}, and, ultimately, to a smaller mass flow rate to be compressed. Thus, the CO₂ compression power consumption decreases with enhanced ultrapure H₂ production. The two effects described act in the same direction, decreasing the power consumption when the ultrapure H₂ throughput increases. The overall result is that both $\eta_{tot 60}$ and η_{tot}^* tend to increase when shifting the production to ultrapure H₂. The thermodynamic factor equalizing the energy performances in all the cases would be ≈ 0.58 , which suggests the plant design point should be one with a significant ultrapure H₂ throughput. As pointed out for the other configuration, the validity of the described trend has not been assessed for a larger range of power output variations.

The performance related to CO₂ separation is similar in all cases. The modifications introduced to the PSA process in order to coproduce H₂, do not hinder significantly the effectiveness of the cycle. The CO₂ purity achieved is stable in a

neighborhood of 99%, thanks to the presence of the flash separation process integrated in the CO₂ compression station. The CO₂ recovery undergoes a slight decrease when coproducing ultrapure H₂.

Discussion of the results

The novel system configurations demonstrated to entail a high degree of flexibility. Shifting between power and ultrapure H₂ allows for a load-following mode of operation with minimal modifications in the process units. PSA technology demonstrated to be rather effective in this sense. Minimal adjustments in the PSA unit arrangement allowed for obtaining different splits of the product outputs, without any significant impact on the upstream processes. Further, PSA can be easily tuned in accordance to the system requirements giving a high degree of freedom in the design phase. For instance, if the plant was requested to produce a lower amount of ultrapure H₂, both PSA configurations could be designed according to that specification (i.e. different sizes of the column, cycle scheduling, etc.).

Previous studies implemented the coproduction by utilizing a PSA process downstream an absorption unit. Absorption is currently believed to be the most effective and mature technology for CO₂ removal from a shifted syngas, while PSA is the benchmark for H₂ purification. However, an issue connected to this configuration consists in the necessity for a compression of the PSA tail gas. The tail gas has a non-negligible H₂ content which must be recovered. The common practice is to compress the gas stream and feed it to the gas turbine as fuel. The tail gas compression increases the plant power consumption and is the main additional source of energy penalty when implementing ultrapure H₂ coproduction. Both the system configurations proposed in this work

enable the avoidance of this tail gas compression. Thereby, it was expected the performance of the system to be enhanced in comparison to the benchmark alternative (i.e. absorption + PSA). With regard to that, some considerations can be drawn by looking at Table 6. A premise is necessary before the analysis. A range of different results can be found in the literature estimating IGCC plant performance. This is due to the various configurations, operating conditions and computational assumptions that can be adopted for these systems. We tried to establish some key assumptions in order to set a common framework for comparison: the set of results chosen from the literature needs to be representative of an IGCC plant as close as possible to the system defined in this paper (and based on EBTF recommendations [32]) and should rely on mature technologies. Furthermore, the plant should be designed to produce power as the primary product, whereas ultrapure H₂ is the byproduct. This last consideration brought us to exclude some studies where the context is overturned (i.e. gasification plant designed for H₂ production with an auxiliary power production). The selected works display performances which are generally lower to what is thought to be the current state-of-the-art, especially in terms of energy efficiency. In a previous work, it was discussed how IGCC plants implementing CO₂ capture through a PSA process are not yet as competitive as the absorption-based counterpart [24]. One main reason behind the relatively low net electrical efficiency displayed by the first work selected [10] is believed to be the gasification technology adopted. A Siemens gasifier with water quench was chosen. The second set of results selected [7] exhibits a more substantial energy penalty. In this case more conservative assumptions seem to have been applied. An example is the adoption of an E-class gas turbine, which results in a significant efficiency reduction compared to the utilization of next generation gas turbines.

First a comparison between the PSA-based cases is carried out. The case termed *Only power* is the result of a process simulation based on the same composite model used for all other cases reported in this work. It represents the IGCC plant with a single PSA train and without ultrapure H₂ production. This set of results is useful to evaluate the change in performance when coproducing H₂. Two other cases are displayed (*Two-train PSA* and *One-train PSA*), representing the two novel configurations proposed. The instances were selected, among those reported in the previous sections, in order to have similar ultrapure H₂ throughput and, thus, to allow easier comparisons of the results. Whilst the coal input is kept almost constant for the cases involving two products, when the output is only power the coal input has been decreased in

order to utilize the same gas turbine working with a similar load factor. In this way, the performance of the gas turbine could not be considered a discriminating factor for different performances.

Coproducing ultrapure H₂ necessarily results in lower η_{el} , since part of the energy is stored in the H₂ (η_{H_2}). η_{tot}^* is enhanced when ultrapure H₂ is produced, in both the two configurations analyzed. However, the *Two-train PSA* case displays a slightly better energy performance. Another advantage over the *One-train PSA* alternative is the H₂ purity which fully matches the requirement. The CO₂ separation performance (represented in the table by R_{CO₂}) displays a small increase when moving to a coproduction layout. The *One-train PSA* case returns a R_{CO₂} slightly higher than the *Two-train PSA* case. Overall the differences are very small, about 1%. It must be stressed that a key benefit of implementing a *One-train PSA* configuration cannot be grasped by the table, as it consists in the utilization of a single separation stage instead of two.

If we broaden the comparative analysis also to the selected results from the literature, the advantage of using PSA for both separating CO₂ and purifying H₂ seems to be supported. Overlooking the absolute numbers, which may be influenced by different assumptions, it is meaningful to analyze the relative variations of the performance indicators (given the lack of enough information for calculating η_{tot}^* in all the cases, the cumulative efficiency term considered is η_{tot60}). When coproducing a similar throughput of ultrapure H₂, η_{tot60} tends to increase in all the cases reported. The largest increase is registered with the *Two-train PSA* case (+0.65%) followed by the *One-train PSA* case (+0.37%). The selected absorption-based literature cases whether report the same value (+0%) [7] or a more limited increase (+0.18%) [10]. Even though the complexity of the systems demands caution with comparison of different sets of results, the reported outcome seems to comply with the beneficial effect of avoiding tail gas compression attained with the novel configurations proposed. This energy saving would be more significant the larger the ultrapure H₂ production is compared to the power output. On a CO₂ separation perspective (i.e. CO₂ recovery), the absorption-based system displays better performance both in an only power and in a coproduction layout. Finally, it is important to point out that the utilization of PSA technology brings along some issues to be addressed. Complexity of the arrangement, possible large footprint and necessity to smooth out fluctuations in the fuel gas to the gas turbine are typical examples. The latter issue is stressed when off-design operating conditions apply, like the cases studied in this work [42].

Table 6 – Performance of IGCC plants implementing CO₂ capture either with or without ultrapure H₂ coproduction.

	Coal input MW	CO ₂ capture technology	R _{CO₂} %	Y _{H₂} %	η_{H_2} %	η_{el} %	$\eta_{el\ prod}$ %	η_{tot60} %	η_{tot}^* %
Only power PSA	971	PSA	84.6	–	–	36.21	64.22	36.21	36.21
Two-train PSA	1095	PSA	85.2	99.991	8.86	31.54	64.78	36.86	37.28
One-train PSA	1088	PSA	85.7	99.983	8.84	31.28	64.85	36.58	37.01
Cormos [10]	1167	Selexol	92.4	–	–	36.02	–	36.02	–
Cormos [10]	1167	Selexol	92.4	99.950	8.57	31.06	–	36.20	–
Dynamis [7]	1396	Selexol	90.3	–	–	33.10	–	33.10	–
Dynamis [7]	1396	Selexol	90.2	99.950	3.00	31.30	–	33.10	–

Conclusions

Two novel system configurations of an IGCC plant coproducing power and ultrapure H₂ with CO₂ capture are presented. Both are based on PSA technology for separating CO₂ from the shifted syngas and purifying H₂. The main reason for the coproduction of ultrapure H₂ is the possibility to increase the flexibility of the power output. The configurations proposed demonstrated to fulfill this requirement as the output of the plant could be shifted to a certain extent between the two energy products without losing in efficiency. Within the cases reported, a load variation of about 13% (net power output reduced from 346 MW to 300 MW) could be reached by increasing the ultrapure H₂ throughput (up to a maximum of 163 MW) while the coal feeding is maintained constant. Larger load variations are realistically achievable given a minimum redesign of the PSA processes. In this sense PSA does not seem to pose limits in the flexibility achievable. Thereby the power plant has the possibility to effectively comply with the variability of electricity demand, characteristic of paramount importance in view of the future energy market. The first configuration relies on two PSA trains in series and was termed *Two-train* PSA. While the main goal of the first train is CO₂ removal from the shifted syngas, the second train further processes part of the H₂-rich off-gas in order to increase the H₂ purity. The utilization of the same technology allows for an advantageous integration scheme between the two processes. The shift between power output and ultrapure H₂ can be achieved with different strategies, allowing for an interesting potential of flexible operation not fully explored in this paper. The cases reported increased the ultrapure H₂ throughput by augmenting the gas sent to the second PSA process and adjusting the relative cycle scheduling in order to fulfill the process requirements. The units upstream the first PSA are basically unaffected by this procedure and are, thus, able to retain good working efficiencies. Accordingly, the plant energy efficiency is stable on a good level at varying power outputs. The CO₂ separation performance is on acceptable levels and slightly increases with the decrease of the power output. The second configuration assessed consists of a single PSA train and was for this reason termed *One-train* PSA. The process is able to concentrate CO₂ from the shifted syngas, while producing two H₂-rich gas streams. A first stream characterized by a high H₂ purity (up to 99.99+% vol.) and a second one with a lower H₂ content (82–85%), which constitutes the continuous fuel feed of the gas turbine. Different shares of power and ultrapure H₂ could be obtained by simply modifying the purge-to-feed ratio of the PSA process. The upstream processes are again unaffected by these modifications of the PSA process and can keep on working at their design point. However, issues arose regarding the possibility of achieving very high H₂ purities in all the operating conditions analyzed. Only one of the cases reported strictly fulfilled the H₂ purity specification established (99.99+% vol.), which is defined considering PEM fuel cells as final application. If such high purity is required, the flexibility of the plant could not be completely realized. More relaxed purity constraints would enable a high degree of flexibility, with relatively good energy and CO₂ separation performance and an easier plant design

(one separation stage instead of two like in all the other alternatives).

In order to complete the overview on the novel PSA-based system configurations, a comparative analysis is carried out with the most common arrangement for power and ultrapure H₂ coproduction in IGCC plants. It consists of an absorption unit for processing the shifted syngas followed by a PSA for further H₂ purification. The related results refer to two studies, selected after a screening of the relevant literature. Introducing the production of ultrapure H₂ appears to be more effective when also the CO₂ separation is carried out through a PSA process, as can be argued by the cumulative efficiency. The main advantage is that PSA technology allows avoiding the power consumption related to PSA tail gas compression, common in the configuration including absorption. Between the two proposed options, the *Two-train* PSA configuration demonstrated to perform better in terms of energy efficiency.

Although the discussed advantages of the novel configurations presented, the general viability has yet to be proven since PSA integration into an IGCC plant has normally a lower overall performance than absorption. It needs to be evaluated if the benefits introduced with ultrapure H₂ coproduction are sufficient to make up for this initial performance gap. The scattering of results in the literature makes this evaluation not straightforward. A possible solution would be to utilize a common modeling framework to assess the performance of both options. Other issues may also arise when adopting PSA technology, among those the need for controlling the fluctuations in the H₂-rich gas rate to the gas turbine due to the PSA cyclic operation. Lastly, this is a very first assessment of such system entirely based on PSA technology. A further optimization is likely feasible, exploiting developments in the processes and in the materials (e.g. adsorbents effectively performing at high temperatures allowing for warm gas cleaning processes). Moreover a simplification of the PSA layout is possible with advantages in terms of footprint. In particular the *Two-train* PSA configuration relies on a fairly complex second PSA cycle, which was developed to obtain high H₂ recovery. Since that is not an important requirement in the case proposed, an easier PSA cycle could be advisable.

In conclusion, the system analysis conducted suggests IGCC plants completely based on PSA as gas separation technology to be rather promising. PSA processes allow shifting between varying power-to-hydrogen ratios without significant energy penalties, increasing so plant flexibility at partial loads.

Acknowledgments

The authors gratefully acknowledge the financial support provided through the Norwegian University of Science and Technology (NTNU).

Nomenclature

- a_i number of neighboring sites occupied by adsorbate molecule for species i
 C_i gas concentration of species i , mol/m³

$C_{ads,i}$	specific heat of species i in the adsorbed phase, $J/(mol\ K)$
$C_{p,G}$	gas specific heat at constant pressure, $J/(mol\ K)$
$C_{p,s}$	particle specific heat at constant pressure, $J/(kg\ K)$
C_{tot}	total gas concentration, mol/m^3
$C_{v,G}$	gas specific heat at constant volume, $J/(mol\ K)$
D	diameter of the adsorption column, m
$D_{ax,i}$	axial dispersion coefficient of species i , m^2/s
d_p	particle diameter, m
$\Delta H_{r,i}$	isosteric heat of adsorption of species i , J/mol
k_i	equilibrium constant of species i , Pa^{-1}
$k_{\infty,i}$	adsorption constant at infinite temperature of species i , Pa^{-1}
$k_{LDF,i}$	linear driving force coefficient of species i , s^{-1}
L	length of the adsorption column, m
P	pressure, Pa
$PSA-R_{CO_2}$	PSA CO_2 recovery
$PSA-Y_{CO_2}$	PSA CO_2 purity
PW/H_2	ratio of net electric output and H_2 energy output
P/F	purge-to-feed mole flow ratio
q_i^*	equilibrium adsorbed concentration of species i , mol/kg
\bar{q}_i	averaged adsorbed concentration of species i , mol/kg
$q_{m,i}$	maximum adsorption capacity of species i , mol/kg
R	universal gas constant, $Pa\ m^3/(mol\ K)$
R_{CO_2}	CO_2 recovery
R_{H_2}	H_2 recovery
t	step time, s
T	temperature, K
u_s	superficial velocity, m/s
Y_{CO_2}	CO_2 purity
Y_{H_2}	ultrapure H_2 purity
Greek letters	
ϵ	bed void fraction
ϵ_p	particle void fraction
η_{el}	net electric efficiency
$\eta_{el\ prod}$	power production efficiency
η_{H_2}	hydrogen efficiency
η_{tot60}	cumulative efficiency (with a factor 0.6)
η_{tot}^*	cumulative efficiency (with a factor $\eta_{el\ prod}$)
λ_{ax}	axial thermal dispersion coefficient, $J/(s\ m\ K)$
ρ_G	gas volumetric mass density, kg/m^3
ρ_p	particle volumetric mass density, kg/m^3

Subscripts

i species

Superscripts

NC number of components

REFERENCES

- [1] IPCC. *Climate change 2014: synthesis report*. Geneva, Switzerland: IPCC; 2014. p. 151.
- [2] IEA. *Energy and climate change – world energy outlook special report*. 2015.
- [3] IEA. *Technology roadmap – carbon capture and storage*. 2013.
- [4] Brouwer AS, van der Broeck M, Seebregts A, Faaij APC. The flexibility requirements for power plants with CCS in a future energy system with a large share of intermittent renewable energy sources. *Energy Procedia* 2013;37:2657–64.
- [5] IEAGHG. *Operating flexibility of power plants with CCS*. 2012.
- [6] Jansen D, Gazzani M, Manzolini G, van Dijk E, Carbo M. Pre-combustion CO_2 capture. *Int J Greenh Gas Control* 2015;40:167–87.
- [7] DYNAMIS. *Towards hydrogen and electricity production with carbon dioxide capture and storage*. 2009.
- [8] Kreutz T, Williams R, Consonni S, Chiesa P. Co-production of hydrogen, electricity and CO_2 from coal with commercially ready technology. Part B: economic analysis. *Int J Hydrogen Energy* 2005;30(7):769–84.
- [9] Chiesa P, Consonni S, Kreutz T, Williams R. Co-production of hydrogen, electricity and CO_2 from coal with commercially ready technology. Part A: performance and emissions. *Int J Hydrogen Energy* 2005;30(7):747–67.
- [10] Cormos C-C. Assessment of hydrogen and electricity co-production schemes based on gasification process with carbon capture and storage. *Int J Hydrogen Energy* 2009;34(15):6065–77.
- [11] Cormos C-C. Evaluation of energy integration aspects for IGCC-based hydrogen and electricity co-production with carbon capture and storage. *Int J Hydrogen Energy* 2010;35(14):7485–97.
- [12] Davison J, Arienti S, Cotone P, Mancuso L. Co-production of hydrogen and electricity with CO_2 capture. *Int J Greenh Gas Control* 2010;4(2):125–30.
- [13] Chen Q, Rao A, Samuelsen S. H_2 coproduction in IGCC with CCS via coal and biomass mixture using advanced technologies. *Appl Energy* 2014;118:258–70.
- [14] Li M, Rao AD, Scott Samuelsen G. Performance and costs of advanced sustainable central power plants with CCS and H_2 co-production. *Appl Energy* 2012;91(1):43–50.
- [15] Cormos C-C. Hydrogen and power co-generation based on coal and biomass/solid wastes co-gasification with carbon capture and storage. *Int J Hydrogen Energy* 2012;37(7):5637–48.
- [16] Cormos C-C, Starr F, Tzimas E. Use of lower grade coals in IGCC plants with carbon capture for the co-production of hydrogen and electricity. *Int J Hydrogen Energy* 2010;35(2):556–67.
- [17] Ahn S, You Y-W, Lee D-G, Kim K-H, Oh M, Lee C-H. Layered two- and four-bed PSA processes for H_2 recovery from coal gas. *Chem Eng Sci* 2012;68(1):413–23.
- [18] Lopes FVS, Grande CA, Rodrigues AE. Activated carbon for hydrogen purification by pressure swing adsorption: multicomponent breakthrough curves and PSA performance. *Chem Eng Sci* 2011;66(3):303–17.
- [19] Ribeiro AM, Grande CA, Lopes FVS, Loureiro JM, Rodrigues AE. A parametric study of layered bed PSA for hydrogen purification. *Chem Eng Sci* 2008;63(21):5258–73.
- [20] Ribeiro AM, Grande CA, Lopes FVS, Loureiro JM, Rodrigues AE. Four beds pressure swing adsorption for hydrogen purification: case of humid feed and activated carbon beds. *AIChE J* 2009;55(9):2292–302.
- [21] Sircar S, Golden TC. Purification of hydrogen by pressure swing adsorption. *Sep Sci Technol* 2000;35(5):667–87.
- [22] Luberti M, Friedrich D, Brandani S, Ahn H. Design of a H_2 PSA for cogeneration of ultrapure hydrogen and power at an advanced integrated gasification combined cycle with pre-combustion capture. *Adsorption* 2014;20(2–3):511–24.
- [23] Riboldi L, Bolland O. Evaluating pressure swing adsorption as a CO_2 separation technique in coal-fired power plants. *Int J Greenh Gas Control* 2015;39:1–16.
- [24] Riboldi L, Bolland O. Comprehensive analysis on the performance of an IGCC plant with a PSA process integrated for CO_2 capture. *Int J Greenh Gas Control* 2015;43:57–69.

- [25] Liu Z, Green WH. Analysis of adsorbent-based warm CO₂ capture technology for integrated gasification combined cycle (IGCC) power plants. *Industrial Eng Chem Res* 2014;53(27):11145–58.
- [26] Gazzani M, Macchi E, Manzolini G. CO₂ capture in integrated gasification combined cycle with SEWGS – Part A: thermodynamic performances. *Fuel* 2013;105:206–19.
- [27] Manzolini G, Macchi E, Binotti M, Gazzani M. Integration of SEWGS for carbon capture in natural gas combined cycle. Part B: reference case comparison. *Int J Greenh Gas Control* 2011;5(2):214–25.
- [28] Baade W, Farnand S, Hutchison R, Welch K. CO₂ capture from SMRs: a demonstration project. *Hydrocarb Process* 2012:63–8.
- [29] Sircar S, Kratz WC. Simultaneous production of hydrogen and carbon dioxide from steam reformer off-gas by pressure swing adsorption. *Sep Sci Technol* 1988;23(14–15):2397–415.
- [30] Alptekin G, Steve D, Jayaraman A, Dubovik M, Amalfitano R. A low cost, high capacity regenerable sorbent for CO₂ capture. In: A&WMA's 102nd annual conference & exhibition; 2009.
- [31] Alptekin G, Ambalavanan J, Copeland R, Dietz S, Bonnema M, Schaefer M, et al. Novel warm gas CO₂ capture technology for IGCC power plants. TDA Research Inc; 2013.
- [32] DECARBit. Enabling advanced pre-combustion capture techniques and plants. European best practice guidelines for assessment of CO₂ capture technologies. European Benchmarking Task Force; 2011.
- [33] Riboldi L, Bolland O. Determining the potentials of PSA processes for CO₂ capture in integrated gasification combined cycle (IGCC). *Energy Procedia* 2016;86:294–303.
- [34] Thermoflex Version 24.0.1. 2014, Thermoflow Inc.
- [35] gPROMS 4.1.0. 2015, Process System Enterprise Limited.
- [36] Aspen HYSYS V7.3. 2011, Aspen Technology Inc.
- [37] Lopes FVS, Grande CA, Ribeiro AM, Loureiro JM, Evaggelos O, Nikolakis V, et al. Adsorption of H₂, CO₂, CH₄, CO, N₂ and H₂O in activated carbon and zeolite for hydrogen production. *Sep Sci Technol* 2009;44(5):1045–73.
- [38] IEA. Power generation from coal: measuring and reporting efficiency performance and CO₂ emissions. 2010.
- [39] de Visser E, Hendriks C, Barrio M, Mølnvik MJ, de Koeijer G, Liljemark S, et al. Dynamis CO₂ quality recommendations. *Int J Greenh Gas Control* 2008;2(4):478–84.
- [40] Siriwardane RV, Shen M-S, Fisher EP, Poston JA. Adsorption of CO₂ on molecular sieves and activated carbon. *Energy & Fuels* 2001;15(2):279–84.
- [41] Ahn H, Yang J, Lee C-H. Effects of feed composition of coke oven gas on a layered bed H₂ PSA process. *Adsorption* 2001;7(4):339–56.
- [42] Najmi B, Bolland O, Colombo KE. Load-following performance of IGCC with integrated CO₂ capture using SEWGS pre-combustion technology. *Int J Greenh Gas Control* 2015;35:30–46.

